SEDIMENTOLOGY AND MICROMORPHOLOGY OF DRUMLIN SEDIMENTS AT CHIMNEY BLUFFS STATE PARK, NEW YORK STATE, UNITED STATES OF AMERICA.

by

DEREK LESLIE DREGER

A thesis submitted to the Department of Earth Sciences

Brock University

in partial fulfilment of the requirements for the degree of

Master of Sciences

Dr. J. Menzies Supervisor

ABSTRACT

The drumlin sediments at Chimney Bluffs, New York appear to represent a block-in-matrix style glacial mélange. This mélange comprises sand stringers, lenses and intraclasts juxtaposed in an apparently massive diamicton. Thin section examination of these glacigenic deposits has revealed microstructures indicative of autokinetic subglacial deformation which are consistent with a deformable bed origin for the diamicton. These features include banding and necking of matrix grains, oriented plasma fabrics and the formation of pressure shadows at the long axis ends of elongate clasts. Preservation of primary stratification within the sand intraclasts appears to suggest that these features were pre-existing up-ice deposits that were frozen, entrained, then deposited as part of a deforming till layer beneath an advancing ice sheet. Multi-directional micro-shearing within the sand blocks is thought to reflect the frozen nature of the sand units in such a high strain environment.

It is also contended that dewatering of the sediment pile leading to the eventual immobilisation of the deforming till layer was responsible for opening sub-horizontal fissures within the diamicton. These features were subsequently infilled with mass flow poorly sorted sands and silts which were subjected to ductile deformation during the waning stages of an actively deforming till layer. Microstructures indicative of the dewatering processes in the sand units include patches of fine-grained particles within a coarser-grained matrix and the presence of concentrated zones of translocated clays. However, these units were probably confined within an impermeable diamicton casing that prevented massive pore water influxes from the deforming till layer. Hence, these microstructures probably reflect localised dewatering of the sand intraclasts.

A layered subglacial shear zone model is proposed for the various features exhibited by the drumlin sediments. The complexity of these structures is explained in terms of

superposing deformation styles in response to changing pore water pressures. Constructional glaciotectonics, as implied by the occurrence of sub-horizontal fissuring, is suggested as the mechanism for the stacking of the sand intraclast units within the diamicton.

The usefulness of micromorphology in complimenting the traditional sedimentology of glacigenic deposits is emphasised by the current study. An otherwise massive diamicton was shown to contain microstructures indicative of the very high strain rates expected in a complexly deforming till layer. It is quite obvious from this investigation that the classification of diamictons needs to be re-examined for evidence of microstructures that could lead to the re-interpretation of diamicton forming processes.

RÉSUMÉ

Le pacquet de sédiments drumlinaire de Chimney Bluffs, New York, représent un "bloc-en-matrice" genre de mélange glaciale. Des structures microscopique comprennent l'évidence pour la déformation intrinsèque attribuée à l'origine lit non résistant du drumlin. Préservation des structures primaires au coeur des blocs arénacés suggère que ceux sont des dépôts préexistant qui furent gelés, entraînés et par la suite sedimentés au milieu d'une couche de débris sous-glaciaires en voie de déformation. Des failles microscopiques à l'interieur des blocs arénacés appuient aussi l'idée d'un bloc cohésif (c'est-à-dire gelé) au centre d'un till non résistant. Des implications significatives s'émergent de cette étude pour les conditions sous-glaciaire et les procéssus de la formation des drumlin.

TABLE OF CONTENTS

LIST OF FIGURES

LIST OF APPENDIX II FIGURES

LIST OF APPENDIX II TABLES

LIST OF PLATES

CHAPTER 1: INTRODUCTION

1.0 General

The late 19th and the early 20th Centuries represented a period of intense Quaternary research in the New York State drumlin field (Fig. 1.1; Miller, 1972). Although such research has been ongoing, much remains to be discovered about the complex glacial record of the field (Coates, 1976; Fullerton, 1980). Numerous researchers have noted that the highly varied topography of the field, the lack of radiocarbon dating controls and the presence of strongly to weakly stratified units within several drumlins have complicated the interpretation of the Late Wisconsinan subglacial conditions that existed at the southern margin of the Laurentide Ice Sheet in New York State (Muller, 1965; Miller, 1972; Coates, 1976; Fullerton, 1980; Mayewski *et al.*, 1981; Mickelson *et al.*, 1983).

The present study involves a detailed macro- and micromorphological (thin section) analysis of an approximately 800 m long drumlin stoss-end exposure on the south shore of Lake Ontario in Chimney Bluffs State Park, 50 km northeast of Rochester, New York (Fig. 1.2). The exposed section is oriented roughly 90° to the long axis of the drumlin which extends approximately 1 km inland. Drumlin deposits in the park form a series of transverse bluff sections up to 50 m high which are bounded by laminated and highly convoluted glaciolacustrine sediments. All of these deposits are actively eroded by lake ice and storm waves which, in addition to normal slumping, are continuously exposing fresh sections at the site.

Until recently, the only description of the drumlin sediments at Chimney Bluffs was a brief account of the "upper bedded stiff clays" and the overlying coarse gravel unit provided by Slater (1928; 1929). More recent work by Brennan and Caulkin (1984), Callkin and Muller (1992) and Menzies and Woodward (1993) has renewed interest in this area. Menzies

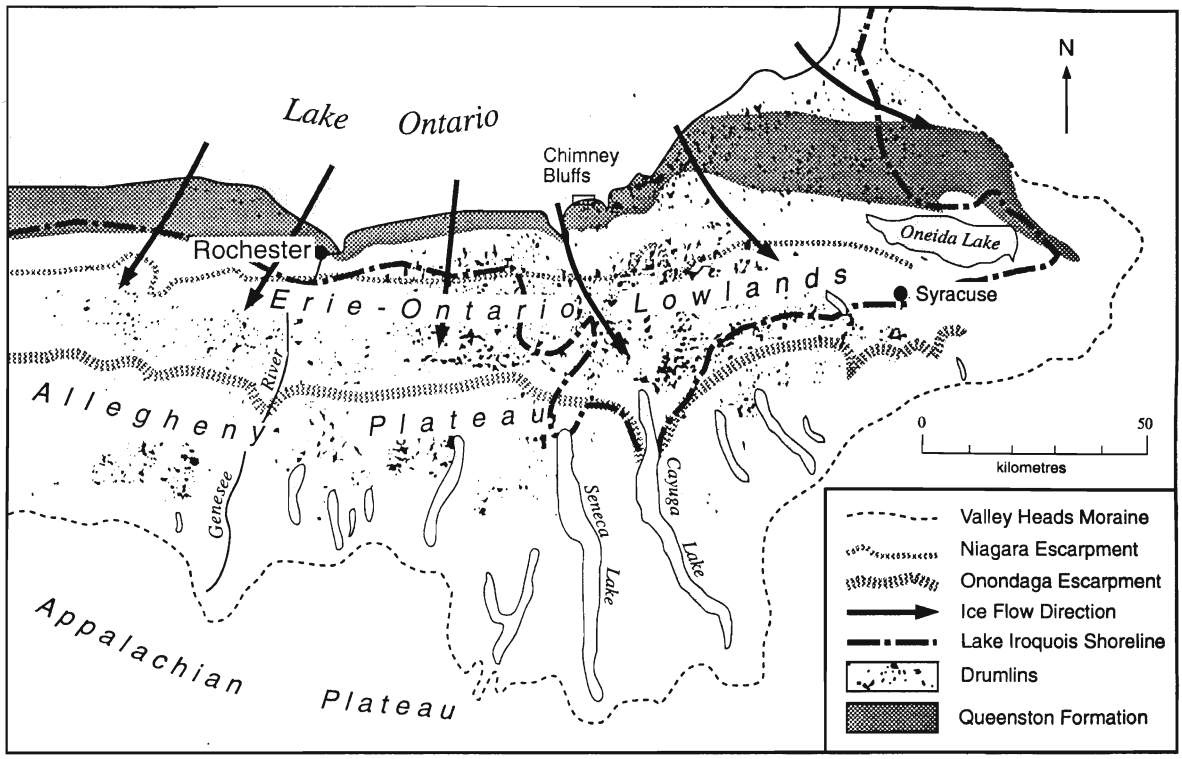

Figure 1.1 Location map for New York drumlin field (after Rickard and Fisher, 1970).

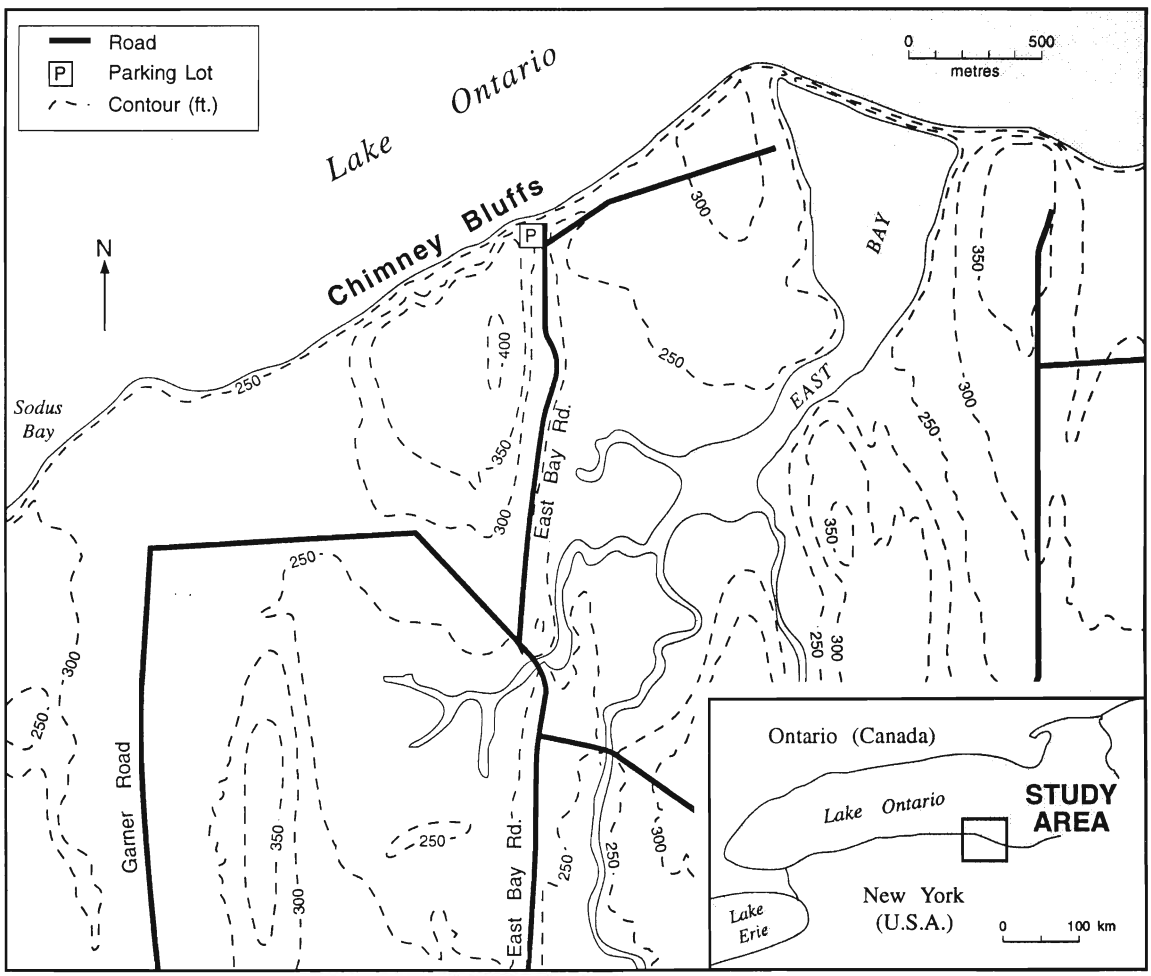

Figure 1.2 Location map for Chimney Bluffs State Park, Wayne Co., New York, U.S.A..

and Woodward (1993) cited the need for a detailed macro- and micromorphological study of these sediments in order to better understand the processes involved in their emplacement within the drumlin landform and their subsequent deposition. Such an investigation is crucial to the reappraisal of the processes involved in the evolution and deposition of glacial landforms (Eyles and Eyles, 1983).

A problem in interpreting the mechanism(s) of drumlinisation arises with the occurrence of stratified units within a drumlin. Investigations concerning the origin of drumlins have traditionally been based on the sedimentology and the macroscale structures of the diamicton comprising the drumlin form. However, results of micromorphological observation have recently shown that an apparently massive (i.e. structureless) diamicton may actually contain microstructures attributable to deformational processes (Meer, 1987; Lagerlund and Meer, 1990; Meer, 1993). Such structures include the development of microfabrics, or rather the orientation of grains in response to applied stresses in addition to structures developped during saturated pore water conditions (Meer, 1987). The usefulness of thin section observations in characterising tills was first noted by Sitler and Chapman (1955) and reiterated more recently by (Meer, 1987; Menzies and Maltman, 1992).

The intent of the present study is to demonstrate that micromorphology can be used to compliment the study of drumlinisation processes. Chimney Bluffs State Park provides an ideal setting for such investigations due to extent of the exposed drumlin section and to the presence of undeformed and deformed sand units within an apparently undeformed diamicton which is difficult to explain using traditional methods. The current study is also intended to compliment ongoing research on drumlinisation processes in former Late Wisconsinan ice-marginal areas (Whittecar, 1979; Dardis and McCabe, 1983; Dardis and McCabe 1987; Hanvey, 1987; McCabe and Dardis, 1989; Shaw and Gilbert, 1990; Boyce and

Eyles, 1991).

1.1 Previous Work

Scant research has been undertaken concerning the drumlin sections on the southern shore of Lake Ontario (Martin, 1901; Fairchild, 1907; Slater, 1929; Calkin and Muller, 1992; Menzies and Woodward, 1993); although a considerable body of literature exists for the New York drumlin field (e.g. Gillette, 1940; Reed *et al.*, 1962; Muller, 1963; Muller, 1965; Miller, 1972; Krall, 1977; Mickelson *et al.*, 1983; Ridky and Bindschadler, 1990; Shaw and Gilbert, 1990; Francek, 1991). Slater (1929) believed that a detailed study of the exposures at Chimney Bluffs State Park, New York was unnecessary due to the paucity of observable structures and only a brief description of the site was given.

Slater (1929) proposed that the drumlins of this area were a composite of upper layers of concentric bedding and "tenacious" cores. These cores, which were noted to contain not only "streaky lenticles" of sandy material, but also contorted beds, were thought to have formed as a response to the differential lateral pressures as ice flowed over an obstruction. This view complemented Fairchild (1907), who saw these drumlins as the geomorphological expression of areas of decreased pressure and lagging flow beneath actively moving ice.

Muller (1963) and Miller (1972) believed that the stratification found in New York drumlins was due to the readvance of Late Wisconsinan ice over pre-existing 'stagnant' glacial deposits, an idea supported by Gravenor (1953), Whittecar and Mickelson (1979), Kruger and Thomsen (1984), McCabe and Dardis (1989), and in part by Francek (1991). However, Muller (1974) considered stratified drift to be evidence of a wet-soled or warm-based ice sheet wherein basal meltwater activity reduced the friction between the subglacial debris (till) layer and the glacier sole allowing for forward movement. Such a water-saturated till layer is thought to represent a deforming till layer which acted as a viscous fluid capable

of transporting clasts in a slurry (Clarke, 1987). The terms *deforming till* and *deformation till* are used in the manner suggested by Alley (1991) in reference to subglacial sediments undergoing pervasive shear deformation and to the diamicton deposited when the sediments cease deforming. Recent work (Evenson, 1971; Muller, 1974; Boulton, 1982; Hicock *et al.*, 1989; Menzies, 1989; Mullins and Hinchey, 1989) has suggested that such a layer could also have provided a nucleus for drumlinisation on the southern margin of the Laurentide Ice Sheet. However, such an origin has been disputed by Clayton *et al.* (1989) who cited the lack of deformational structures and the preservation of primary stratification. Instead, subglacial meltwater flooding and channelised flows have been used to explain the drumlinisation process in the New York drumlin field (Mickelson *et al.* 1983; Shaw and Gilbert, 1990).

1.2 Geological Setting

Chimney Bluffs is located at the northernmost extent of the New York drumlin field (Fig. 1.1) which is bounded by Lake Ontario to the north, Lake Erie in the west, the Adirondack Mountains in the east and the Appalachian Plateau to the south (Coates, 1976; Ridky and Bindschadler, 1990). A distinguishing feature of the drumlin field is its apparent genetic relationship (discussed in detail below) to the series of elongate lakes that comprise the Finger Lakes region south of the Onondaga Escarpment (Fig. 1.1). The southern boundary of the Finger Lakes Region is marked by the Valley Heads moraine complex. The maximum advance of the Late Wisconsinan Laurentide Ice Sheet in this region is the terminal moraine in northern Pennsylvania (Muller and Caulkin, 1993). Source rocks for the unnamed diamicton comprise > 85% red and green Upper Ordovician and Lower Silurian sandstones, shales and siltstones of the Queenston Formation (Fig. 1.1) which extend outward into the Ontario basin (Holmes, 1952), whilst the remainder are derived from unidentified

Precambrian rocks.

1.2.1 Valley Heads Moraine Complex

The Valley Heads Moraine complex is topographically controlled by the Allegheny Escarpment, the northern limit of the Appalachian Plateau. Ice probably began to retreat from the Valley Heads moraine by 14 000 BP (Muller and Calkin, 1993). These ages are consistent with isotopic data for the rapid melting of the Laurentide Ice Sheet between 13 000-14 000 yr. B.P. (Ruddiman, 1987). The Valley Heads is not viewed as a single moraine, but rather as a complex belt of ridges representing a series of ice re-advances that were unable to advance beyond the regional divide south of the Finger Lakes region (Muller, 1965; Mickelson *et al.*, 1983; Bloom, 1986). However, the nature, number and extent of the ice re-advances following the Erie Interstade have not been established (Fullerton, 1986).

1.3 Glacial Setting

The interpretation of Late Wisconsinan glacial deposits and associated landforms in New York State is essential to the understanding of the subglacial conditions of the southern margin of the Ontario Lobe (Mayewski *et al.*, 1981). The Ontario Lobe, which has been further subdivided into the Finger Lakes, Oneida and Black River sub-lobes (Coates, 1976; Fullerton, 1980; Mickelson *et al.*, 1983), represented a transition from a marine-based Laurentide Ice Sheet in the east to a terrestrial-based ice sheet in the south (Mayewski *et al.*, 1981). The thickness of the locally derived till exceeds 50 m in some locations (Holmes, 1952; Moss and Ritter, 1962; Clayton, 1965; Mickelson *et al.*, 1983) and indicates the high intensity of glacial scouring in northern New York. However, the scarcity of radiometric ages from the deposits limited the establishment of a proper sequence of glacial events in northern New York State, despite the well preserved sedimentological record of Late Wisconsinan ice marginal fluctuations in the Erie-Ontario Lowlands (Fig. 1.1; Coates, 1976).

Meltwater channels occur throughout the New York drumlin field and are considered to be related to the Finger Lakes (Mullins and Hinchey, 1989). These elongate lakes are cut into Devonian limestone and shale and radiate outward from the Lake Ontario shoreline in a fashion similar to the drumlin field (Fullerton, 1986). A possible explanation for the lakes is that they represent part of a Late Wisconsinan subglacial drainage system that formed during the collapse of the Laurentide Ice Sheet (Mullins and Hinchey, 1989).

1.3.1 Ice-Streaming

The Finger Lakes region and the Erie-Ontario Lowlands together form a topographic depression directly south of the deepest part of Lake Ontario that also coincides with the northern boundary of the New York drumlin field (Holmes, 1952; Clayton, 1965; Muller, 1965; Ridky and Bindschadler, 1990; Shaw and Gilbert, 1990). The suggestion that this depression was the focus of more rapid ice flow (Moss and Ritter, 1962) or rather of a Late Wisconsinan ice stream (Mullins and Hinchey, 1989) is consistent with current views regarding the nature of Laurentide Ice Sheet (Wright, 1973; Hughes, 1981; Boulton *et al.*, 1985; Hughes, 1987; Hicock, 1988; Dredge, 1988; Hicock *et al.*, 1989; Alley, 1991; Hicock and Dreimanis, 1992).

Ice streams have been described as zones of ice within an ice sheet that flow more rapidly than, but not necessarily in the same direction as the surrounding ice (Bentley, 1987). However, the distribution of ice streams within the Laurentide Ice Sheet need not have been controlled by areas of low relief, but rather by other factors such as subglacial water content and sediment type (Hughes, 1987; Clarke, 1987a; Hicock and Dreimanis, 1992). Deformation of a subglacial till layer in response to changing subglacial water pressures may be the principal component of ice stream movement (Blankenship *et al.*, 1987; Alley *et al.*, 1987; Hicock and Dreimanis, 1992). Hence, sediments having a low conductivity (i.e. diamicton)

would be conducive to rapid ice flow without the benefit of a depressed topography (Hicock and Dreimanis, 1992). However, due to rapidly changing subglacial conditions, water content would tend to fluctuate and therefore the presence of an interconnected series of low conductivity (i.e. easily deformable) sediments within a topographic depression would facilitate the formation of an ice stream.

Seismic and borehole data from the Finger Lakes region has revealed that the lakes are contained within deep bedrock scours infilled with large volumes of proglacial and subglacial sediment which tend to support the ice-streaming hypothesis (Mullins and Hinchey, 1989). Such an origin has been disputed by Ridky and Bindschadler (1990) who suggested that outlet glaciers, rather than ice streams in the Finger Lakes depression could have produced the same features. However, the New York drumlin field, which lies north of this region, could be analogous to the ridges parallel to the ice flow direction beneath Ice Stream B in the Antarctic (Rooney *et al.*, 1987) and would therefore appear to support the ice streaming hypothesis. Similarly, short-lived ice streaming activity has also been suggested as the origin for the Peterborough drumlin field by Boyce and Eyles (1991).

1.3.2 New York Drumlin Field

The New York Drumlin field (Fig. 1.1) may represent the geomorphic expression of a subglacially deforming till layer (*sensu* Boyce and Eyles, 1991). The mean orientation of the field is 353° (Francek, 1991) with the long axes of the drumlins forming a southward pattern splaying outward from Lake Ontario over a 12 000 km^2 area. This is consistent with ice flowing from the centre of the lake onto a less confined lowland (Miller, 1972; Mickelson *et al.*, 1983; Ridky and Bindschadler, 1989). Similar splayed patterns of ice flow have also been observed in modern ice streams (Hicock *et al.*, 1989). Such a pattern could reflect changes in subglacial conditions beneath ice sheets (Vernon, 1966; Sugden, 1977) or even

flow conditions beneath the marginal areas of ice sheets (Boulton, 1987). Muller (1963), Shaw and Gilbert (1990), and Francek (1991) believed that given the uniformity of the pattern, the field represented a single drumlinisation episode during which the flow lines remained constant. This uniformity has also been interpreted as the result of a period of stable active flow at the ice margin position, during the most recent glacial maximum (Ridky and Bindschadler, 1990). It should be noted that drumlin orientations in the Finger Lakes region do not follow the overall trend and may, in fact, reflect the change in basal shear stress that occurred when the ice encountered the Allegheny Plateau (Ridky and Bindschadler, 1990; Francek, 1991).

1.4 Drumlinisation Processes

The processes involved in drumlinisation are the subject of much debate (Menzies, 1987) and are centred around two very different theories involving either a deforming basal till layer (Boulton, 1987; Menzies, 1987) or a catastrophic subglacial meltwater flood event (Shaw, 1983; Shaw et al, 1987; Dardis et al., 1987; Shaw *et al.* 1989). Mickelson *et al.* (1983) and Shaw and Gilbert (1990) suggested a subglacial catastrophic flood origin for the drumlins in northern New York State, whilst Fairchild (1907) and Slater (1929) proposed a "constructional" origin involving basal obstructions to ice flow. Menzies and Woodward (1993) invoked a complexly deforming subglacial till layer to explain the origin of the drumlin at Chimney Bluffs. Whether drumlins are of a polygenetic origin or represent a single erosional episode, it is expected that certain properties associated with these processes would be preserved in the sediment record (Hicock and Dreimanis, 1992). The occurrence of stratified sediments, and even their sedimentary characteristics, which until recently have been overlooked (Hanvey, 1987), should therefore be explained in terms of the drumlinisation process(es).

1.4.1 Drumlin Stratification

The distribution of stratified sequences within the New York drumlin field is far from uniform (Fairchild, 1907; Slater, 1929; Gravenor, 1953), ranging from "lenses" within a diamicton matrix, to drumlin cores, to the lee-side of drumlins and to the bulk of a drumlinised landform (Muller, 1974; Whittecar and Mickelson, 1979; Hanvey, 1987; Shaw *et al.*, 1989; Menzies, 1990). The degree of stratification within drumlins may reflect the rate of ice advance (i.e., little stratification develops with rapid advance; McCabe and Dardis, 1989), but is not necessarily related to drumlin morphology (Hanvey, 1987; Shaw *et al.*, 1989). Stratified units have been found in "classical" drumlins (i.e., blunt up-ice end and tapered down-ice end), "megadrumlins" (drumlin clusters), and parabolic and brachanoidal drumlins as well as in ice-marginal flutes (Paul and Evans, 1974; Dardis and McCabe, 1983; Shaw, 1983; Sharpe, 1987; Hanvey, 1987). Several theories exist for the internal stratification of drumlins. Until recently, stratification within drumlins was generally attributed to the streamlining or moulding of pre-existing proglacial lake and/or outwash or subaqueous glaciomarine deposits by overriding ice (Slater, 1929; Whittecar and Mickelson, 1979; McCabe and Dardis, 1989). Such a view is consistent with the occurrence of proglacial lakes and outwash plains that formed during glacial retreat along the southern margin of the Laurentide Ice Sheet (Mickelson *et al.*, 1983). It is therefore possible that the stratified drift found within New York drumlins originated from these proglacial deposits.

A mechanism was proposed by Whittecar and Mickelson (1979) for similar stratified deposits observed in drumlins in Wisconsin, in which repeated ice advances over proglacial outwash resulted in these "deformation" structures. These advances were considered to result in a thickening of the ice, which generated compressive flow conditions and hence more meltwater. The drumlin form is therefore the result of sediment accretion through subglacial

deposition and the subsequent compression and erosion by overriding ice. Recently, this theory was modified by Boyce and Eyles (1991) who proposed that drumlinisation occurred as the result of a deforming subglacial till layer overriding proglacial sediments in marginal areas. Such a layer may have been the principle component of movement for ice streaming. Hence, within the context of ice marginal areas of glacial lobes, drumlinisation and ice streaming processes are considered to be interrelated.

These deformational theories are summarised by Boulton (1987), who suggested that a deforming subglacial till layer, or even its interaction with subglacial cavity infill (discussed in detail later) and lodgement processes is the main source of drumlinisation. A similar origin has also been proposed for the Peterborough drumlin field north of Lake Ontario (Boyce and Eyles, 1991). According to Boulton (1987), lodgement is the process whereby movement of clasts in the basal zone of a glacier is inhibited due to the frictional drag exerted on them by an underlying rigid bed. Furthermore, there are three distinct subglacial deformational processes that could produce the drumlin landform. Local inhomogeneities in the deforming till layer related to zones containing more slowly deforming (i.e., more cohesive) sediment could provide nuclei for a mobile drumlin form in the first scenario. Secondly, pressure fluctuations caused by irregularities in the plane of décollement over which deforming sediment moves could provide the focus for a "static" drumlin. Lastly, relatively resistant (i.e., non-deforming) sediment masses within a deforming till layer could be isolated and hence form "erosional" drumlins.

The depositional processes that produced stratified sand, silt, clay and/or gravel lenses within drumlins are still the subject of much debate (Menzies, 1979; Shaw *et al.*, 1989). Clayton *et al.* (1989) argued that similar lenses within a till sheet were deposited by subglacial water flowing through intratill openings. Accordingly, it has been suggested by

Clayton *et al.* (1989) that in the absence of high strain structures, subglacial bed material likely flowed laterally into the drumlin form. In such an environment, associated fabric, flow structures and clastic dikes would be expected. Although the association of interconnected glacial troughs and ice-marginal meltwater drainage/"tunnel" channels with the drumlins of northern New York State (Tarr, 1905; Mickelson *et al.*; 1983; Bloom, 1986) are supportive of the foregoing deformable bed (i.e., ice streaming) and the lateral flow models, drumlinisation could also be of a subglacial meltwater origin.

1.4.2 Subglacial Meltwater Origin

Mullins and Hinchey (1989) proposed that these "tunnel" channels were genetically related to the drumlins and were indicative of Late Wisconsinan ice-streaming. However, it should also be noted that such channels provide another possible explanation for the origin of stratified drift within drumlins (Paul and Evans, 1974; Dardis and McCabe, 1983; Hanvey; 1987; Sharpe, 1987; Hanvey, 1989; Mooers, 1989). The actual drumlinisation process, according to the channel hypothesis, is thought to occur beneath the ice margin in response to constantly changing subglacial pressure zones (Vernon, 1966; Paul and Evans, 1974; Dyson, 1952). Streamlining of the tunnel deposits is considered to occur after deposition (Paul and Evans, 1974; Dardis and McCabe, 1983; Hanvey, 1989). Shaw and Gilbert (1990); however, proposed that these tunnels were evidence of a catastrophic meltwater flood, or rather an erosional drumlinisation episode.

Similar "anastomosing" channel systems have been identified in other drumlin fields (Whittecar and Mickelson, 1979; Dardis and McCabe, 1983; Grube, 1983; Sharpe, 1987) and have been likened by Shaw *et al.* (1989) to subglacial tunnel valleys associated with a catastrophic meltwater flooding episode. The association of such tunnel systems with ice-marginal flute formation in a modern glacial environment has already been demonstrated

(Paul and Evans, 1974), and the suggestion by Mickelson *et al.*(1983) that frozen bed conditions (i.e., an impermeable substrate) existed underneath the Ontario Lobe in the Late Wisconsinan appear to support the catastrophic flood hypothesis. In this model, drumlins are thought to be "erosional" marks formed at ice margins in response to an enormous subglacial meltwater discharge (Shaw, 1983). Therefore, each drumlin field is considered to represent a single discharge event (i.e., drumlinisation episode). Shaw *et al.* (1989) suggested that thick stratified sand units within drumlins could have accumulated in a single flood event, either in a subglacial cavity or channel. Accordingly, the finer grained diamicton could represent the waning stages of the flood and/or normal drainage. A further explanation is that the sand units could represent secondary flooding episodes. However, a deforming basal till layer has been shown to exist under conditions similar to those proposed by Shaw *et al.* (1989) at the Urumqi glacier in China (Echelmeyer and Zhongxiang, 1987). Furthermore, the possibility that changing pore water content could lead to rapid ice marginal fluctuations (i.e., ice streaming) and to drumlinisation has been ignored by Shaw and Gilbert (1990) and inadequately explained by Mickelson *et al.* (1983).

An alternative to the catastrophic meltwater flood theory is the "sheetwash" model, as proposed by Dardis and McCabe (1987). This is essentially an accretionary model in which successive layers of sediment are built-up into the drumlin form under melt-out conditions. Thus, high-energy well-sorted stratified inter-till sand layers develop in response to periods of increased subglacial meltwater flow within a shallow water layer (i.e., sheetwashing). Oscillating high and low water discharges would therefore result in interlayered sand and diamicton layers within a drumlin form. Accordingly, if low discharge conditions were to prevail, multiple diamicton layers would produce an apparently homogeneous diamicton drumlin. However, both the Dardis and McCabe (1987) and the

Shaw *et al.* (1989) theories consider the drumlin landform to be the result of subglacial meltwater sheetwashing subglacial sediments.

CHAPTER 2: METHODS

2.0 General

A detailed sedimentological lithofacies study is integral to the re-evaluation of any depositional environment (Eyles *et al.*,1983). Accordingly, the micro- and macromorphological aspects of the sediments that form Chimney Bluffs are examined in order to better characterise the depositional and post-depositional history of the drumlin. Micromorphological analyses, which until recently were the focus of fabric and mineral analysis of soils, have been successfully applied to the study of glacial sediments. They provide a useful tool for the determination of penecontemporaneous and post-depositional processes (Meer, 1987; Meer and Laban, 1990; Menzies and Maltman, 1992).

2.1 Field Work

Prior to the commencement of field work, a series of photographs of Chimney Bluffs was taken from a boat on Lake Ontario to assist in choosing appropriate sample sites. However, sampling methods based on Menzies (1987a) were somewhat hampered by the dangerous nature of the bluffs, resulting in a lack of complete vertical stratigraphic sections. In general, gently sloping vegetated areas were avoided, and readily accessible near-vertical freshly exposed areas were favoured.

Active slumping and sliding, especially after rainstorms, were responsible for the majority of these fresh exposures. However, during the course of the study, several large sections of the bluff-forming diamicton, some up to 15 m^2 in areal extent, were observed to collapse in the absence of rain. Thus, on the more dangerous and sometimes heavily fissured vertical slopes, only photographs were taken. Interpretations of the latter sites are therefore made on the basis of neighbouring and more accessible ones.

At each site, the outer 50 cm of bluff sediment was cleared away to reveal a fresh

surface. Bulk sediment samples were then collected for grain size analysis and their dry colour was determined using the Munsell Soil Colour Charts. The roundness, long axis orientation and basic lithology of the clasts within the diamicton were also noted in addition to any observable macrostructures. Wherever fissility was observed, careful inspection was required to determine whether it was of a primary origin or simply the product of post-depositional slumping. This determination was made by rejecting fissures that essentially mimicked the vertical slope angle of a bluff face. Because of the thinness and the near vertical nature of the transverse north-south bluff ridges, it was assumed that the majority of the original fissures had been over-printed by those related to the gravitationally-induced stresses presaging a slumping episode. This assumption was dramatically reinforced by the observed collapse of a 10 m^2 section along a previously examined near-vertical fissure. Similarly, fissility may have been over-printed by near-vertical stress fissures in the easternmost section of the bluffs. At sites where the fissility was determined to be of a primary origin, twenty strike and dip fissure measurements were made within a 1 m^2 area as per the method described by Kazi and Knill (1973) and McGown and Radwan (1974).

2.2 Sampling Methods

Samples of diamicton and sand and clay lenses were also taken at several sites using the Kubiëna box method as outlined by Kemp (1985) and Meer (1993). Together with the standard-sized aluminium Kubiëna box (8 x 6 x 4 cm), a larger (15 x 8 x 5 cm) box was also used. The open-ended boxes were cut into the bluff faces with a knife following the removal of 50 cm of surficial material. Occasionally, in areas where the diamicton was strongly compacted, a hammer and a block of wood were used to imbed the sample box. The sediment around the box was then scraped away and a lid was placed on the exposed end. A Brunton compass was used to measure the orientation of the box sample. Photographs of

the bluffs were then used to determine the elevation and location of each sample site.

2.3 Sample Processing

2.3.1 Grain Size Analysis

Bulk sediment samples were processed using a combination of the hydrometer methods as outlined by Gee and Bauder (1986) and Menzies (1993). For the purposes of this study, the method was modified so that 100 ml of distilled water and 100 ml of a 50 $g \cdot l^{-1}$ solution of sodium hexametaphosphate (a dispersant) were added to each of three beakers containing approximately 40 g of a given sediment. The beakers were left overnight after which the samples were transferred to a metal dispersing cup and stirred at full speed for 5 minutes with a Hamilton-Beach mixer. The samples were subsequently transferred to a 1000 ml (@ 20 °C) glass cylinder and made up to the 1 litre mark with distilled water yielding a sediment concentration of 40 $g \cdot l^{-1}$ as recommended by Allen (1974).

A plunger was used to mix the suspensions and Bouyouces Scale ($g \cdot l^{-1}$) ASTM Soil Hydrometers 152H (Temp. 68 °F) were placed therein and left to equilibrate for 30 s. Specific gravity readings were taken at 30 sec., 1 min., 2min., 3 min., 5 min., 10 min., 30 min., 1 h., 1.5 h., 2 h., 3 h., 6 h. and 24 h. following their initial mixing. A "blank" or "control" hydrometer cylinder containing distilled water and 100 ml. of sodium hexametaphosphate was also monitored during this period. A thermometer was also placed in the control solution because temperature variations lead to thermal expansion (or contraction) of the meniscus and hence, inaccurate hydrometer readings (Allen, 1974). It should be noted, however, that Allen (1974) cited that errors from reading the top of rather than the bottom of the meniscus can be disregarded. For each set of three cylinders, hydrometers were left undisturbed for the initial 10 min. period, following which they were removed and slowly placed into the next set of cylinders. By using this technique, a total of

5 samples or 15 hydrometer cylinders were processed during a 24 hour period.

In order to separate out the sand fraction from the original 40 g sample, the sediment and suspension of each cylinder were then passed through a 53 µm (+ 4.25 ϕ) sieve, the contents of which were emptied onto an evaporating dish and oven dried at 105°C overnight. The oven dried sample, which weighed up to 20 g, was then weighed and transferred to a nest of US Standard Series brass frame, steel mesh Endecotts Ltd. sieves (- 4.0, - 3.5, - 3.0, - 2.5, - 2.0, - 1.5, - 1.0, - 0.5, 0.0, + 0.5, + 1.0, + 1.5, + 2.0, + 2.5, + 3.0, + 3.5, + 4.0, + 4.5 ϕ and pan) and shaken for 3 min. The contents of each sieve were then weighed using a Mettler Type PJ360 Delta Range scale.

Grain sizes were determined from the raw hydrometer data according to the procedure outlined by Gee and Bauder (1986), a summary of which can be found in Appendix I.

2.3.2 Thin Section Preparation

Thin sections were prepared by Dr. J. J. M. van der Meer at the University of Amsterdam according to the procedure as outlined by Kemp (1985) and Meer (1993). The rigid construction of the Kubiëna boxes in addition to cohesive clays in the sediment helped to maintain the integrity of the samples which were left to dry at room temperature for several months and subsequently shipped to the Netherlands where they were oven-dried at 40° C. Impregnation of the samples took place in a vacuum with Frencken Synolite type 544-A-3 resin, which had been thinned with monostyrene, catalysed by cyclonox LNC and accelerated with cobaltoctate (1 %). Pressurised (6 atm.) $N_{(g)}$ was used to facilitate the resin impregnation, following which the samples were left to harden over a 6 week period.

At Brock University, the boxes were removed from the hardened samples with a hacksaw, hammer and chisel. The samples were then cut parallel to their exposed end (see Sampling Methods) in addition to three separate cuts taken perpendicular to this plane with

a water diamond saw. Samples were then mounted on an object glass, 1 mm thick, and were subsequently ground to a thickness of 20 μm and covered with a 0.17 mm thick cover glass. Dimensions of the thin sections for the exposed end cuts were 5.0 x 7.5 cm, whilst those for the perpendicular planes were 2.5 x 4.5 cm. The larger thin sections proved to be invaluable to the study of microstructures within the collected samples.

2.4 Microscope Analysis

The thin sections were examined with a Leitz Labrolux 12 POL stereomicroscope using a X 4 objective lens. Composition, roundness (based on Powers, 1953), average grain size and modal distribution (visually estimated) of the skeleton grains (*sensu* Meer, 1987) were noted for each thin section. Similarly, plasma (*sensu* Brewer, 1976) composition, distribution and fabric in addition to microstructures (e.g. shears) and sediment boundaries were also described. Negative prints were made by placing individual thin sections into a photo enlarger whereupon their image was projected onto photographic print film which was subsequently developed. Photographs of notable microstructures contained in the thin sections were then taken with a WILD Photoautomat MPS 45/51 which was connected to a mounted 35 mm camera.

CHAPTER 3: FIELD OBSERVATIONS

3.0 General

The glacigenic sediments at Chimney Bluffs (see Fig. 3.1) can be divided into two major facies units comprising (i) massive sandy diamicton (unit A) containing many sand and sandy silt/clay units (Figs. 3.2a, b); and (ii) glaciolacustrine / glaciofluvial sediments comprising an overlying laterally continuous unit of stratified sands and gravels (Unit B), a discontinuous unit of intercalated sand and silt/clay rhythmites (subunit Bs), and rhythmically laminated silts and clays (subunit Br; Figs. 3.2a, b). The height of the drumlin increases from < 10 m at either end of the section to over 50 m in the central portion of the drumlin. Figure 3.1 was drafted using a style similar to that of Menzies (1990) and grain size classification in the following descriptions is based on the Wentworth scale (see appendix II). Stratigraphic sections 1, 2 and 7 on Figure 3.1 represent complete sections, whereas 3, 4, 5, and 6 are composite sections based on data from similar elevations, but not always from the same transect. Such a method was necessary due to the nature of the bluffs. Complete site descriptions are contained in appendix II. Arrows on plates indicate described features.

3.1 Facies Descriptions

3.1.1 Diamicton Slump Facies

At the base of the diamicton is a 2 - 5 m thick laterally continuous zone of slumped diamicton sediment (Fig. 3.1). The sequence comprises sub-horizontal and occasionally convolute light grey (10YR7/2) sand, grey (10YR6/1) sandy silt and pinkish grey (7.5YR6/2) sandy diamicton strata (Plate 3.1). Boudinaged or fragmented sandy silt layers which in some cases are observed to wrap around large clasts and deformed sand lenses are also present. Soft sediment deformation structures are visible on the eastern flank of the drumlin form where folded convolute medium and coarse sand layers (Plate 3.2) are contained in a flow

CHIMNEY BLUFFS

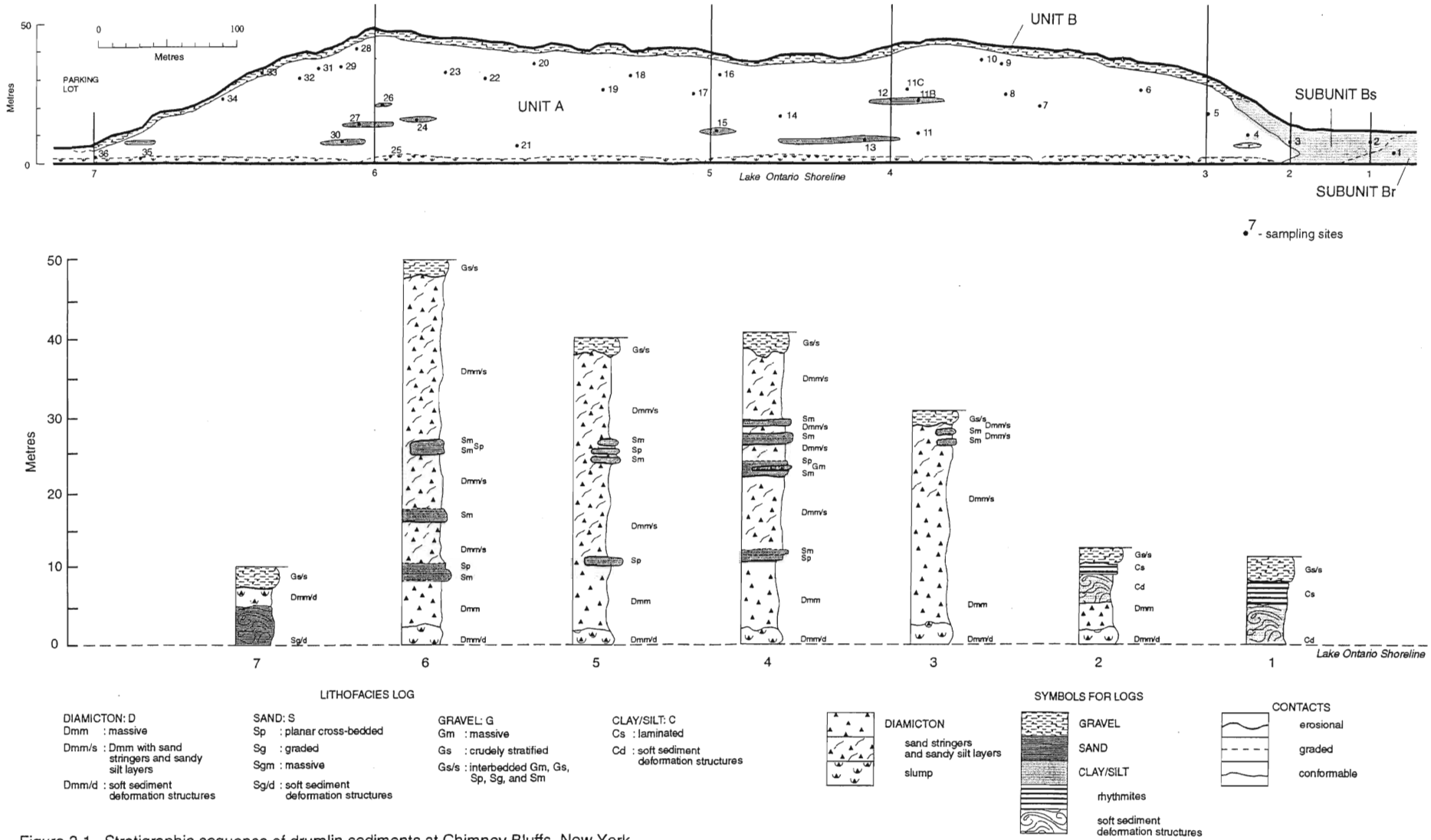

Figure 3.1 Stratigraphic sequence of drumlin sediments at Chimney Bluffs, New York.

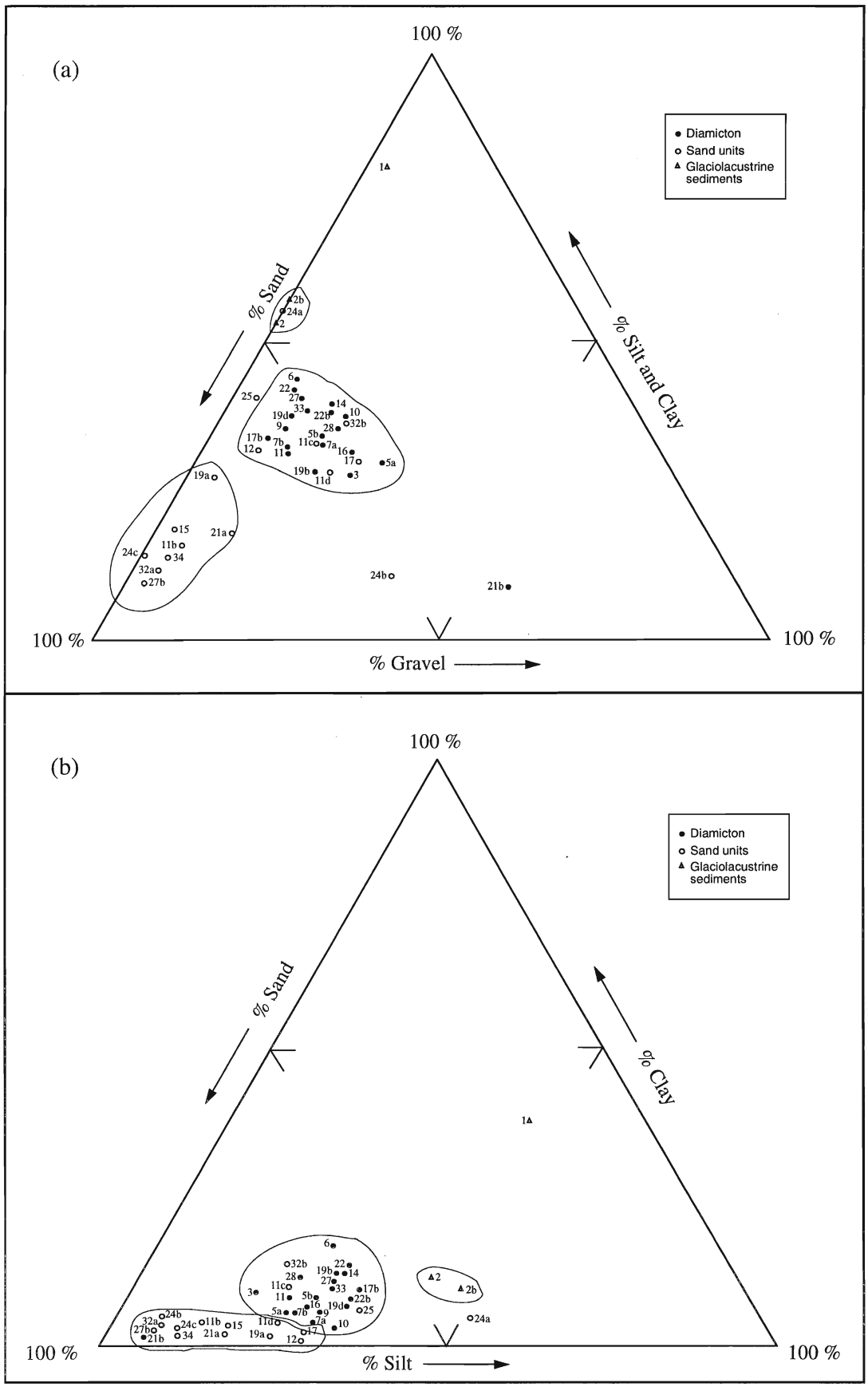

Figure 3.2 Grain size distribution data for sand, gravel and silt/clay fractions (a) and (b) sand, silt and clay fractions (see Tables 3.1 a, b {Appendix II} for numerical data).

Plate 3.1 Sand and clay layers within diamicton in beach level slump at *site 5* (note: trowel is approximately 25 cm long).

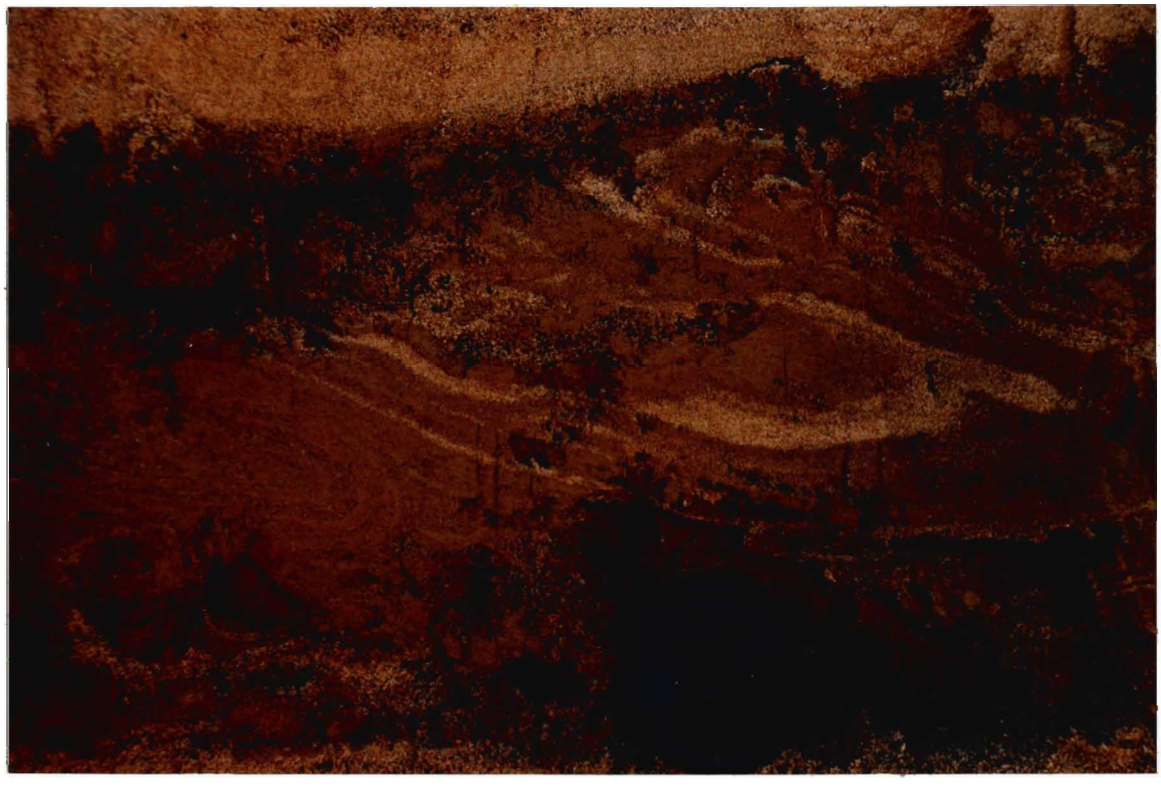

Plate 3.2 Folded sand layers in diamicton slump at *site 36*.

nose of diamicton. The slump facies at the western flank is characterised by a flow of pinkish grey (7.5YR6/2; 5YR6/2; 5YR7/2), very pale brown (10YR7/3), light brown (7.5YR6/4) and light yellowish brown (10YR6/4) banded massive sandy diamicton with grey (10YR6/1) sandy silt layers (unit A) and coarse sand lenses into the adjacent highly convoluted light grey (10YR7/1) glaciolacustrine rhythmites of subunit Bs (Plate 3.3; Fig. 3.1). The upper slump contact along the base of the drumlin is sharp and irregular with the overlying diamicton mélange.

3.1.2 Diamicton-Sand Intraclast Mélange Facies (unit A)

The matrix-supported sandy diamicton is massive, but possesses a pervasive sub-horizontal fissility that varies from weak- to well-defined (Plate 3.4). The fissility does not appear to cross-cut the various sand bodies and sandy silt layers contained within the diamicton. Furthermore, this fissility could not have formed during the post-depositional consolidation of the drumlin because the stresses associated with this process could not have penetrated to the considerable depths (i.e., > 20 m) where fissuring was observed (Anderson, 1983). Pinkish grey (7.5YR6/2; 5YR6/2; 5YR7/2), very pale brown (10YR7/3), light brown (7.5YR6/4) and light yellowish brown (10YR6/4) colour banding (Plate 3.5) is typical of the diamicton in this bluff-forming (Plate 3.6) unit. The very pale brown (10YR7/3) and the light yellowish brown (10YR6/4) bands tend to have a higher concentration of sand intraclasts and stringers (Plate 3.7) than the other diamicton bands. The term "intraclast" is taken from Menzies (1990) where it is defined as sediments incorporated into the diamicton that have an origin in the same depositional basin as the diamicton. Clasts throughout the banded diamicton range in size from pebbles to boulders up to 2 m in diameter and are generally angular to sub-rounded. They are derived from local Queenston Formation sandstones, siltstones and shales (> 85 %) and unidentified

Plate 3.3 Slump of diamicton into glaciolacustrine sediments at *site 3*.

Plate 3.4 Strongly fissile diamicton at *site 14* (note: hammer is approximately 30 cm long).

Plate 3.5 Colour banded diamicton at *site 7*.

Plate 3.6 Transverse bluff section at *site 29* (note: figure is approximately 1.8 m high).

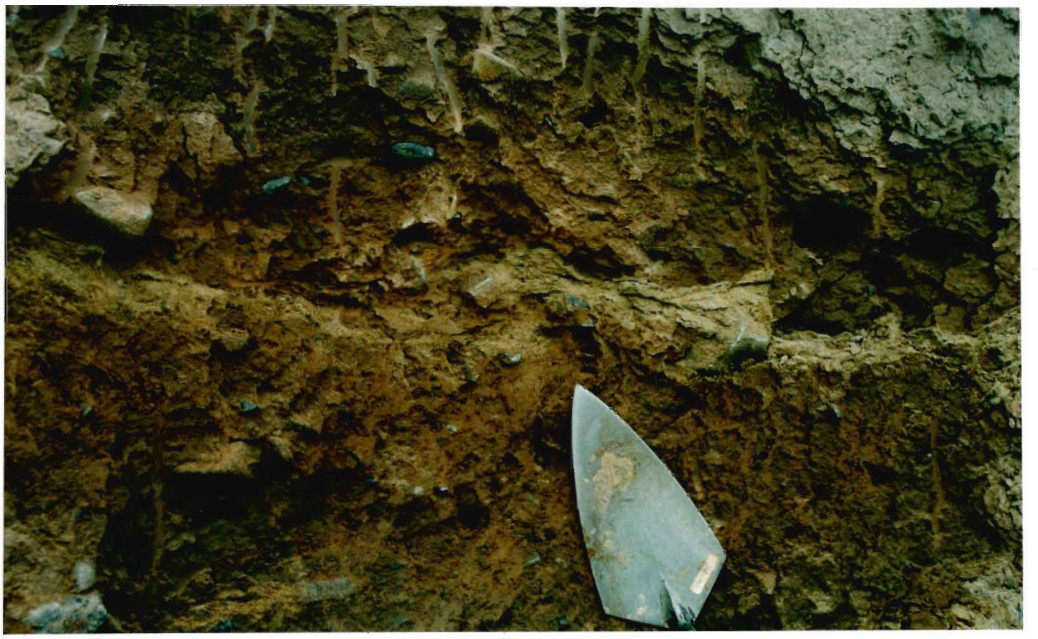

Plate 3.7 Folded sand stringer in fissile diamicton at *site 11C*.

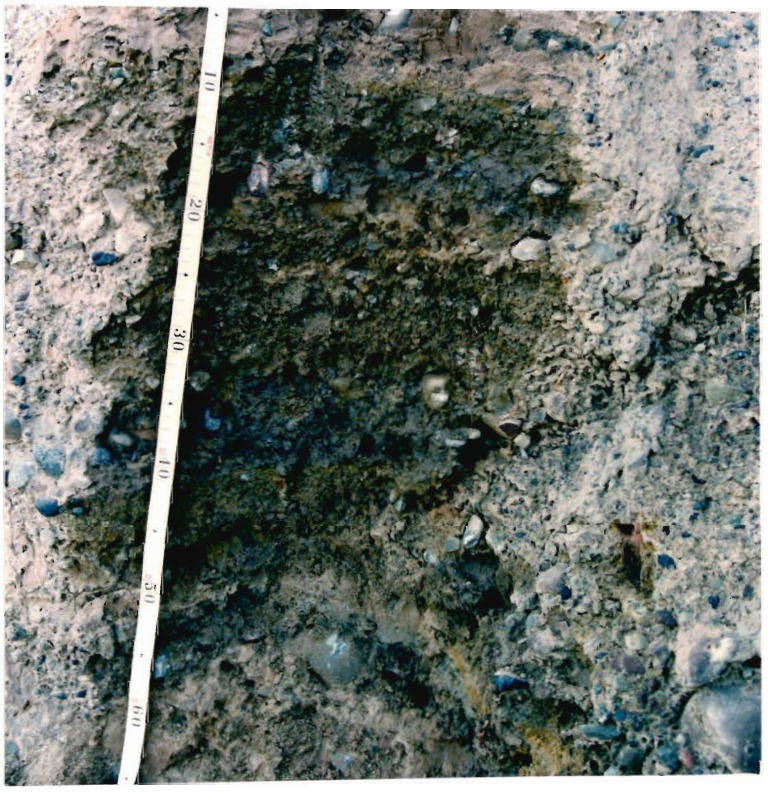

Plate 3.8 Crudely stratified gravel lens at *site 4*.

Precambrian rocks (< 15 %).

Sand intraclasts tend to be confined to, but not restricted to an approximately 20 m thick zone in the mid- (10 - 20 m high) vertical range of the drumlin (Fig. 3.1). Sand stringers and lenses are also ubiquitous within this range, but can also be found throughout the upper and lower reaches of the diamicton. Although the occurrence of lenses of well-sorted gravel has been noted by Menzies and Woodward (1993), only one such lens was found by the present writer (Plate 3.8). In general, the intraclasts and lenses have sharp contacts with the diamicton (Plate 3.9), although in some instances, contacts that were gradational over a short distance were observed (Plates 3.10; 3.11). The intraclasts range in thickness from 0.5 to over 2 m and in length from ten to tens of metres. Although their extension into the vertical bluff faces was difficult to determine, the intraclast at *site 11B* (Fig. 3.1) was found to extend for over 30 m into the diamicton. By this point, the same intraclast had narrowed to only 10 cm in thickness. Internal multi-directional shearing and micro-faulting of primary stratification were typical of the sand intraclasts (Plates 3.12; 3.13). Occasionally, fractures infilled with diamictic sediments were noted extending inward from the edge of an intraclast (Plate 3.14), but not outward into the surrounding diamicton. Grey (10YR6/1) sandy silt layers (Plate 3.15) have a similar distribution, but tend to thicken in the mid-vertical zone of the drumlin. The dominant sediments within the intraclasts and lenses are very fine to coarse sand (Plates 3.10; 3:13). Vague cross-bedding and normally graded fining up sequences within several of the intraclasts are indicative of fluctuating flow conditions and imply that the units have not been rotated (Plates 3.10; 3.13); however, some sand blocks had obviously been rotated (Plate 3.16). Intercalated sand and clay layers are also suggestive of variable flow conditions. The slightly distorted layers in Plate 3.10 were also typical of several of the intraclasts. Sand intraclasts varied from saucer-shaped (Plate

Plate 3.9 Saucer-shaped sand intraclasts in diamicton approximately 10 m above *site 11B* (note: shovel is approximately 1 m long).

Plate 3.10 Intercalated fine sand and clay layers within a sand intraclast at *site 13*. (note: vague cross-beds marked by heavy mineral separation in central sand layer).

Plate 3.11 Sharp upper and gradational lower contacts of sand intraclast at *site 11B*.

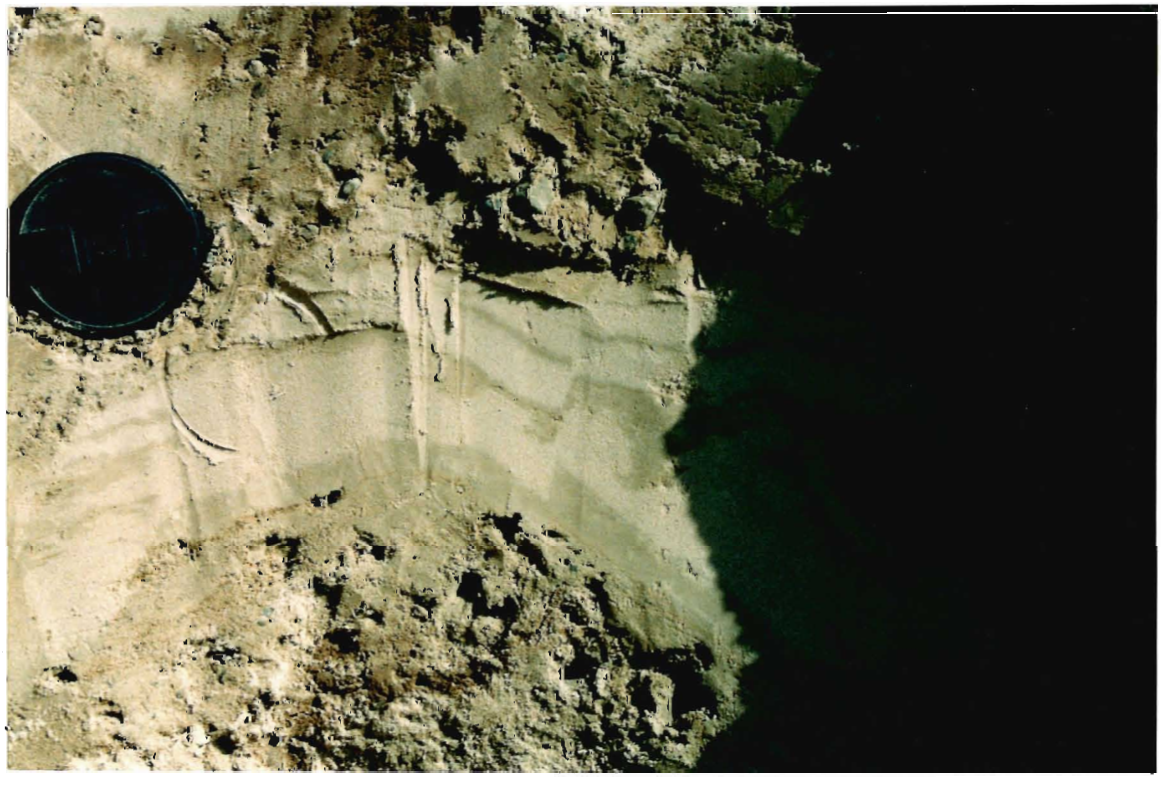

Plate 3.12 Micro-shears and irregularly shaped sheared dark clay lens in clay-rich layer within sand intraclast at *site 13*.

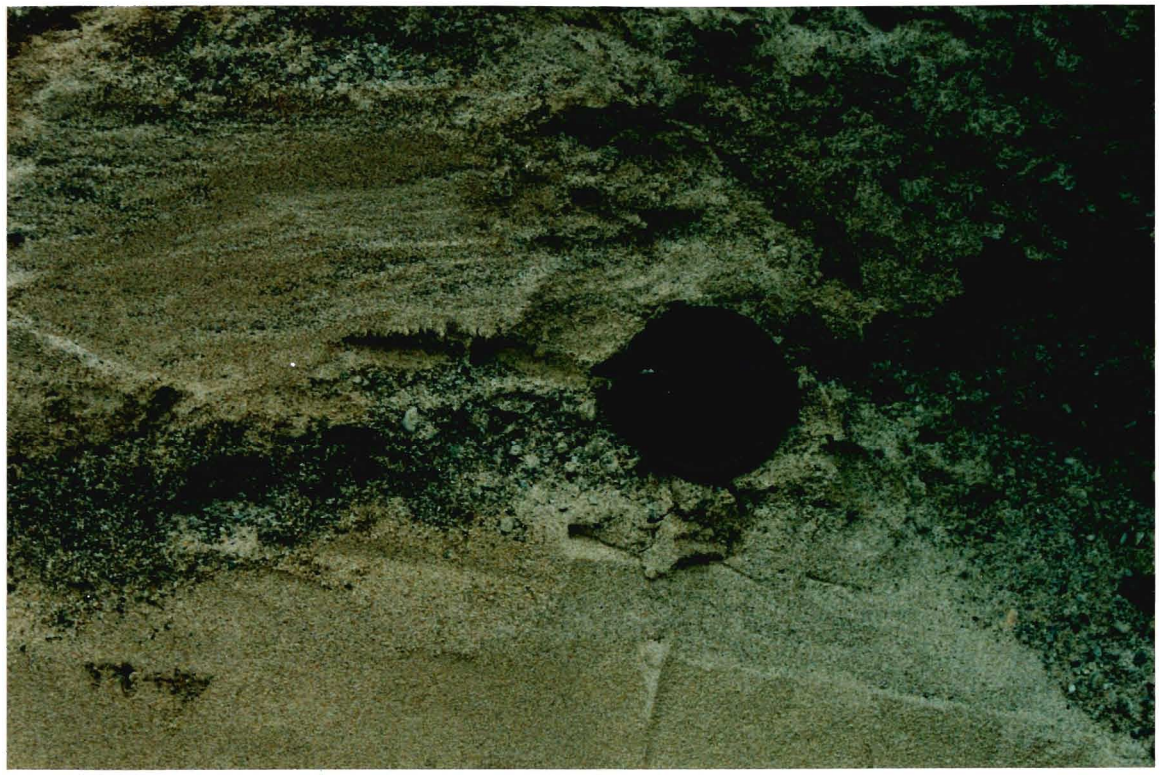

Plate 3.13 Detail of coarse sand lens within sheared fine sand layers. Note the silt-infilled fissures.

Plate 3.14 Diamicton infilled fissure (top right to centre left) in intraclast at *site 24*.

Plate 3.15 Folded sand silt layer in fissile diamicton at *site 22* (note: canine figure is approximately 46 cm long).

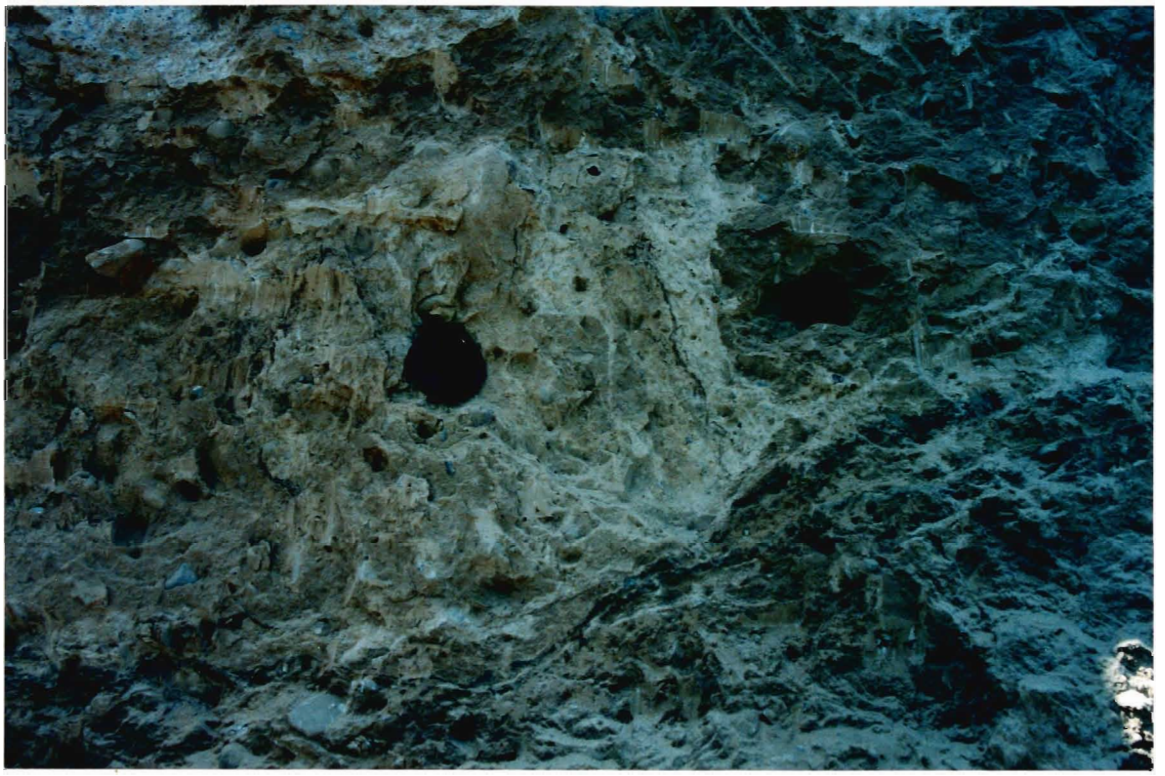

Plate 3.16 Triangular block of sand within diamicton at *site 17*.

3.9) to boudins (Plate 3.17) to more tabular forms. The smaller sand lenses tended to be more streamlined (Plate 3.18) and "wispy" (Plate 3.19) than the intraclasts. The grossly lenticular morphology of these sand units within the diamicton is consistent with the type III block-in-matrix mélange as described by Cowan (1985).

3.1.3 Glaciolacustrine Facies (unit B; subunits Br, Bs)

3.1.4 Reworked Glacigenic Sediments (unit B)

Matrix-supported imbricate gravels ranging in size from pebbles to cobbles are intercalated with light yellowish brown (10YR6/4) very fine- to coarse-grained massive and locally stratified sands in this unit (Plate 3.20). The sediments are restricted to a 1 - 2 m thick veneer at the top of the drumlin landform which has a sharp erosive contact with the underlying diamicton mélange (Fig. 3.1). Clasts are sub-angular to sub-rounded and appear to be similar in composition to those of the underlying diamicton (i.e., mostly local Queenston Formation sandstones, shales and siltstones and some unidentified Precambrian rocks). Occasionally discontinuous beds of vaguely cross-bedded sands are interdigitated with the poorly sorted gravels, but are predominantly preserved at the base of the sequence. Lenses of underlying diamicton have also been incorporated into the sediments near the underlying erosive contact of the sequence.

3.1.5 Rhythmites (subunit Br)

This subunit is exposed at the easternmost extent of the site and comprises light grey (10YR7/1) rhythmically laminated glaciolacustrine silts and clays and massive silts with individual laminae ranging up to 0.5 cm thick (Plate 3.21). Occasional massive beds up to 20 cm thick with no laminae are also present throughout the subunit. These fine grained sediments contain rare randomly oriented pebble-sized clasts. Most of the laminae are undisturbed; however, highly convoluted laminae, containing faulting and thrusting are

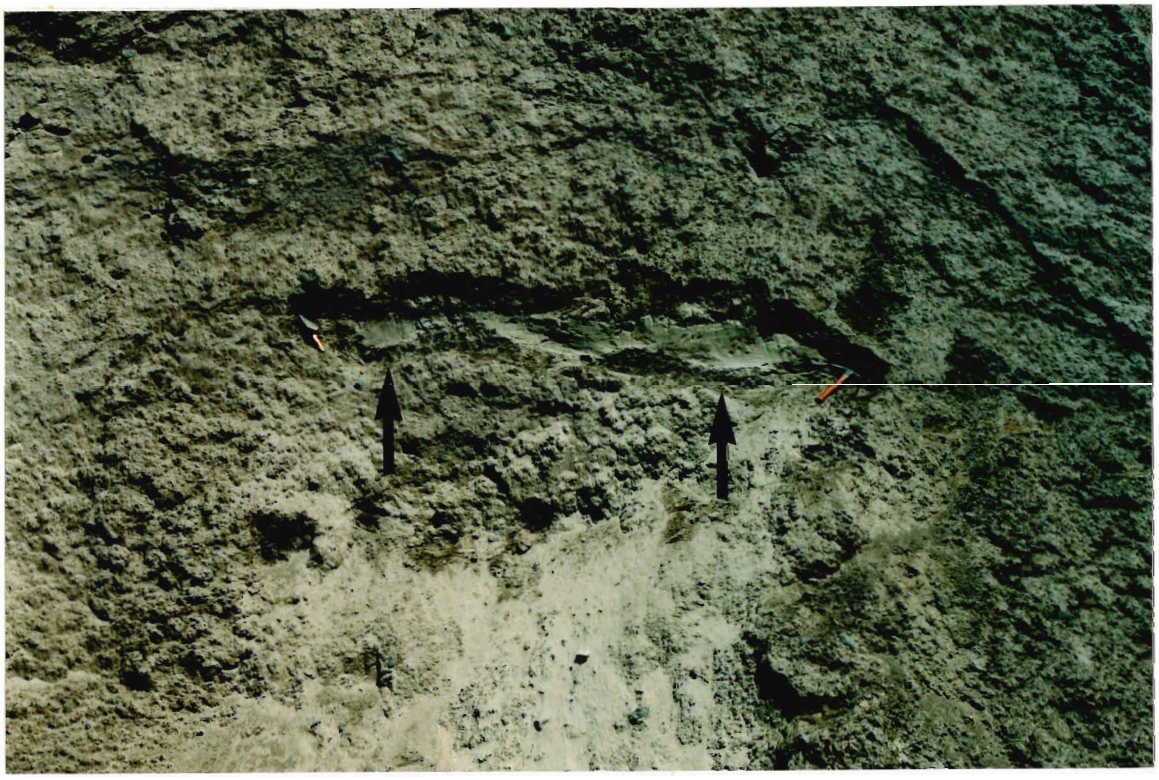

Plate 3.17 Two sand intraclast boudins in diamicton at *site 15*.

Plate 3.18 Streamlined sand lens in diamicton at *site 17*.

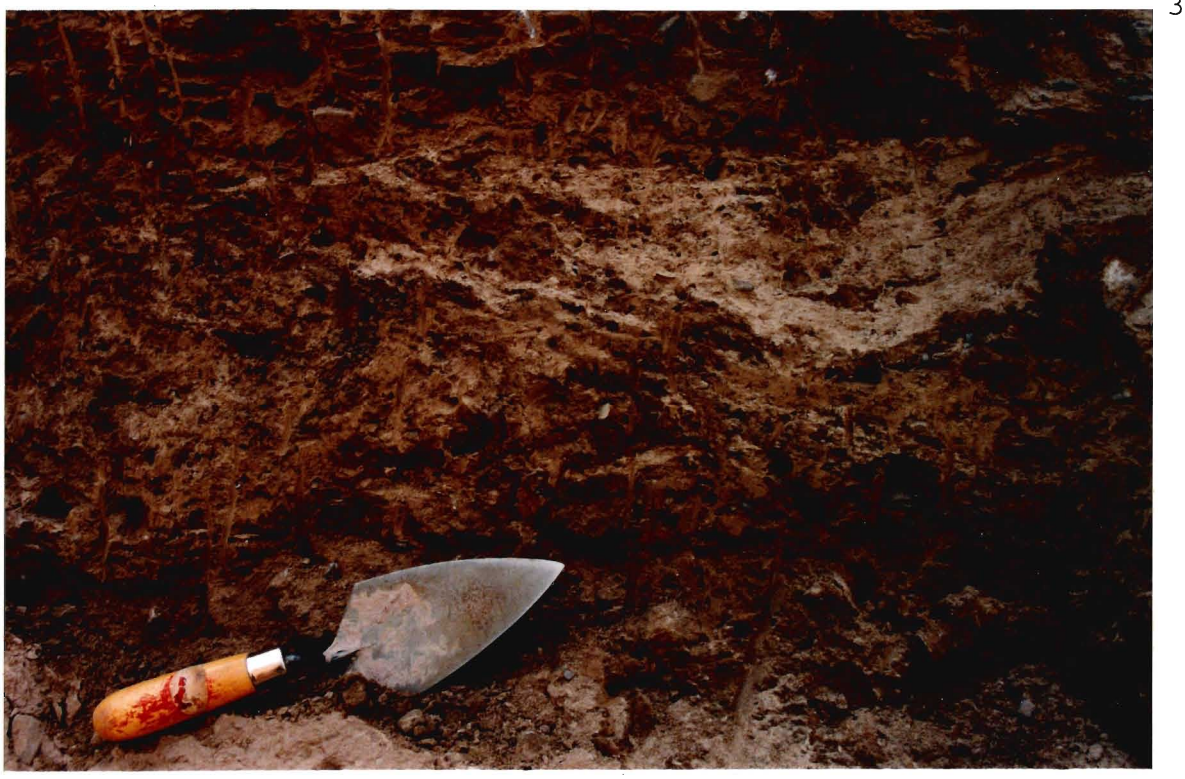

Plate 3.19 "Wispy" sand lens in diamicton at *site 17.*

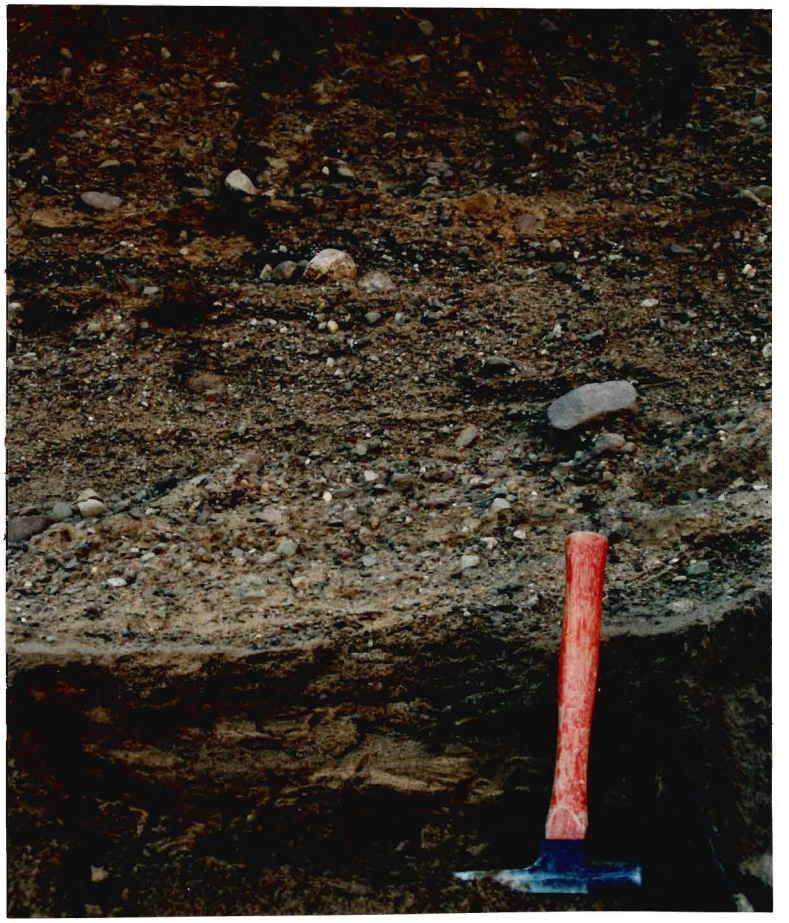

Plate 3.20 Sharp erosional contact between unit B and underlying diamicton at *site 33.*

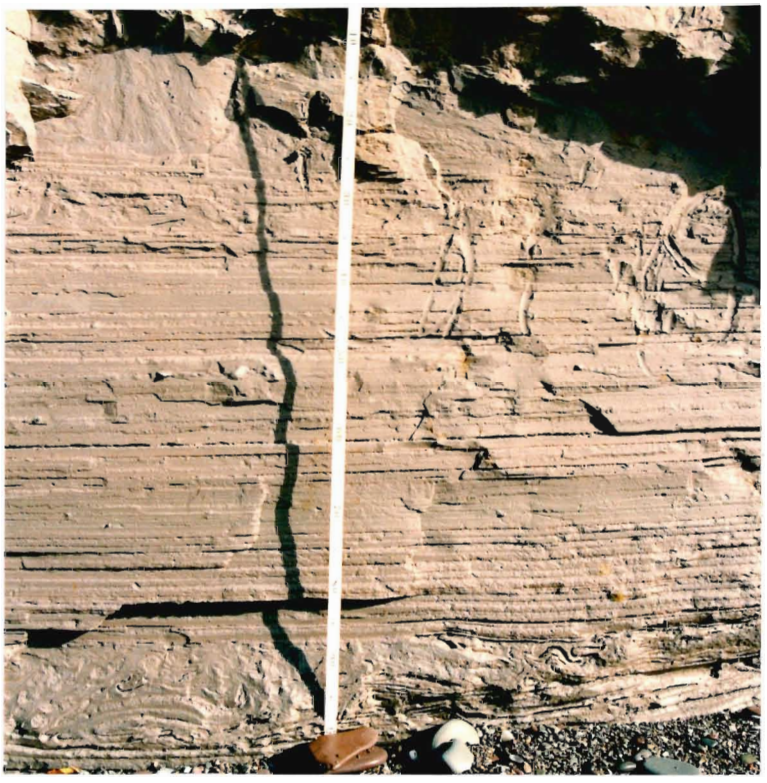

Plate 3.21 Rhythmically laminated glaciolacustrine silts and clays at *site 1*.

Plate 3.22 Silt and clay laminae intercalated with fine sands at *site 2*.

present within a 20 cm thick zone at the base of the sequence (i.e., beach level). The upper contact of this subunit is irregular and gradational over a short vertical distance and close examination reveals laminae crossing over into subunit Bs.

3.1.6 Laminated sands, silts and clays (subunit Bs)

The base of subunit Bs (Fig. 3.1) consists of a 2 m thick sequence of light grey (10YR7/1) rhythmically laminated glaciolacustrine silts and clays overlying a 0.5 m thick convoluted laminae unit. In some instances the tops of convoluted beds have been truncated by the overlying horizontal laminae, whilst faulting is quite common in the contorted beds. The upper sequence comprises silt and clay laminae intercalated with discontinuous laminae, stringers (up to 3 mm thick) and inclusions up to 0.5 cm thick consisting of very fine light yellowish brown (10YR6/4) sand (Plate 3.22). Alternatively, there are a few relatively thick beds (up to 10 cm) of massive silts and clays within the facies in addition to rare randomly oriented pebble-sized clasts. The lower contact of the subunit with the diamicton slump facies is sharp and irregular, whilst its upper contact with the sands and gravels of unit B is gradational over a very short distance.

3.2 Interpretation

The sediments at Chimney Bluffs appear to have been deposited by what Menzies (1990) called "a multistage process of derivation and deposition." Drumlin sediments at the present site can therefore be thought of as a mélange of sand units and diamicton. It is also evident, as will be soon discussed, that these sediments have clearly been deformed in a high shear environment during or quickly after their deposition.

The origin of the sands, sandy silts and gravels within the diamicton is of particular interest. Primary structures which occur within some of these sediments in addition to the overall banded nature of the diamicton may reflect pre-existing and/or penecomtemporaneous

depositional conditions. Consequently, the stratigraphic sequence at Chimney Bluffs could represent a mélange of glacigenic sediment derived from a single ice source and deposited through inter-related melt-out and flow processes (DeJong and Rappol, 1983). However, the absence of expected melt-out structures and the presence of attenuated sand lenses in the diamicton tend to suggest that these sediments are not strictly the result of melt-out or flow tills (Menzies, 1990; Hicock and Dreimanis, 1992). Instead, they probably reflect a deformation till (Boulton, 1987) or a soft bed till (Hart and Boulton, 1991) origin. A third possibility is that the drumlin sediments at the site represent a hybrid of lodgement, deforming and melt-out tills deposited in response to constantly changing subglacial pore water conditions (Hicock and Dreimanis, 1992). Characteristics of such a sediment would therefore be expected to reflect the interaction of erosional, depositional and deformational processes (Hart, 1994). However, Hart and Boulton (1991) noted that a highly deformed till may in fact be homogeneous, so that the primary fabric is obliterated; hence the massive diamicton at Chimney Bluffs may have undergone significant bulk strain. Due to the complex nature of unit A, the diamicton and sand units will be discussed separately.

3.2.1 Diamicton-Sand Intraclast Mélange Facies (unit A)

3.2.2 Diamicton

Proof that the diamicton may have been subjected to extremely high strain rates is therefore given by its lack of primary fabric and its apparently massive nature (Hart and Boulton, 1991). Pervasive fissility in the diamicton in addition to the occurrence of sand intraclasts, sand and clay boudins, streamlined sand and gravel lenses are inconsistent with both lodgement and subglacial melt-out flow processes (Menzies, 1990; Hicock and Dreimanis, 1992). Lodgement would be expected to produce more consistent fabrics including the long axes orientation of clasts pointing up ice (Dreimanis, 1989). Abundant

rounded clasts and strong parallel fabrics attributed to subglacial melt out tills (Shaw, 1979) are also absent. Instead a combination of brittle and ductile shear within the mid sheared zone (see Fig. 5.2 a) of a deforming till layer is thought to have generated these features. It is also possible that these features could be the product of a subaquatic facies that was deformed while its water content was still significant (Menzies, 1990). However, given the absence of macroscale dewatering and soft sediment deformation structures within the drumlin sediments, the latter is not very likely.

Finally, the contacts between the sand intraclasts and the diamicton range from sharp to gradational and may reflect the compact clayey nature of the diamicton. The "wispy" contacts of the highly deranged sand lenses and the sand stringers in the mid- to upper portion of the drumlin could reflect homogenisation of these units with the diamicton under super-saturated pore water conditions associated with a deforming till layer. Another possibility, is that this diamicton-sand stringer association could be interpreted as a crudely stratified diamicton sequence that accumulated as the result of melt-out and sediment flow interaction in a subglacial cavity (Shaw, 1983; Dardis and McCabe, 1983; Sharpe, 1987; Hanvey, 1987). It is expected that the morphology of such a deposit in addition to the long axis orientation of clasts would be conformable to the shape of the subglacial conduit wherein it formed. Since neither of these features are observed, a deforming till layer seems to be the most likely origin for the diamicton.

3.2.3 Sand Units

The following discussion will focus on the possible primary origin(s) of these sediments by first concentrating on the larger sand intraclasts. It is possible that the intraclasts, especially in the mid-vertical zone, are somehow related. Their internal stratification, namely intercalated coarse sand lenses/layers and vaguely cross-bedded sands

reflect a highly variable flow regime, possibly associated with or proglacial deposits (Allen, 1982; Menzies, 1990). The absence of clasts within these units further supports a proglacial origin for the sand units or may even reflect a deep-water subglacial conduit origin (Menzies, 1990). The latter also suggests that the lenticular sand bodies could have formed *in situ* during periods of fluctuating subglacial meltwater flow (Shaw, 1983, Sharpe, 1987; Clayton *et al.* 1989; McCabe, 1991), but this hypothesis may only be partly correct. The distribution of the sand intraclasts within the drumlin landform in addition to their morphology and internal structures strongly suggests that some translocation of the sand units has occurred following their deposition.

Several sand intraclasts at the site can be attributed to a subglacial origin. Saucer-shaped tablate sand bodies (Plate 3.9) could be analogous to the broad and low subglacial conduits described by Hooke *et al.* (1990) or even to the "till canals" proposed by Walder and Fowler (1994). Similar lenses of stratified sediment within a diamicton have also been attributed to subglacial conduit formation under effective pressures close to ice overburden pressure by Brown *et al.* (1987) and Eyles *et al.* (1982). Such pressures in addition to related subglacial melting during periods of low ice flow, basal drag and water movement over non-cohesive material could contribute to the overall conduit shape (i.e., broad and low; Hooke *et al.*, 1990). However, only low effective pressures were considered necessary by Walder and Fowler (1994) for the formation of a channelised subglacial meltwater flow over a deformable bed. Thus the sand units may be the vestiges of a complex subglacial drainage system involving interconnected cavities and incised braided "till canals" that existed beneath the Laurentide Ice Sheet which were subsequently abandoned and remobilised within a subglacial deforming till layer.

The sand intraclasts could reflect the confinement of water and sediment within a

subglacial till conduit (Hanvey, 1989; McCabe and Dardis, 1989; Menzies, 1990). Although poorly sorted sediments can be attributed to the highly concentrated sediment flows within a closed conduit (Saunderson, 1977), well-sorted cross-bedded sediments cannot (Hanvey, 1989; Menzies, 1990). However, enhanced differential settling in response to the fluctuating flow conditions attested to by intercalated clays, sands and coarse sand layers and lenses within the intraclasts is possible where subglacial conduits debouch into a glaciomarine/glaciolacustrine environment (Hanvey, 1989). Such deposits also reflect the episodic nature of subglacial meltwater discharge (Gustavson and Boothroyd, 1982; Hook *et al.*, 1985). The crudely stratified gravel lens located at the western edge of the drumlin section (Fig. 3.1) is also indicative of the highly variable discharges expected in such an environment (Hanvey, 1989). Similarly, high energy flows are implied by the inclusion of pellets derived from the diamicton surrounding the boundaries of several sand intraclasts and by the occurrence of massive sand layers within all of the intraclasts. These layers possibly reflect periods during which high concentrations of suspended particles prevented segregation of the sands based on particle size and settling velocities (Middleton and Southard, 1978). Finally, decreasing water depths within the conduits in response to dewatering processes could have resulted in the formation of conditions conducive to the generation of cross-beds (Hanvey, 1987).

However, all of these features can also be attributed to a proglacial origin for the sand intraclasts (Menzies, 1990). In this scenario, the sands would be derived from englacial and subglacial melt-out at the margin of a marine-based ice sheet. Such an origin would also imply that diamicton debris flows would be part of this sequence (DeJong and Rappol, 1983; Menzies, 1990) which would explain the presence of diamicton-derived inclusions in the intraclasts. However, the implication that the sediment pile at Chimney Bluffs is a melt-out

till is rather simplistic. The diamicton is characterised by features attributable to a deforming till origin and as will be shown, the internal structures of the intraclasts give credence to this hypothesis.

The infilled fractures and fissures traceable to the surrounding diamicton revealed in several of the sand intraclasts are similar to those described by Menzies (1990), attributed to external stresses applied during their transposition within a deforming till layer. Microfaulting and/or shearing of the primary stratification within the intraclasts are also indicative of the stresses associated with the viscous flow of such a deforming subglacial till layer (Menzies, 1990; Hart and Boulton, 1991; Hicock and Dreimanis, 1992). The attenuated and streamlined sand lenses (boudinaged structures) further support this hypothesis. Contorted intercalated sand and clay layers within the sand intraclasts may reflect a period of plastic deformation within a water saturated deforming bed (Menzies, 1990; Hicock and Dreimanis, 1992). It is possible that the saucer-shaped sand intraclasts reflect deformation under high strain rates (Hart and Boulton, 1991).

A distinguishing feature of several of the intraclasts is their gradational contacts with the diamicton. Such contacts tend to be intercalated sand layers and diamicton and although they can be attributed to the high energy flows expected in subglacial conduits (Hanvey, 1989), they could also reflect lateral shearing of the units within a deforming till layer. In some instances it appeared as if a portion of the intraclast had been "broken off" and tilted (Plate 3.16). Such a feature attests to the hypothesis that the sand intraclasts where transported in a deforming till layer subsequent to their up-ice deposition. Unlike the smaller sand lenses and stringers, the intraclasts tend be immiscible (i.e sharp boundary) with the diamicton. Furthermore, the preservation of primary structures within such a theoretical high strain environment is rather significant. The intraclasts may be the product of a subglacial

conduit/canal system, or possibly even the remnant of a former proglacial sand unit(s) that has been frozen by an overriding ice sheet and subsequently "plucked" and entrained by a deforming till layer (Menzies, 1990). Such a frozen sand unit would act as a cohesive substance and would be susceptible to brittle deformation (Owen 1987) especially under high strain rates (Ladanyi and Morel, 1990). However, Owen (1987) and Hicock and Dreimanis (1989) also noted that a saturated un-lithified sand unit could also act as a cohesive unit. Therefore, longitudinal shearing coupled with lateral shearing, during transposition of either a frozen or a saturated sand block, could have produced the internal shearing of the primary stratification within the sand intraclasts of the diamicton mélange at Chimney Bluffs. The similarity of the internal structures and thicknesses of the sand units within this zone is consistent with this theory.

The massive nature of the diamicton may be the product of very high rates of strain. This is also supported by the high degree of intermixing implied by "wispy" sand stringers and lenses within the diamicton. However, such homogenisation could also reflect saturated pore water conditions during which un-lithified sediments were remobilised along pressure induced fissures (Hicock and Dreimanis, 1992; Kumpulainen, 1994). It is further plausible that high strain rates and high pore water content are inter-related (Hicock and Dreimanis, 1992).

3.2.4 Sandy Silt Layers

The sandy silt layers have a number of possible origins. Their consistent sub-horizontal orientation could be indicative of a period of high subglacial pore water pressures during which subglacial waters forced their way along planes of weakness in the deforming diamicton in the manner described by Huntley and Broster (1993). In this scenario, lateral extensional and flow and stress fields associated with an advancing ice sheet (Boulton, 1987)

produce localised groundwater flow and deposition along shear planes. However, the till fabric or oriented clasts predicted by the Hunter and Broster (1993) glacigenic deformation model were not observed at the present site. Furthermore the distribution of the sandy silt layers appears to parallel that of the sand intraclasts by having a higher concentration in the mid-vertical zone of the drumlin and the observed cross-cutting of the sandy silt layers by sub-horizontal/vertical fissure planes appear to contradict such a scenario.

Similar layers have been attributed to sediments deposited by meltwater movement through intratill openings within a rigid debris and ice mixture (Clayton *et al.*, 1989). Accordingly, the presence of these layers is evidence against a deforming subglacial till layer. Intratill sand layers have also been ascribed to a melt-out origin by (Dardis and McCabe, 1987) who further stated that such layers do not occur in lodgement tills. However, Dardis and McCabe (1987) also suggested that deformed sand lenses are found exclusively in lodgement tills and hence the association of such lenses with the sandy silt layers at the present site appears to negate this hypothesis.

Another possibility is that these layers formed in sub-horizontal fissures that were opened in response to excessive hydrostatic pressures (Kumpulainen, 1994). According to this model, groundwater flow and sediment transport were initiated beneath a frozen (i.e., impermeable) crust in glacier-margin conditions. However, the somewhat contorted appearance of these layers implies that some ductile deformation has occurred. Therefore, it is suggested that these layers could have a similar history to the translocated sand units. However, if it is possible that these sediments, unlike the cohesive sand bodies, were not frozen or compacted to the same degree during transport, it would explain why they were plastically, rather than brittly deformed. The likelihood that these layers are simply part of the banded diamicton unit is improbable due to the absence of clasts and their sharp contacts

with the diamicton. The occurrence of fissility that passes through both the sandy silt layers and the diamicton, but not visibly through the sand intraclasts, imply that the sandy silt layers could pre-date intraclasts. Finally, in considering the distribution of the layers, it is apparent that they could have formed within a strained environment during the dewatering of the saturated diamicton as it started to immobilise.

Regardless of the primary origin of these layers, partially frozen, or at least saturated conditions during their transport are implied. Preservation of primary laminae within some of the larger layers in addition to the wrapping of some of the layers over and under large clasts within the diamicton appear to support this possibility. A remobilisation of sandy silts along shear planes developped in response to post-depositional consolidation is not favoured because the layering is too contorted and obviously unrelated to the near-vertical gravity-induced fissures observed at the site. The occurrence, albeit rare, of S-folded sandy silt layers within the mid-vertical to upper zones of the drumlin section is also consistent with partially cohesive transport within a soft deforming till layer (Hart and Boulton, 1991; Hicock and Dreimanis, 1992).

3.2.5 Glaciolacustrine Facies (unit B; subunits Br, Bs)

Due to the shoreline location of the drumlin, the stratified sands and gravels of unit B are interpreted as the product of high energy reworking of the underlying diamicton in the context of a rapidly falling wave base during a period of rapid isostatic rebound. Similar deposits on drumlin summits within the New York drumlin field have also been attributed to near-shore wave erosion in addition to stratified deposits in wave cut notches on the flanks of drumlins situated on former Lake Iroquois shorelines (Fairchild, 1907; Gillette, 1940; Francek, 1991). The sharp erosional contact with the underlying diamicton mélange (Fig. 3.1) implies that the depositional history of this unit is distinct from the drumlinisation

process. However, it could be argued that this facies reflects the waning stages of a subglacial meltwater flood event as discussed by Shaw *et al.* (1989). The presence of distal lacustrine facies (subunit Br) which grades rather abruptly into a more proximal lacustrine facies (subunit Bs) as evidenced by the increasing number of sand laminae appears to contradict such a flood event. Instead, these facies in conjunction with the reworked glacigenic veneer appear to support a fairly rapid uplift of the drumlin landform and its subsequent exposure to wave erosion.

CHAPTER 4: THIN SECTION OBSERVATIONS

4.0 Background

Although thin section observations are commonly used in pedology, they have rarely been applied to the study of glacigenic sediments (Mücher and Morozova, 1983). Pioneering work on microfabrics in till by Sitler and Chapman (1955) recognised the potential of such investigations to compliment the study of large scale till fabrics. Recently, Meer (1987) reaffirmed this potential by citing the usefulness of micromorphological observations in characterising till depositional environments and the post depositional changes that occurred within tills and related glacial deposits. Due to the paucity of published material on this subject (Meer, 1987), a standardised approach to the micromorphology of glacigenic sediments does not exist. For the purposes of the present study, the classification scheme outlined by Meer (1993) will be used to describe the thin sections made from the collected Kubiëna box samples. This scheme is based on the Brewer soil thin section classification system (1976) with additions from that of Baratt (1969).

Accordingly, nomenclature outlined by Brewer (1976) is used extensively in the following section. As this terminology is not ubiquitous to the various geological disciplines, a brief discussion of it is necessary. *Skeleton grains* are defined as individual mineral grains larger than the thickness of a thin section (approximately 20 μm), or rather those grains which were larger than plasma-sized particles. *Plasma* comprises all colloidal size (< 2 μm) material (clay minerals, oxides and hydroxides of Fe, AL, Mn, soluble salts, etc.) that is not bound up in skeleton grains. For the thin sections described in this chapter, plasma most commonly occurs as amorphous zones of indistinct reddish brown Fe-stained(?) particles under plane polarised light. Typically, with cross polars, unconsolidated clay-sized particles (plasma) have a "speckled" extinction pattern and similarly oriented plasma domains (plasmic

fabric) display a high birefringence (Meer, 1993). *Plasmic fabric* observed comprised *skelsepic* plasmic fabric, or rather the orientation of plasma particles around a skeleton grain and *argillasepic* plasmic fabric in which oriented clay-rich plasma particles occur as isolated patches amongst the skeleton grains. Finally, the term *argillan* is used to describe an accumulation of translocated clay minerals in pores, structural units or on the surfaces of skeleton grains (Meer, 1987).

The black and white plates are negative prints of the thin sections studied in this chapter. Colour plates are photographs of the thin sections taken with a X 4 objective lens (plate width approximately 3 mm) under plane polarised light, unless otherwise stated. Arrows indicate described features.

4.1 Thin Section Descriptions

Sample 93-CBB-1

The sample was taken from the contact zone of a possible slump of drumlin diamicton into the adjacent glaciolacustrine silts and clays approximately 5 m above the shoreline at *site 3*. Strike of the sample is 55° with a dip of 9°.

A. Macroscopic

The section can be divided into two zones based on texture and clast content (Plate 4.1). The lower zone comprises a diamicton with fine clay bands. Near the bottom edge of the photograph, elongate skeleton grains appear to be oriented parallel to the surface of the larger sandstone grains. Very thin "wavy" darker clay bands occur in the central portion of the lower zone and have a random distribution. The lighter colour of the upper portion of this zone is a grey (10YR6/1) sandy silt layer which has obviously thoroughly intermixed with the diamicton.

Poorly sorted coarse sands intermixed with diamictic inclusions and fine diamictic

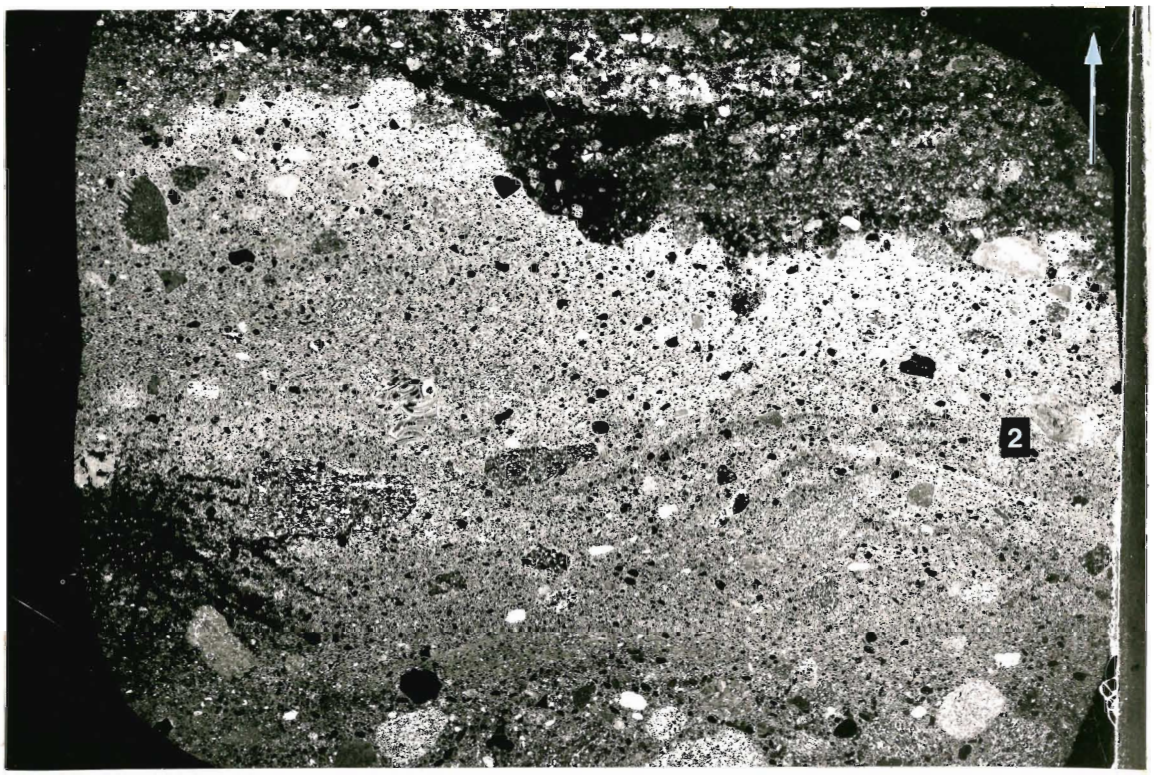

Plate 4.1 Sample 93-CBB-1 taken from contact zone of diamicton slump facies and the laminated sands, silts and clays of subunit Bs at *site 3*.

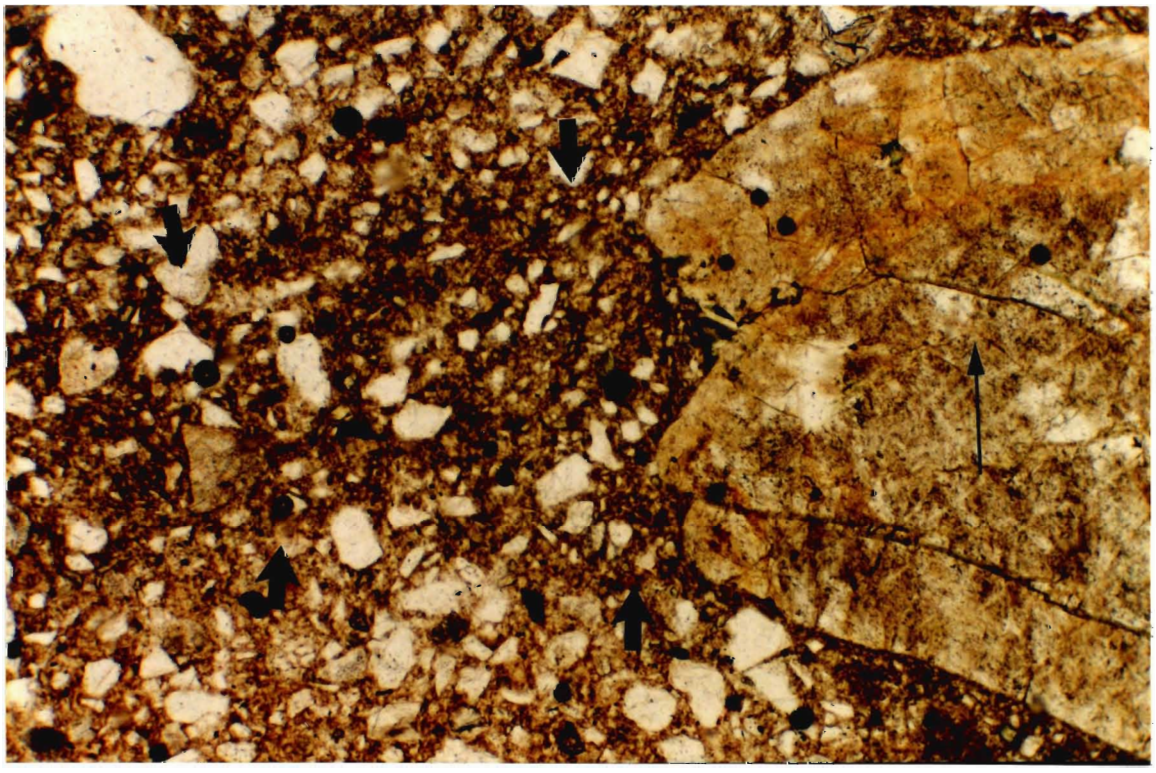

Plate 4.2 Detail of location 2 illustrated in Plate 4.1 showing clay-rich "tail" extending from limestone clast (left).

Plate 4.3 Sample 93-CBB-3 taken from sand lens in diamicton slump facies at *site 5*.

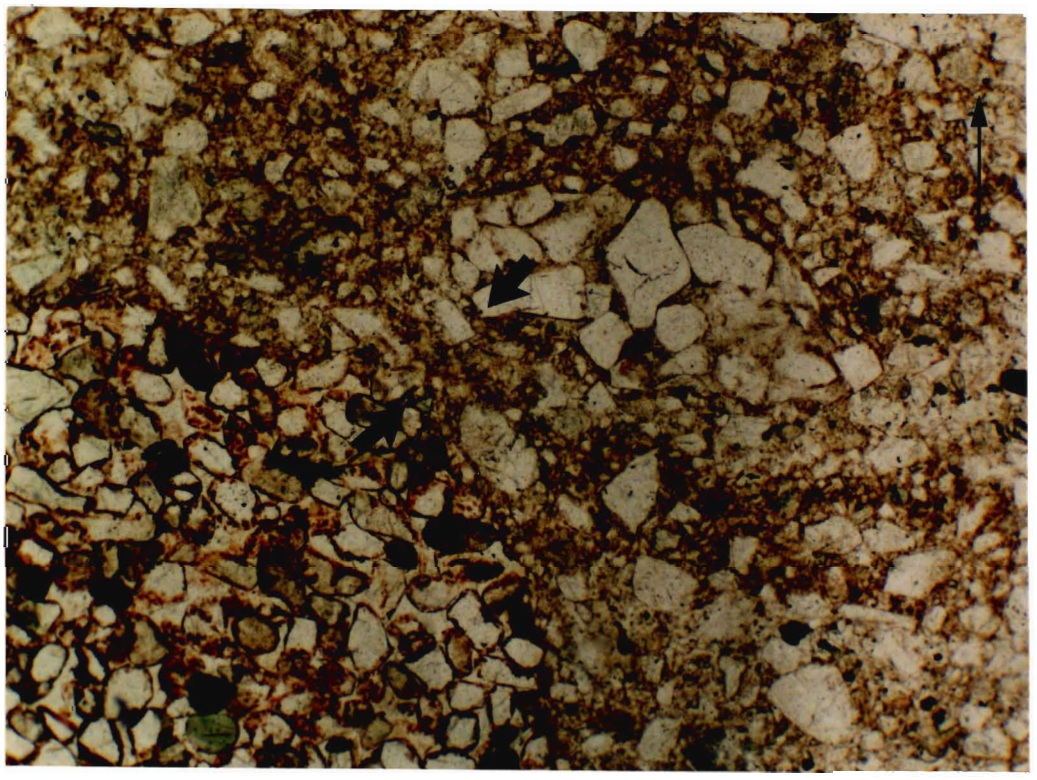

Plate 4.4 Detail of location 4 illustrated in Plate 4.3 showing deflection of clay-rich laminae around elongate sandstone clast (upper right) and necking of laminae between the same clast and the larger sandstone clast on the lower left.

bands comprise the upper zone. The coarse sands in this zone form crude laminae, which are similar to the "wavy" clay bands" in the lower diamicton. The boundary of the two zones is irregular and slightly gradational as demonstrated by the inter-fingering of the diamictic laminae and the coarse sands in the upper zone.

B. Microscopic

skeleton:

size: grains vary in size from < 50 µm to approximately 250 µm with a mode of approximately 150 µm in both zones.

shape: grains range from angular in the lower zone to rounded in the upper zone; larger grains (> 2 mm) tend to be rounded.

distribution: random throughout the sample.

composition: mainly quartz; some plagioclase, chlorite, and clinopyroxene; the larger grains tend to be sandstone and fossiliferous limestone.

plasma: mostly homogenous clays in the lower zone and finely laminated clay bands in the upper zone.

structure: clay bands in diamicton tend to wrap over and under larger clasts. "Tails" or plasma rich bands of skeleton grains are observed at one end of some elongate clasts throughout the diamicton (Plate 4.2). Secondary mineralisation forming a diffuse ring of carbonates around several limestone clasts is also apparent in addition to casings of skeleton grains. Occasional flow structures comprising re-mobilised plasma within diamictic pellets similar to the one illustrated in Plate 4.24 are also observed.

aggregates: reddish-brown Fe-staining(?) is texturally restricted to the diamicton in the lower zone and the diamictic bands in the upper zone.

plasmic fabric: weakly-developped skelsepic fabric.

C. Interpretation

The casings of skeleton grains oriented parallel to the surface of larger grains and the weakly-developped skelsepic plasmic fabric can be ascribed to the rotational and/or differential movement of these particles in response to pressure (Meer, 1987; Meer and Laban, 1990) and are indicative of strain application (Menzies and Maltman, 1992). "Tails" and bands of skeleton grains, flow structures and irregularly shaped fine clay bands are also indicative of differential movement within the diamicton unit during autokinetic deformation (Menzies and Woodward, 1993; Menzies and Maltman, 1992). Secondary carbonates also imply saturated conditions (Meer, 1987) and depending on the timing of their formation, could support the above observations indicative of a slump origin for the drumlin diamicton at this site.

Sample 93-CBB-3

The sample was taken from a sand lens in the slumped zone of drumlin sediments approximately 0.5 m above the shoreline at *site 5*. Strike of the sample is 65° with a dip of 3°.

A. Macroscopic

The central portion of the thin section is a large sub-angular sandstone clast (Plate 4.3). A further distinguishing feature of this sand unit is the fine clay-rich diamictic bands that appear to "flow" around the larger clast. Similarly, elongate skeleton grains are tangentially oriented around the lower right edge of the clast. In general, the diamictic bands are irregular and discontinuous whilst the sand portion of the thin section tends to be poorly sorted and heavily intermixed with the clay-rich bands.

B. Microscopic

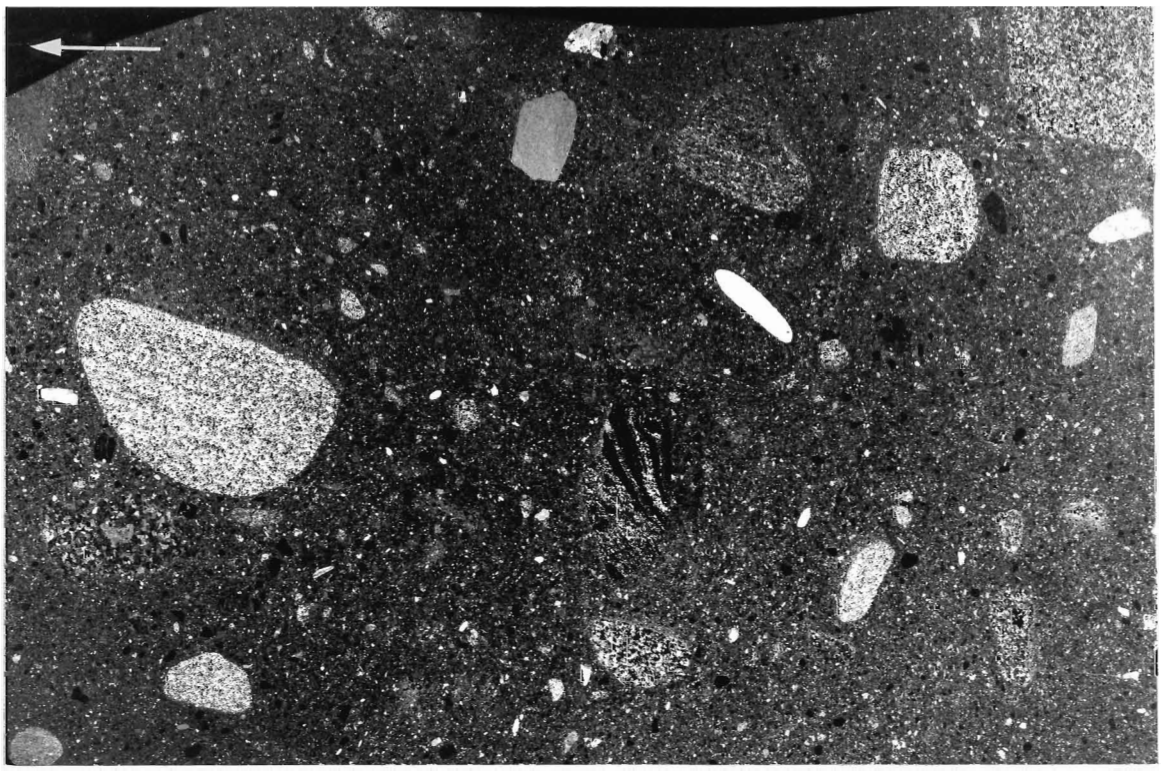

0 10 mm

Plate 4.5 Sample 93-CBB-11 taken from central portion of sand intraclast at *site 11B*.

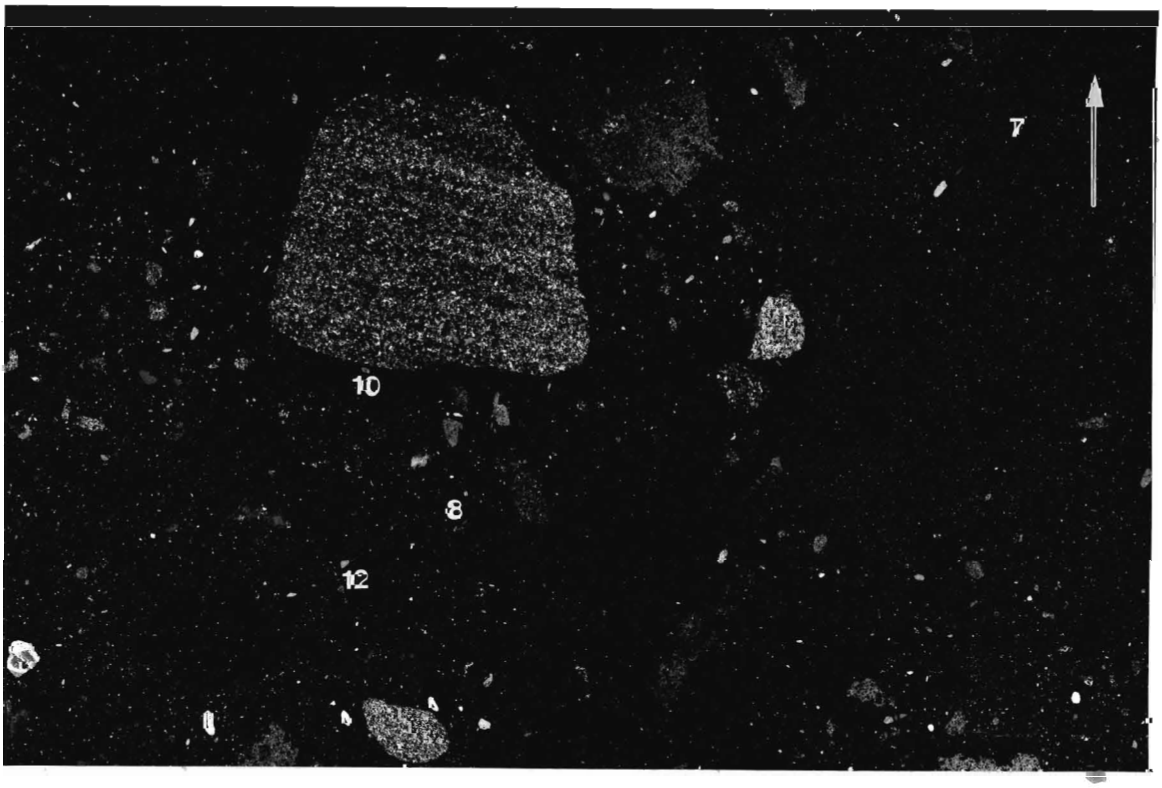

0 10 mm

Plate 4.6 Sample 93-CBB-11B taken from massive sand layer near upper boundary of same intraclast as sample 93-CBB-11.

skeleton:

size: grains range from < 50 μm to approximately 1 cm, but most tend to be 150 μm; larger grains (> 2 mm) tend to be rounded.

shape: grains range from (well) rounded (most) to angular.

distribution: mostly random with occasional vague banding.

composition: mainly quartz; some plagioclase, chlorite and clinopyroxene; the larger grains tend to be sandstone and fossiliferous limestone.

plasma: scarce throughout, except in clay-banded areas.

structure: deformation of plasma rich diamicton laminae around an elongate sandstone clast and "necking" or squeezing of the laminae between this clast and the large sandstone clast is also apparent (Plate 4.4). Oriented grains on the upper left side of the Plate form a "tail" at one end of the smaller clast. A streamlined diamictic flow structure around an elongate sandstone clast similar to the one illustrated in Plate 4.8 is also apparent. Elsewhere in the thin section, vague circular arrangements of skeleton grains (circular structures) may be observed.

aggregates: reddish-brown Fe-staining(?) is texturally restricted to the diamictic derived clay-bands.

plasmic fabric: argillasepic fabric in clay-bands.

C. Interpretation

Structures observed within the sample are consistent with a slump origin for the sand lens. Menzies and Maltman (1992); Meer and Laban (1990) suggest that streamlined flow structures reflect differential movement within highly saturated porewater conditions. Circular arrangements of skeleton grains could therefore represent differential or possibly even rotational movement (Meer, 1993) within the sand lens. Bending of laminae and "necking"

of skeleton grains also imply a slumping or mass movement episode.

Sample 93-CBB-11

The sample was taken from the central portion of a sand intraclast approximately 20 m above the shoreline at *site 11B*. Strike of the sample is 85° with a dip of 28°.

A. Macroscopic

Poorly sorted medium- to coarse-grained structureless sand and gravel with clusters of silt-dominated areas comprise the sample (Plate 4.5). The long-axes of many skeleton grains tend to be oriented parallel to the surfaces of the larger clasts; forming an encasement of finer grains. The clasts, however, are randomly oriented.

B. Microscopic

skeleton:

size: grains range from < 50 μm to ˜0.5 cm with a mode of approximately 100 μm, except within occasional silt domains.

shape: grains throughout range from (well) rounded(most) to angular.

distribution: mostly random except for occasional clustering of smaller grains in scattered silt domains.

composition: mainly quartz; some plagioclase, chlorite and clinopyroxene; the larger grains tend to be sandstone and fossiliferous limestone.

plasma: rare and restricted to small amounts of clay in various silt domains (concentrations of silt-sized particles).

structure: several small discontinuous shear planes at various angles to each other are found throughout the sample. Weakly-defined banding of skeleton grains occur randomly or as "tails" at one end of some of the larger clasts. "Necking" of the skeleton grains between the two clast is also apparent. Other notable features include "lineations" of grain-to-grain

oriented skeleton particles up to 1 cm in length and occasional diffuse rims of plasma (secondary carbonates?) around limestone clasts.

aggregates: none.

plasmic fabric: none.

C. Interpretation

Differential movement in response to stress application within the sand unit is implied by the bands, tails, lineations and necking of skeleton grains in the sample. The poorly sorted nature of the sediments in this thin section are consistent with a closed-pipe (Saunderson, 1977) subglacial conduit origin or even a proglacial glaciofluvial origin for the intraclast sediments (discussed in chapter 3). The high degree of rounding displayed by the clast in Plate 4.5 also reflect a saturated mass flow origin for the sediment. The intrinsic and multi-directional shearing may reflect deformation under very high bulk strain rates. In conjunction with the previously mentioned structures, the shearing attests to a mélange-type environment wherein a frozen intraclast is transported within a saturated deforming till layer (Menzies and Maltman, 1992). As discussed earlier, the secondary carbonates could represent post-depositional porewater movement through the intraclast. However, according to Hallet (1976) and Souchez and Lorrain (1991), such mineralisation could also reflect pressure-melting and regelation within a saturated subglacial environment.

Sample 93-CBB-11B

The sample was taken from a "massive" sand layer near the upper boundary of the same sand intraclast as sample 93-CBB-11. Strike of the sample is 71° with a dip of 5°.

A. Macroscopic

Areas dominated by silt-sized particles are visible throughout the massive, poorly sorted sand and gravel with a higher concentration of silts to the left of the large sandstone

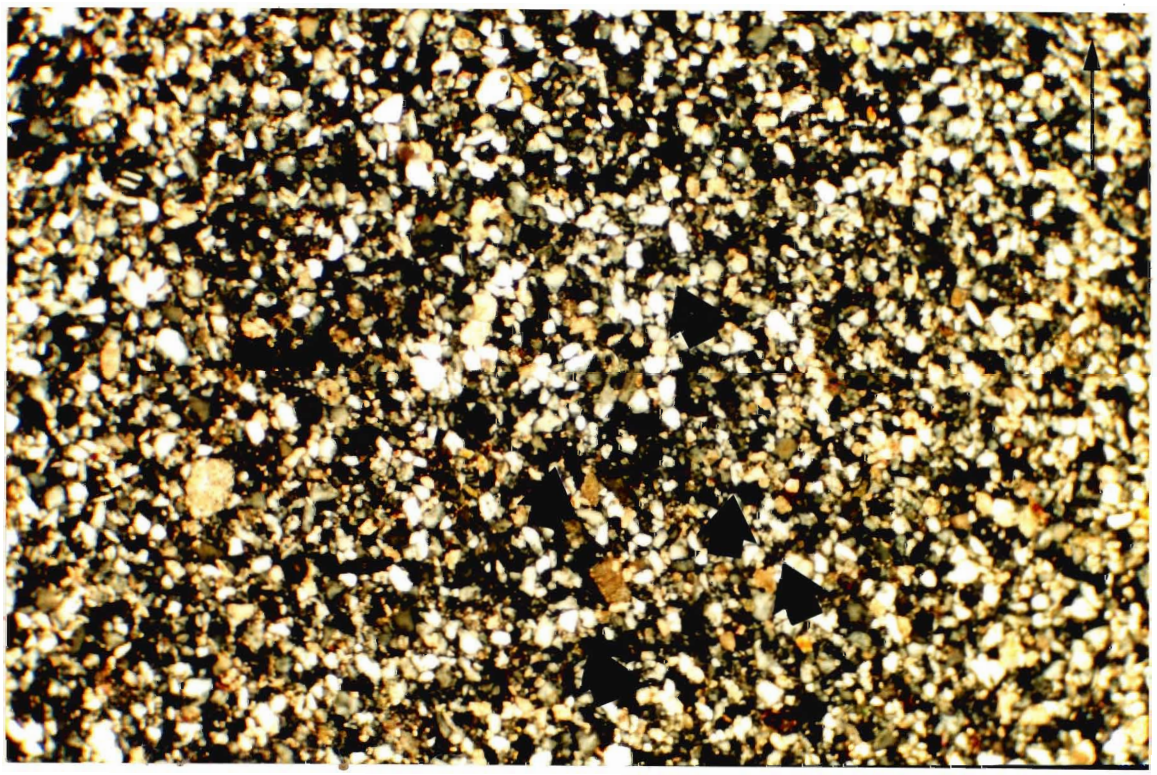

0 1.0 mm

Plate 4.7 Detail of location 7 illustrated in Plate 4.6 with cross-polars showing folded shear plane.

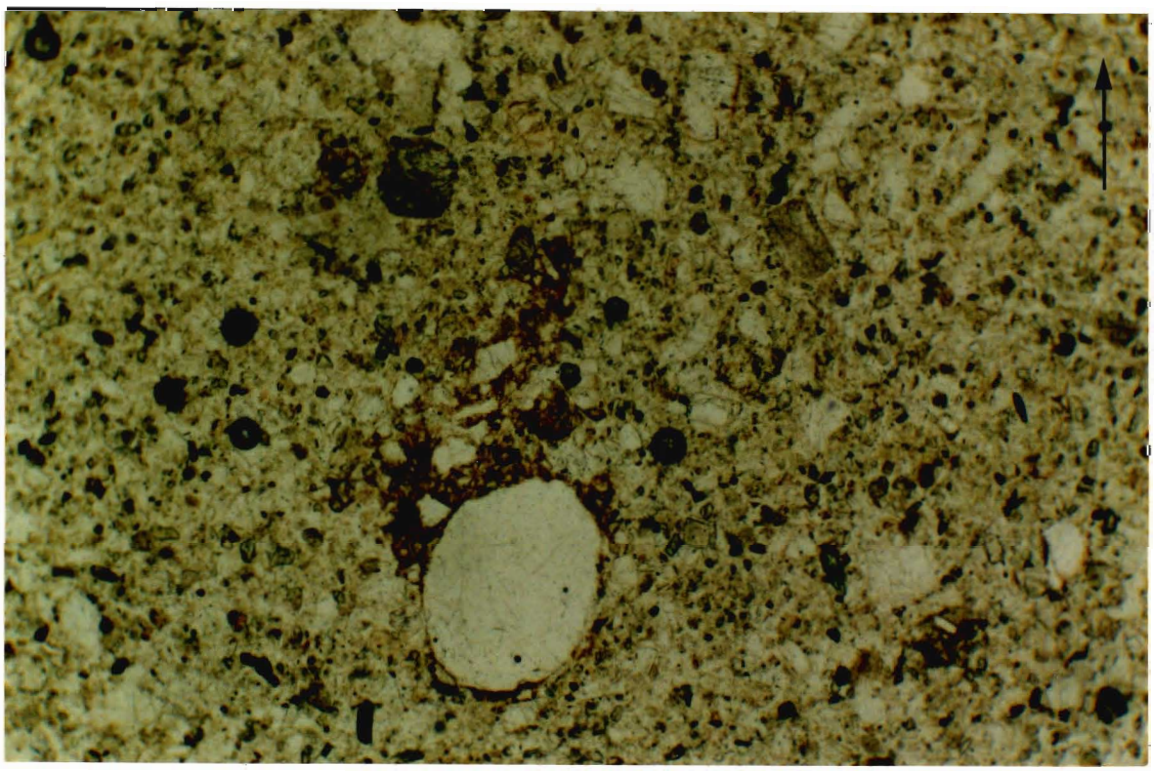

0 1.0 mm

Plate 4.8 Detail of location 8 illustrated in Plate 4.6 showing a clay-rich comet trail extending from a quartz clast

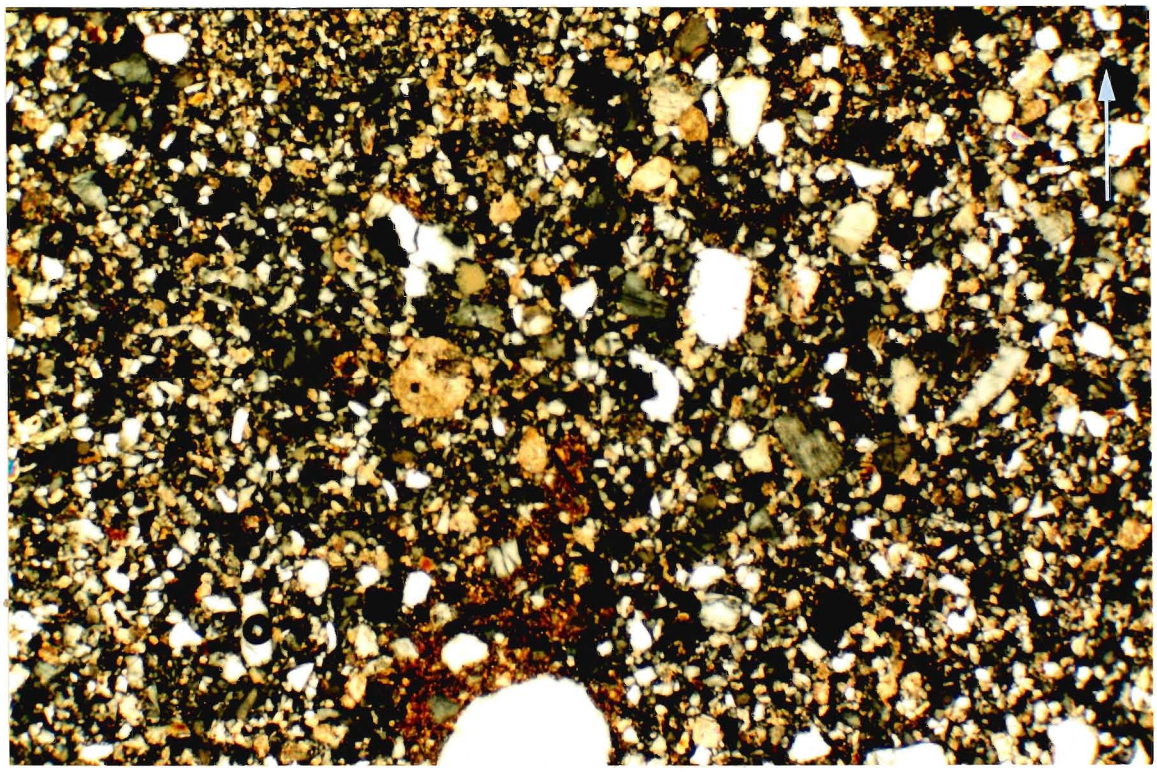

0 1.0 mm

Plate 4.9 Detail of location 9 illustrated in Plate 4.6 with cross-polars showing discontinuous shears radiating outward from a clay-rich comet trail extending from a quartz clast.

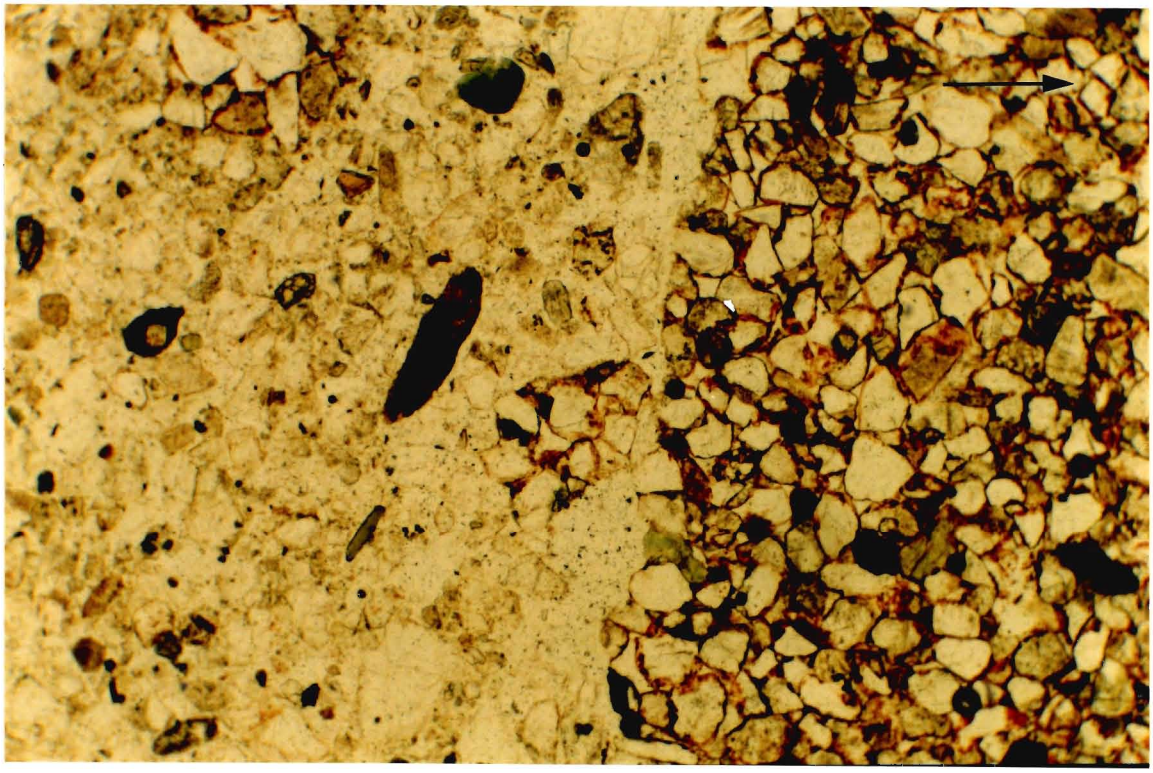

0 1.0 mm

Plate 4.10 Detail of location 10 illustrated in Plate 4.6 showing an angular sandstone fragment.

clast (Plate 4.6). These domains are relatively free of coarse grains and appear to be massive. Diamictic inclusions are interspersed randomly in the coarser grain and silt dominated zones. The inclusions tend to be sub-angular to sub-rounded and irregularly shaped. Smaller inclusions appear to be better rounded than the larger ones. Again, skeleton grains encase larger grains within this sample.

B. Microscopic

skeleton:

size: grains range from < 50 µm to over 2 cm with a mode of approximately 150 µm, except in the numerous silt domains; larger grains (> 2 mm) tend to be rounded.

shape: grains throughout the sample range from (well) rounded(most) to angular.

distribution: mostly random, but absent from the silt domains.

composition: mainly quartz; some plagioclase, chlorite and clinopyroxene; the larger grains tend to be sandstone and fossiliferous limestone.

plasma: rare; restricted to fine clay bands scattered throughout the thin section.

structure: randomly oriented discontinuous shear planes, some at oblique angles to each other, are the main feature of the sample. In some instances the shear planes are folded (Plate 4.7); however these tend to be isolated occurrences. A quartz clast with a plasma rich tail (Plate 4.8) appears to be the focus for a radiating group of discontinuous shear planes in cross-polarised light (Plate 4.9), whilst elsewhere streamlined silt boudins appear to be separated by cross-cutting discontinuous shear planes. The intensity of the shearing is exemplified by the fracturing of several of the larger clasts. Plates 4.10 and 4.11 are of a fragment of the adjacent sandstone clast which is clearly related to the diagonal discontinuous shear plane seen in cross-polarised light. A similar discontinuous shear plane extends outwards from the clast towards the lower left of the Plate upon rotation of the stage. A

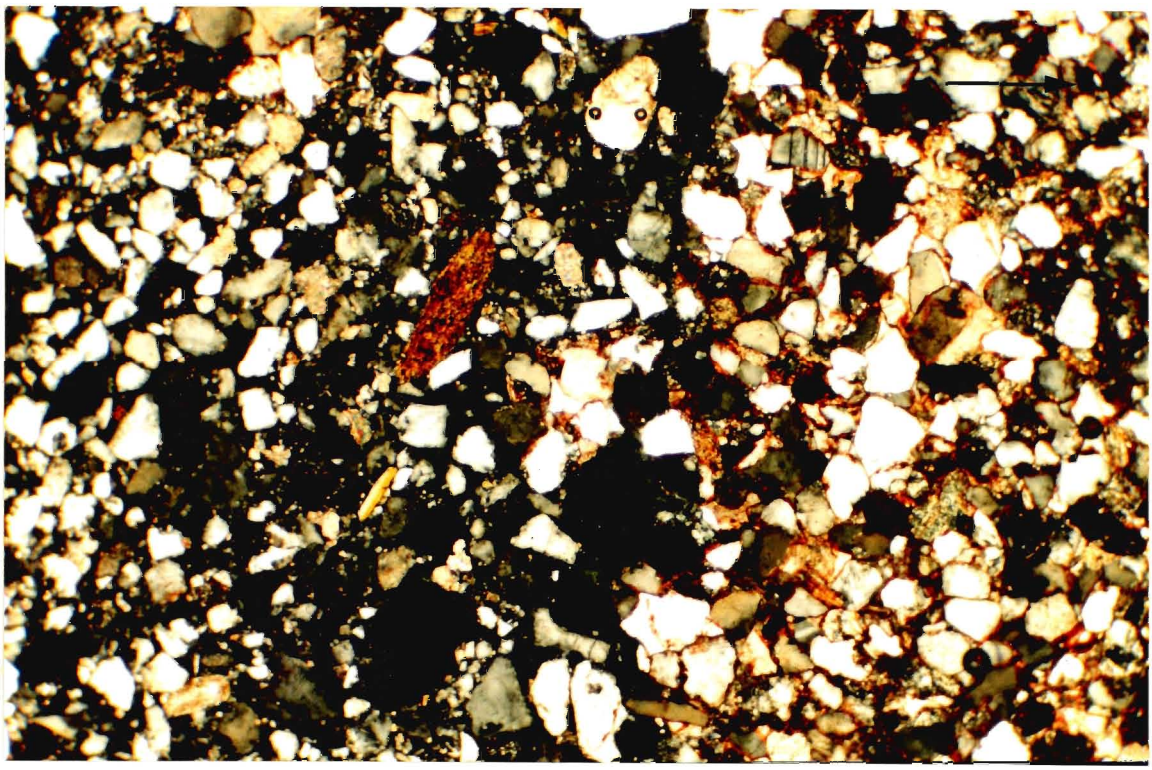

Plate 4.11 Detail of location 10 illustrated in Plate 4.6 with cross-polars showing relationship of diagonal shear with angular sandstone fragment.

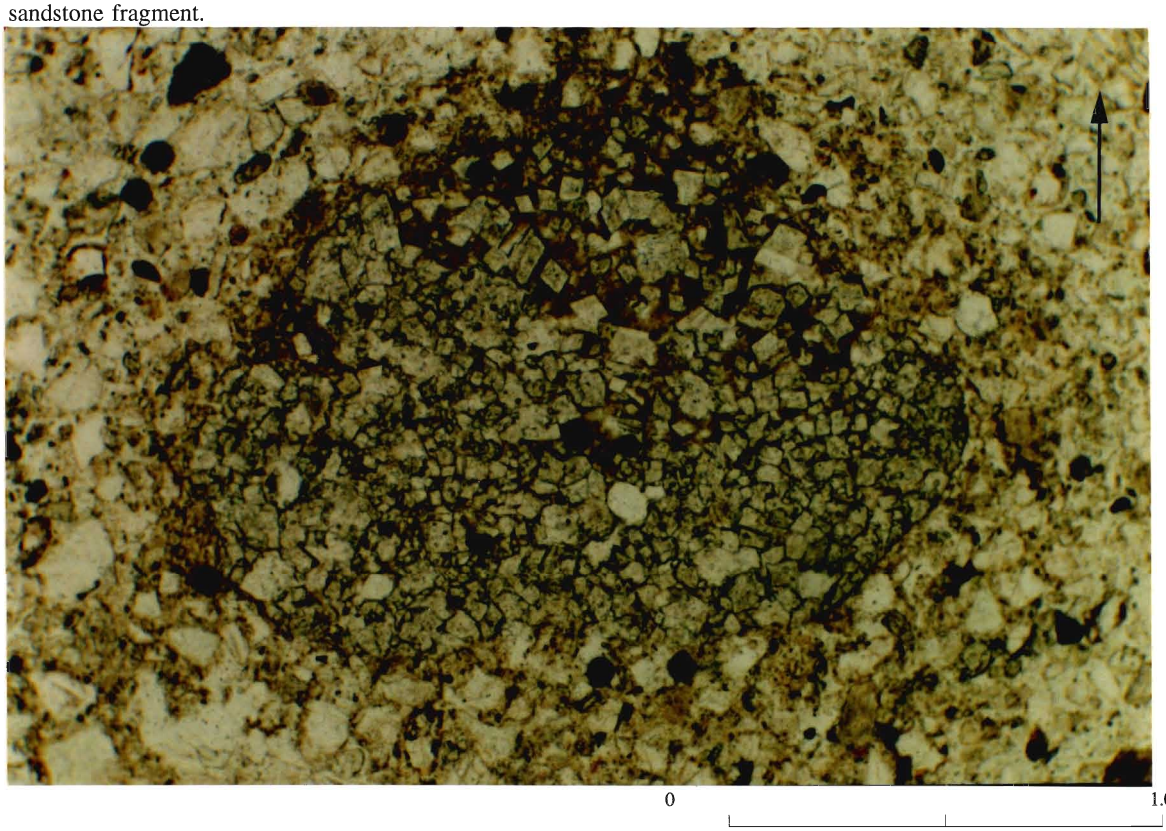

Plate 4.12 Detail of location 12 illustrated in Plate 4.6 showing a ring of secondary carbonates around a fractured limestone clast.

fractured crystalline limestone clast (Plate 4.12) appears to be surrounded by secondary carbonates (diffuse ring of clay-sized particles).

aggregates: reddish-brown Fe-staining(?) is texturally restricted to the diamictic inclusions.

plasmic fabric: vague skelsepic fabric within diamictic inclusions.

C. Interpretation

A complex evolution is suggested by the features observed in the sample. The diffuse silt-dominated areas may reflect porewater dissipation (Menzies and Maltman, 1992) subsequent to the entrainment of the sand intraclast in a deforming till layer. Such structures could therefore reflect the transition through water loss from saturated pore water conditions (ductile shear) to subglacial conditions conducive to brittle-ductile deformation (discussed in chapter 5). Boudins of silt appear to confirm this hypothesis in addition to the intense nature of the cross-cutting multi-directional shear planes. Skelsepic fabric within the diamictic inclusions probably reflects pre-existing conditions in the surrounding diamicton; however, the rounding of the inclusions is probably indicative of discrete differential movement within the sand unit during its formation. However, Plate 4.9 seems to imply that this discrete differential movement is somehow associated with the shearing in the sample and hence is associated with the deforming till layer. Again, the secondary carbonates could reflect high porewater pressures in the subglacial zone.

Sample 93-CBB-11C

The sample was taken from a coarser sand lens within the central portion of a sand intraclast approximately 20 m above the shoreline at *site 11B*. Strike of the sample is 110° with a dip of 7°.

A. Macroscopic

Coarse sand dominates and large clasts are absent from the sample (Plate 4.13).

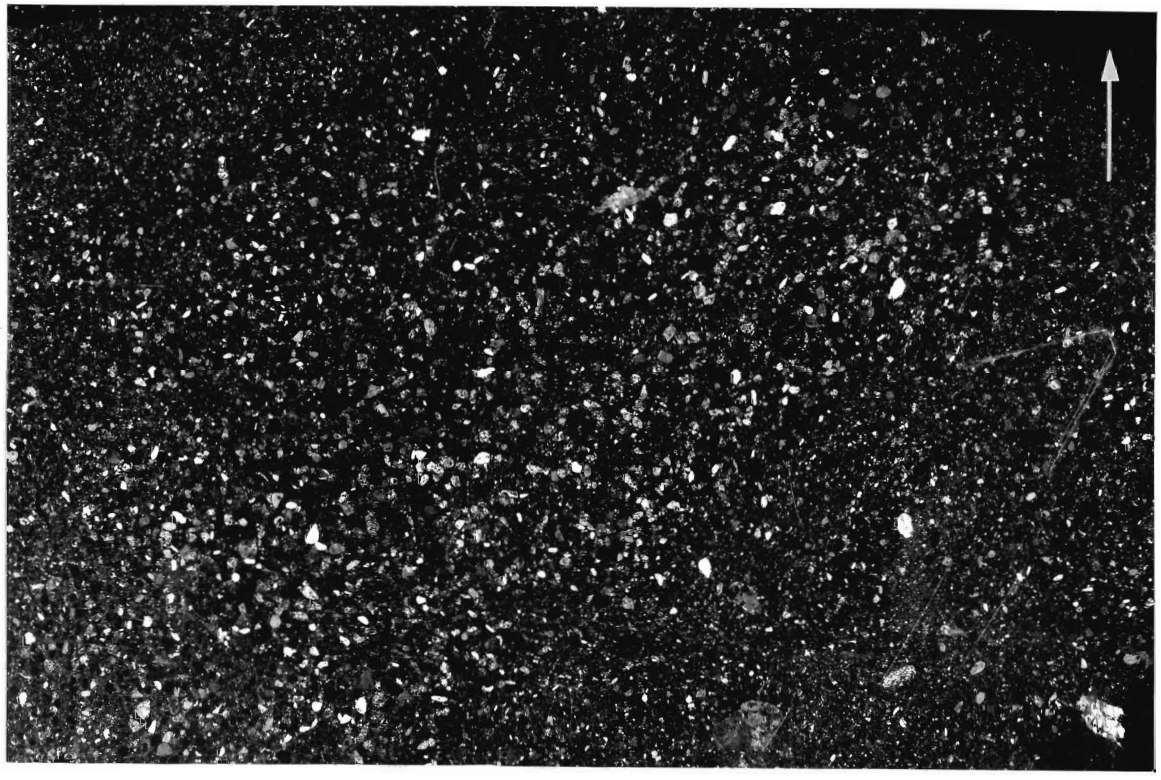

Plate 4.13 Sample 93-CBB-11C taken from coarse sand lens within sand intraclast at *site 11B*.

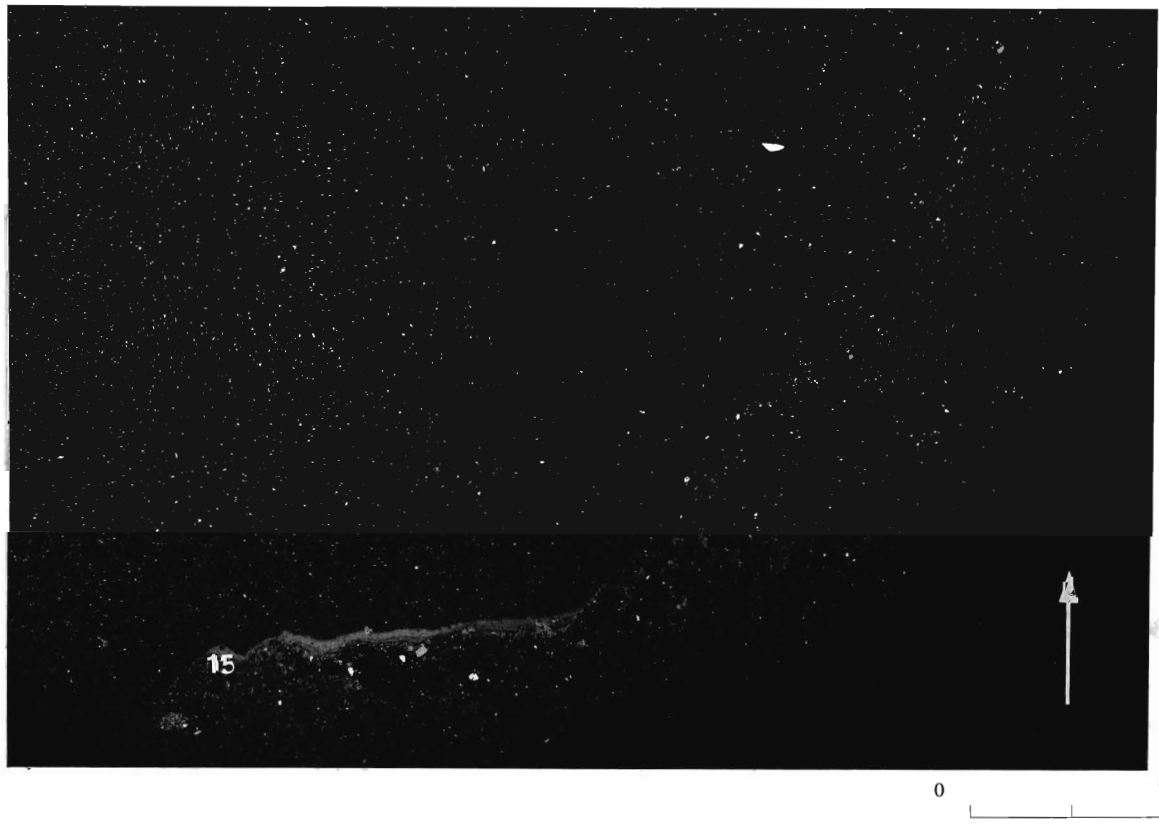

Plate 4.14 Sample 93-CBB-12A taken from lower contact of sand intraclast with the diamicton at *site 12*.

Crude stratification is visible within the coarser grains central portion of the sample. The finer grained sands in the lower right appear to be massive, though some banding is evident. This area also contains a possible fault that runs horizontally through the finer sand area and stops at the coarser sand boundary. A band of clayey material within the latter appears to have been displaced approximately 0.5 cm by the fault. A diagonal shear zone trending towards the top left of the sample into the coarser sands branches at the midpoint of the fault. Note that the apparent fold in the upper right corner of the sample is a scratch on the cover slip of the thin section.

B. Microscopic

skeleton:

size: grains range from < 50 µm to approximately 0.5 cm with a mode of approximately 200 µm and domains of 500 µm.

shape: grains throughout the sample range from (well) rounded(most) to angular; larger grains (> 2 mm) tend to be rounded.

distribution: mostly random with domains of coarser grained material.

composition: mainly quartz; some plagioclase, chlorite and clinopyroxene; the larger grains tend to be sandstone and fossiliferous limestone.

plasma: none.

structure: circular structures of skeleton grains are quite common in the sample, but the most pervasive feature are the various cross-cutting discontinuous shear planes. Occasionally, these zones are at right angles to each other, but the overall impression is that they intersect at oblique angles and have a random distribution. Banded zones of coarser grained material with no preferred orientation in addition to the tangential arrangement of grains around coarser skeleton grains are also observed.

aggregates: none.

plasmic fabric: none.

C. Interpretation

Circular structures and the casings of skeleton grains around larger clasts can be attributed to rotational and/or differential movement within the sand unit and could be indicative of mass flow conditions. Banding observed in the sample is probably of a primary depositional origin. The rather diffuse bifurcating shear zone could reflect a saturated environment which experienced an extended period of compressive strain (Menzies and Maltman, 1992). Hence, the intraclast may have been partially frozen within a high strain environment, thereby allowing for saturated conditions in which primary structures would have been obliterated.

Sample 93-CBB-12A

The sample was taken from the lower contact between a very fine sand layer within the sand intraclast at *site 12* and the diamicton. This is a continuation of the sand intraclast from *site 11B*. Strike of the sample is 62° with a dip of 9°.

A. Macroscopic

The sample can be divided into two zones based on texture and clast content. Massive fine sand with rounded silt domains comprise the left zone, whilst diamicton the right (Plate 4.14). The silt domains appear to be inclusions of the silty layer seen at the lower boundary of the two zones. Two diamictic inclusions, one rounded the other angular can be seen in the upper central portion of the sample. A sharp, mostly linear boundary separates the two zone.

Finely laminated diamicton with "wispy" clay bands is found in the right zone. The lower boundary of the two zones is formed by a massive silt band overlying a slightly folded

finely laminated clay band which has a sharp contact with the underlying diamicton. The diamicton contains shrinkage cracks and has a visible fabric of oriented grains in addition to the clay layers encasing the large clast on the upper right portion of the sample.

B. Microscopic

skeleton:

size: grains range from < 50 µm to approximately 1.5 cm with a mode of approximately 150 µm in the diamicton and 100 µm in the sand layer. Domains of silt are also present.

shape: grains range from mostly rounded in the sand layer to angular in the diamicton.

distribution: random throughout the sample, but absent from silt domains.

composition: mainly quartz; some plagioclase, chlorite and clinopyroxene with some limestone and sandstone.

plasma: mostly homogeneous clays in the diamicton.

structure: clusters of fine-grained sands in which weak circular structures have developped are found throughout the sand unit. Coarser skeleton grains are oriented parallel to the surfaces of the diamictic inclusions seen in the upper right and top centre of Plate 4.14. A vague diagonal discontinuous shear plane from the lower right to the upper left of the Plate continues into the surrounding coarse sands. Shears are also observed to cross-cut diamictic inclusions in the sand unit. Note the lack of plasma in the surrounding coarse sands. Multiple, apparently randomly oriented discontinuous shear planes, cross-cutting each other at oblique angles also occur throughout the sand unit. At the lower boundary of the diamicton, folded clay laminae (fining upwards) are apparent (Plate 4.15). The clay in these laminae does not appear to intermix with the sand or the diamicton unit, although it does have a very narrow gradational contact with the latter. Another feature of the sand/diamicton contact zone are flow structures of diamicton in the laminated clay bands, and banding of

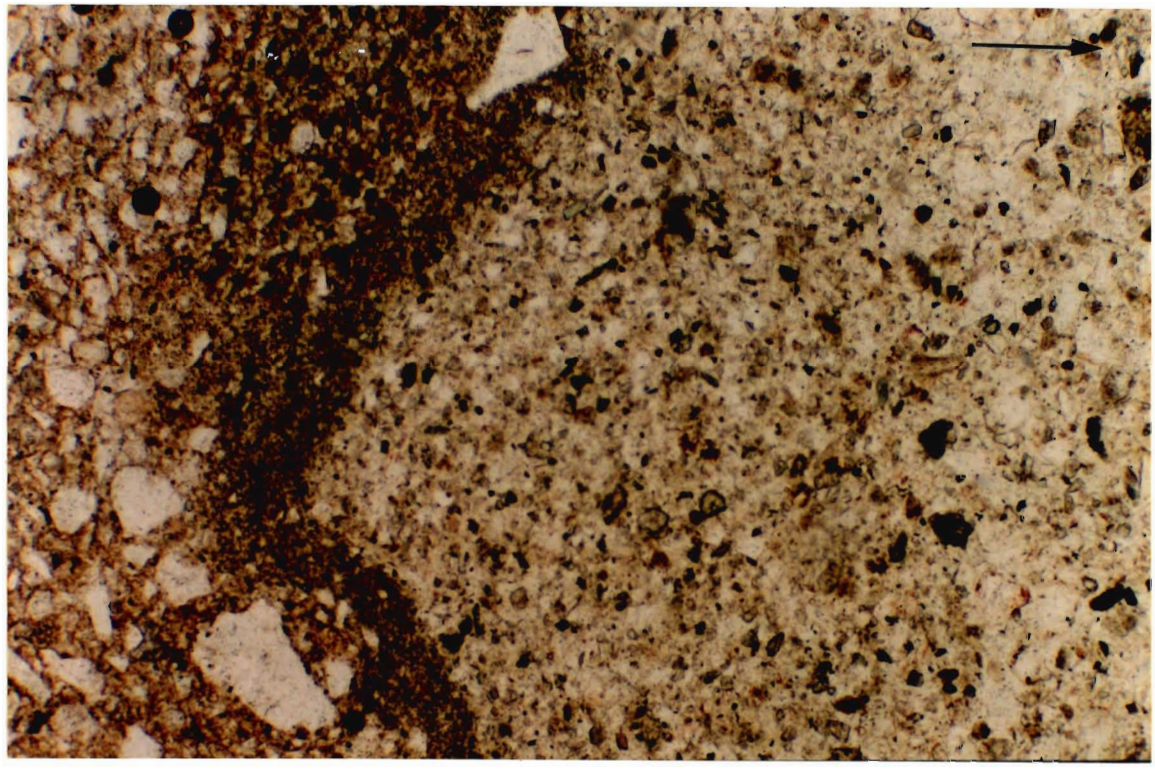

0 1.0 mm

Plate 4.15 Detail of location 15 illustrated in Plate 4.14 folded clay laminae at base of sand unit.

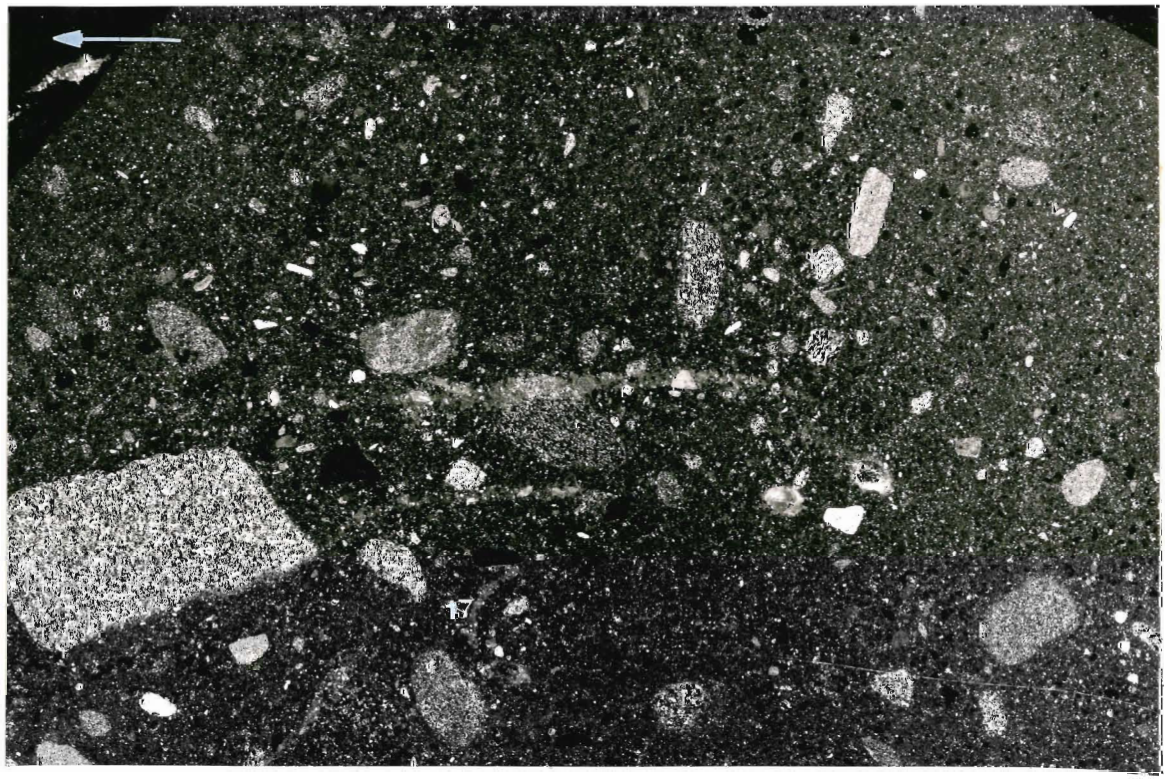

0 10 mm

Plate 4.16 Sample 93-CBB-12B taken from a sandy silt layer at *site 12*.

coarser grains with the diamicton.

aggregates: reddish-brown Fe-staining(?) is texturally restricted to the clay-rich diamicton.

plasmic fabric: strongly-developped skelsepic fabric in the diamicton.

C. Interpretation

Structures observed within this sample suggest a saturated, highly strained environment. Banding and circular arrangements of skeleton grains in addition to the rounded clusters of fine-grained sands are indicative of differential and/or rotational movement under saturated porewater conditions. The clusters of fines could also be re-worked fragments of the lower silt and laminated clay sequence, which is supported by the presence of discontinuous shear planes that cross-cut the diamictic inclusions. This sequence appears to partially derived from the diamicton that attests to the possible conduit or even proglacial melt-out origin of this sand unit. According to the fining upwards sequence of the clay laminae, the intraclast appears to have not been rotated during its transport history. Such laminae would reflect low flow conditions and the re-worked fragments and massive sands would therefore reflect the transition to higher energy flow conditions. Similarly, the aforementioned fine-grained clusters could be indicative of dewatering processes during transport. The folded clay laminae of this sequence at the boundary of the sand layer and the diamicton could be the result of vertical differential loading during the transport of the intraclast. Flow structures can also be attributed to such an environment (Menzies and Woodward, 1993).

Sample 93-CBB-12B

The sample was taken from a grey (10YR6/1) sandy silt layer approximately 21 m above the shoreline at *site 12*. Strike of the sample is 81° with a dip of 6°.

A. Macroscopic

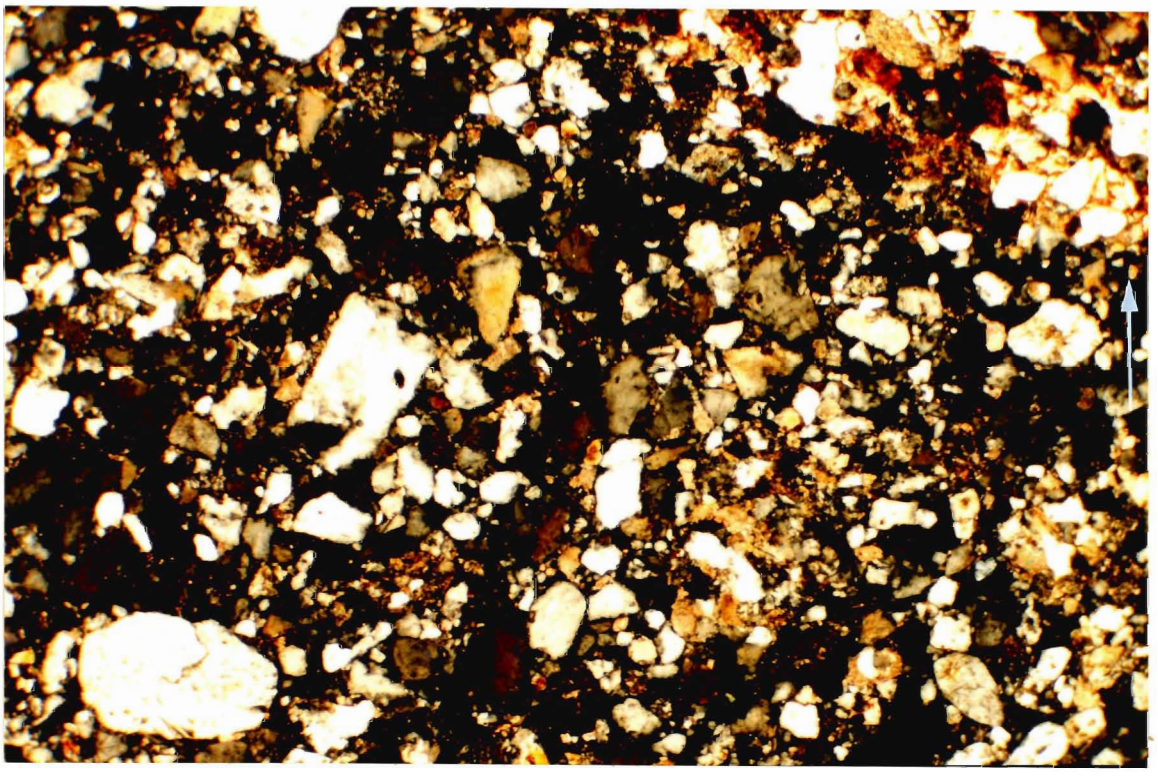

Plate 4.17 Detail of location 17 illustrated in Plate 4.16 with cross-polars showing the intersection of a near vertical shear plane with two diagonal (top right to lower left and from the white arrow to bottom centre) shear planes.

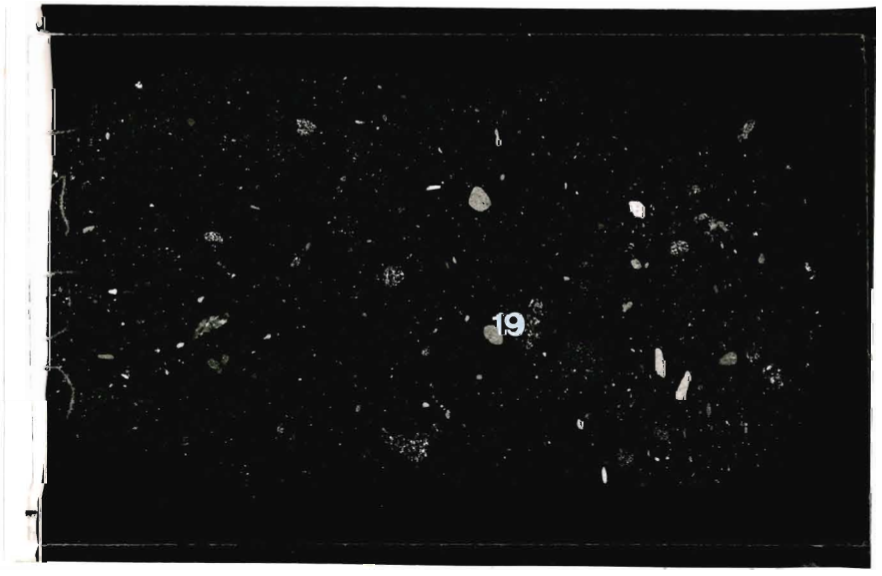

Plate 4.18 Thin section from the lower portion of sample 93-CBB-12B cut at 90° to the long axis illustrated in Plate 4.16.

Massive poorly sorted sand and gravel comprise the sample (Plate 4.16). Skeleton grains form "casings" around the larger grains, but no other fabric is visible. The two lighter coloured streaks in the centre of the Plate are scratches on the thin section. Plate 4.18 is a thin section taken at 90 to the lower portion of the long axis of the sample illustrated in Plate 4.16.

B. Microscopic

skeleton:

size: grains range from < 50 μm to approximately 1.5 cm with a mode of approximately 100 μm.

shape: grains range from angular to (well) rounded(most); larger grains (> 2 mm) tend to be rounded.

distribution: random throughout the sample.

composition: mainly quartz; some plagioclase, chlorite and clinopyroxene; the larger grains tend to be sandstone and fossiliferous limestone.

plasma: rare clay patches.

structure: circular structures, some with "ghost" (voids) clasts occur throughout the sample. Discontinuous shear planes having no preferred orientation are typical of the thin section (Plate 4.17). Occasionally, casings of skeleton grains around elongated clasts form a triangular patch of fines at one end of the clast and in some instances, a "halo" or a void at the other end (Plate 4.19). Skeleton grains also form lineations, "tails" (Plate 4.19) and vague banding throughout the sample. Weakly-defined kinks are sometimes present in the bands, but this occurrence is rare.

aggregates: none.

plasmic fabric: none.

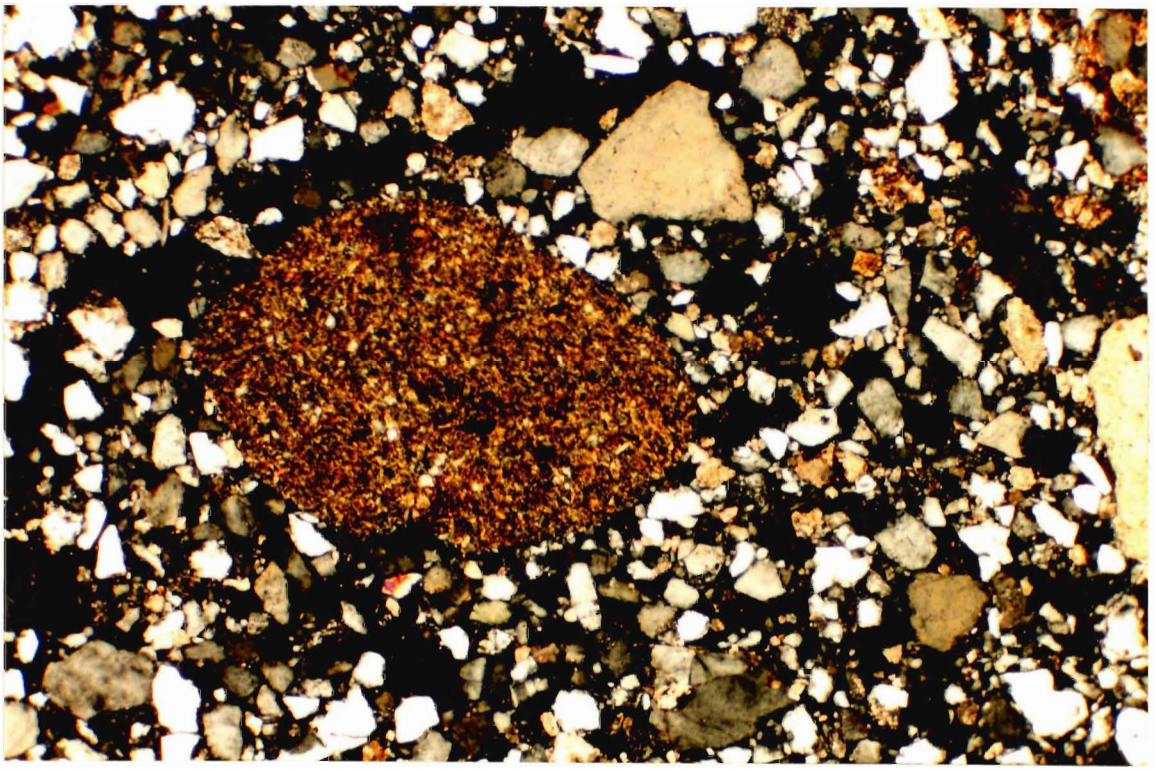

Plate 4.19 Detail of location 19 illustrated in Plate 4.18 with cross-polars showing rounded siltstone clast with "halo" or void space (upper left) and a casing of skeleton grains that terminates in a triangular shape (right) .

Plate 4.20 Sample 93-CBB-13A taken from a faulted clay layer within a sand intraclast at *site 13.* .

C. Interpretation

Circular structures and casings of skeleton grains around larger clasts are indicative of rotational and/or differential movement within the sample. The elongate clast with associated triangular patches of fines are somewhat analogous in shape to augens (Sitler and Chapman, 1955) and have been described as "pressure shadows" by Meer (1993). Although these patches reflect deformation associated with augen development, they could also be the result of differential flow within the sample whereby the clasts moved through the matrix leaving a "trail" of fines behind it. Associated void spaces mimicking the opposite end of the elongated clasts could also be the result of this type of movement (Menzies and Maltman, 1992). The presence of discontinuous shear planes and kink-banding suggest that brittle deformation, possibly while the silty sand unit was frozen has occurred during transport. Again, the poorly sorted character of this thin section could reflect mass flow conditions in a closed-pipe system. The angularity of some of the larger clasts implies that they have been derived from a local source (i.e., the diamicton). All of these features suggest a complex origin for the sandy silt layer involving deposition, entrainment and deformation of the sediments within a deforming till layer.

Sample 93-CBB-13A

The sample is of a faulted clay layer in a very fine sand layer within a sand intraclast approximately 8 m above the shoreline at *site 13*. Strike of the sample is 84° with a dip of 22°.

A. Macroscopic

Well-sorted, structureless fine sands constitute the bulk of this sample and larger grains are absent (Plate 4.20). The upper left portion of the sample is a zone of deformed clay-rich inclusions ranging from angular to rounded. The shape of the finely laminated

(similar to the laminae illustrated in Plate 4.15) angular clay-rich inclusions suggests faulted blocks, around which skeleton grains have formed casings.

B. Microscopic

skeleton:

size: grains range from < 50 µm (most) to approximately 150 µm.

shape: grains range from angular to (well) rounded(most).

distribution: random, but absent from the clay "layers".

composition: mainly quartz; some plagioclase, chlorite and clinopyroxene with some sandstone(?) and fossiliferous limestone(?).

plasma: some clay rich areas which are mostly confined to the clay-rich intraclasts.

structure: weakly-defined randomly oriented shears planes are the most notable feature of the sample. Vague lineations and "necking" of skeleton grains are also quite common. The contact between the clay and diamictic inclusions and the sand unit are sharp and range from straight-edged to irregular.

aggregates: reddish-brown Fe-staining(?) is texturally restricted to those areas of high clay content.

plasmic fabric: none.

C. Interpretation

Lineations and "necking" of skeleton grains in addition to the presence of some rounded clay-rich inclusions suggest that some differential movement has occurred after and/or during the emplacement of the clay-rich inclusions. These inclusions could be derived from clay laminations deposited during low flow conditions which were subsequently fragmented, possibly while frozen, and mixed with the sand during high energy flow conditions, or possibly even during transport within a mélange. The absence of plasma in the

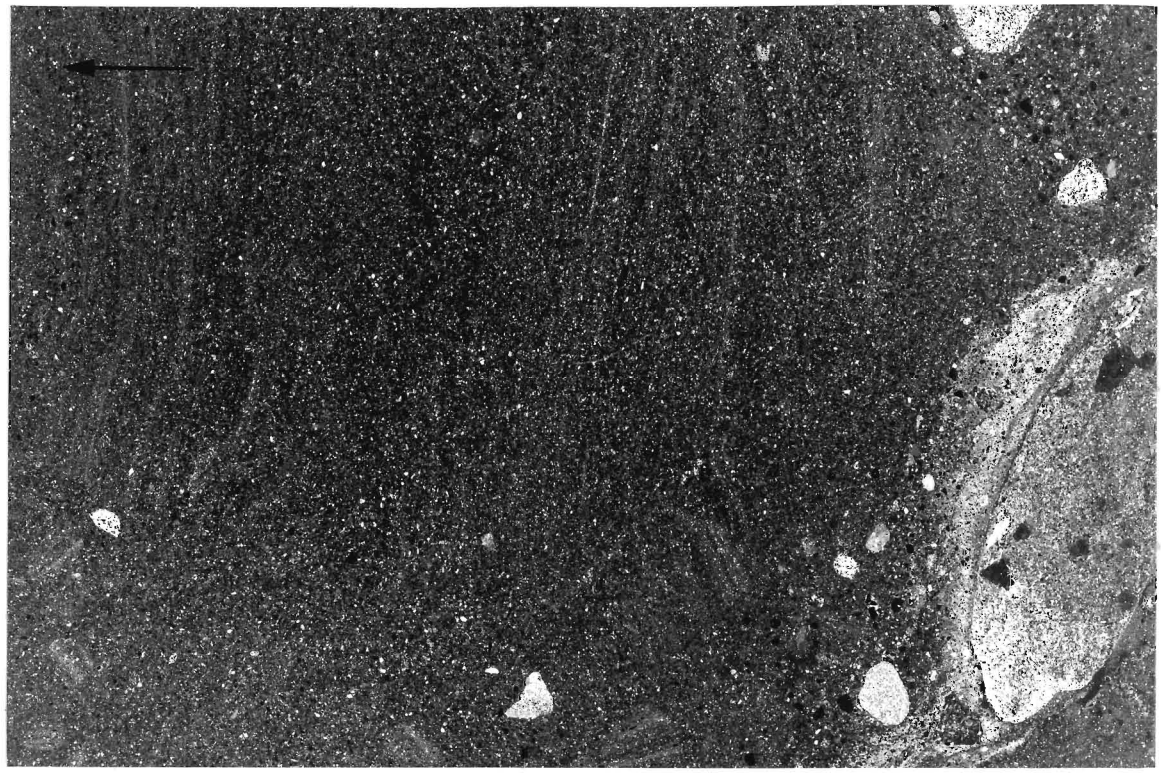

0 10 mm

Plate 4.21 Sample 93-CBB-13B taken from a very fine sand layer in the same sand intraclast as sample 93-CBB-13A illustrated in Plate 4.20 at *site 13*.

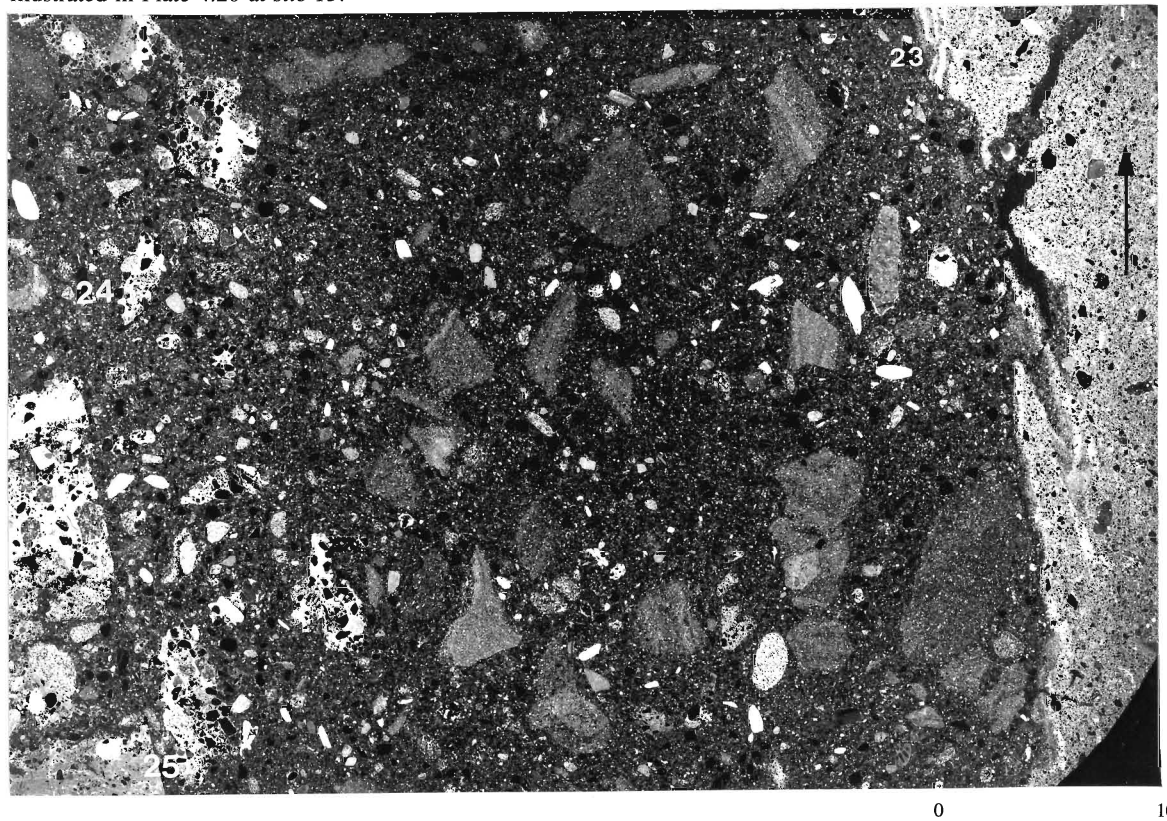

0 10 mm

Plate 4.22 Sample 93-CBB-15 taken from the contact between a sand boudin and the diamicton at *site 15*.

sand unit tends to support the idea that the inclusions may have been at least partially frozen prior to their incorporation within the sand unit. The intense nature of the internal shearing implied by the faulted block and the observed pervasive shearing tend to support the idea of high bulk strain in a partially frozen environment.

Sample 93-CBB-13B

The sample was taken from a similar very fine sand layer within the same sand intraclast as 93-CBB-13A, only 2 m eastward. Strike of the sample is 330° with a dip of 16°.

A. Macroscopic

The well-sorted sands of this sample are finely laminated and apparently sheared. The stratification of the sands in the upper left corner of Plate 4.21 is terminated by a near vertical micro-fault. A diamictic inclusion is visible at the bottom of the Plate and consists of a large clast with a casing of clay-rich diamicton. The boundary of the inclusion is very irregular with the diamicton essentially intermixing with the sand unit. Casings of skeleton grains around larger clasts are also visible.

B. Microscopic

skeleton:

size: grains range from < 50 µm to approximately 2 cm with a mode of approximately 100 µm.

shape: grains range from angular to (well) rounded(most); larger grains (> 2 mm) tend to be rounded.

distribution: random throughout.

composition: mainly quartz; some plagioclase, chlorite, pyroxene with some sandstone and fossiliferous limestone.

plasma: restricted to clay in diamictic inclusion in the lower zone.

structure: several features are apparent in the thin section, the most pervasive being weakly- to strongly-defined cross-cutting discontinuous shear planes. Elsewhere, "teardrop"-shaped diamictic inclusions with stretched out tails similar to the large inclusion described above are visible. Circular structures, lineations, bands and "necking" of skeleton grains can also be observed in the thin section.

aggregates: reddish-brown Fe-staining(?) is texturally restricted to the diamictic inclusion.

plasmic fabric: strongly-developped skelsepic fabric in the inclusion.

C. Interpretation

The sample could reflect a partially frozen conditions during and/or after transposition. Saturated porewater conditions are suggested by the strong intermixing of the diamictic inclusion with the surrounding sand unit. Casings of skeleton grains around the inclusion and adjacent clast and the structureless appearance of the sand in this zone appears to support this conclusion. Fine laminations in the sand suggest that some differential sorting has occurred and in conjunction with the diamictic inclusion, probably reflect fluctuating flow processes. Frozen conditions are suggested in the upper laminated sands in which circular structures and necking of skeleton grains is apparent. Although the latter are indicative of discrete relative motion, remnant primary structures in the sand unit, albeit discretely sheared, suggest that this zone was frozen during transport and subsequent deformational episodes. Teardrop diamictic inclusions in this zone could reflect porewater dissipation as the unit thawed.

Sample 93-CBB-15.

The sample was taken from the contact zone between the sand intraclast boudin and the diamicton approximately 10 m above the shoreline at *site 15*. Strike of the sample is 352° with a dip of 2°.

A. Macroscopic

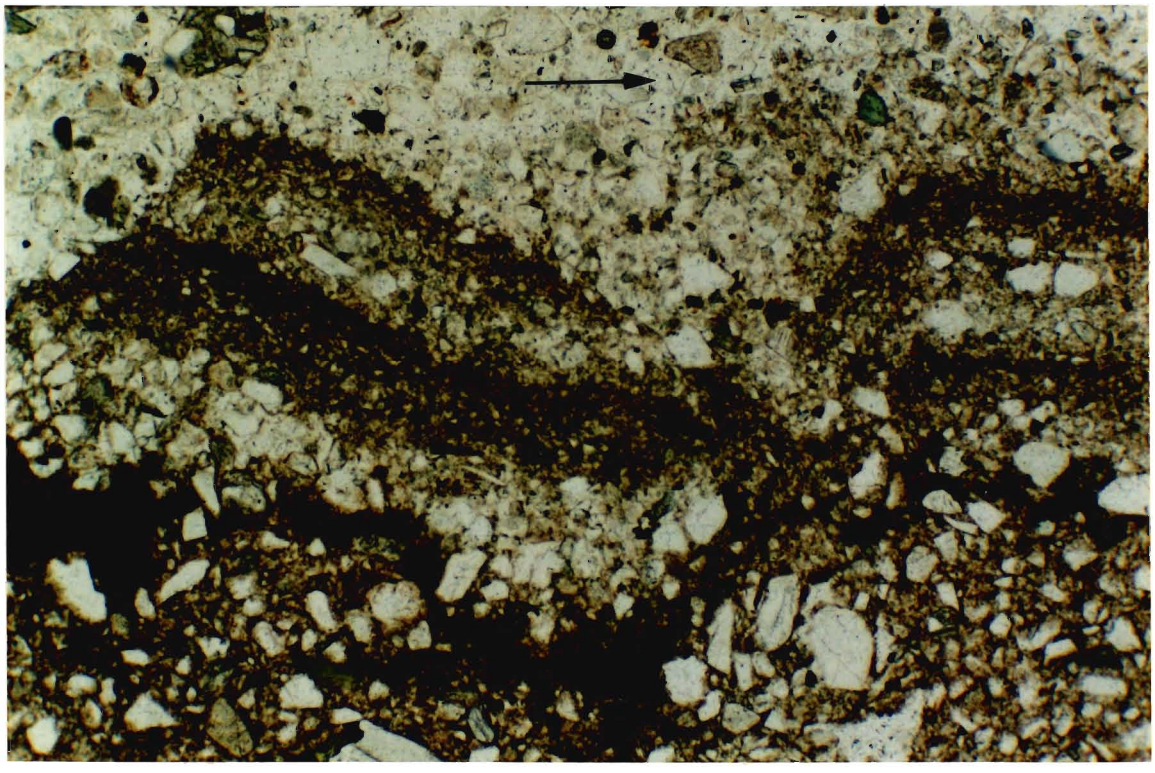

0 1.0 mm

Plate 4.23 Detail of location 23 illustrated in Plate 4.22 showing pinched normally graded fine-grained laminae at contact between diamicton (plate) and sand lens (plate).

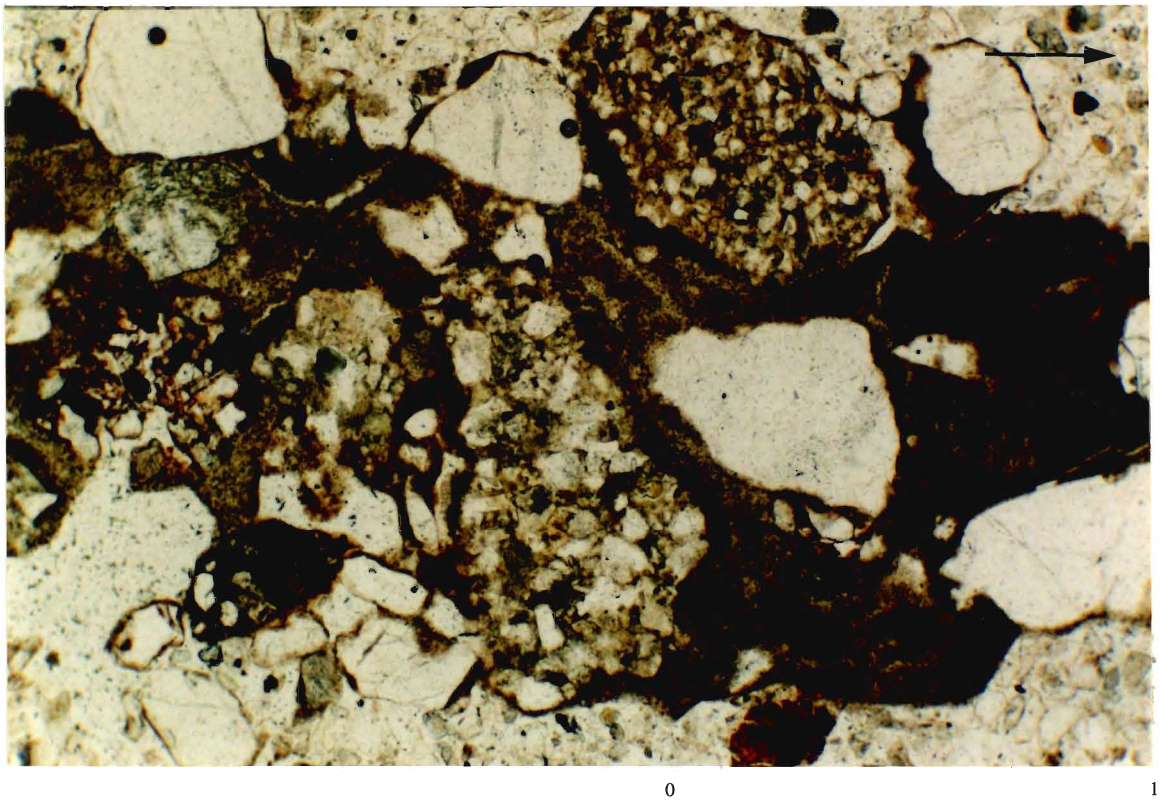

0 1.0 mm

Plate 4.24 Detail of location 24 illustrated in Plate 4.22 showing Fe-stained flow structure.

The sample can be divided into three zones based on texture and clast content (Plate 4.22). The zone on the far right is diamictic with skeleton grains of various sizes and no obvious sorting. Bedding in this zone is restricted to very thin and discontinuous, partially folded discontinuous clay-rich bands at the contact between the outer right and the central zones. The boundary is sharp although some inter-fingering and fracturing of the diamicton is evident.

The central zone has a more dense concentration of skeleton particles. The sand grains are unsorted, but the distinguishing feature of this zone are the numerous angular to sub-angular clay-rich inclusions. Banding is visible in several of the inclusions whose distribution is apparently random. The boundary with the zone on the left is gradational and consists of intermixed sands and clay-rich diamictic inclusions.

The left zone comprises angular to sub-rounded clay-rich inclusions which appear to be remobilised diamicton. The straight edge of the lower left inclusion is possibly a fault. The inclusions in all zones are "envelopped" by a thin casing of skeleton grains. Plate 4.27 is a thin section taken at 90° to the upper portion of the long axis illustrated in Plate 4.22.

B. Microscopic

skeleton:

size: grains range from < 50 µm to approximately 1 mm with a mode of approximately 100 µm in the central zone and 150 µm in the outer zones.

shape: grains range from (well) rounded in the central zone to angular in the outer zones; larger grains (> 2 mm) tend to be rounded.

distribution: random.

composition: mainly quartz; some plagioclase, chlorite and clinopyroxene; the larger grains tend to be sandstone and fossiliferous limestone.

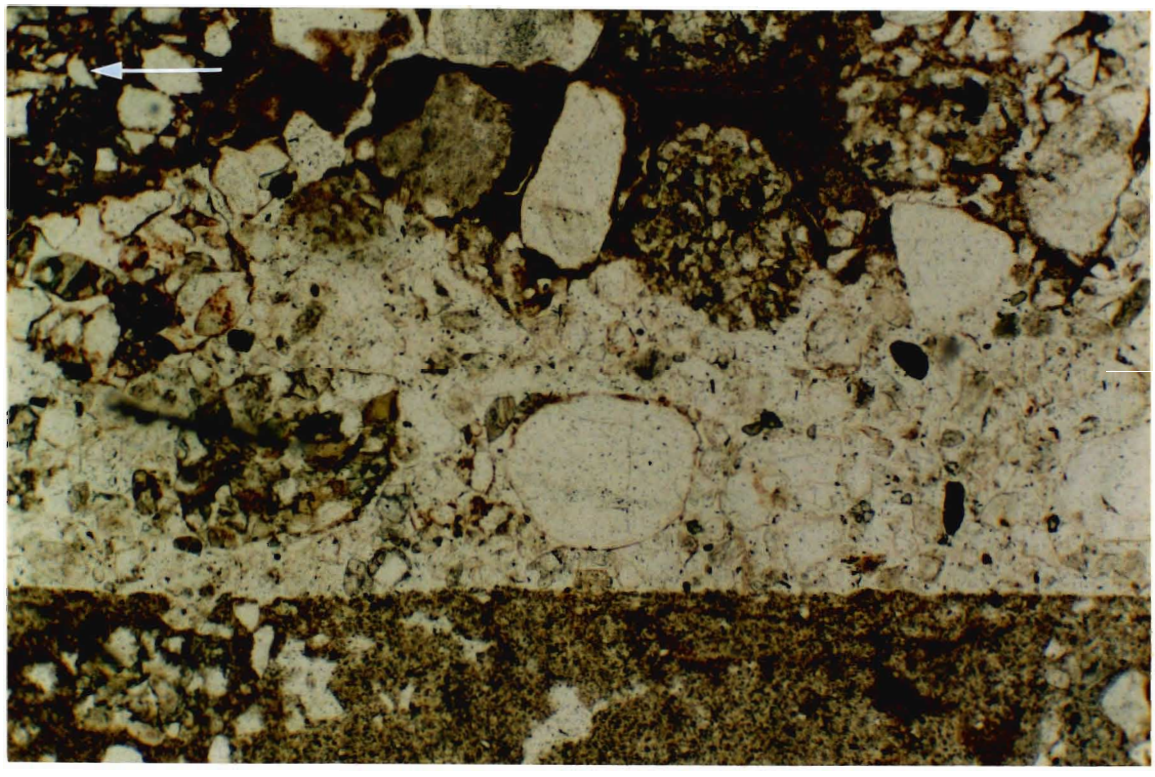

0 1.0 mm

Plate 4.25 Detail of location 25 illustrated in Plate 4.22 showing a possible fault (straight edge at bottom) and a flow structure (top).

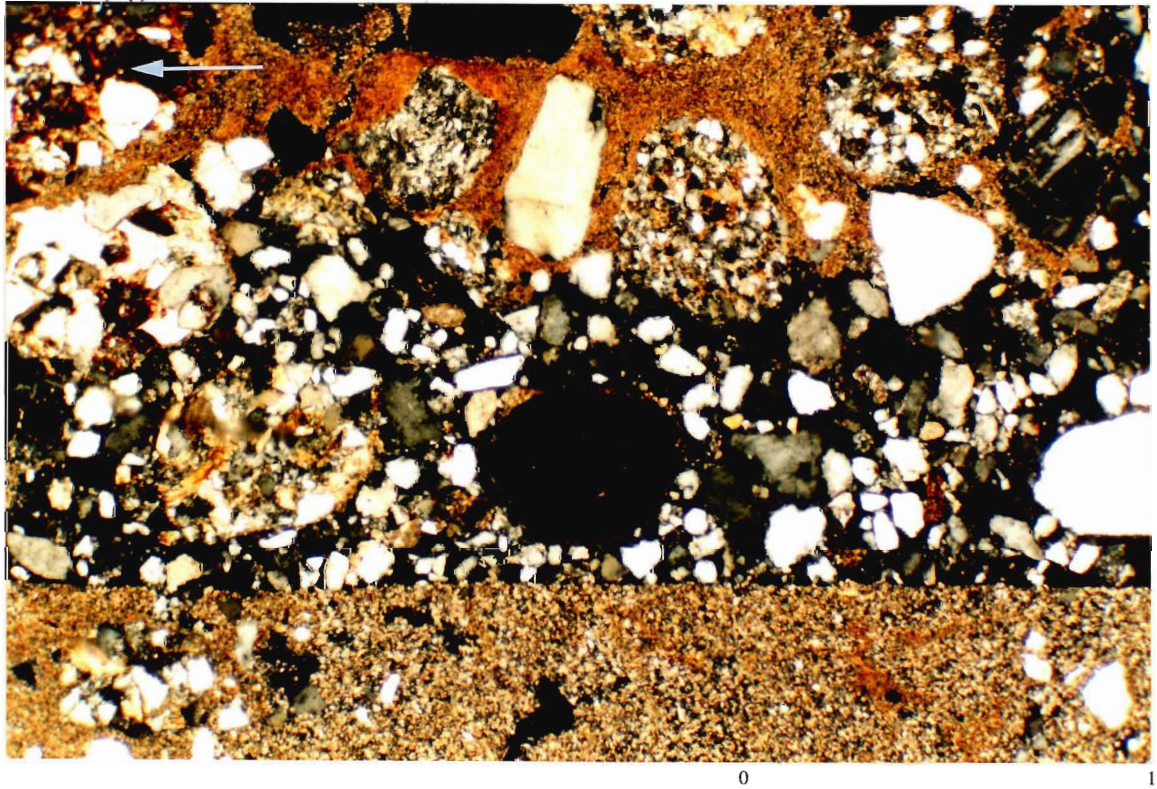

0 1.0 mm

Plate 4.26 Same as Plate 4.25, but with cross-polars. Note the casing of skeleton grains around the quartz clast (opaque) and the absence of fines in the fault zone.

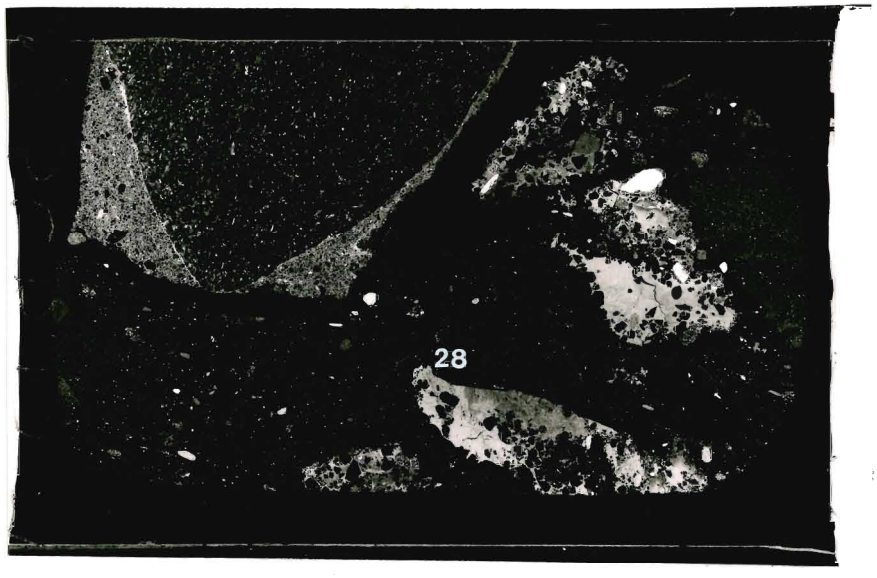

0 1.0 mm

Plate 4.27 Thin section from the upper portion of sample 93-CBB-15 cut at 90° to the long axis illustrated in Plate 4.22.

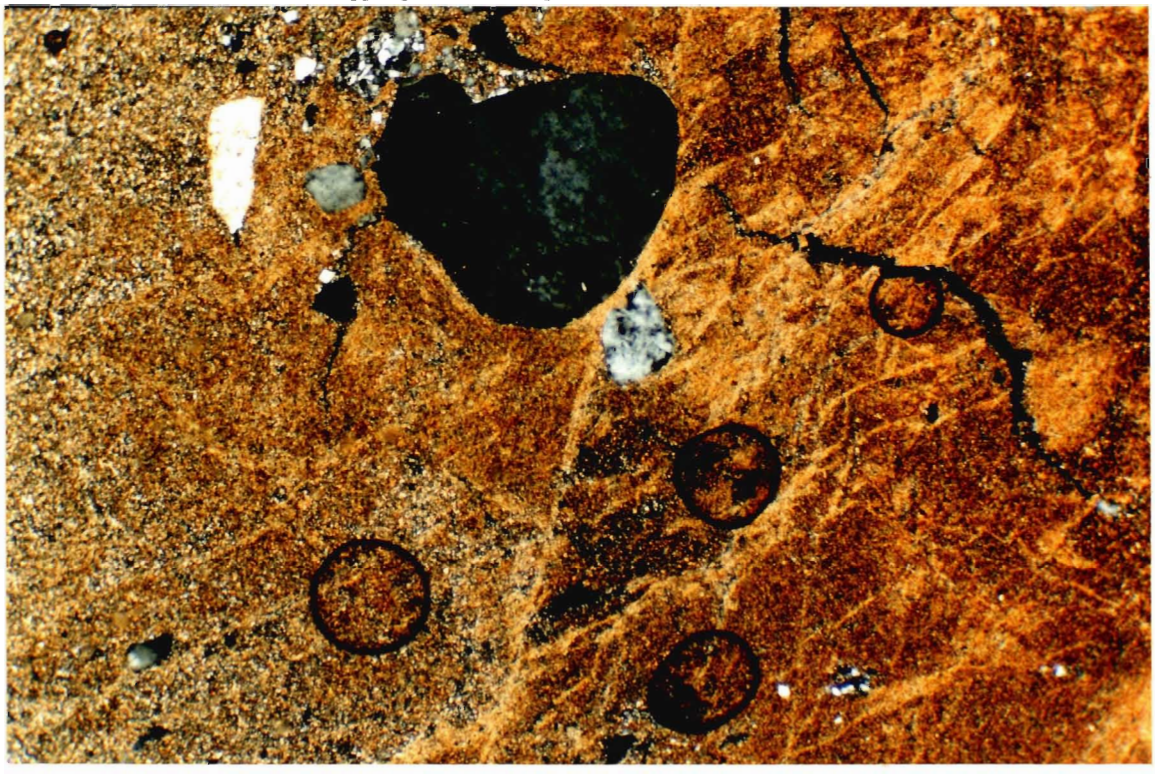

0 1.0 mm

Plate 4.28 Detail of location 28 illustrated in Plate 4.27 with cross-polars showing compound fabric in Fe-rich zone within a diamictic inclusion.

plasma: mostly homogeneous clays confined to the outer zones and the diamictic inclusions.

structure: laminae within the clay-rich inclusions are deformed and in the discontinuous clay band at the boundary between the diamicton and the sand lens the laminae are almost pinched off (Plate 4.23). This laminae clearly has a fining up sequence as shown by the high concentration of reddish-brown Fe-staining(?). The "collapsed" section of the laminae is infilled with sands from the adjacent sand lens. Diamictic inclusions in the left outer zone consisting of deformed and laminated Fe-stained clays form flow structures within the sand lens (Plate 4.24). The straight-edged diamictic inclusion in the outer left zone suggests a fault (Plates 4.25 and 4.26). Note how the coarse grain is encased by a circle of fines under crossed-polars. "Necking" of fines between coarser grains and occasional randomly oriented ill-defined discontinuous shear planes are also evident in the central zone. A compound plasma (unistrial?) fabric within a very fine-grained Fe-rich zone within a diamictic inclusion can be observed in Plate (4.28).

aggregates: reddish-brown Fe-staining(?) is texturally restricted to the diamictic inclusions.

plasmic fabric: strongly-developped skelsepic fabric in the deformed diamictic fragments.

C. Interpretation

The thin section represents a gradational contact between the diamicton and the sand lens. Pieces of the surrounding diamicton have been broken off and rotated within the sand lens where they have undergone extensive deformation. Casings of skeleton grains around the larger clasts and the presence of flow structures suggest autokinetic deformation; however, the latter also implies saturated porewater conditions. The clay-rich inclusions may have been part of a pre-existing laminated silty-clay band within the diamicton or the sand lens. Their sharp boundaries imply that they were probably frozen prior to their incorporation into the sand lens. However, the normally graded silty laminae illustrated in Plate 4.23 appear to be

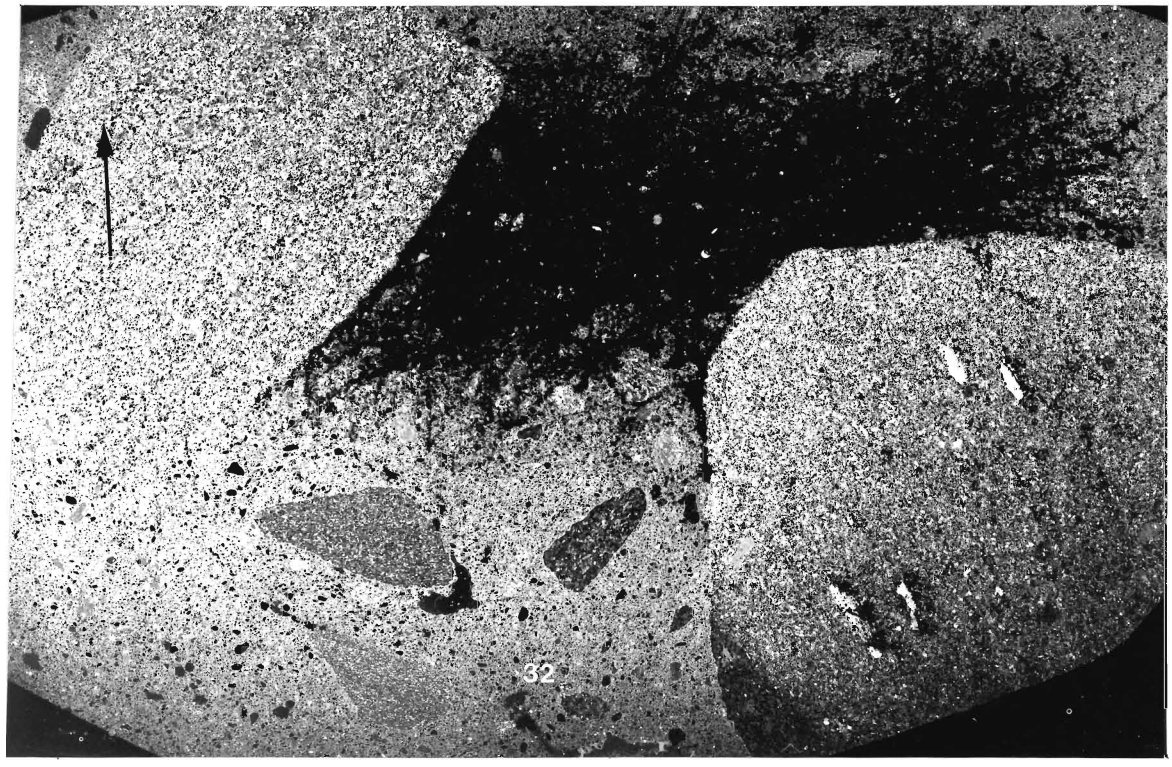

Plate 4.29 Sample 93-CBB-21 taken from diamicton at *site 21*.

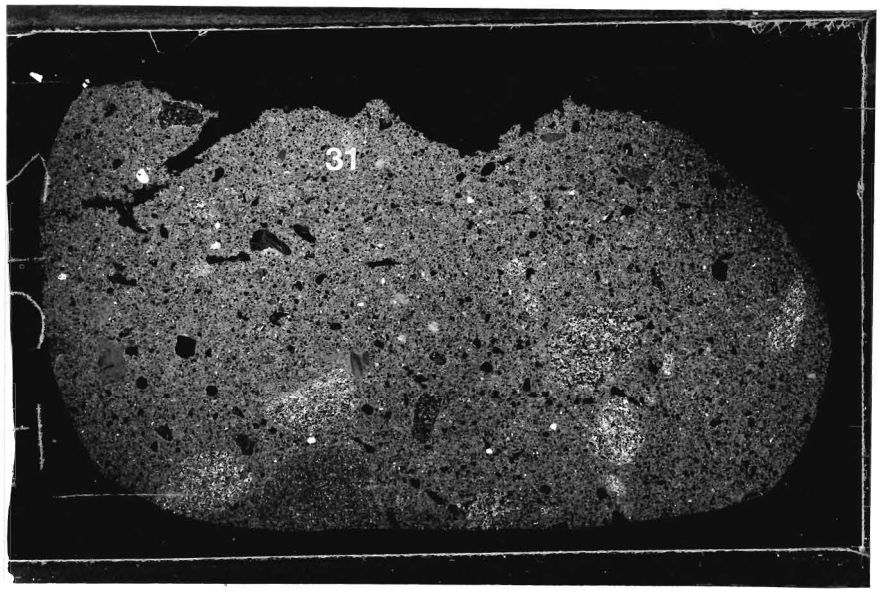

Plate 4.30 Thin section from the lower portion of sample 93-CBB-21 cut at 90° to the long axis illustrated in Plate 4.29.

derived from the diamicton and their normal grading implies that they have been rotated subsequent to their deposition. Such evidence suggests variable flow conditions for the deposition of the sediments within this sand unit. Low energy flow conditions are suggested by the occurrence of the silty laminae and the silty clay layer, which was subsequently eroded and brecciated when the high energy flow conditions prevailed . The possible fault seen on the left side of Plate 4.22 is consistent with the type of high energy environment suggested by the observed features. The ill-defined multi-directional discontinuous shear planes could be related to the extensional and compressive strains associated with boudin formation during the transport of this intraclast within a deforming till layer subsequent to deposition.

Sample 93-CBB-21

Sample of diamicton taken approximately 8 m above the shoreline at *site 21*. Strike of the sample is 195° with a dip of 8°.

A. Macroscopic

Apparently massive diamicton and two large sandstone clasts comprise the sample (Plate 4.29). The only distinguishable feature of the sample is the casings of skeleton grains around the larger grains within the diamicton. Note the black area of the Plate is the result of improper preparation. Plate 4.30 is a thin section cut 90° to the lower portion of the long axis of the sample illustrated in Plate 4.29.

B. Microscopic

skeleton:

size: grains range from < 50 μm to approximately 1 cm with a mode of approximately 100 μm.

shape: grains range from angular(most) to rounded; the larger grains (> 2 mm) tend to be rounded.

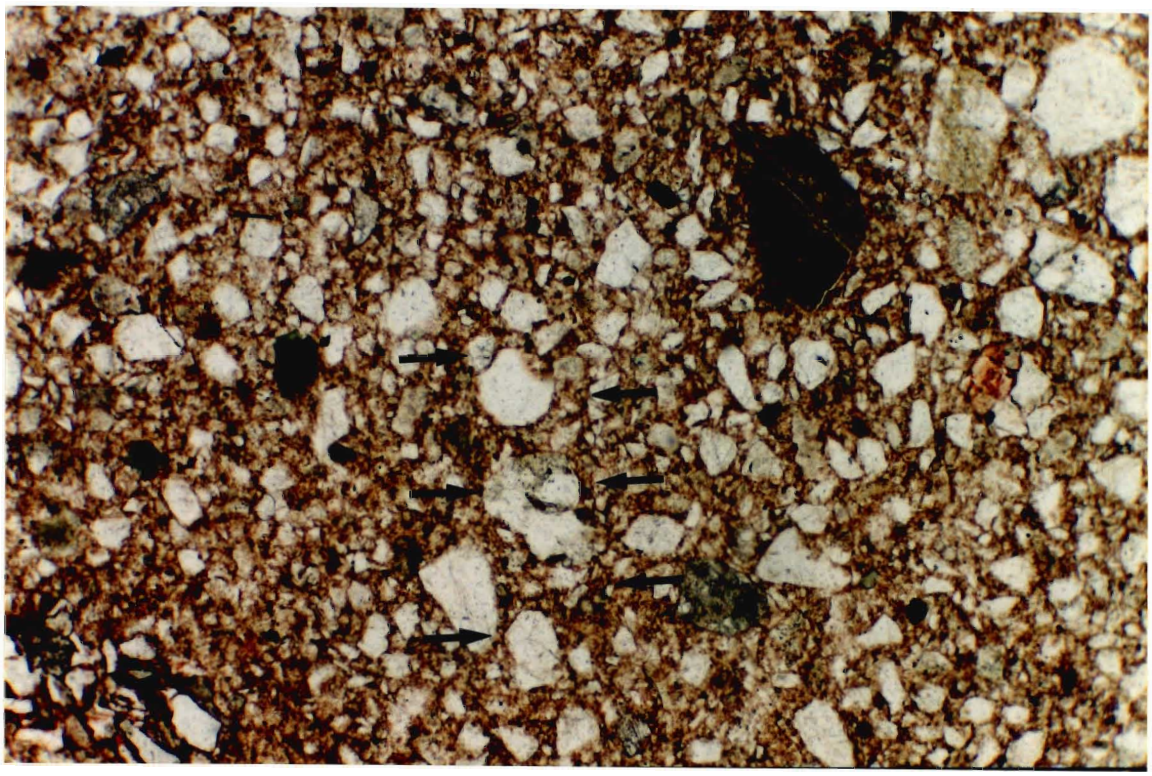

0 1.0 mm

Plate 4.31 Detail of location 31 illustrated in Plate 4.30 showing a band of skeleton grains (small arrows) within the diamicton.

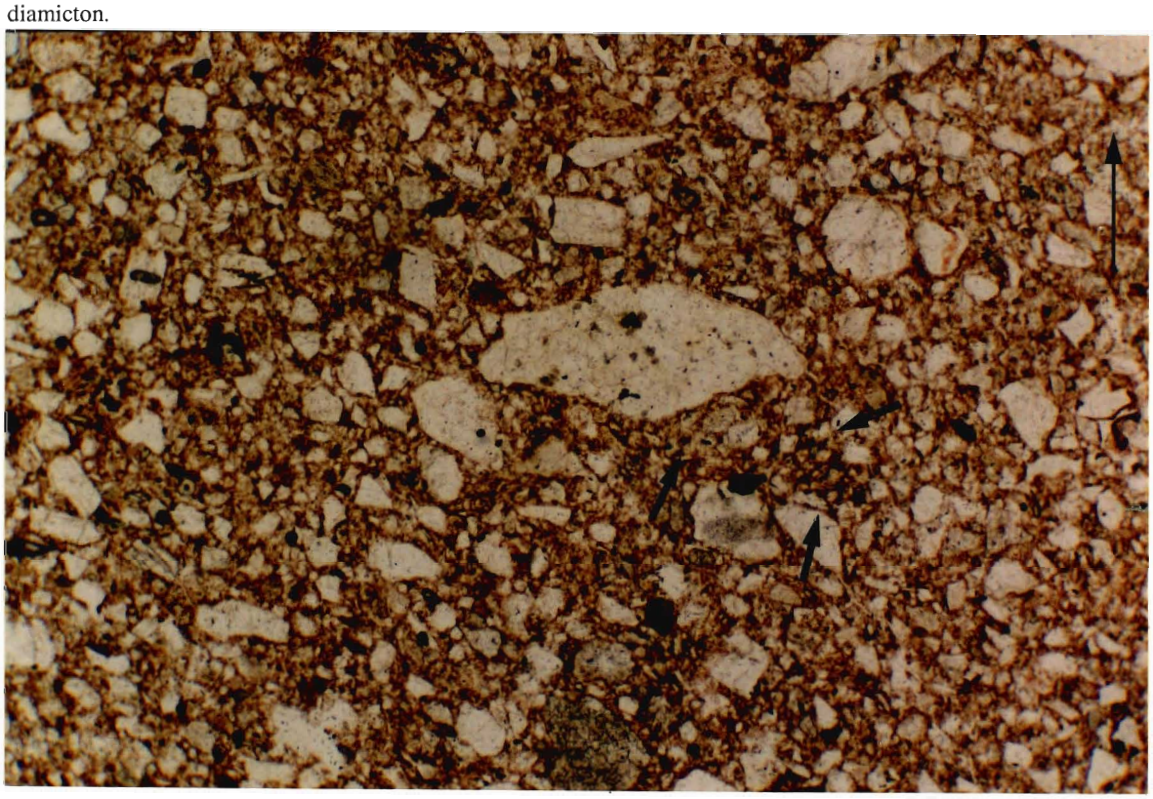

0 1.0 mm

Plate 4.32 Detail of location 32 illustrated in Plate 4.29 showing a triangular patch (small arrows) of finer-grained material.

distribution: random throughout the sample.

composition: mainly quartz; some plagioclase, chlorite and clinopyroxene; the larger grains tend to be sandstone and fossiliferous limestone.

plasma: homogeneous clay.

structure: banding of skeleton grains is the most common feature of the sample (Plate 4.31) in conjunction with skeleton grains oriented parallel to the surface of the larger clasts. Triangular patches of fines are also found at one or both ends of elongate clasts within the diamicton (Plate 4.32) in addition to "lineations" which occasionally form "tails" at one end of some of the larger clasts.

aggregates: reddish-brown Fe-staining(?) of the plasma is uniform throughout the sample.

plasmic fabric: strongly-developped skelsepic fabric.

C. Interpretation

Differential movement within the diamicton is indicated by the various features observed in the sample. Banding and lineations of skeleton grains suggests zones of discrete relative motion as do the casings of skeleton grains around the larger clasts and the well-defined skelsepic plasmic fabric. Similarly, tails of skeleton grains stretching out from one end of a larger clast in addition to the triangular patches of fines suggest that differential movement has occurred within the diamicton matrix. The sample could reflect the saturated and high bulk strain environment associated with a deforming till.

Sample 93-CBB-22

Sample of diamicton surrounding to sandy silt layer approximately 30 m above the shoreline at *site 22*. Strike of the sample is 330° with a dip of 29°.

A. Macroscopic

This is a sample of apparently massive diamicton with several shrinkage cracks and

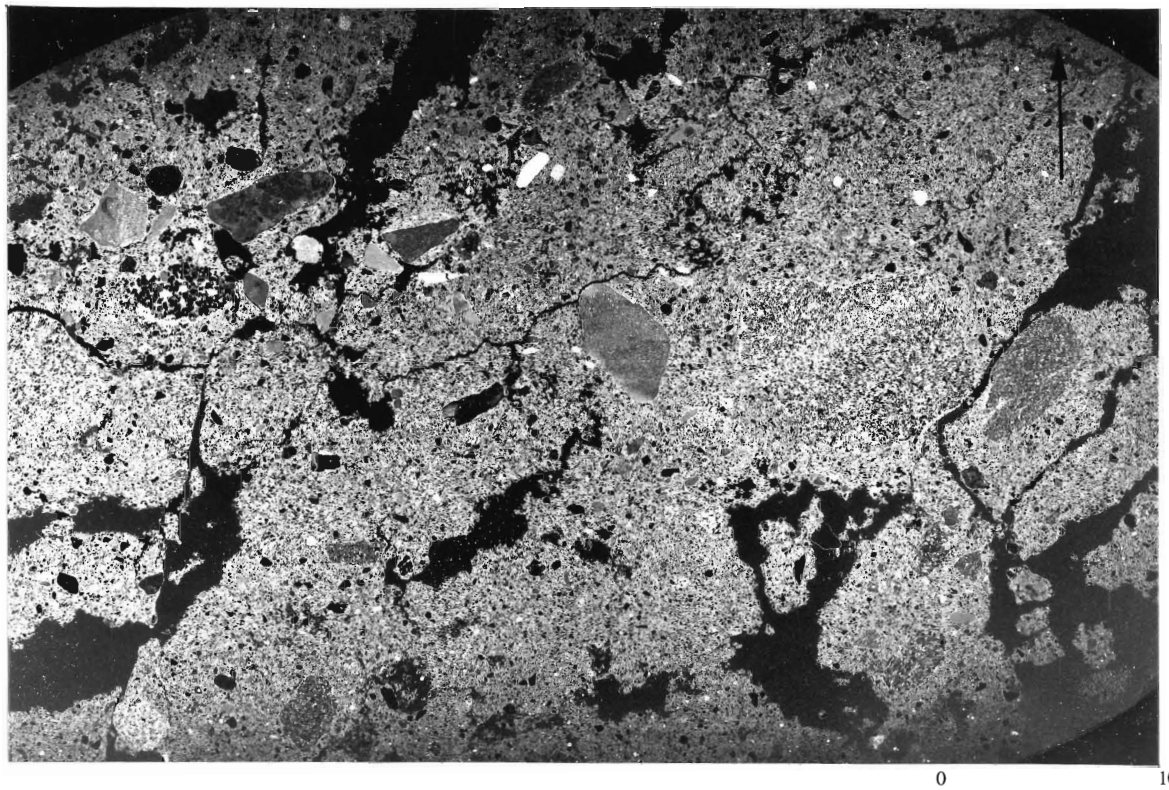

Plate 4.33 Sample 93-CBB-22 taken from diamicton surrounding the sandy silt layer at *site 22*.

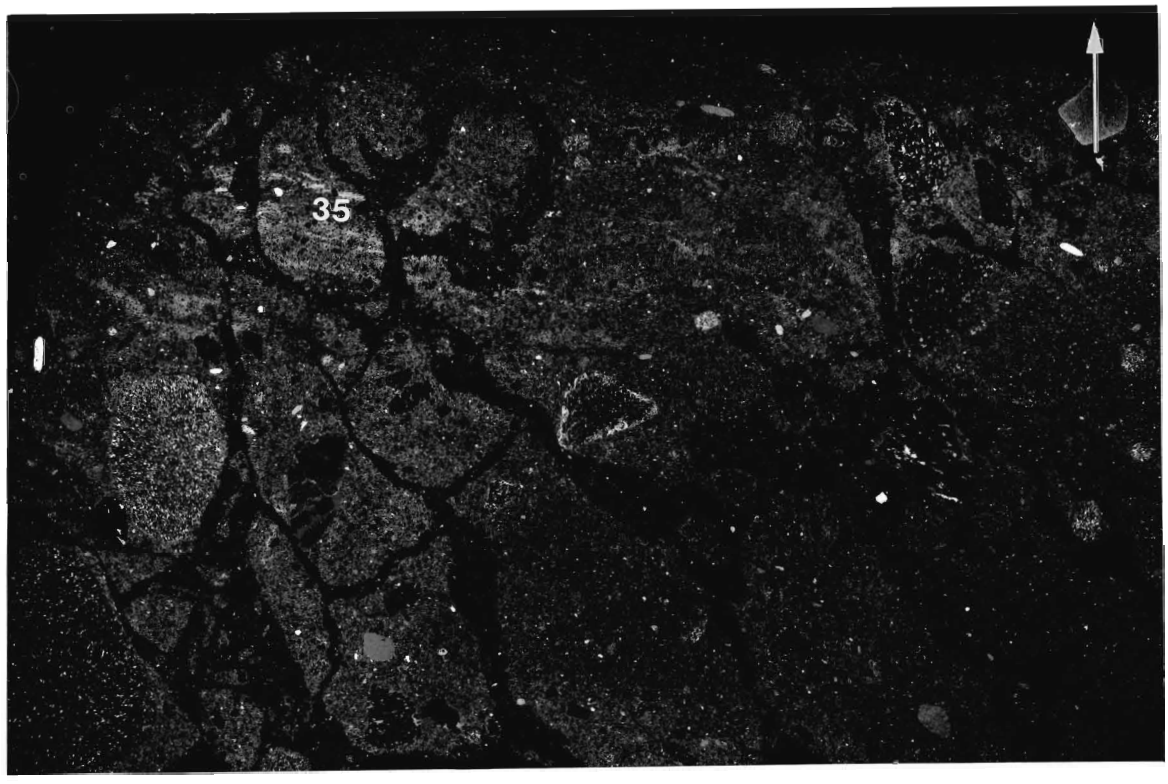

Plate 4.34 Sample 93-CBB-23 taken from fissile diamicton at *site 23*.

voids caused by improper preparation (Plate 4.33). A feature that is not clear on the Plate is a zone of grey (10YR6/1) diamicton in the upper left corner of the sample. Vague casings of skeleton grains around the larger grains are also apparent.

B. Microscopic

skeleton:

size: grains range from < 50 µm to approximately 1 cm with a mode of approximately 150 µm.

shape: grains range from angular(most) to rounded; larger grains (> 2 mm) tend to be rounded.

distribution: random throughout the sample.

composition: mainly quartz; some plagioclase, chlorite and clinopyroxene; the larger grains tend to be sandstone and fossiliferous limestone.

plasma: homogeneous clays throughout.

structure: massive diamicton with uniform dense matrix and occasional casings of skeleton grains and plasma around larger clasts.

aggregates: reddish-brown Fe-staining(?) of the plasma is uniform throughout the sample.

plasmic fabric: strongly-developped skelsepic fabric.

C. Interpretation

Differential movement or autokinetic deformation has occurred in response to an applied strain as suggested by the occurrence of casings of skeleton grains around larger clasts and the well-defined skelsepic plasmic fabric. The grey diamicton within the upper left zone cannot be distinguished on a structural or textural basis from the underlying diamicton and the two are thought to have been affecting by the same deformational processes.

Sample 93-CBB-23

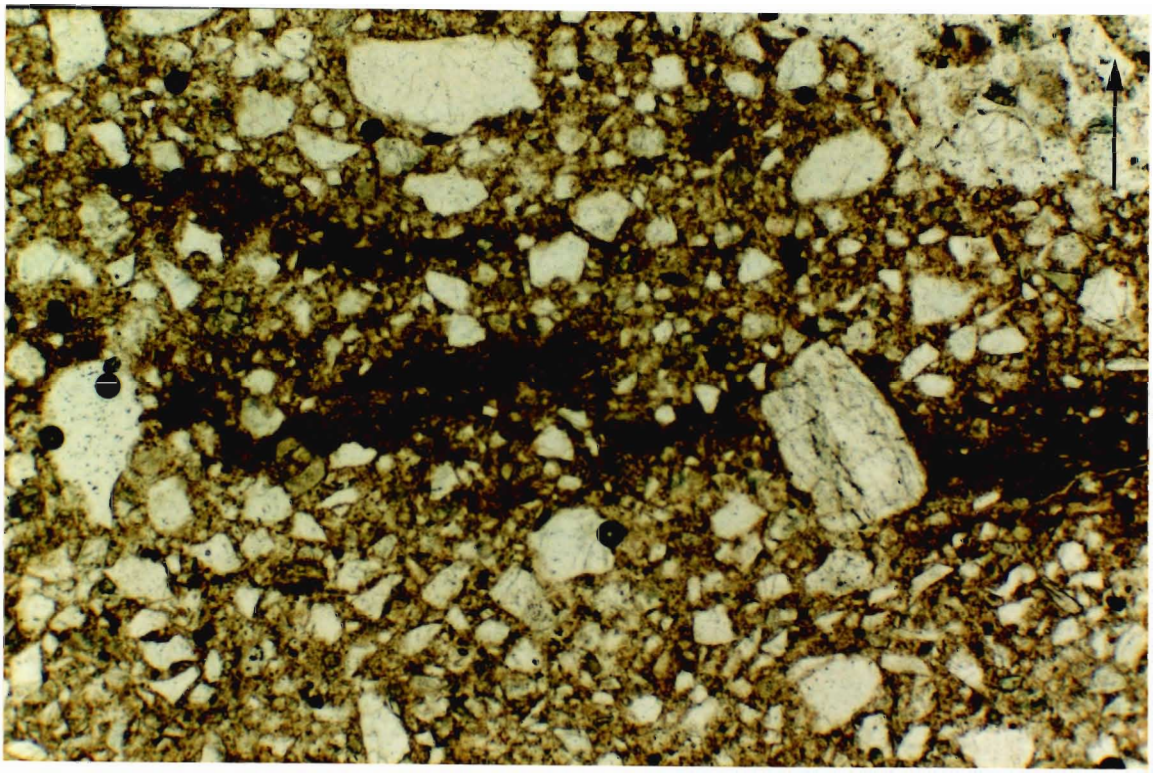

0 1.0 mm

Plate 4.35 Detail of location 35 illustrated in Plate 4.34 showing folded clay bands that attenuate into boudinage structures.

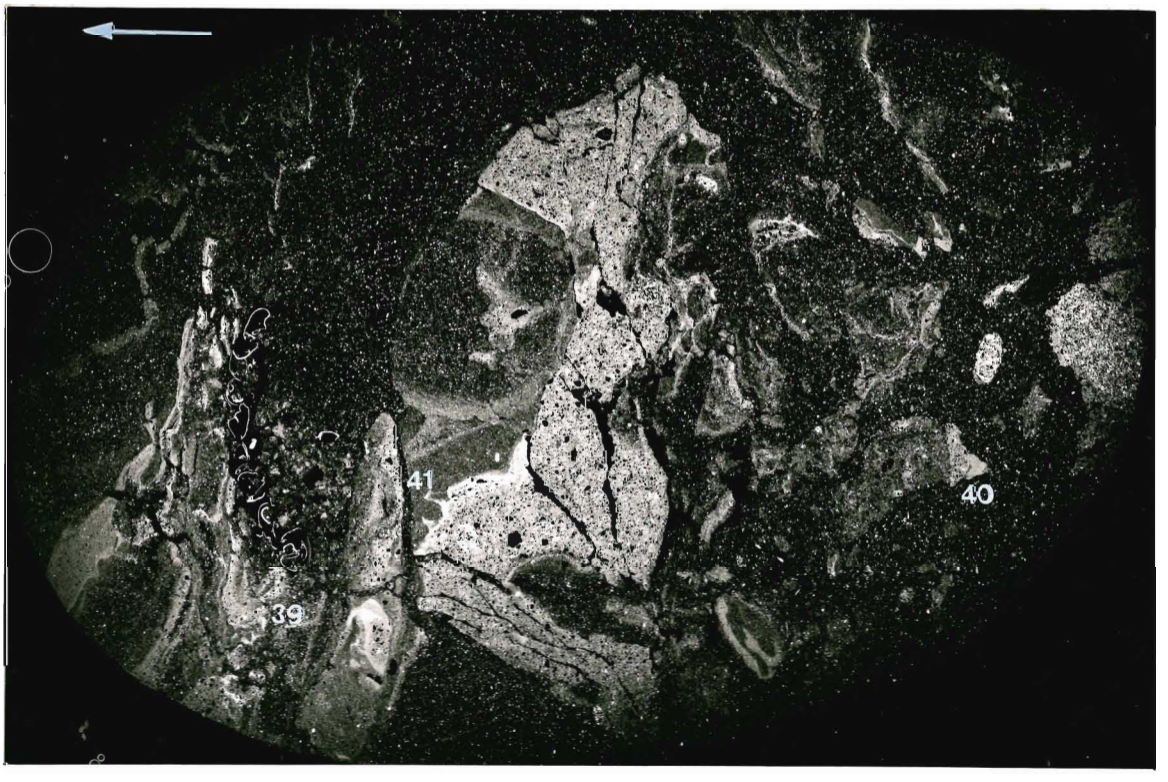

0 10 mm

Plate 4.36 Sample 93-CBB-24A of diamictic pellets taken from central portion of sand intraclast at *site 24*.

Sample of fissile diamicton taken approximately 32 m above the shoreline at *site 23*. Strike of the sample is 304° with a dip of 5°.

A. Macroscopic

The overall fractured appearance of this diamicton sample is the result of drying and sample preparation (Plate 4.34). Hence, not much can be said about the macromorphology of the sample apart from the presence of "wispy" clay-rich bands and vague casings of skeleton grains around the larger grains.

B. Microscopic

skeleton:

size: grains range from < 50 µm to approximately 0.5 cm with a mode of approximately 150 µm. Domains of silt are also present.

shape: grains range from angular(most) to rounded; larger grains (> 2 mm) tend to rounded.

distribution: random throughout the sample, but absent from the silt domains.

composition: mainly quartz; some plagioclase, chlorite and clinopyroxene; the larger grains tend to be sandstone and fossiliferous limestone.

plasma: homogeneous clay throughout the sample.

structure: discontinuous vague discontinuous shear planes(?) appear to be associated with clay bands. Deformed clay bands are observed to wrap over and under clasts and in places appear to attenuate to form boudinage structures (Plate 4.35).

aggregates: reddish-brown Fe-staining(?) of the plasma is uniform throughout the sample.

plasmic fabric: strongly-developped skelsepic fabric.

C. Interpretation

"Wispy" clay-rich bands, casings of skeleton grains around larger clasts and the strongly-developped skelsepic plasmic fabric suggest differential movement under very high

bulk strain. The ill-defined discontinuous shear planes could actually be fissures within the diamicton as their appearance is similar to those described by Meer (1993). Hence a deforming till bed origin could be applied to the sample.

Sample 93-CBB-24A

Sample of the diamictic pellets taken from the central zone of the sand intraclast approximately 18 m above the shoreline at *site 24*. Strike of the sample is 130° with a dip of 29°.

A. Macroscopic

The sample has several distinguishing features, the most notable being diamictic inclusions (Plate 4.36). Starting at the top, a folded and micro-faulted light coloured clay band is present. Underneath and to the left of this band is a zone of highly convoluted diamictic and laminated clay inclusions whose layering appear to "flow" into a large underlying void space. The space appears to be a series of inter-connected pores containing remarkably preserved argillans. Beneath this zone a few isolated pores, one containing a single argillan, are present.

At the centre of the sample is a large angular diamictic inclusion with shrinkage cracks. The apparent sandstone clast at the top of this inclusion is actually a silt-rich zone containing a smaller diamictic inclusion. Between the large diamictic inclusion and the finer-grained zone is a sharp, almost linear boundary with only a slight amount of inter-fingering on the far left.

Beneath the inclusion is a zone of highly deformed laminated(?) clay bands and diamictic(?) inclusions. Plate 4.37 is a thin section taken at 90° to the upper portion of the long-axis of the sample illustrated in Plate 4.36.

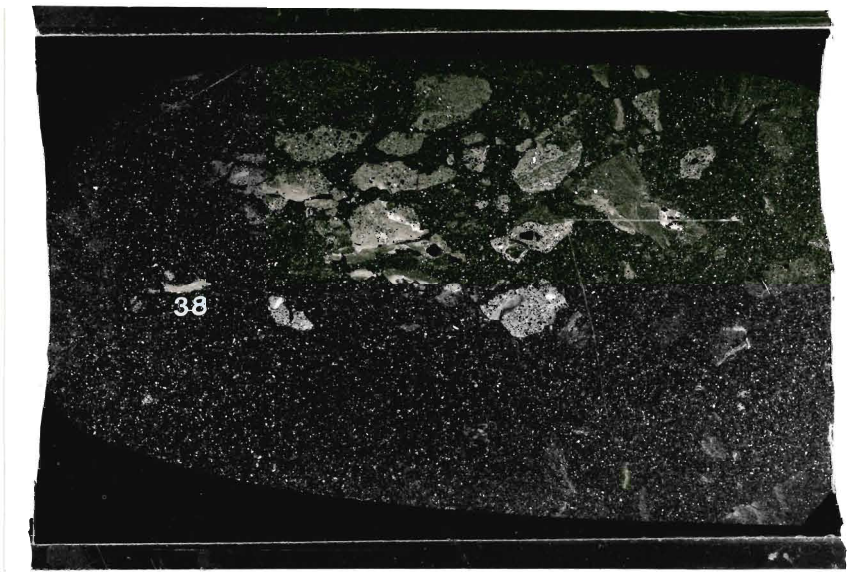

0 1.0 mm

Plate 4.37 Thin section from the upper portion of sample 93-CBB-24A cut at 90° to the long axis illustrated in Plate 4.36.

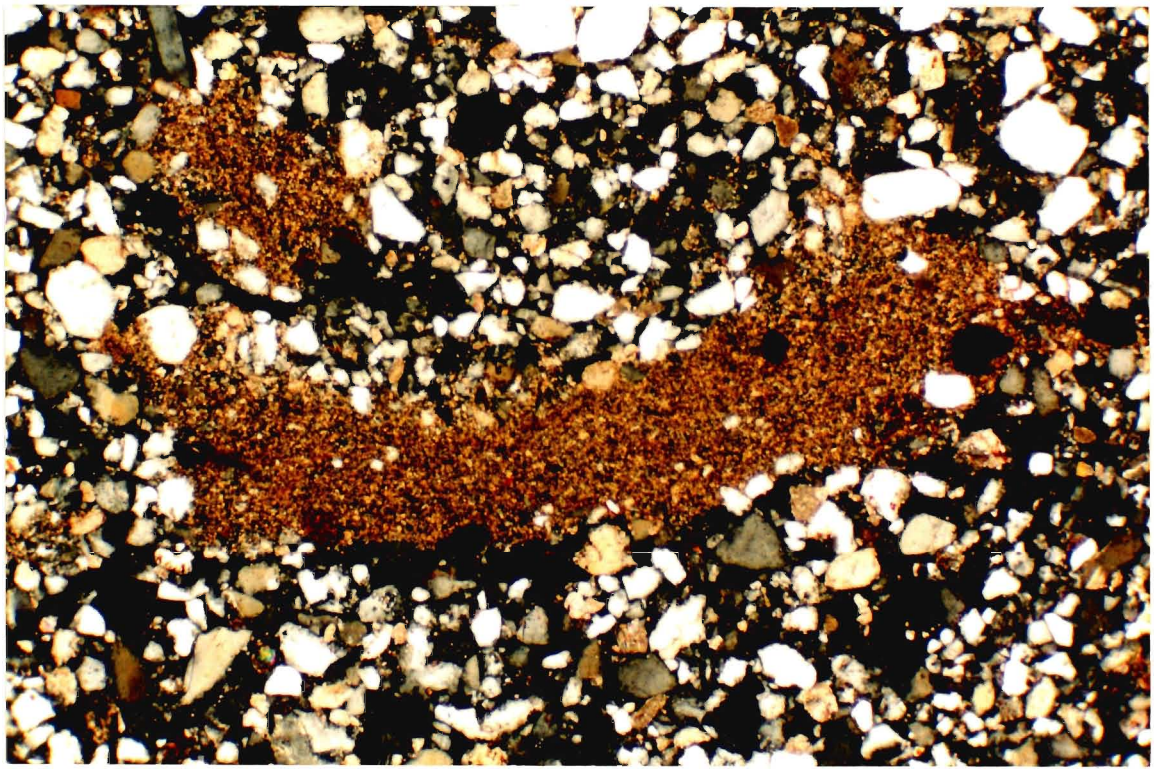

0 1.0 mm

Plate 4.38 Detail of location 38 illustrated in Plate 4.37 with cross-polars showing massive clay boudins.

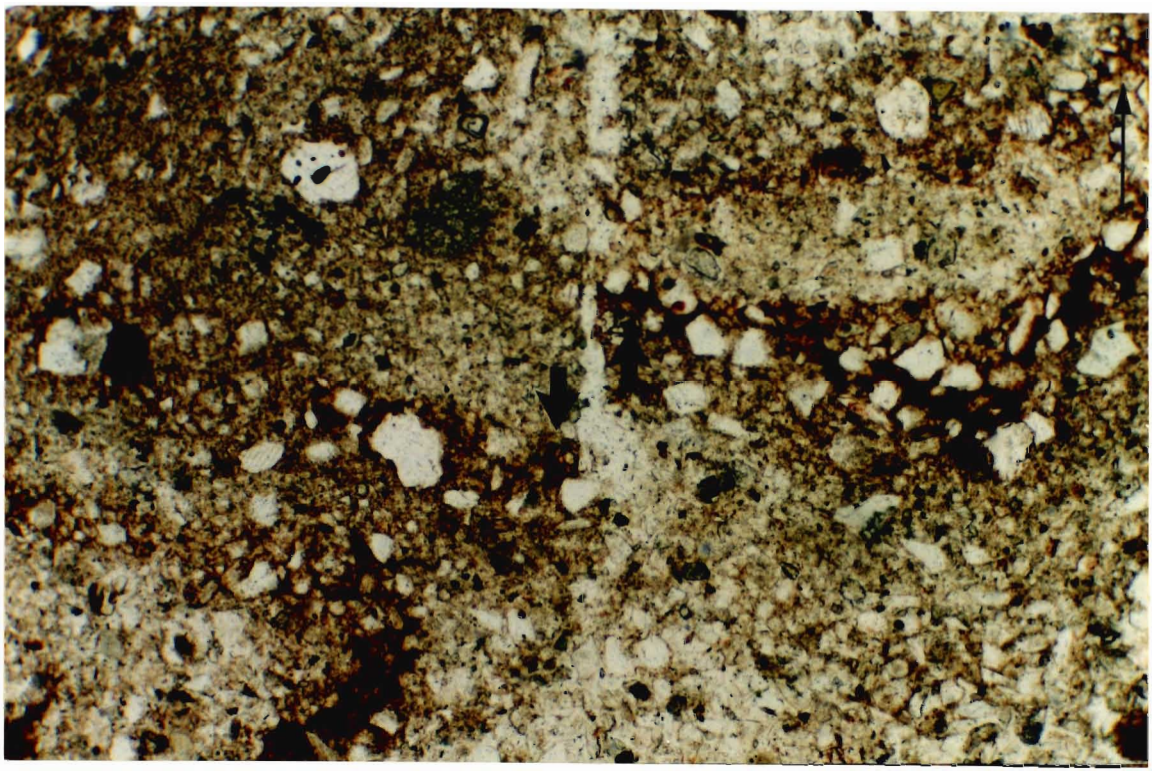

0 1.0 mm

Plate 4.39 Detail of location 39 illustrated in Plate 4.36 showing faulted clay laminae.

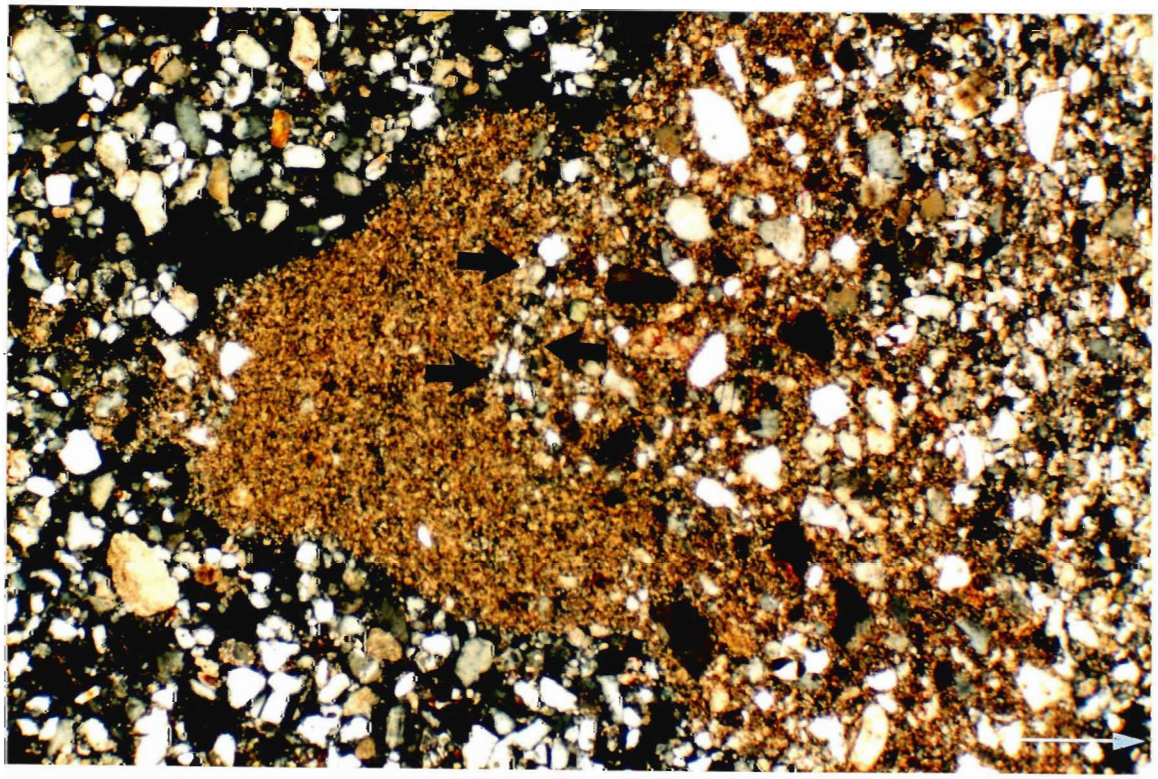

0 1.0 mm

Plate 4.40 Detail of location 40 illustrated in Plate 4.36 with cross-polars showing the formation of a fine grained diamictic clast. Note the infilled fracture to the right of the partially formed clast.

B. Microscopic

skeleton:

size: grains range from < 50 µm to approximately 500 µm with a mode of approximately 50 µm in the sand unit and 100 µm in the diamictic inclusions.

shape: grains range from angular in the diamictic inclusions to (well) rounded in the sand unit; larger grains (> 2 mm) tend to be rounded.

distribution: in both sediments is random.

composition: mainly quartz; some plagioclase, chlorite and clinopyroxene; the larger grains tend to be sandstone and fossiliferous limestone.

plasma: mostly homogenous clays in the diamictic inclusions and clay bands.

structure: a well-preserved zone of argillans similar to the one illustrated in Plate 4.49 is apparent in the thin section. Clays within these structure range from massive to laminated and do not appear to have been deformed. In some areas finely-laminated to massive clayey boudins (Plate 4.38) are observed. In the case of the latter, note the discontinuous shear plane that cross-cuts the inclusion. Elsewhere, laminated clay inclusions have been deformed and faulted (Plate 4.39) whilst others have been fragmented and separated by bifurcating "necking" structures of fine- to medium-grained sands similar to those illustrated in Plate 4.45. Discontinuous shear planes appear to be random and are observed to cross-cut each other at oblique angles in the sand portion of the sample. Plate 4.40 is an example of the formation of fine-grained diamictic "clast" at the edge of a diamictic inclusion. Note the partially developped fracture at the top of the sub-rounded "clast" infilled with medium-grained sand in addition to the slight diffusion of plasma into the sand unit at the lower edge of the "clast". A similar feature is seen in Plate 4.41 wherein flow-noses of clay protrude into a silt-rich zone. Observe also the infilled fracture in the upper left of the Plate that

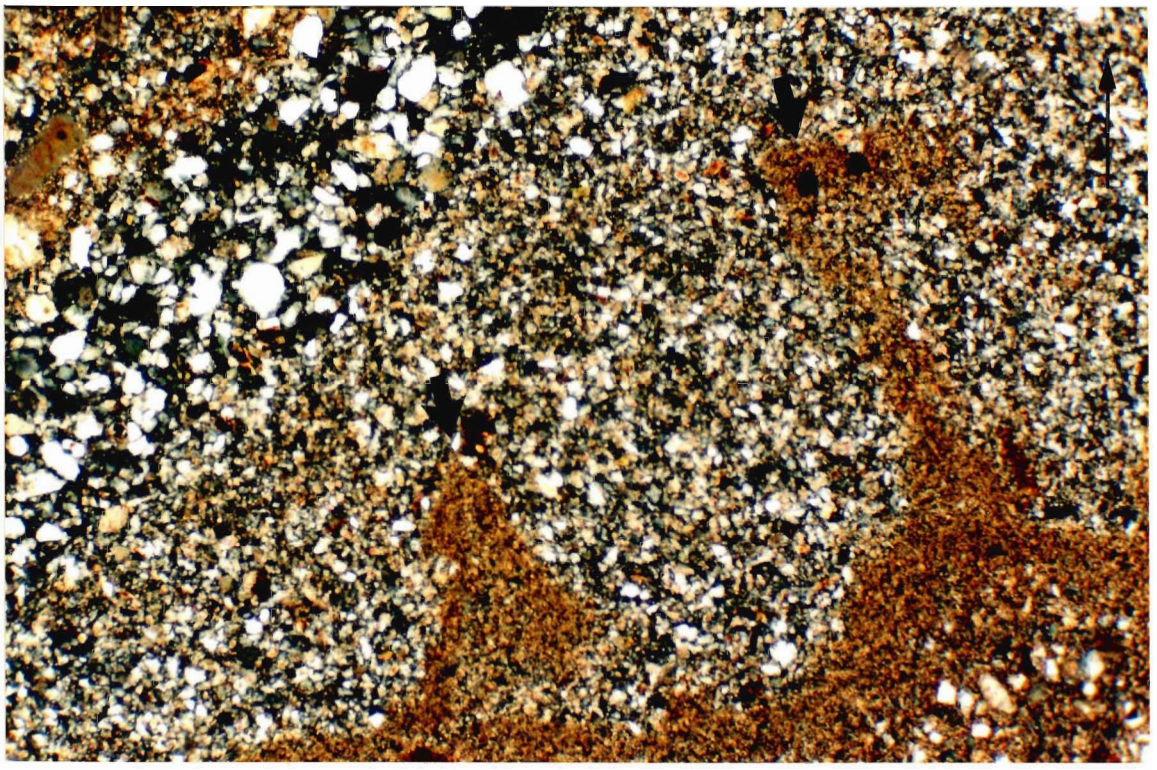

0 1.0 mm

Plate 4.41 Detail of location 41 illustrated in Plate 4.36 with cross-polars showing the flow-type nose of clay-rich material into a fine grained sand.

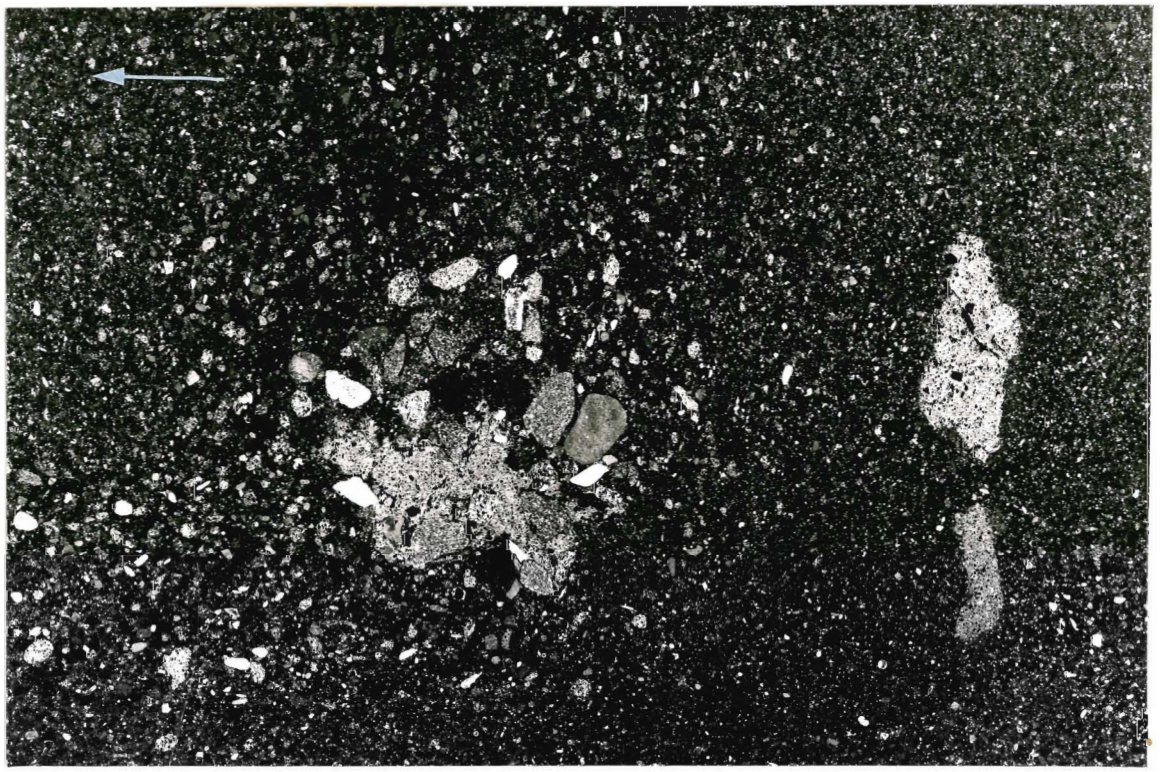

0 10 mm

Plate 4.42 Sample 93-CBB-24B taken from coarse sand lens within sand intraclast at *site 24*.

separates two large diamictic fragments/inclusions. Lineations and bands of skeleton grains are also prevalent in the sand unit.

aggregates: reddish-brown Fe-staining(?) is texturally restricted to the diamictic and clay bands.

plasmic fabric: weakly-developped skelsepic fabric within the clay-rich areas.

C. Interpretation

The sample appears to have been subjected to high porewater pressures and associated stresses during its development. The highly convoluted laminae and the sub-rounded character of the lower clay band inclusions suggest differential and/or rotational movement within the sand unit. Again, the laminated clay bands probably reflect low flow conditions, which changed to a high energy flow as implied by the fragmenting of these laminae and the surrounding diamicton. Autokinetic deformation during transport of the intraclast is suggested by banding, necking and casings of skeleton grains and the partial development of a diamictic "clast" in the matrix of the larger diamictic inclusion and flow-noses of finer grained material. However, the presence of clay boudins, infilled fractures and obliquely intersecting discontinuous shear planes are indicative of the very high shear stresses necessary to incorporate the diamictic inclusions. During transport, high subglacial porewater pressures could have saturated the contact zone of the intraclast, thereby distorting primary structures and allowing for the rounding and deformation of the diamictic inclusions. The occurrence of argillans is indicative of clay translocation due to groundwater flow associated with soil formation (Meer, 1987). However Meer (1987) has also suggested that this process could also occur immediately following till deposition and therefore the argillans could be related to the fine-grained domains illustrated in Plates 4.6 and 4.14 which were attributed to pore water dissipation. In any case, the lack of deformed argillans would appear to suggest that

they formed after the application of high strain rates, possibly after the till became immobile.

Sample 93-CBB-24B

The sample was taken from a coarse sand lens within the sand intraclast approximately 18 m above the shoreline at *site 24*. Strike of the sample is 135° with a dip of 20°.

A. Macroscopic

The sample can be divided into two zones based skeleton grain sizes with the upper zone having a higher concentration of larger grains (Plate 4.42). The focus of the larger grains is a rounded diamictic inclusion about which they appear to be arranged in a circular pattern. The boundary of the inclusion with the coarser grains is rather sharp with only a slight amount of intermixing observed.

The lower zone comprises fine skeleton grains and two horizontal elongate diamictic inclusions with sharp boundaries. Skeleton grains encase both of the inclusions, but no other structures are noted.

B. Microscopic

skeleton:

size: grains range from < 50 µm to approximately 2 mm with a mode of approximately 150 µm. A domain of coarser grains with a mode of approximately 500 µm is found in the upper zone of the sample.

shape: grains in both zones range from angular to (well) rounded(most).

distribution: in both zones is random.

composition: mainly quartz; some plagioclase, chlorite and clinopyroxene with some sandstone and fossiliferous limestone.

plasma: mostly homogenous clay restricted to the diamictic inclusions.

structure: the coarse sand zone around the diamictic inclusion in the centre of the sample has a high concentration of rounded diamictic "clasts". The clasts are obviously derived from the central inclusion as evidenced by discontinuous "strings" of plasma extending outward from the central inclusion into the coarse sand zone. Various ill-defined discontinuous shear planes cross-cutting each other at oblique angles occur throughout the sands and in some instances, in the diamictic inclusions. Lineations and possible kink banding of skeleton grains tends to be confined to the finer grained lower zone of the sample.

aggregates: reddish-brown Fe-staining(?) is texturally restricted to the diamictic inclusions.

plasmic fabric: vague skelsepic fabric in the diamictic inclusions.

C. Interpretation

The zonation of coarser grains around the rounded diamictic inclusion suggests a water saturated matrix in which "sieving" of the finer grains has occurred. Rounded diamictic clasts within this zone are indicative of differential and rotational movement within the sand unit. These features could be or a primary origin, but are more likely due to post-depositional dewatering and transport of the intraclast in a deforming till layer. The boudinaged diamictic inclusion in the lower zone could reflect a partially frozen matrix to which very high bulk strain has been applied. The presence of randomly oriented discontinuous shear planes, some of which cross-cut the boudins, appear to support this idea as does the occurrence of kink banding and lineations in the lower zone.

Sample 93-CBB-26

Sample of a the irregular contact between a small "wispy" sand lens and the surrounding diamicton taken approximately 21 m above the shoreline at *site 26*. Strike of the sample is 146° with a dip of 20°.

A. Macroscopic

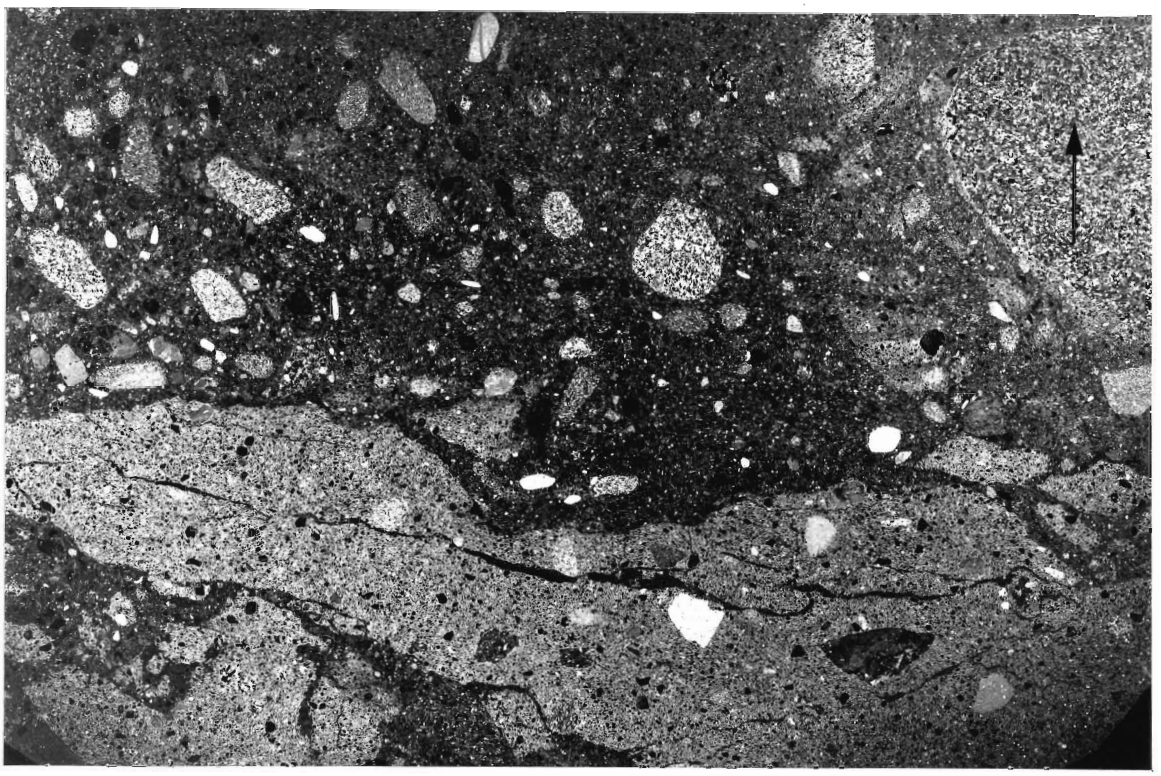

0 10 mm

Plate 4.43 Sample 93-CBB-26 taken from contact between "wispy" sand lens and diamicton at *site 26*.

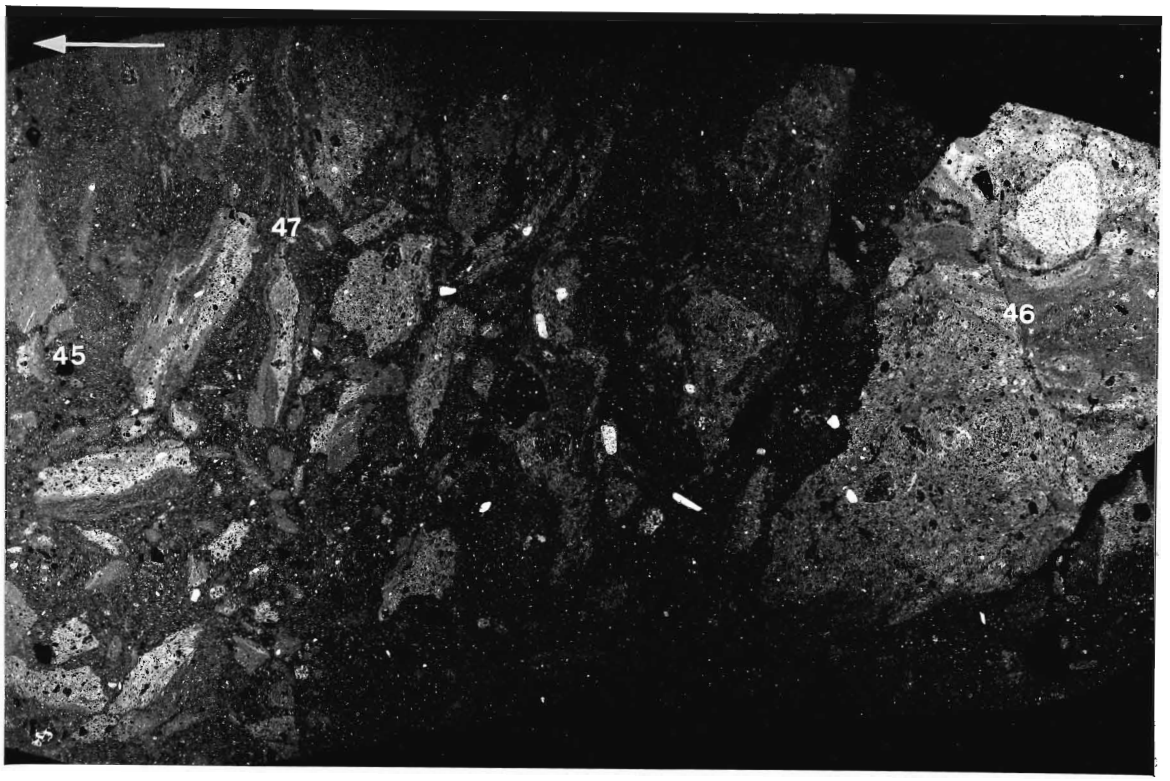

0 10 mm

Plate 4.44 Sample 93-CBB-26B of sandy silt and diamictic inclusions within sand intraclast at *site 26*.

A lower diamicton zone and an upper poorly sorted sand and gravel zone are apparent in the sample (Plate 4.43). The diamicton is inter-fingered with the sand unit and a zone of brecciated diamicton inclusions surrounds the main diamicton "finger". The boundary between the diamicton and the sand unit may therefore be thought of as being gradational in addition to sharp and irregular.

The upper zone contains many rounded clasts that appear to be randomly oriented. A large clast on the upper right is encased by zone of fine-grained diamictic layers approximately 1 cm wide. Skeleton grains throughout the sand unit encase the various clasts and diamictic inclusions.

B. Microscopic

skeleton:

size: grains range from < 50 µm to approximately 0.5 cm with a mode of approximately 100 µm in the upper zone and 150 µm in the lower zone.

shape: grains range from mostly angular in the lower zone to rounded in the upper zone; larger grains (> 2 mm) tend to be rounded.

distribution: in both zones is random.

composition: mainly quartz; some plagioclase, chlorite and clinopyroxene; the larger grains tend to be sandstone and fossiliferous limestone.

plasma: rare in the upper zone where non-homogeneous clays are mostly found around the larger grains; homogenous clay in the throughout the lower zone diamicton.

structure: circular structures can be observed throughout the sands of the upper zone in addition to slight intermixing of plasma from the diamictic inclusions with the sand unit. Ill-defined banding and skeleton grains oriented parallel to larger clasts in the upper zone are also apparent.

aggregates: reddish-brown Fe-staining(?) is texturally restricted to the diamicton in the lower zone and the diamictic inclusions in the upper zone.

plasmic fabric: strongly-developped skelsepic fabric within the diamicton.

C. Interpretation

The irregular and gradational contact observed in this sample indicates that stress has been applied at least to the edges of the sand lens. Angular inclusions of unmodified (?) diamicton at the contact attest to the intensity of the strain applied. Furthermore, the massive poorly sorted sediment of the lens and the slight intermixing of plasma from the diamictic fragments implies that this contact zone was saturated at the time of deposition. These features are also adducible to mass flow conditions, possibly within a subglacial conduit or in a proglacial glaciofluvial sequence. Other structures for differential and/or rotational movement within the unit, namely banding and casings of skeleton grains around the larger clasts and inclusions and the well-defined skelsepic fabric in the diamicton can be ascribed to transport within a deforming till layer.

Sample 93-CBB-26B

Sample of sandy silt and diamictic pellets within the sand intraclast approximately 20 m above the shoreline at *site 26*. Strike of the sample is 125° with a dip of 18°.

A. Macroscopic

Several angular to sub-angular diamictic inclusions are contained within a massive fine-grained sand unit (Plate 4.44). Most of the inclusions contain deformed(?) bands of finely laminated clays, some of which appear to continue into the surrounding sand. The orientation of the inclusions is apparently random. Skeleton grains are noticeably rare within the clay-rich bands, a feature that is noticeable in the clay-band that wraps around the side of the sandstone clast in the large inclusion at the bottom of the sample. It is not obvious

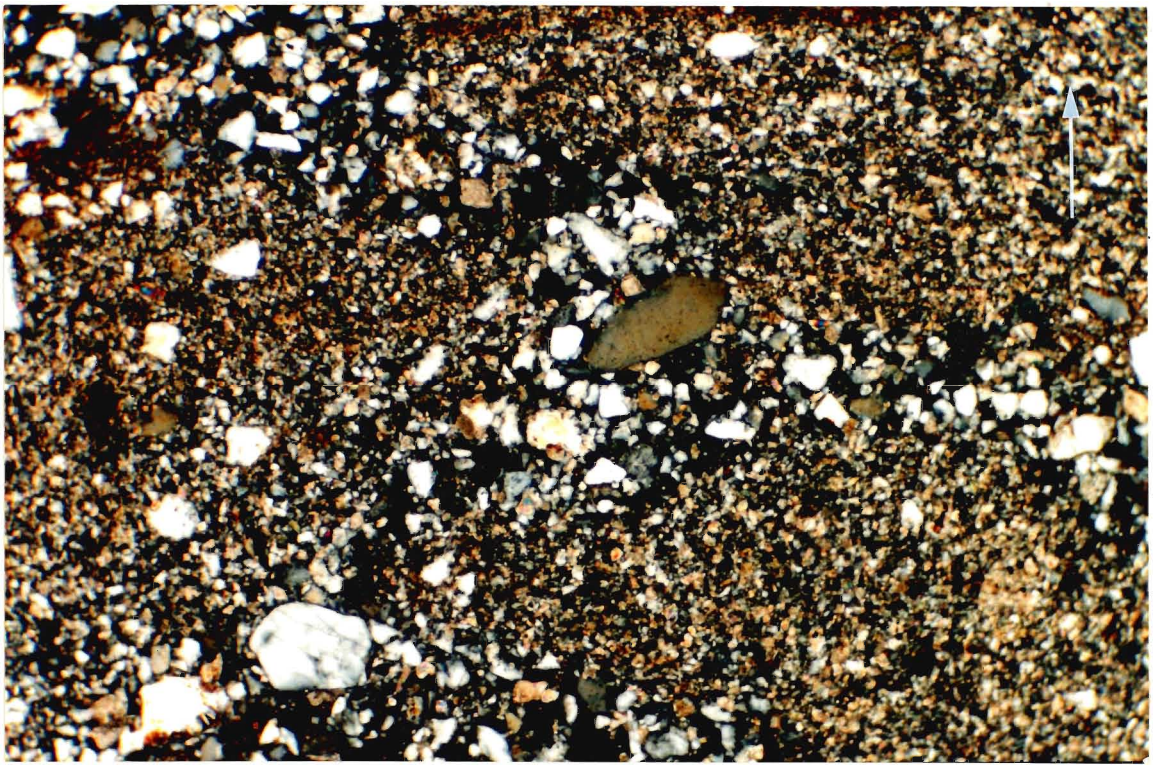

0 1.0 mm

Plate 4.45 Detail of location 45 illustrated in Plate 4.44 with cross-polars showing a bifurcating band of fine sands separating three rounded sandy silt fragments.

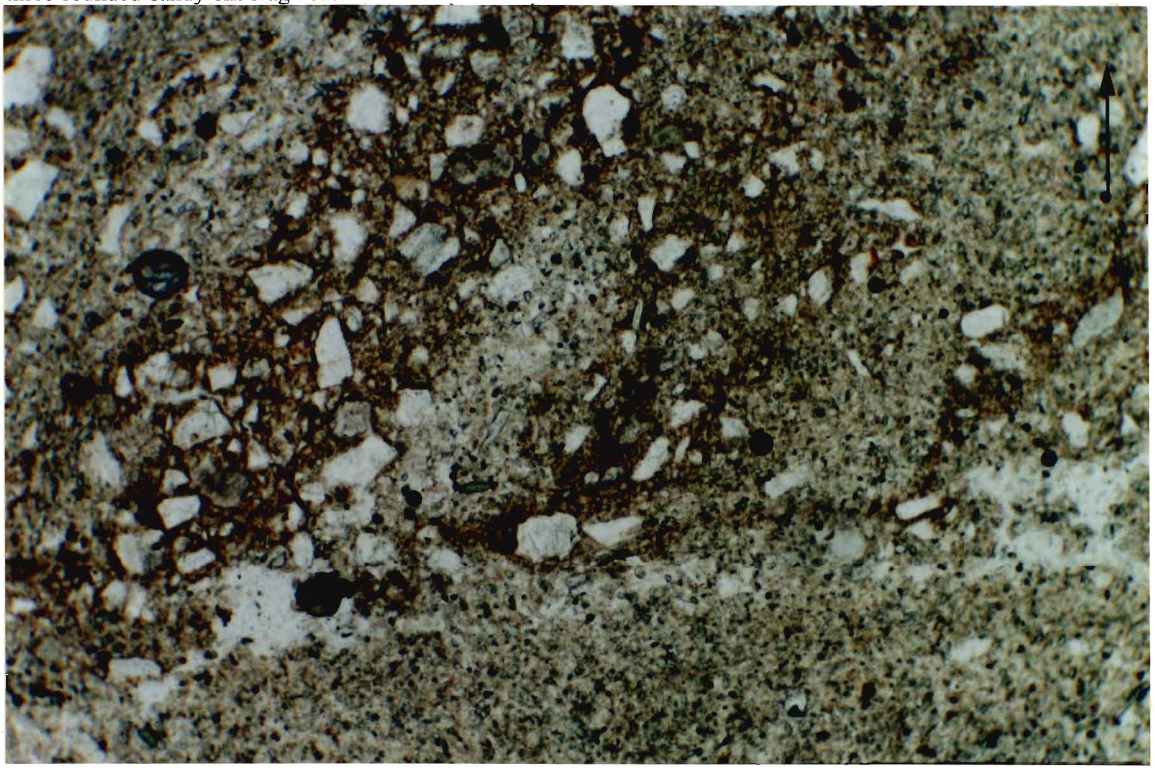

0 1.0 mm

Plate 4.46 Detail of location 46 illustrated in Plate 4.44 showing the inter-fingering of diamictic and laminated silts terminated by a possible fault (bottom).

if the skeleton grains of the sand unit form casings around the larger grains and inclusions.

B. Microscopic

skeleton:

size: grains range from < 50 μm to approximately 0.5 cm with a mode of approximately 100 μm in the upper zone and 150 μm in the diamictic inclusion in the lower zone.

shape: grains range from angular in the diamictic inclusions to rounded in the sandy areas; larger grains (> 2 mm) tend to be rounded.

distribution: in both zones is random, except in the clay-rich inclusions where both sets of modal grains are absent.

composition: mainly quartz; some plagioclase, chlorite and clinopyroxene; the larger grains tend to be sandstone and fossiliferous limestone.

plasma: rare clays in the sand unit, but mostly confined to the homogenous clays of the diamictic inclusions.

structure: the most distinguishing feature of the thin section is the numerous inclusions, some of which are themselves fragmented. Rounded fragments of a clay band are seen in Plate 4.45 are separated by a bifurcating band of fine sands in which some intermixing of plasma has occurred. Note the semicircular arrangement of skeleton grains around the quartz clast near the centre of the Plate. Inter-fingering and possible faulting of Diamicton and laminated silts is apparent within the large diamictic inclusion (Plate 4.46). Note the diffuse edges of the diamictic bands on the left and the sheared/faulted zone delineated by the upper silt laminae. The fracture fragments a silt band and its orientation appears to be controlled by the surface of the sandstone clast. Silt laminae and diamicton wrap around a limestone clast in Plate 4.47 and terminate in a flow-nose structure within the sand unit.

aggregates: reddish-brown Fe-staining(?) is texturally restricted to the diamictic inclusions.

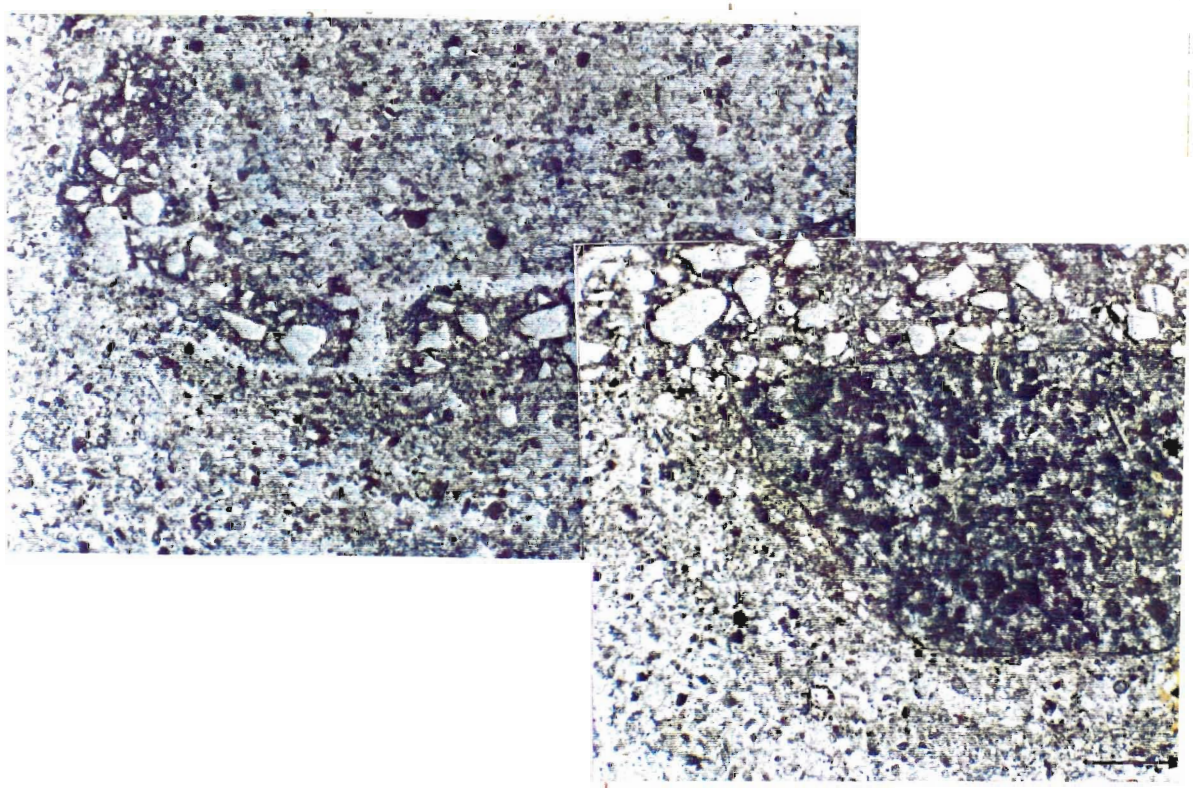

Plate 4.47 Detail of location 47 illustrated in Plate 4.44 showing the wrapping of silt laminae and diamicton around a limestone clast. Note how they terminate in a flow-type nose structure.

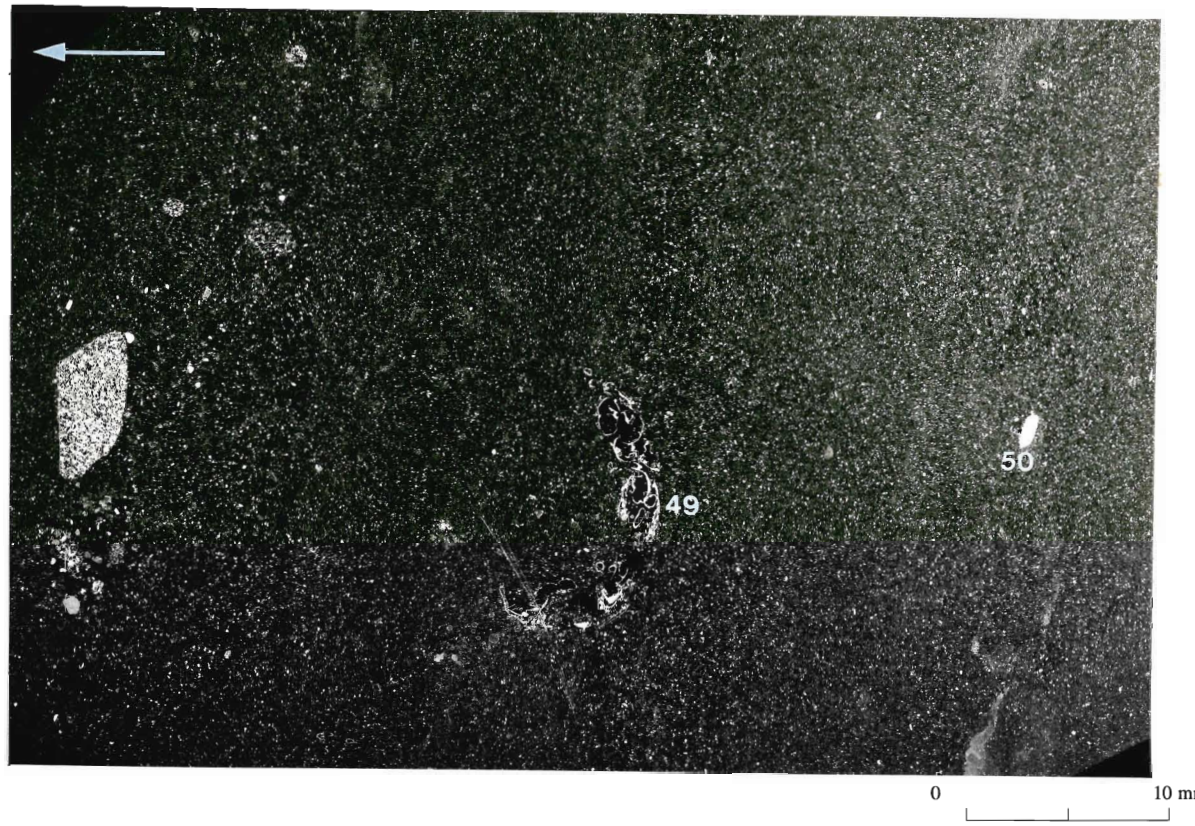

Plate 4.48 Sample 93-CBB-26C taken from the central portion of a sand intraclast at *site 26C*.

plasmic fabric: strongly-developped skelsepic fabric in the diamictic inclusions.

C. Interpretation

Saturated high porewater pressure conditions are suggested by the observed structures. Rounding of the diamictic inclusions and the re-mobilisation or the differential movement of finer grained material into flow noses and wrap around laminae are indicative of such an environment. Further examples of saturated conditions are the intermixing and inter-fingering of plasma with the massive sand unit, infilled fractures and the arrangement of skeleton grains parallel to the surface of the inclusions and larger clasts. However, brittle deformation associated with the entrainment of the intraclast within a deforming till layer is also apparent in the faulted zone of the large diamicton inclusion. This could reflect the greater density of the material, or possibly even that a thin layer of the surrounding diamicton the intraclast had been frozen upon its emplacement and subsequently broken off and emplaced within the sand unit.

Sample 93-CBB-26C

Sample of sand from the central portion of the sand intraclast approximately 20 m above the shoreline at *site 26*. Strike of the sample is 128° with a dip of 6°.

A. Macroscopic

Vague banding of coarser grains can be seen throughout the sample (Plate 4.48). Apart from the casing of skeleton grains around the clast at the top of the sample, the most interesting feature is the semi-circular void near the centre. The void is a series of inter-connected pores containing well-preserved argillans. The feature appears to cross-cut pre-existing "laminae" as defined by the coarser sand layer.

B. Microscopic

skeleton:

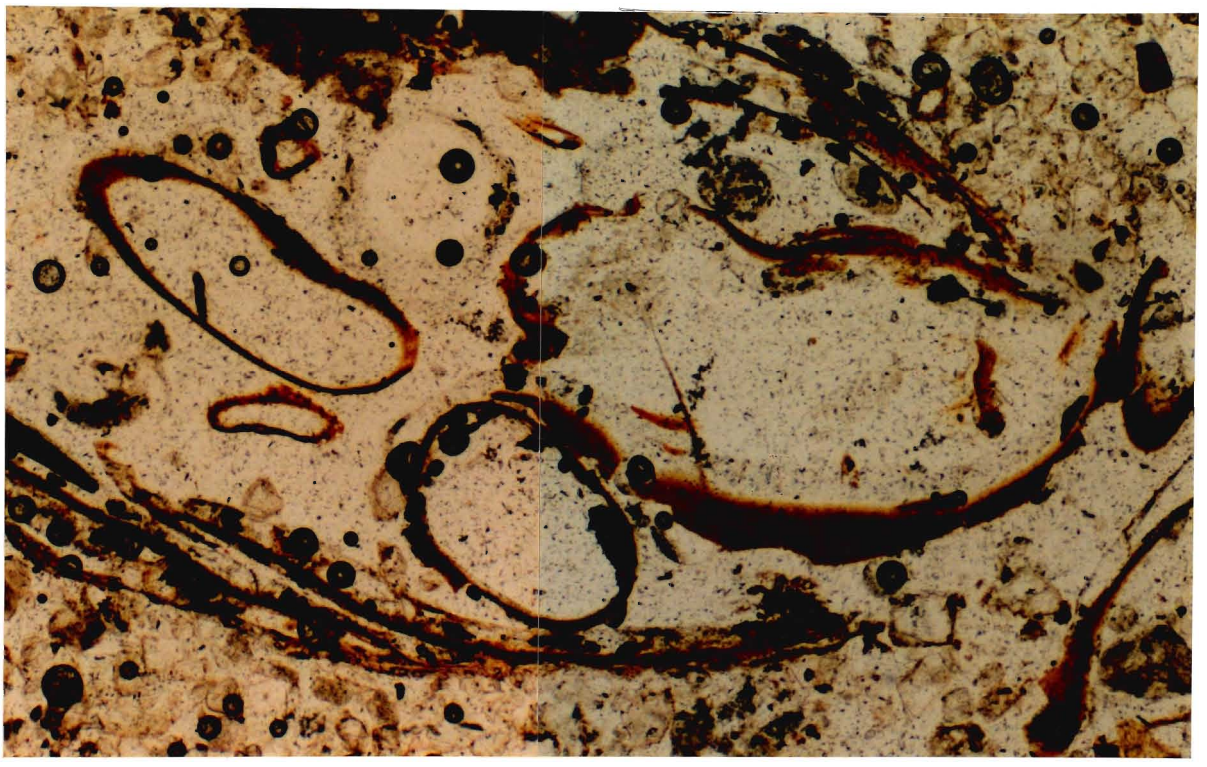

Plate 4.49 Detail of location 49 illustrated in Plate 4.48 of a zone of well-preserved argillans.

Plate 4.50 Detail of location 50 illustrated in Plate 4.48 showing a diffuse ring of secondary carbonates around a limestone clast.

size: grains range from < 50 µm to approximately 1 cm with a mode of approximately 100 µm.

shape: grains range from (well) rounded(most) to angular.

distribution: is random throughout the sample with some areas of vague banding.

composition: mainly quartz; some plagioclase, chlorite, clinopyroxene and some fossiliferous limestone.

plasma: none.

structure: the semi-circular cluster of argillans are essentially undeformed (Plate 4.49) although the argillans on the upper left appear to be slightly flattened. Indistinct discontinuous shear planes radiate outward from this semi-circular pore structure in the surrounding fine sand unit. Throughout the sand unit various circular structures and weakly-defined randomly oriented discontinuous shear planes are present, some of which intersect each other at oblique angles. Diffuse zones of secondary carbonates are also observed around several limestone clasts within the sand unit (Plate 4.50).

aggregates: reddish-brown Fe-staining(?) is restricted to casing of secondary carbonates around the large limestone clast in the upper portion of the thin section.

plasmic fabric: none.

C. Interpretation

Circular structures of skeleton grains imply that differential movement has occurred within the sand matrix. As discussed earlier, secondary carbonates could reflect high pressures within the subglacial environment which is supported by the presence of discontinuous shear planes, albeit indistinct, within the sand unit. The discontinuous shear planes radiating outward from the argillan zone are obviously related to the structure and could reflect stress applied by the circulating porewaters on the surrounding sands. As these

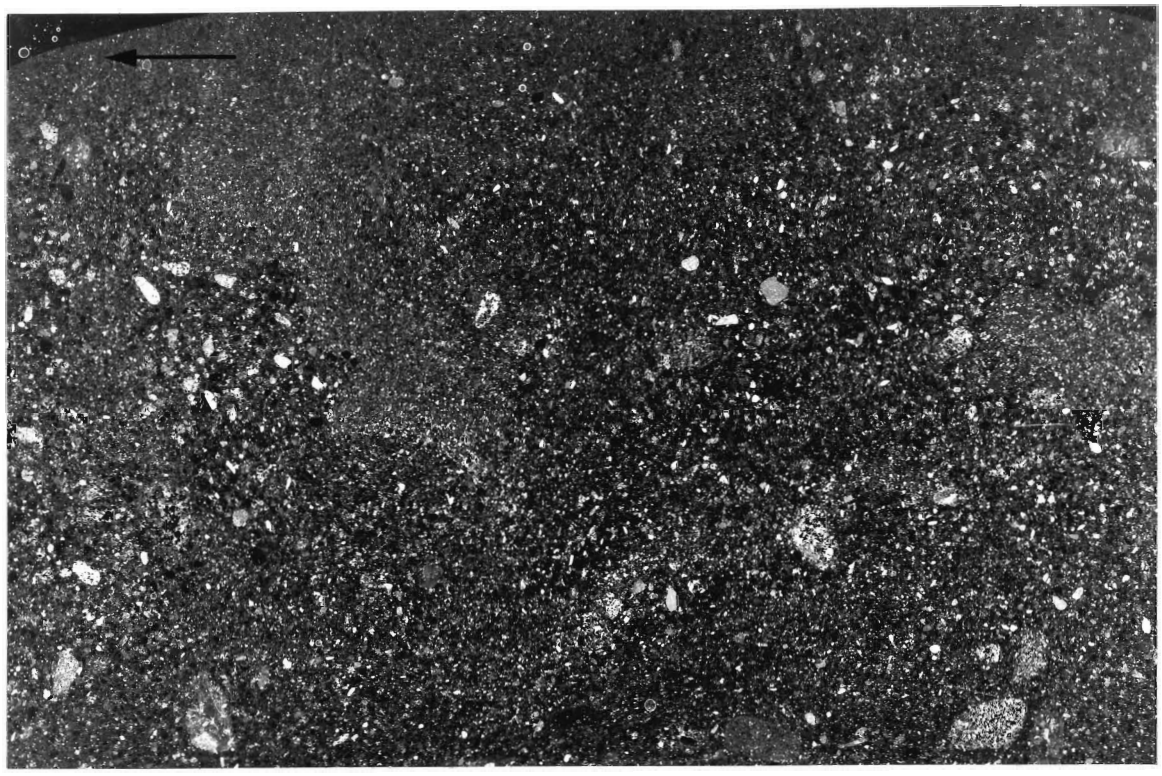

0 10 mm

Plate 4.51 Sample 93-CBB-30 taken from topmost sand layer in sand intraclast at *site 30.*

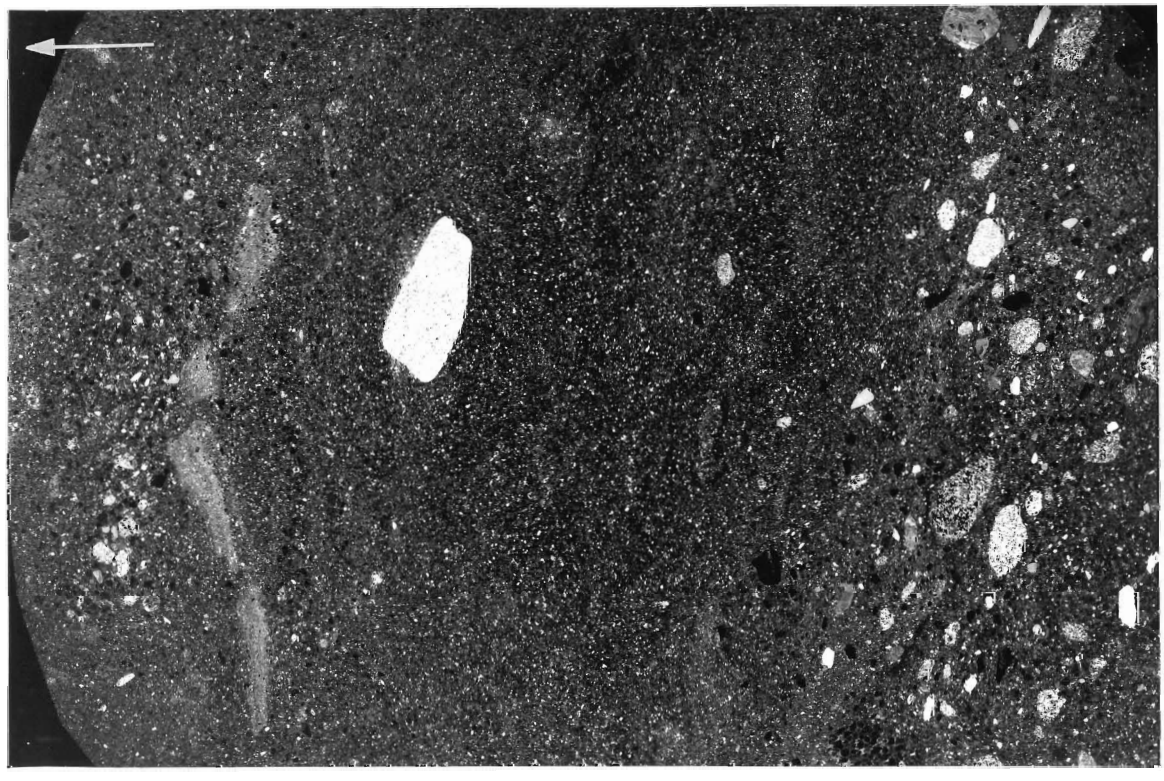

0 10 mm

Plate 4.52 Sample 93-CBB-30B taken from finer grained sand layer within the same intraclast as Plate 4.51 at *site 30.*

structures are relatively undeformed, they appear to have been emplaced after the till layer had ceased deforming. Hence, the argillan zone could be related to the dewatering processes that contributed to till immobilisation. Since argillans are thought to be associated with soil formation (Brewer, 1976), their occurrence at such considerable depth is unusual and tends to support the proposed till dewatering origin.

Sample 93-CBB-30

The sample was taken from the topmost sand layer within a sand intraclast approximately 10 m above the shoreline at *site 30*. Strike of the sample is 65° with a dip of 19°.

A. Macroscopic

The sample comprises structureless coarse grained sands and scattered silt-dominated zones (Plate 4.51). Skeleton grains form casings around the larger grains in the otherwise featureless sample.

B. Microscopic

skeleton:

size: grains range from < 50 µm to approximately 0.5 cm with domains having modes of 150 µm and 100 µm.

shape: grains in all zones range from angular to (well) rounded(most); larger grains (> 2 mm) tend to be rounded.

distribution: sample has bimodal distribution.

composition: mainly quartz; some plagioclase, chlorite, clinopyroxene; larger grains tend to be sandstone and fossiliferous limestone.

plasma: none.

structure: closer examination reveals a poorly sorted sand unit containing vague randomly

oriented discontinuous shear planes and coarse-grained bands. Occasional ill-defined clusters of finer grained sand units and possible circular structures are also evident.

aggregates: none.

plasmic fabric: none.

C. Interpretation

The sample appears to have been saturated during its transposition as illustrated by the differential movement implied by structures present. Circular structures and casings of skeleton grains around larger clasts suggest discrete relative movement within the matrix. Clusters of fine-grained sands could be the product of saturated porewater conditions or possibly even porewater dissipation during dewatering of the deforming till. The vague discontinuous shear planes throughout the sample indicate that the intraclast was subjected to high bulk strain. All of these features are consistent with subglacial conduit or proglacial sediments which have been subjected to a high strain environment.

Sample 93-CBB-30B

Sample of finer sand layer within the same intraclast as sample 93-CBB-30. Strike of the sample is 60° with a dip of 11°.

A. Macroscopic

A lower zone containing a high concentration of larger grains within a fine sand has a gradational boundary with the upper weakly-laminated(?) fine sand zone (Plate 4.52). The larger grains have a weakly-developped fabric as defined by the somewhat parallel orientation of their long axes.

Finely laminated clay "boudins" are found near the top of the sample and appear to be part of a diamictic inclusion within the sand unit. In both zones, casings of skeleton grains are visible around the larger grains. Note that the casing around the elongate clast in

the upper zone is almost augen shaped.

B. Microscopic

skeleton:

size: grains range from < 50 μm to approximately 0.5 cm with a mode of approximately 100 μm in the upper zone and 250 μm in the lower zone.

shape: grains in both zones range from angular to (well) rounded(most); larger grains (> 2 mm) tend to be rounded.

distribution: in both zones is random.

composition: mainly quartz; some plagioclase, chlorite and clinopyroxene; the larger grains tend to be sandstone and fossiliferous limestone.

plasma: none.

structure: small domains of silt concentrations in addition to discontinuous shear planes with no preferred orientation, are randomly distributed throughout the sample. Casings of skeleton grains around larger clasts and circular structures are also quite common. A "necking" structure formed by skeleton grains squeezed between two closely spaced clasts similar to the one illustrated in Plate 4.4 is also observed. A void space defined by lineations of coarse sand grains similar to the one illustrated in Plate 4.19 seems to mimic the surface of large sandstone clast.

aggregates: none.

plasmic fabric: none.

C. Interpretation

This thin section closely resembles sample 93-CBB-24B (Plate 4.42) and probably has a similar origin. The clay-rich boudins and the multi-directional discontinuous shear planes are indicative of a high bulk strain environment, whilst casings of skeleton grains around

Plate 4.53 Sample 93-CBB-33 taken of the diamicton underlying the lower contact of the stratified sands and gravels of unit B at *site 33*.

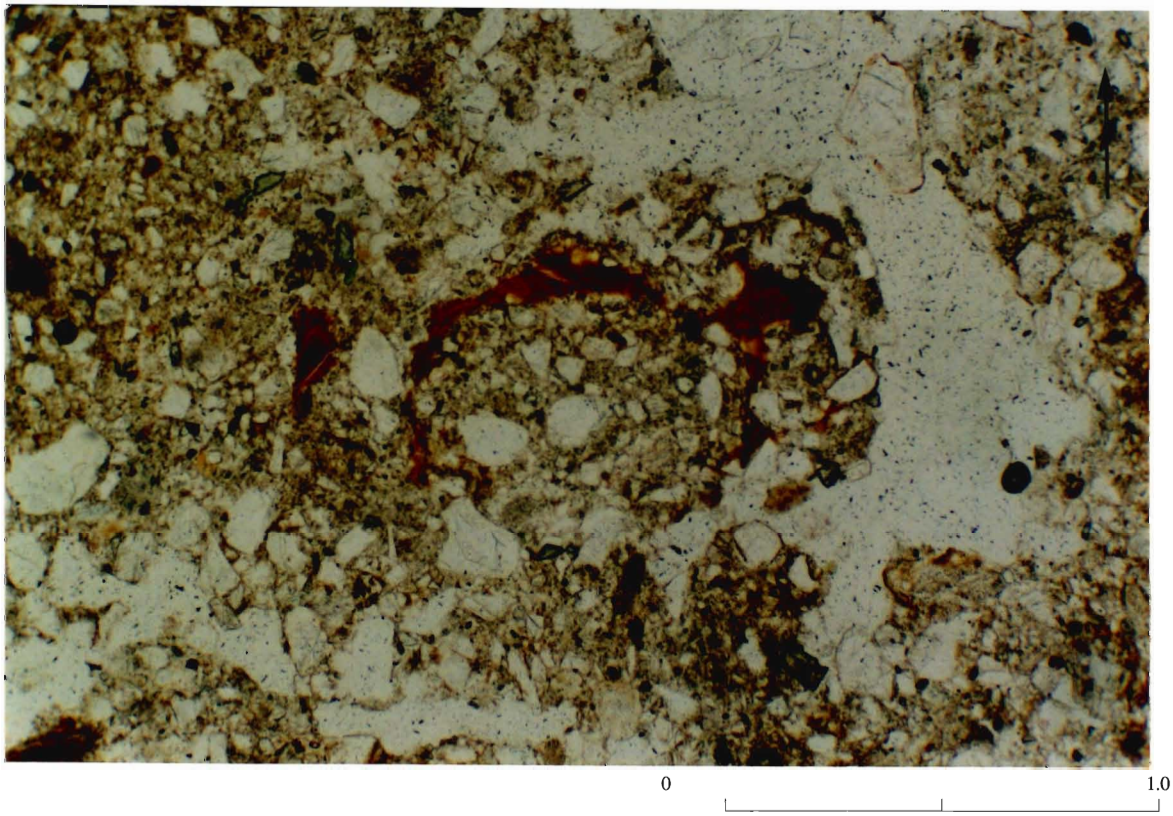

Plate 4.54 Detail of location 54 illustrated in Plate 4.53 showing an argillan (red-brown) around a diamictic clast.

larger clasts and necking and circular structures suggest that differential movement has also occurred. Both sets of features could be ascribed to deformation processes in a confined environment; however the silt dominated areas could also represent the preferential passage of porewater through the sand unit during till dewatering. Again these features imply variable flow deposition followed by *en masse* transport within a deforming till layer.

Sample 93-CBB-33

Sample of diamicton underlying the stratified sands and gravels approximately 31 m above the shoreline at *site 33*. Strike of the sample is 178° with a dip of 71°.

A. Macroscopic

The intense fracturing within the sample is the result of drying and sample preparation (Plate 4.53). Therefore, the only discernable feature of the diamicton is the casing of skeleton grains around the larger grains.

B. Microscopic

skeleton:

size: grains range from < 50 µm to approximately 0.5 cm with a mode of approximately 150 µm.

shape: grains range from angular(most) to rounded; larger grains (> 2 mm) tend to be rounded.

distribution: is random throughout the sample.

composition: mainly quartz; some plagioclase, chlorite and clinopyroxene; the larger grains tend to be sandstone and fossiliferous limestone.

plasma: homogeneous clays.

structure: fine "wavy" Fe-stained clay bands are found throughout the sample and tend to "flow" around coarser grains (similar to structure illustrated in Plate 4.35). Isolated clay balls

similar to the diamictic clast illustrated in Plate 4.62 are also typical of the diamicton in this sample. However, the most interesting features of the sample are the numerous argillans and associated pores found throughout. Plate 4.54 is an example of a finely laminated argillan formed around a diamictic "clast" within the diamicton. Plate 4.55 clearly illustrates a perfectly preserved finely laminated argillan within an oblong pore. Note that the clay also slightly inter-fingers into the surrounding diamicton. Near the top of the sample the concentration of argillans increase as seen in Plate 4.56.

aggregates: reddish-brown Fe-staining(?) of the clays is mostly uniform throughout the sample.

plasmic fabric: weakly-developped skelsepic fabric.

C. Interpretation

The diamictic "clast", clay bands and vague skelsepic plasmic fabric all suggest that differential movement has occurred within the diamicton. These features are consistent with the idea of autokinetic deformation as the sediment moved as a massive unit (Menzies and Woodward, 1993). Argillans within the diamicton are probably related to porewater movement and clay translocation that occurred subsequent to the deposition of the overlying stratified sand and gravel unit.

Sample 93-CBB-34

Sample of stratified coarse sand/gravelly unit overlying the drumlin diamicton approximately 23 m above the shoreline at *site 34*. Strike of the sample is 55° with a dip of 19°.

A. Macroscopic

Fining upward sequence of poorly sorted sand and gravel and fine-grained diamictic laminae (Plate 4.57). Plates 4.58 is a thin section cut at 90° to the lower portion of the long

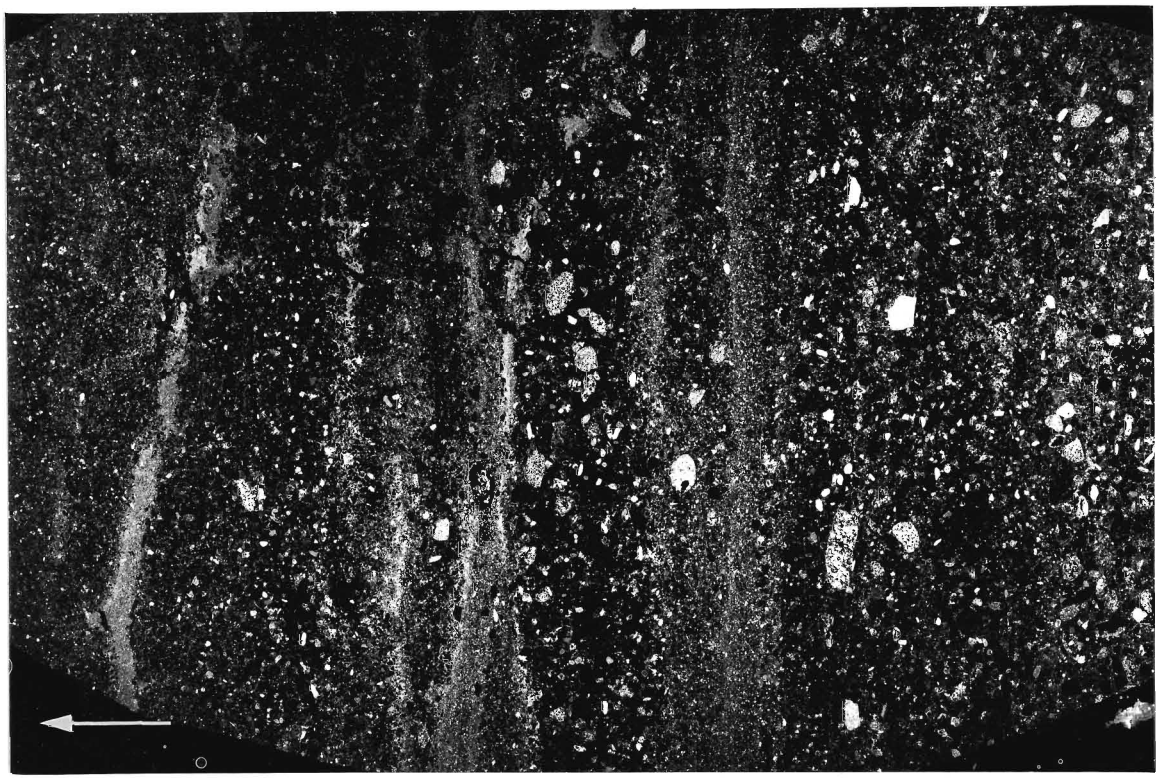

0 10 mm

Plate 4.57 Sample 93-CBB-34 taken from the stratified sands and gravels of unit B at *site 34*.

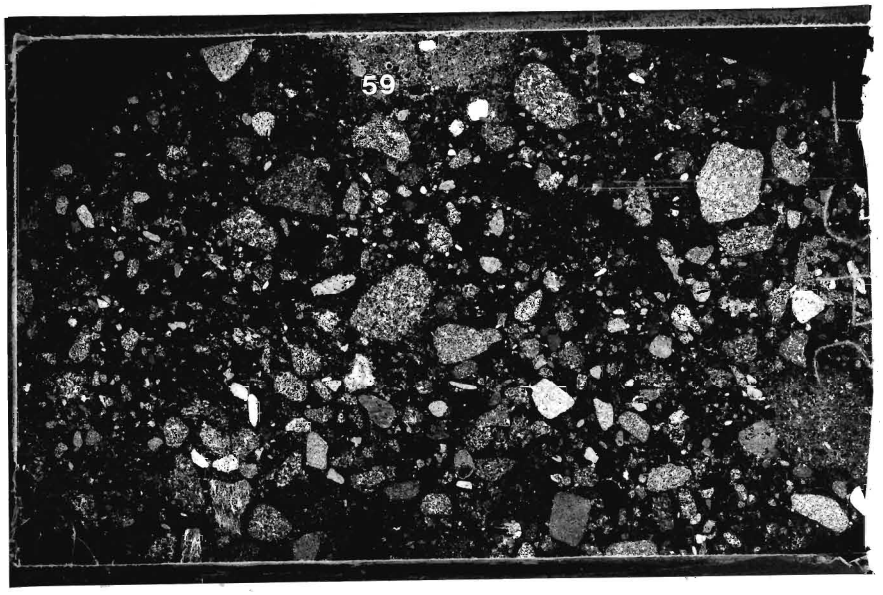

0 1.0 mm

Plate 4.58 Thin section from the lower portion of sample 93-CBB-34 cut at 90° to the long axis illustrated in Plate 4.57.

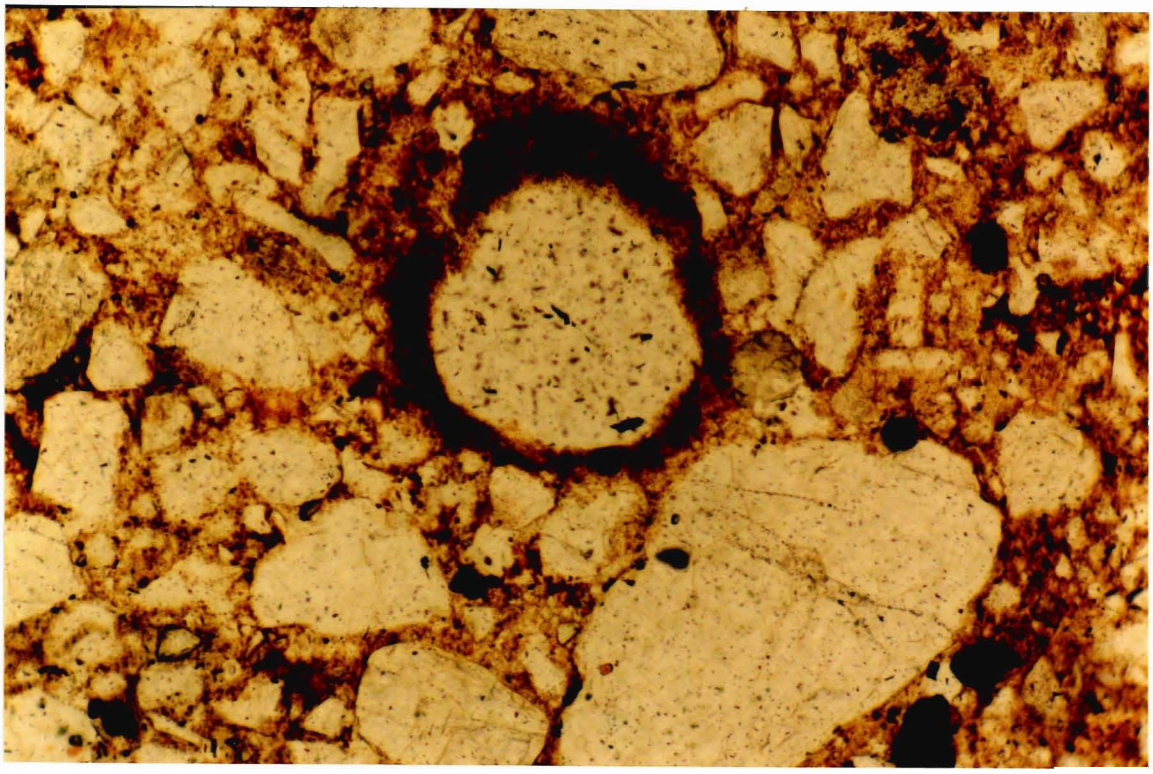

0 1.0 mm

Plate 4.59 Detail of location 59 illustrated in Plate 4.58 showing a near circular pore with a massive clay rim (argillan).

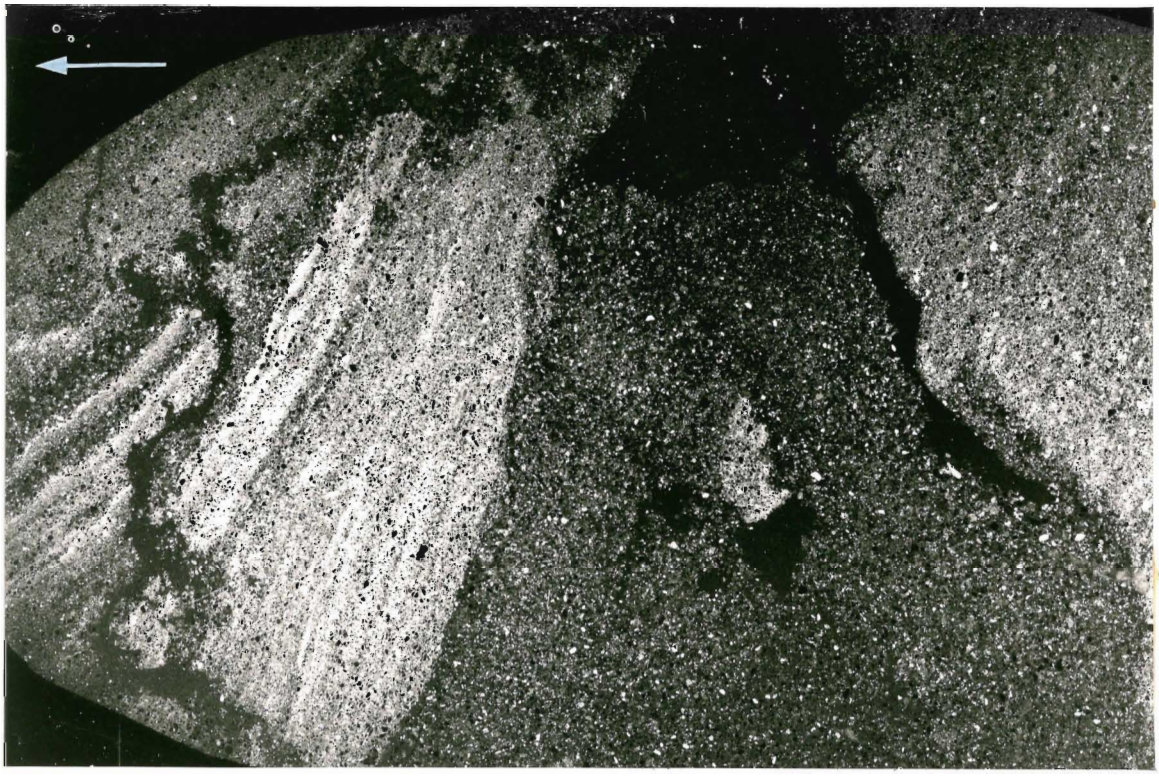

0 10 mm

Plate 4.60 Sample 93-CBB-36 taken of folded sand and diamicton layers in the slump zone at *site 36*.

axis of the sample illustrated in Plate 4.57.

B. Microscopic

skeleton:

size: grains range from < 50 μm to approximately 0.5 cm with a mode of approximately 250 μm.

shape: grains range from rounded(most) to angular; larger grains (> 2 mm) tend to be rounded.

distribution: mostly random, but rare to absent in diamictic beds.

composition: mainly quartz; some plagioclase, chlorite and clinopyroxene; larger grains tend to be sandstone and fossiliferous limestone.

plasma: non-homogeneous clays confined to the diamictic beds within the sandy unit.

structure: diamictic layers are significantly intermixed with the coarser grained laminae. Argillans are also found throughout the sample, but the clays in this sample tends to be massive rather than laminated (Plate 4.59).

aggregates: reddish-brown Fe-staining(?) is texturally restricted to the clay-rich layers.

plasmic fabric: finely laminated clays.

C. Interpretation

The most distinguishing feature of this sample is the absence of brittle deformation structures (i.e., shear planes and banding of skeleton grains). Hence, the stratified sediments of this sample were not transported within a deforming till layer. Furthermore, it is unlikely that they represent the waning flow of a subglacial meltwater flood since the expected grounding of the ice sheet subsequent to this event should have produced brittle deformation structures. The presence of obviously diamicton derived layers within the stratified unit attests to the wave-reworked diamicton origin of the unit as discussed in chapter 3. Due to

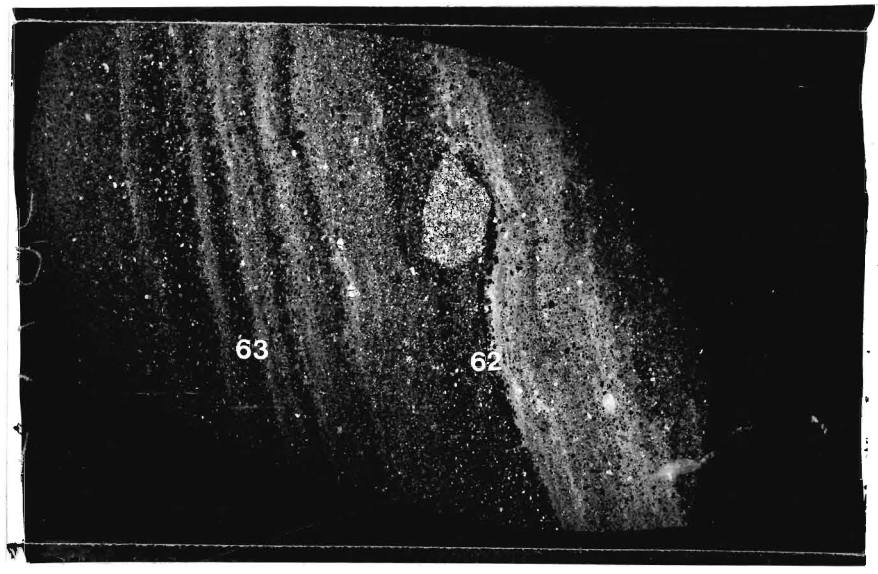

0 1.0 mm

Plate 4.61 Thin section from the upper portion of sample 93-CBB-36 cut at 90° to the long axis illustrated in Plate 4.60.

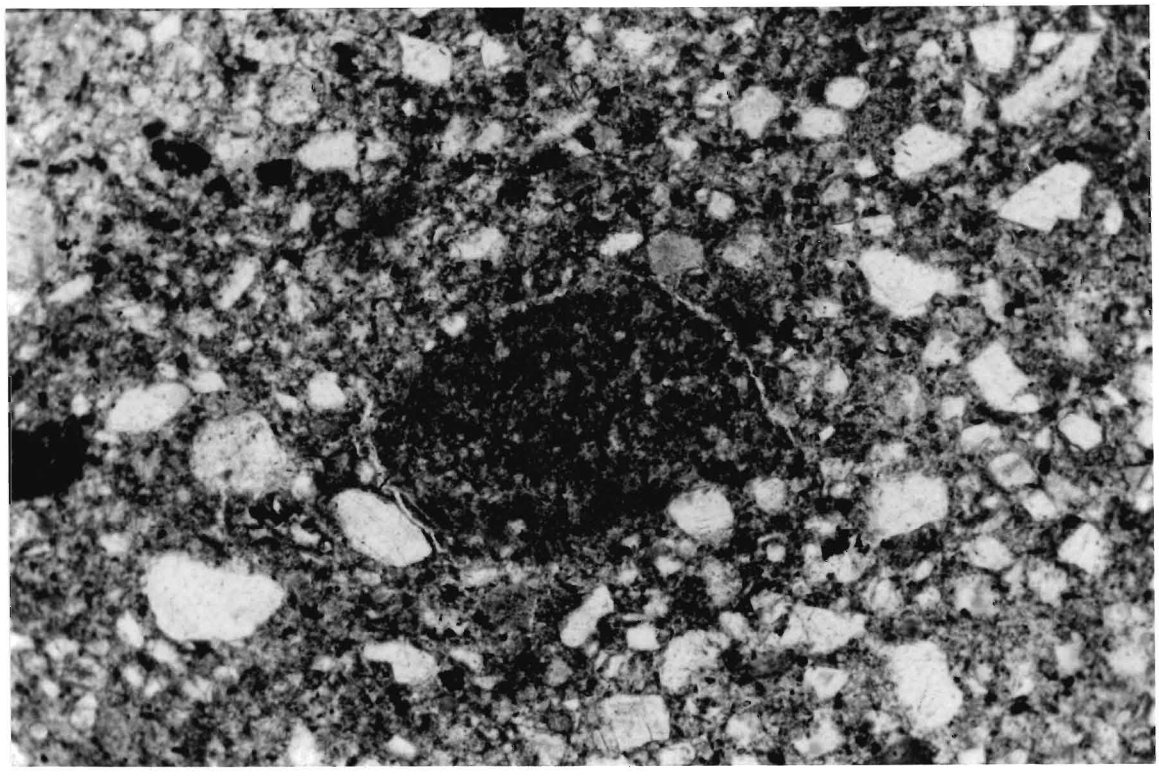

0 1.0 mm

Plate 4.62 Detail of location 62 illustrated in Plate 4.61 showing a fine grained diamictic clast within the diamicton.

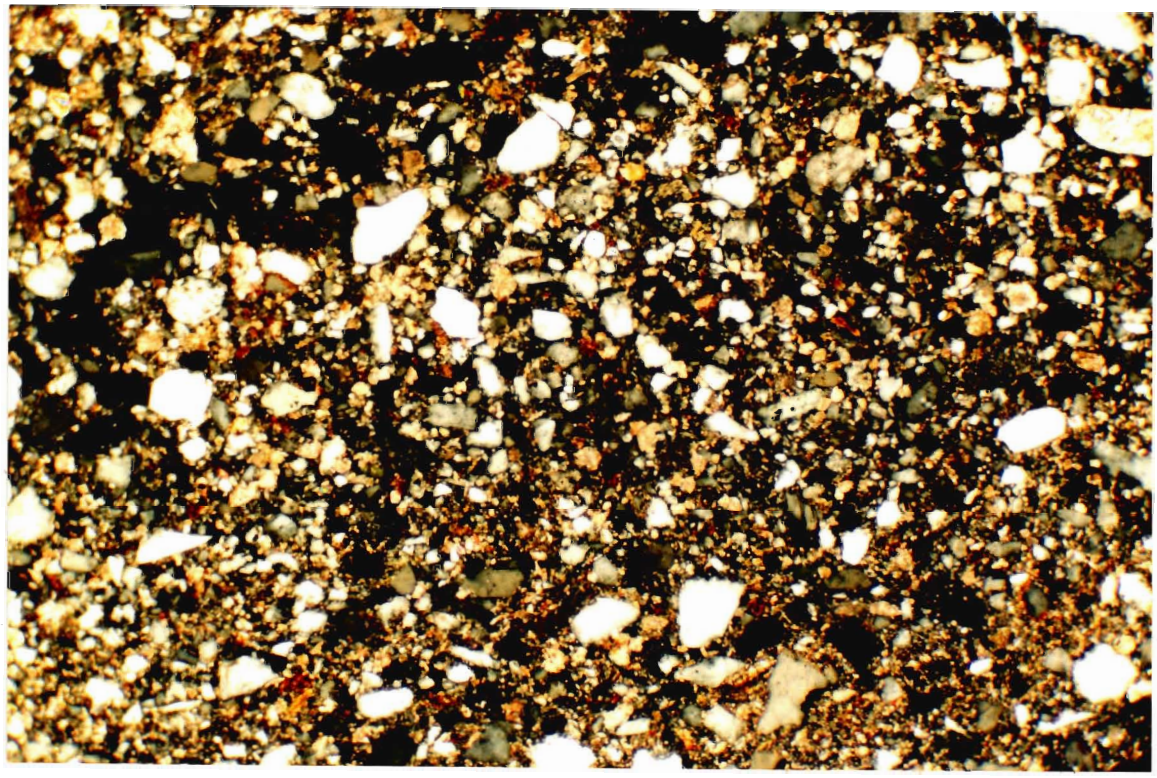

Plate 4.63 Detail of location 63 illustrated in Plate 4.61 with cross-polars showing discontinuous shear planes radiating outward from a void.

the near surface location of the site, the argillans are likely the product of infiltrating meteoric waters.

Sample 93-CBB-36

The sample was taken of folded sand and silty layers in the eastern slump zone of the diamicton into the adjacent glaciolacustrine sediments approximately 2 m above the shoreline at *site 36*. Strike of the sample is 145° with a dip of 4°.

A. Macroscopic

The sample comprises two outer zones of diamictic material and a central zone of massive coarse sand (Plate 4.60). Fine clay laminations occur in the upper zone, some of which appear to be inter-bedded with coarse sand layers. The boundary between this zone and the central sand unit is sharp. A sub-rounded diamictic inclusion in the centre of the sample has a sharp boundary with the sand unit. The lower diamictic zone appears to be vaguely laminated. Fractures and large void spaces on the sample are the result of sample preparation. Plates 4.61 is a thin section cut at 90° to the upper portion of the long axis of the sample illustrated in Plate 4.60.

B. Microscopic

skeleton:

size: grains range from < 50 µm to approximately 1 mm with a mode of approximately 100 µm in the central zone and 150 µm in the upper and lower zones.

shape: grains range from (well) rounded in the central zone to angular in the outer zones.

distribution: in all zones is random.

composition: mainly quartz; some plagioclase, chlorite and clinopyroxene with minor amounts of sandstone and fossiliferous(?) limestone.

plasma: abundant clays in the upper and lower zones and scattered clays in the central zone.

structure: bands and lineations of skeleton grains are found throughout the sample. A fine-grained clay-rich "clast" in a diamictic layer is located at the centre of Plate 4.62 , whilst similar structures or possibly even boudins are observed elsewhere in other diamictic layers. "Necking" structures of skeleton grains are also common to the thin section. Furthermore, clay from these clasts is observed to extend into the surrounding sand unit. The sandy areas of the sample contain randomly oriented discontinuous shear planes, some of which radiate outward from voids (Plate 4.63).

aggregates: reddish-brown Fe-staining(?) is texturally restricted to the upper and lower zones.

plasmic fabric: weakly-developped skelsepic fabric in the upper and lower zones.

C. Interpretation

The sample appears to have formed mostly due to slumping of the diamicton into adjacent lake sediments whilst the lake levels were high enough to buttress the sides of the drumlin. The diamictic "clasts", necking and casings of skeleton grains around larger clasts and the intermixing of plasma with the sand unit are all indicative of rotational movement which in this case was most likely in response to gravitational forces. Shearing within the sand portion of the thin section is consistent with a sand layer being translocated by a sediment gravity flow as are the numerous folded sand layers or rather, soft sediment deformation structures.

4.2 Summary

Micromorphological observations of the various samples imply a series of complex processes leading to the final deposition of the drumlin sediments at Chimney Bluffs. Several structures associated with relative sediment motion and ductile deformation are found throughout the sediments. Flow structures in the guise of banding of skeleton grains and re-

mobilised clay-rich zones were not restricted to a particular sediment type or zone within the drumlin. Furthermore, differential and/or rotational movement as illustrated by the orientation of the long axes of skeleton grains parallel to the surface of larger clasts was typical of all the thin sections examined. Cowan (1985) noted that in a type III block-in-matrix mélange such intergranular movement would be expected under high fluid pressures in partly consolidated sediments. However, the timing of this deformation is difficult to determine from the observed microstructures. These features may be indicative of earlier depositional processes or could be a combination of superposed structures and fabrics from all processes prior to the final deposition of the sediments (Menzies and Maltman, 1992). It is also possible that pre-existing structures could have been overprinted during or immediately following the formation of the drumlin landform (Menzies and Woodward, 1993).

A clear indication that the sand intraclasts represent transposed up-ice deposits is made by the structures observed in these samples. The saturated pore water conditions suggested by the poorly sorted massive sands described in several of the thin sections are also implied by various other features. Circular arrangements of skeleton grains, casings of oriented skeleton grains around larger clasts and, where present, diamictic inclusions exhibiting a small degree of intermixing with the sands are all indicative of saturated conditions (Meer, 1987). Furthermore, flow structures of plasma from the surrounding diamicton were seen extending into normally graded clay laminae in several of the samples. Such laminations imply low energy flow conditions and in conjunction with the possible dropstone in Plate 4.21 could reflect a primary subglacial conduit or a ice-proximal primary origin for the sand intraclasts. High energy flow conditions are suggested by medium sand laminae, coarse sand layers and diamicton derived inclusions noted in the intraclast samples. The combination of these features with clay laminations and angular clay-rich inclusions apparently derived from a pre-

existing layer in the deposit attest to the highly variable flow regime expected in proglacial glaciofluvial deposits and subglacial conduit deposits formed at the point of debouchure into an open marine environment (Hanvey, 1989).

The samples appear to have be derived from a complex stress environment involving brittle deformation (Broster and Clague, 1987; Menzies, 1990). The preservation of primary structures in the sand blocks suggests that these blocks were likely frozen during transport within such a layer. Because frozen sands experience brittle deformation at high strain rates (Ladanyi and Morel, 1990), the occurrence of multi-directional shear planes within the intraclast samples would appear to support this argument. Similarly, micro-faulting of primary structures (i.e clay laminae) and possibly even the angular diamictic inclusions in the sand intraclasts also attest to brittle deformation under frozen conditions. This style of deformation is consistent with high strain applied to cohesive units of damp or frozen sand in which yield strength decreases in response to increased pore water content (Owen, 1987). Owen (1987) also noted that tangential shearing by ice overriding a non-liquified bed would result in erosion or deformation of a thin near-surface layer. It is possible that at Chimney Bluffs, the deforming till layer eroded and subsequently entrained frozen blocks of subglacial or proglacial sands.

It is not surprising that the high bulk strain features noted in the thin sections suggest both saturated and dry/frozen conditions. Such conditions are expected in a glacial mélange environment (Menzies and Maltman, 1992). Hence both brittle and ductile deformational structures could be indicative of a partially frozen and partially saturated deforming till environment. Since primary structures are still apparent in some of the sand intraclast samples, whilst absent in others, it is suggested that at least some of the intraclasts had been frozen during and possibly subsequent to transposition. Although the occurrence of argillans

in these units could be ascribed to a pre-emplacement origin, an alternate explanation seems likely. These features, in conjunction with the diffuse plasma domains observed in several of the thin sections, may reflect periods of pore water dissipation associated with the immobilisation of the deforming till layer. The shape of the argillan-containing void in Plate 4.48 is reminiscent of a dish structure formed in response to dewatering as described by Lowe and LoPiccolo (1974). However, in considering the proposed depositional environment in which this feature is likely to have developed, its shape could reflect strain conditions within an immobilising till layer. Banding of skeleton grains exhibited in various diamicton samples and the occurrence of possible "pressure shadows" associated with augen development are indicative of high strain rates (Menzies, 1990; Menzies and Maltman, 1992; Hicock and Dreimanis, 1992). The lack of macroscale structures is not surprising since rapid stress dissipation is expected in dense materials (i.e., diamicton) (Menzies, 1982). Furthermore, a massive diamicton could reflect homogenisation in response to very high rates of strain (Hart and Boulton, 1991).

Thin section examination has also revealed that the sand units and the sandy diamicton appear to have been derived from similar source areas. Such an observation is based on similarities in grain composition between the two facies, although the sand units are bereft of plasma-sized material. The skeleton grains of the sand intraclasts tend to be more rounded than those comprising the diamicton. The primary bedding structures exhibited by the sand units are indicative of subaquatic conditions, but whether these were in a proglacial glaciofluvial environment or in subglacial conduits can not be inferred from the thin sections. Slight intermixing of plasma with sand grains occurs at the contact between diamicton and sand intraclasts, but the sharpness of this contact is rather remarkable. Essentially the larger sand units are intact/cohesive blocks that have experienced minimal ductile deformation, but

pervasive brittle deformation. Conversely, the massive "wispy" sand lenses are replete with rotational structures and patches of fines that are strongly suggestive of pore water movement and/or severe plastic deformation. Such features were also found within the sand intraclasts implying that at least some pore water movement had occurred sometime during or after the original and subsequent depositional process. It is proposed that the "wispy" sand lenses therefore behaved in the manner expected of a non-cohesive material (i.e., un-lithified sand) in a complexly deforming environment (Clayton *et al.*, 1989) and based on the foregoing discussion, they were not frozen during transport.

Finally, the homogeneity of reddish-brown Fe-staining(?) throughout the diamicton samples, especially those taken at considerable depths within the drumlin, imply that it was not strictly the product of water movement through a soil horizon. An alternative to this theory is that the dissolution and precipitation of Fe could reflect changing Eh/Ph conditions in the subglacial meltwater and may even be related to changes in porewater pressure gradients (Whalley *et al.*, 1990). Although these conditions may be related to those necessary for the precipitation of secondary carbonates (Hallet, 1976), two slightly different and, as of yet, unknown subglacial meltwater environments may be required (Whalley *et al.*, 1990). Perhaps the fractured limestone clast with its rim of secondary carbonates in Plate 4.12 reflects a change in pressure gradient conducive to carbonate precipitation; however, this is conjecture at best. Nevertheless, both Fe-staining and secondary carbonate mineralisation could be related to the subglacial conditions present in a deforming till layer in a way that has not yet been determined.

CHAPTER 5: DISCUSSION

5.0 General

Evidence suggests a water saturated deforming till origin for the sediments of Chimney Bluffs. Both macro- and micro-scopic structures indicate that the main style of deformation in the sediment pile was probably autokinetic (during *en masse* movement of the sediment). Discrete relative movement as implied by banding, circular arrangements and casings of skeleton grains around larger clasts in addition to necking and skelsepic plasma fabric appears to support this hypothesis. The lack of macroscale deformation structures at the site has several implications. Hanvey (1989) suggests that such an absence implies that the drumlinisation process cannot be solely the result of a deforming till layer, nor of the erosion of pre-existing sediments. Another possibility is that the diamicton is so highly sheared that any glacigenic deformation structures are no longer visible (Broster and Clague, 1987; Hart *et al.*, 1990; Hart and Boulton, 1991) or rapid stress dissipation within the denser diamicton could also result in a lack of deformation structures (Menzies, 1982). Consolidation of sediments to greater densities is a function of the overriding ice (Alley, 1991; Boulton and Dobbie, 1994). It is further expected that the sedimentological record of this consolidation should reflect glacial loading, subglacial deformation and melt water flow. The microstructures encountered at Chimney Bluffs imply that such processes have occurred, especially in the ductile re-organization of the skeleton grains and plasma. However the complexity of these features suggests that they were not all formed penecontemperaneously. Overprinting of various structures is likely to have occurred during the "evolution" of the diamicton-sand intraclast mélange prior to its final deposition. The key to this "evolution" was probably the highly variable pore water content expected in a deforming till layer which would have controlled the style of deformation (Hicock and Dreimanis, 1992).

5.1 Soft Deforming Till Layer

Since all subglacial diamictons encounter some form of deformation during a number of different depositional process(es), the term deforming till will be modified in the manner after Menzies (1990a) and Hart (1994) to *soft deforming till.* Essentially it is a specific type of deformation till that has been deposited by both depositional and deformational processes in which sediment moves laterally in response to high basal ice shear strains, possibly under a zone of rapidly moving ice (i.e., an ice stream; Alley *et al.*, 1987; Hart, 1994). Cowan (1985) noted that such high bulk strain was integral to the mélange environment. However, it is misleading to assume that the stress patterns produced by a soft deforming till, especially within an inhomogeneous sediment layer, are unidirectional (Boulton, 1987). As will be discussed later, the complex subglacial conditions implied by a glacial mélange could result in multidirectional and highly localised stresses.

Sedimentary structures observed at Chimney Bluffs are consistent with those expected in a soft deforming till layer. According to Alley (1991) and Hicock and Dreimanis (1992), a number of characteristics are associated with the high basal water pressures and saturated porosity conditions within this environment. Matrix-dominated diamictons, a lack of deformational structures and overconsolidated diamictons are all ascribed to a soft deforming layer. Furthermore, boudinaged sand lenses, pressure shadows and fissuring in addition to necking and flow banding of diamicton sediments are representative of the changing shear stresses within such an environment.

Figures 5.1a and 5.1b illustrate the various deformation styles and associated features within the context of a layered subglacial shear zone. Necking and flow banding are attributed to the very high strain rates within the upper ductile zone (Fig. 5.1a) of the

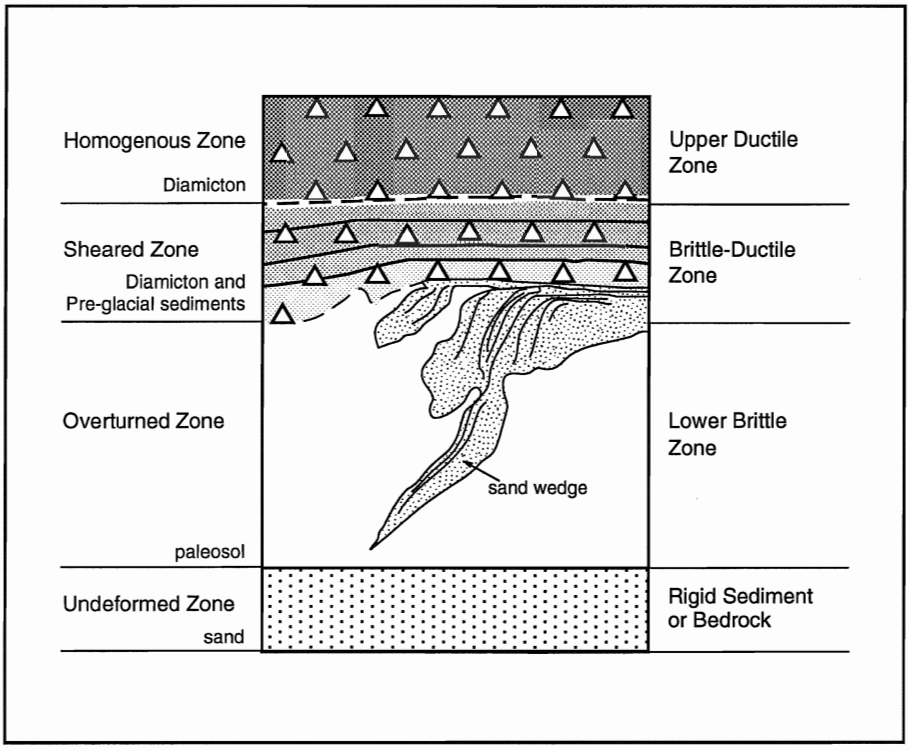

Figure 5.1a Schematic diagram of layered subglacial shear zones (after Hart and Boulton, 1991; Hicock and Dreimanis, 1992).

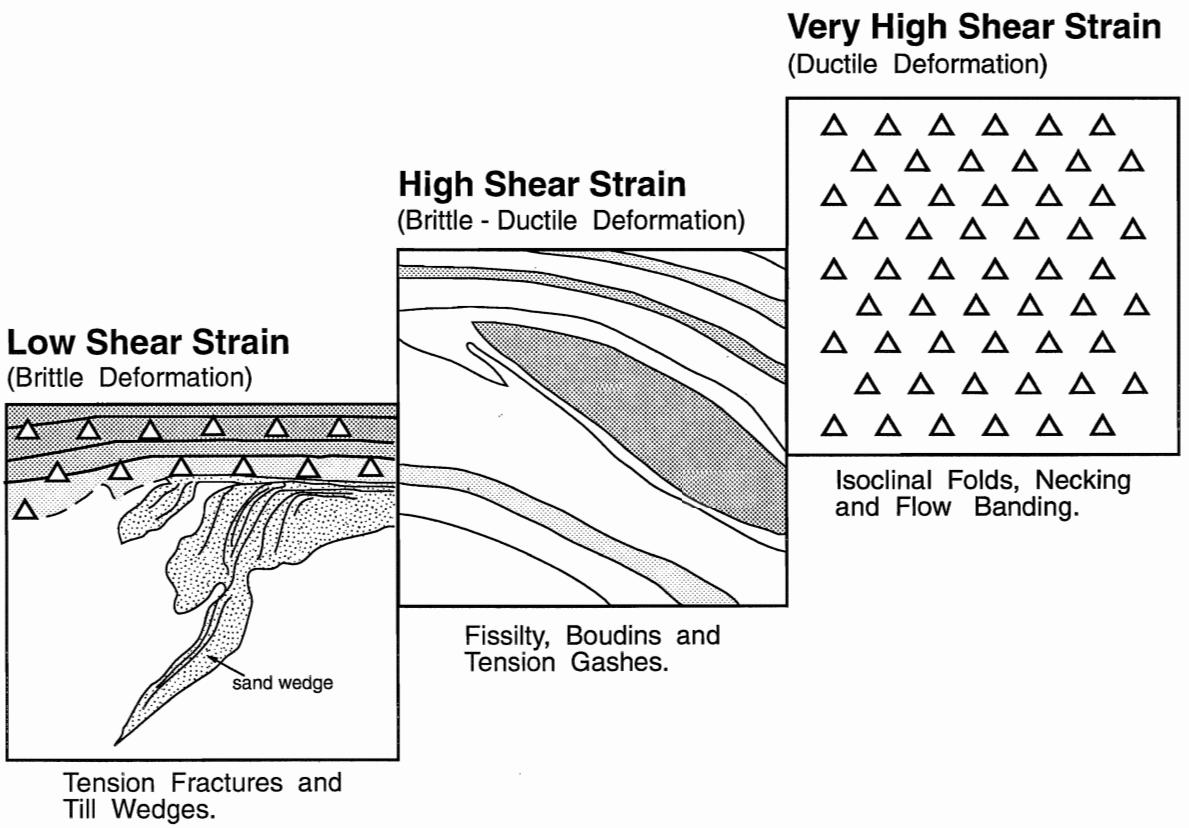

Figure 5.1b Schematic diagram of different styles and of subglacial deformation and related structures associated with different amounts of shear strain (after Hart and Boulton, 1991; Hicock and Dreimanis, 1992).

deforming till model proposed by Hicock and Dreimanis (1992). Similarly, fissility and boudinaging may reflect a combination of brittle and ductile deformation styles in response to till stiffening brought on by decreasing pore water content (Hicock and Dreimanis, 1992). The formation of pressure shadows, as described in the previous chapter, is illustrated in Figure 5.2. Essentially, as the long axis of an elongate clast is re-oriented parallel to the direction of shear in the brittle-ductile zone of Figure 5.1a, pressure shadows develop at the ends of the long axis. Furthermore, the attenuation of sand bodies into boudins may have a similar origin. Figure 5.2 illustrates the process whereby a boudin may form from an inhomogeneity within a deforming till layer, which in this case would be a sand intraclast at the macroscale, or a fine clay laminae at the microscale. Finally, the deformation of sandy silt layers and fine clay laminae around clasts and grains described in the previous chapters can also be attributed to subglacial shearing. The orientation of this deformation would be dependent on ice flow direction (Fig. 5.2), or rather the main direction of shearing within the subglacial environment. Although such shearing could be indicative of lodgement tills (Dreimanis, 1989), the expected strongly oriented clast fabric was not observed. However, since till-forming processes are intrinsically related to changing subglacial pore water pressure conditions (Hart and Boulton, 1991; Hicock and Dreimanis, 1992), the diamicton at Chimney Bluffs could be a hybrid of lodgement and deformation tills.

5.2 Sand Units

A complication in the soft deforming till layer theory arises with the presence of sand stringers, lenses and relatively intact intraclasts. The latter has been cited as evidence against a pervasively deforming layer by Clayton *et al.* (1989) who contended that such features would be destroyed in such an environment. Darker coloured sandy silt layers and colour banding within the apparently homogeneous diamicton further compound the problem. In

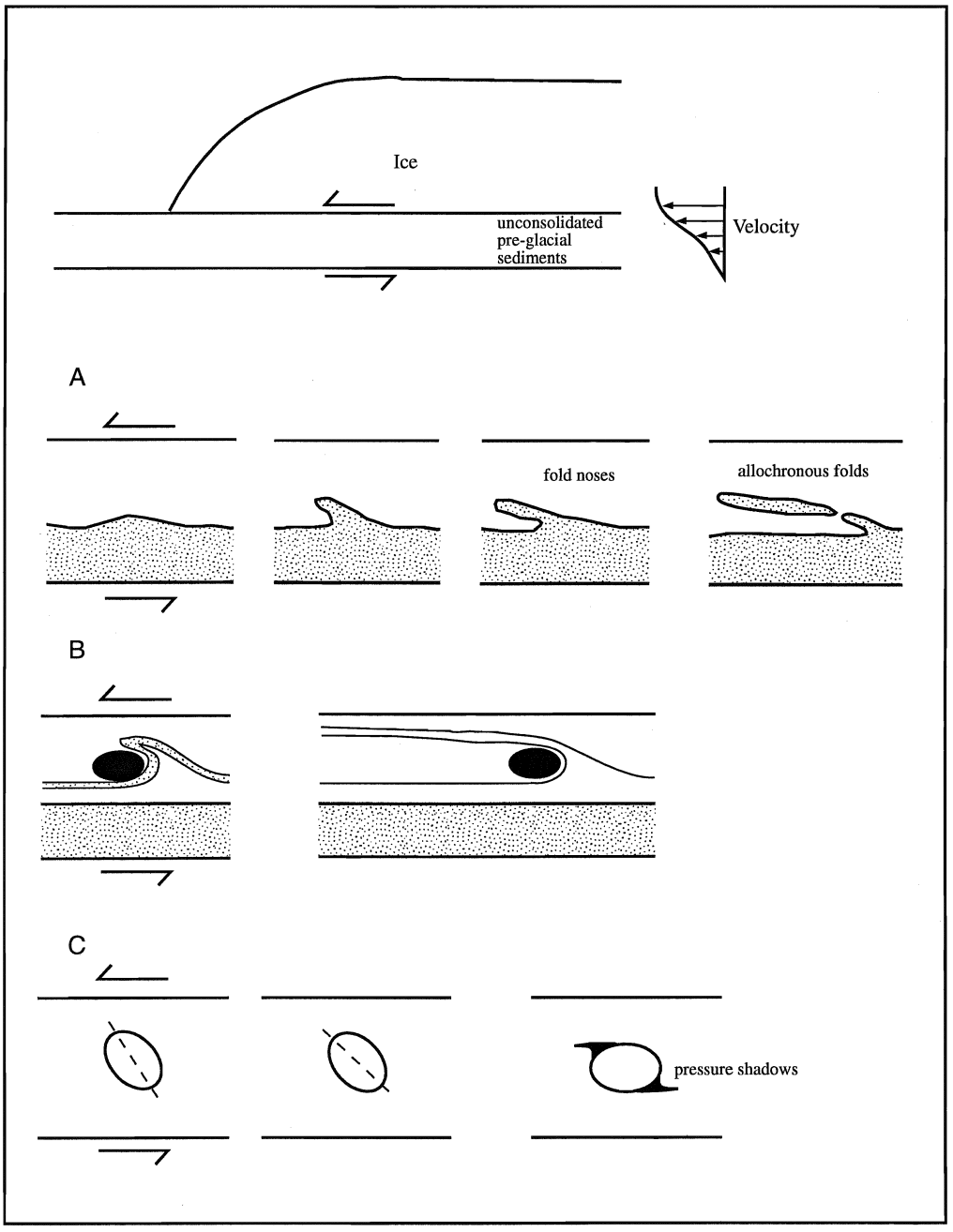

Figure 5.2 Summary of subglacial deformation. (A) Attenuation of inhomogeneity into a fold and then into a lamination. (B) Clast deformation of lamination. (C) Clast within deforming mass rotates in direction of tectonic shear produces pressure shadows (after Hart and Boulton, 1991).

order to interpret these features, it is necessary to consider that the stratigraphy observed at this site could be analogous to a type III block-in-matrix mélange as described by Cowan (1985). Such a mélange is dominantly polymict with chaotically dispersed inclusions of various sizes and shapes. Grossly lenticular blocks within the matrix is the most distinguishing feature of this type of deposit. The dissimilar rheologies of the diamicton and the sand intraclasts may have resulted in the sediments being subjected to heterogeneous bulk deformation. It is expected that due to these processes, some of the blocks will remain intact whilst others will become flattened and/or contorted during or after emplacement. Blocks of this variety can easily be compared to the sand units and associated structures described at the current site.

Boudinaged and/or rotated sand lenses/blocks, and the persistence of sorted intraclasts are consistent with and even expected in a deformation till (Figs. 5.1b, 5.1a; Boulton, 1987; Alley, 1991). Some have suggested that such units comprise locally-derived sediments which have not been subjected to the same degree of strain as the host diamicton (Alley, 1991); however, Menzies (1990a) contended that the blocks could have been transported for quite some distance as long as they were to remain frozen before, during and subsequent to till immobilisation. Entrainment of low shear strength (i.e., non-cohesive) sand blocks in a pervasively deforming till layer should result in their complete destruction (Clayton *et al.*, 1989; Menzies, 1990a) unless the blocks were frozen during transport (Dardis and McCabe, 1987; Broster and Clague, 1987; Menzies, 1990; Alley, 1991; Menzies and Maltman, 1992; Menzies and Woodward, 1993). Thus, destruction of unfrozen *in situ* subglacial cavity/channel sediments is more likely in a deforming till layer than that of entrained frozen up-ice stratified deposits.

The possibility remains though, that the sand units need not have been frozen to be

transported as cohesive blocks. A relatively impermeable (see Table 1, appendix III) layer or "envelope" of sandy diamicton could have protected a water saturated sand block from destruction in a soft deforming till layer. The "cushioning" capability of fine tills (i.e., having a high matrix content) has been noted by Hicock and Dreimanis (1992) who also indicated that such tills would have relatively sharp contacts with the protected units. This hypothesis is consistent with the sharp contacts observed between the sand intraclasts and the surrounding diamicton at the present site. Hence, coupled with ice overburden pressures, the impermeable diamicton layer would tend to assist in the preservation of primary structures within a sand unit by preventing large influxes of subglacial water (Menzies, 1990; Hicock and Dreimanis, 1992). Such a protective layer could also have maintained a stable thermal environment prior to and subsequent to deposition; hence a frozen block would have remained frozen during and after transport. It also follows that an unfrozen sand block which has been transported in this fashion would be expected to exhibit some evidence of plastic deformation. Such evidence could be the occurrence of slightly contorted layering in some of the intraclasts observed at Chimney Bluffs. Whether the sand units are of an ice-proximal proglacial or of a subglacial conduit origin cannot be adequately determined from the current data. However, evidence tends to suggest that they were derived from the same or a similar up-ice area as the diamicton.

The most puzzling characteristic of the large sand intraclasts is the remarkable preservation of primary stratification. Sharp unconformable boundaries with the surrounding diamicton tend to support the distal origin of the units, but could also reflect a subglacial conduit origin (Menzies, 1990). Brittle deformation as suggested by the pervasive conjugate micro-shearing both at the macro- and micro-scopic levels, and the absence of liquefaction structures appear to be indicative of very high strain rates applied to frozen sands (Ladanyi

and Morel, 1990), but could also reflect compact unfrozen conditions (Owen, 1987; Broster and Clague, 1987). In any case, these structures are attributable to the upper brittle zone illustrated in Figure 5.1a and therefore could attest to a subglacial deformational origin for the diamicton-sand intraclast mélange at Chimney Bluffs. Furthermore, although the incorporation of diamictic fragments within the sand intraclasts could reflect primary depositional processes (i.e., high energy flow conditions), it could also be indicative of a high strain environment (Menzies, 1990). If these units have a frozen block origin, erosion of the surrounding denser diamicton in response to changing shear variable stress levels and/or lateral shearing within a deforming layer could occur. However, the high pore water saturation implied by the occurrence of circular arrangements of skeleton grains and of plasma and/or silt domains in the sand intraclast thin sections examined in the previous chapter, appears to contradict the possible frozen block transport mechanism. These microstructures, in conjunction with the sandy silt layers may actually be the vestiges of the dewatering process attributed to the transition from upper ductile shear zone to brittle-ductile shear zone conditions illustrated in Figure 5.1a.

5.3 Dewatering Processes

Dewatering processes may account for some of the structures observed in the sand intraclasts. Although the highly permeable sand intraclasts are the obvious foci for subglacial meltwater movement, the presence of primary structures within these bodies appears to negate this hypothesis. It has been suggested that the relatively impermeable diamicton that surrounds the intraclasts acted as a "protective" layer in the manner outlined by Hicock and Dreimanis (1992). Therefore, mass water movement during dewatering of the soft deforming till layer would have had minimal impact on the intraclasts and would mostly have been limited to the water contained within these units. Accordingly, the dewatering structures

exhibited by the sand intraclasts were restricted to microscale argillans and diffuse zones of fine-grained sediment within a coarser grained matrix. Conversely, sandy silt layers may be macroscale dewatering features. They could represent hydrostatically induced fissures within the diamicton in which mass sediment flows were deposited (Kumpulainen, 1994). Because such deposits would therefore reflect the transition from ductile to brittle-ductile subglacial shear conditions (Hicock and Dreimanis, 1992), the slight degree of ductile deformation exhibited by these layers would be expected.

5.4 Depositional Model

The following discussion is based on the assumption that the sand intraclasts represent ice-marginal proglacial deposits or subglacial conduit melt-out deposits that have been transposed from an up-ice location. It is also possible that these intraclasts in addition to the banded diamicton are derived from a proglacial melt-out sequence that was later overridden and actively deformed by an advancing ice sheet. Regardless of their primary origin, these deposits were then frozen *in situ* and subsequently entrained by the overriding soft deforming till layer (Menzies, 1990). Such a hypothesis is consistent with the observation that overridden material can readily be frozen to a glacier sole (Broster and Clague, 1987) and that saturated un-lithified sands would freeze before a fine-grained till would (Dardis and McCabe, 1987; Menzies, 1990). Once inside a deforming till layer, the degree of strain experienced by the frozen blocks would be a function of both their material shear strengths and subglacial porewater pressures (Menzies, 1990a). Thus, if such pressures were to locally increase, the underlying substrate could be mobilised if its internal shear strength were at or below the critical level of shear strength necessary for mobilisation (entrainment) and vice versa (Menzies, 1990). Within the resulting block-in-matrix glacial mélange, fragmentation and shearing of the entrained sediment package could produce the features observed at the

present site. Due to localised pressure gradients and polythermal conditions of a deforming till layer, a complexity in structures could arise.

Relatively small, unfrozen or partially frozen sand lenses would be heavily deformed or completely destroyed in such an environment (Boulton, 1987; Clayton *et al.*, 1989; Menzies, 1990.; Alley, 1991). The highly convoluted (wispy) and folded sand lenses observed at the present site would appear to support this idea. Similarly, sand stringers could reflect periods re-mobilisation of unfrozen sand units along fissure planes within the diamicton in response to changing pore water conditions. Sandy silt layers may also represent similar conditions and the sub-horizontal orientation of these layers and the sand intraclasts within the mid- to upper-vertical zone of the drumlin could be indicative of constructional glaciotectonics (Hart *et al.*, 1990). Associated diamicton fissility and colour banding, possibly reflecting a multiple diamicton origin are also consistent with this subglacial style of deformation which has a net plane of failure moving upwards within the deforming layer. Thus, once entrained at the base of a deformable bed, there would be a tendency for the whole package to move upwards during which time lateral shearing would possibly attenuate the unit into large-scale boudins. The result would be a mélange of stacked transposed up-ice deposits within an intensely sheared diamicton.

The features at Chimney Bluffs so far discussed can be attributed in part to the glaciotectonic processes outlined in the model Hart and Boulton (1991) and to the layered subglacial till model proposed by Hicock and Dreimanis (1992). According to the latter, all three deformational states (ductile, brittle-ductile, and brittle) could occur within the same soft deforming layer. Such conditions would be controlled by pore water content and unlike the Hart and Boulton (1991) model, the lateral, vertical and temporal variations in these states are not thought to be predictable on the basis of advancing and retreating ice sheets. Rather

these processes would be spontaneous and would be consistent with the constantly changing polythermal conditions and localised pressure gradients within a glacial mélange of frozen sand blocks and saturated deforming till. Accordingly, the sediments would have been subjected to a variety of stresses, each creating structures that obliterated or modified those formed by earlier stresses.

Initially, at the margin of an ice sheet in a marine basin, basal melt-out debris would mix with deformable muds while simultaneously deforming in response to ductile shear (Hicock and Dreimanis, 1992). Subsequent to the freezing and plucking of the sand units (described above), supersaturated viscous flow combined with continuing ductile shear would then produce necking and flow banding structures within the diamicton and eventually at high enough strain rates, a homogeneous (massive) diamicton (Hart and Boulton, 1991). Gradually, water loss would initiate immobilisation of the deforming till layer from the base upward (Boulton and Hindmarsh, 1987; Menzies, 1989; Hart *et al.*, 1990) resulting in a the longitudinal extension and boudinage of less competent units (i.e., partially frozen sandy silts and smaller sand lensoid units; Hart and Boulton, 1991; Hicock and Dreimanis, 1992). The near horizontal fissures and the observed folding, albeit rare, of the sandy silt layers are also consistent with the expected unidirectional folds and fabric of these conditions. Therefore with decreasing pore water conditions, lodgement and/or brittle deformation would be expected (Hicock and Dreimanis, 1992). Accordingly, the massive diamicton, formed at high strain rates under high pore water pressures, would then develop fissures associated with ductile-brittle shearing. Therefore, the massive diamicton in addition to the occurrence of heavily deformed sand lenses within the upper portion of the drumlin at Chimney Bluffs could be analogous to the homogenous zone of the Hart and Boulton model and the upper ductile shear zone of the Hicock and Dreimanis model (Fig. 5.1a). These sediments were

then fissured and fractured in response to decreasing pore water conditions. Such a zone is consistent with the idea that the most intensive subglacial deformation occurs in immediate contact with the over-riding ice (Banham, 1977).

5.5 Conclusions

The glacial sediments at Chimney Bluffs probably represents a block-in-matrix style glacial mélange in which polythermal conditions existed. Localised pore water pressure variations and shear stresses associated with deformable bed conditions are possible mechanisms for the plucking and entrainment and eventual deposition of blocks of overridden proglacial sediments or even the displacement of subglacial conduits or sediments. Preservation of primary stratification within the sand intraclasts implies that they were transported as cohesive or partially frozen blocks enveloped by an impermeable diamicton. During entrainment, constructional glaciotectonics transported the still-frozen or cohesive sand blocks and sandy silt layers up into the mid-vertical zone of the drumlin. Longitudinal and possibly lateral shearing within the soft deforming till layer attenuated some sand units into boudinage structures. The overall massive appearance of diamicton could be the result homogenisation caused by very high bulk strain within a complexly deforming and heavily stressed subglacial till environment.

Several questions concerning the sediments at Chimney Bluffs are raised by the current study. The three dimensional aspects of the sand intraclasts were not adequately investigated. The long axis orientation of these units could provide useful information in determining the style of their emplacement (i.e a transverse orientation to ice flow would imply viscous flow conditions; Hicock and Dreimanis, 1992). Similarly, a more detailed examination of the orientation of the sandy silt layers and the fissility within the diamicton could provide a clearer indication of the mechanics involved in subglacial till deformation and

drumlinisation. It would also be interesting to conduct a lee-side investigation of this drumlin to determine how continuous these features are along the long axis of the landform. Although a model has been proposed for the emplacement of the sediment package at the current site, it does not account for the overall drumlinisation process.

However, several implications for future research arise from the foregoing discussion. The usefulness of micromorphological research in the study of glacigenic deposits has already been demonstrated by several authors (Meer, 1987; Menzies, 1990; Menzies and Maltman, 1992). The current study reaffirms this usefulness by showing that an apparently massive diamicton and undisturbed stratified sands within the diamicton contain microstructures indicative of high bulk strain rates. Investigations of subglacial environments can therefore benefit from the application of this technique in conjunction with traditional sedimentology. Considering the latter, it is obvious that apparently massive diamictons need to be re-examined for evidence of microstructures that could lead to the re-interpretation of diamicton forming processes.

REFERENCES

ALLEN, T. 1974. Particle Size Measurement. Chapman and Hall Ltd., pp. 191-220.

ALLEN, J. R. L. 1982. Sedimentary Structures: Their Character and Physical Basis, 2 Volumes. Elsevier, New York, 633pp.

ALLEY, R. B. 1991. Deforming-bed origin for southern Laurentide till sheets? Journal of Glaciology, **37**: 67-76.

ALLEY, R. B., BLANKENSHIP, D. D., ROONEY, S. T., and BENTLEY, C. R. 1987. Till beneath ice stream B 4: a coupled ice-till flow model. Journal of Geophysical Research, **92**: 8931-8940.

ANDERSON, W. F. 1983. Foundation engineering in glaciated terrain. *In* Glacial geology: an introduction for engineers and earth scientists. *Edited by* N. Eyles. Pergamon, New York, pp. 275-301.

BANHAM, P. H. 1977. Glacitectonics in till stratigraphy. Boreas, **6**: 101-105.

BARATT, B. C. 1969. A revised classification of the microscopic soil materials with particular reference to organic components. Geoderma, **2**: 257-272.

BENTLEY, C. R. 1987. Antarctic ice streams: a review. Journal of Geophysical Research, **92**: 8843-8858.

BLANKENSHIP, D. D., BENTLEY, C. R., ROONEY, S. T., and ALLEY, R. B. 1987. Till beneath ice stream b1: properties derived from seismic travel times. Journal of Geophysical Research, **92**: 8903-8911.

BLOOM, A. L. 1986. Geomorphology of the Cayuga Lake Basin. Cornell University Press, Ithica, pp. 261-279.

BOULTON, G. S. 1982. Subglacial processes and the development of glacial bedforms. *In* Research in glacial, glaciofluvial and glaciolacustrine systems. *Edited by* R. Davidson Arnott, W. Nickling, and B. D. Fahey. Geobooks, Norwich, pp. 1-31.

BOULTON, G. S. 1987. A theory of drumlin formation by subglacial sediment deformation. *In* Drumlin symposium. *Edited by* J. Menzies, and J. Rose. A. A. Balkema, Rotterdam, pp. 25-80.

BOULTON, G. S., and HINDMARSH, R. C. A. 1987. Sediment deformation beneath glaciers: rheology and geological consequences. Journal of Geophysical Research, **92**: 9059-9082.

BOULTON, G. S. and DOBBIE, K. E. 1993. Consolidation of sediments by glaciers: relations between sediment geotechnics, soft-bed glacier dynamics and subglacial ground-water

flow. Journal of Glaciology, **39**: 26-44.

BOYCE, J. I., and EYLES, N. 1991. Drumlins carved by deforming till streams below the Laurentide ice sheet. Geology, **19**: 787-790.

BRENNAN, S. F., and CALKIN, P. E. 1984. Analysis of bluff erosion along the southern coastline of Lake Ontario, New York. New York Sea Grant Institute, 74 pp.

BREWER, R. 1976. Fabric and Mineral Analysis of Soils. Robert E. Krieger, New York, 482 pp.

BROSTER, B. E., and CLAGUE, J. J. 1987. Advance and retreat glacigenic deformation at Williams Lake British Columbia. Canadian Journal of Earth Sciences, **24**: 1421-1430.

BROWN, N. E., HALLET, B., and BOOTH, D. B. 1987. Rapid soft bed sliding of the Puget glacial lobe. Journal of Geophysical Research, **92**: 8895-8997.

CALKIN, P. E., and MULER, E. H. 1992. Pleistocene stratigraphy of the Lake Erie and Ontario lake bluffs in New York. Quaternary coast of the United States: marine and lacustrine systems. SEPM Special Publication, **48**: 385 -396.

CLARKE, G. K. C. 1987. Subglacial till: a physical framework for its properties and processes. Journal of Geophysical Research, **92**: 9023-9036.

CLARKE, G. K. C. 1987a. Fast glacier flow: ice streams, surging, and tidewater glaciers. Journal of Geophysical Research, **92**: 8835-8841.

CLAYTON, L., MICKELSON, D. M., and ATTIG, J. W. 1989. Evidence against pervasively deformed bed material beneath rapidly moving lobes of the southern Laurentide ice sheet. Sedimentary Geology, **62**: 203-208.

COWAN, D. S. 1985. Structural styles in Mesozoic and Cenozoic mélanges in the western Cordillera of North America. Geological Society of America Bulletin, **96**: 451-462.

CRAIG, R. F. 1987. Soil Mechanics. Van Nostrand Reinhold, Wokingham. 410 pp.

DARDIS, G. F., and MCCABE, A. M. 1983. Facies of subglacial channel sedimentation in late Pleistocene drumlins, Northern Ireland. Boreas, **12**: 263-278.

DARDIS, G. F., and MCCABE, A. M. 1987. Subglacial sheetwash and debris flow deposits in late Pleistocene drumlins, Northern Ireland. *In* Drumlin symposium. *Edited by* J. Menzies, and J. Rose. A.A. Balkema, Rotterdam, pp. 225-240.

DE JONG, M. G. G., and RAPPOL, M. 1983. Ice marginal debris-flow deposits in western Allgau, southern West Germany. Boreas, **12**: 57-70.

DREDGE, L. A. 1988. Drift carbonate on the Canadian Shield. II: carbonate dispersal and

ice-flow patterns in northern Manitoba. Canadian Journal of Earth Sciences, **25**: 783 -787.

DREIMANIS, A. 1989. Tills: their genetic terminology and classification. *In* Genetic classification of glacigenic deposits. *Edited by* R. P. Goldthwait and C. L. Matsch. A. A. Balkema, Rotterdam, pp. 17-83.

ECHELMEYER, K., and ZHONGXIANG, W. 1987. Direct observation of basal sliding and deformation of basal drift at sub-freezing temperatures. Journal of Glaciology, **33**: 83 -98.

EVENSON, E. B. 1971. The relationship of macro and microfabrics of till and the genesis of glacial landforms in Jefferson County, Wisconsin. *In* Till/ a symposium. *Edited by* R. P. Goldthwait. Ohio State University Press, pp. 345-364.

EYLES, C. H., and EYLES, N. 1983. Sedimentation in a large lake: a reinterpretation of the late Pleistocene stratigraphy at Scarborough Bluffs, Ontario, Canada. Geology, **11**: 146-152.

EYLES, N., SALDEN, J. A., and GILROY, S. 1982. A depositional model for stratigraphic complexes and facies superimposition in lodgement till. Boreas, **11**: 317-333.

EYLES, N., EYLES, C., and MIALL, A., 1983. Lithofacies types and vertical profile models; an alternative approach to the description and environmental interpretation of glacial diamict sequences. Sedimentology, **30**: 393-410.

FAIRCHILD, H. L. 1907. Drumlins of central western New York State. New York State Museum, Bulletin 111, pp. 391-443.

FRANCEK, M. A. 1991. A spatial perspective on the New York Drumlin Field. Physical Geography, **12**: 1-18.

FULLERTON, D. S. 1980. Preliminary correlation of post-Erie Interstadial events (16,000 10,000 radiocarbon years before present), central and eastern Great Lakes region, and Hudson, Champlain, and St.-Lawrence lowlands, United States and Canada. Geological Survey Professional Paper 1089. pp. 1-52.

FULLERTON, D. S. 1986. Stratigraphy and correlation of glacial deposits from Indiana to New York and New Jersey. *In* Quaternary glaciations in the northern hemisphere. *Edited by* V. Sibrava, D. Q. Bowen, and G. M. Richmond. Pergamon Press, Toronto, pp. 23-36.

GEE, G. W., and BAUDER, J. W. 1986. Particle size analysis. *In* Methods of soil analysis. *Edited by* A. Klute. American Society of Argonomy and Soil Science of America, pp. 383-411.

GILLETTE, T. 1940. Geology of the Clyde and Sodus quadrangles, New York. New York

State Museum Bulletin, **320**: 1-179.

GRAVENOR, C. P. 1953. The origin of drumlins. American Journal of Science, **251**: 674-681.

GUSTAVSON, T. C., and BOOTHROYD, J. C. 1982. Subglacial fluvial erosion: a major source of stratified drift, Malaspina Glacier Alaska. *In* Research in glacial, glaciofluvial and glaciolacustrine systems. *Edited by* R. Davidson-Arnott, W. Nickling, and B. D. Fahey. Geobooks, Norwich, pp. 93-116.

HALLET, B. 1976. Deposits formed by subglacial precipitation of $CaCO_3$. Geological Society of America Bulletin, **87**: 1003-1015.

HANVEY, P. M., 1987. Sedimentology of lee-side stratification sequences in late Pleistocene drumlins, north-west Ireland. *In* Drumlin symposium. *Edited by* J. Menzies, and J. Rose. A.A. Balkema, Rotterdam, pp. 241-253.

HANVEY, P. 1989. Stratified flow deposits in a late Pleistocene drumlin in northwest Ireland. Sedimentary Geology, **62**: 211-221.

HART, J. K. 1994. Till fabric associated with deformable beds. Earth Surface Processes and Landforms, **19**: 15-32.

HART, J. K., and BOULTON, G. S. 1991. The interrelation of glaciotectonic and glaciodepostional processes within the glacial environment. Quaternary Science Reviews, **10**: 335-350.

HART, J. K., HINDMARSH, R. C., and BOULTON, G. S. 1990. Styles of subglacial deformation within the context of the Anglian ice-sheet. Earth Surface Processes and Landforms, **15**: 227-241.

HICOCK, S. R. 1988. Calcareous till facies north of Lake Superior, Ontario: implications for Laurentide ice streaming. Géographie Physique et Quaternaire, **42**: 120-135.

HICOCK, S. R., and DREIMANIS, A. 1992. Deformation till in the Great Lakes region: implications for rapid flow along the south-central margin of the Laurentide Ice Sheet. Canadian Journal of Earth Sciences, **29**: 1565-1579.

HICOCK, S. R., KRISTJANSSON, F. J., and SHARPE, D. R. 1989. Carbonate till as a soft bed for Pleistocene ice streams on the Canadian Shield north of Lake Superior. Canadian Journal of Earth Sciences, **26**: 2249-2254.

HOLMES, C. 1952. Drift dispersion in west-central New York. Geological Society of America Bulletin, **63**: 993-1010.

HOOKE, R. L., WOLD, B., and HAGEN, J. O. 1985. Subglacial hydrology and sediment transport at Bondhusbreen, southwest Norway. Geological Society of America

Bulletin, **96**: 388-397.

HOOKE, R. L., LAUMANN, T., and KOHLER, J. 1990. Subglacial water pressures and the shape of subglacial conduits. Journal of Glaciology, **36**: 67-71.

HUGHES, T. J. 1981. Numerical reconstruction of paleo-ice sheets. *In* The last great ice sheets. *Edited by* G. H. Denton and T. J. Hughes. Wiley, New York, pp. 222-261.

HUGHES, T. J. 1987. Ice dynamics and deglaciation models when ice sheets collapsed. *In* North America and adjacent oceans during the last deglaciation, the geology of North America, Vol. K-3. *Edited by* W. R. Ruddiman, and H. E. Wright, JR. Geological Society of America, Boulder, pp. 183-220.

HUNTLEY, D. H., and BROSTER, B. E. 1993. Polyphase glacigenic deformation of advance glaciofluvial sediments, near Big Creek, British Columbia. Géographie Physique et Quaternaire, **47**: 211-219.

KAZI, A. and KNILL, J. L. 1973. Fissuring in glacial lake clays and tills on the Norfolk coast, United Kingdom. Engineering Geology, **7**: 35-48.

KEMP, R. A. 1985. Soil micromorphology and the quaternary. Q.R.A. Technical Guide, **2**: pp. 1-80.

KRALL, D. B. 1977. Late Wisconsinan ice recession in east-central New York. Geological Society of America Bulletin, **88**: 1697-1710.

KRUGER, J., and THOMSEN, H. H. 1984. Morphology, stratigraphy, and genesis of small drumlins in front of the glacier Myvdaljokull, South Iceland. Journal of Glaciology, **30**: 94-105.

KUMPULAINEN, R. A. Fissure-fill and tunnel-fill sediments: expressions of permafrost and increased hydrostatic pressure. Journal of Quaternary Science, **9**: 59-72.

LADANYI, B., and MOREL, J. F. 1990. Effect of internal confinement on compression strength of frozen sand. Canadian Geotechnical Journal, **27**: 8-18.

LAGERLUND, E., and van der MEER, J. J. M. 1990. Micromorphological observations on the Lund diamicton. Lundqua Report, **32**: 37-38.

LOWE, D. R., and LOPICCOLO, R. D. 1974. The characteristics and origins of dish and pillar structures. Journal of Sedimentary Petrology, **44**: 484-501.

MARTIN, J. O. 1901. The Ontario coast between Fairhaven and Sodus Bays, New York. American Geologist, **27**: 331-334.

MAYEWSKI, P. A., DENTON, G. H., and HUGHES, T. J. 1981. Late Wisconsin ice sheets of North America. *In* The last great ice sheets. *Edited by* G. H. Denton, and T. J.

Hughes. John Wiley & Sons, Toronto, pp. 67-178.

MCCABE, A. M. 1991. The distribution and stratigraphy of drumlins in Ireland. *In* Glacial deposits in Great Britain and Ireland. *Edited by* J. Ehlers, P. L. Gibbard, and J. Rose. Balkema, Rotterdam, pp. 421-435.

MCCABE, A. M., and DARDIS, G. F., 1989. Sedimentology and depositional setting of late Pleistocene drumlins, Galway Bay, western Ireland. Journal of Sedimentary Petrology, **59**: 944-959.

MCGOWN, A. and RADWAN, A. M. 1974. Fissures in boulder clays. Canadian Geotechnical Journal, **12**: 84-97.

MEER, J. J. M. van der. 1987. Micromorphology of glacial sediments as a tool in distinguishing genetic varieties of till. Geological Survey of Finland Special Paper, **3**: 77-89.

MEER, J. J. M. van der. 1993. Micromorphology of Glacial Sediments, a Workshop. University of Amsterdam Press, Fysisch Geografisch en Bodemkundig Laboratorium, pp. 1-42.

MEER, J. J. M. van der., and LABAN, C. 1990. Micromorphology of some North Sea till samples, a pilot study. Journal of Quaternary Science, **5**: 95-101.

MENZIES, J. 1979. A review of the literature on the formation and location of drumlins. Earth Science Reviews, **14**: 315-359.

MENZIES, J. 1982. A till hummock (proto-drumlin) at the ice glacier bed interface. *In* Research in glacial, glaciofluvial and glaciolacustrine systems. *Edited by* R. Davidson-Arnott, W. Nickling, B. D. Fahey. Geo Books, pp. 33-48.

MENZIES, J. 1987. Towards a general hypothesis on the formation of drumlins. *In* Drumlin symposium. *Edited by* J. Menzies, and J. Rose. A.A. Balkema, Rotterdam, pp. 9-24

MENZIES, J. 1987a. Manual for Field Description of Glacial and Associated Sediments. Brock University, pp. 1-59.

MENZIES, J. 1989. Subglacial hydraulic conditions and their possible impact upon subglacial bed formation. Sedimentary Geology, **62**: 125-150.

MENZIES, J. 1990. Sand intraclasts within in a diamicton mélange, southern Niagara Peninsula, Ontario, Canada. Journal of Quaternary Science, **5**: 189-206.

MENZIES, J. 1990a. Brecciated diamictons from Mohawk Bay, S. Ontario, Canada. Sedimentology, **37**: 481-493.

MENZIES, J. 1993. Laboratory Manual for Soil Science. Brock University, pp. 13-17.

MENZIES, J., and MALTMAN, A. J. 1992. Microstructures in diamictons-evidence of subglacial bed conditions. Geomorphology, **6**: 27-40.

MENZIES, J. and WOODWARD, J. 1993. Preliminary study of subglacial diamicton microstructures as reflected in drumlin sediments at Chimney Bluffs, New York. *In* Glaciotectonics and mapping glacial deposits. *Edited by* J. S. Abers. University of Regina, Regina, pp. 36-45.

MICKELSON, D. M., CLAYTON, L., FULLERTON, D. S., and BORNS, H. W., JR. 1983. The late Wisconsin glacial record of the Laurentide ice sheet in the United States. *In* Late Quaternary environments of the United States. *Edited by* H. E. Wright, JR. Vol. 1: The late Pleistocene. *Edited by* S. C. Porter. University of Minnesota Press, Minneapolis, pp. 3-37.

MIDDLETON, G. V., and SOUTHARD, J. B. 1978. Mechanics of sediment movement. SEPM Short Course Notes, 3.

MILLER, J. W., JR. 1972. Variations in New York drumlins. Annals of the Association of American Geographers, **62**: 418-423.

MOOERS, H. D. 1989. Drumlin formation: a time transgressive model. Boreas, **18**: 99-107.

MOSS, J., and RITTER, D. 1962. New evidence regarding the Binghampton substage in the region between the Finger Lakes and Catskills, New York. American Journal of Science, **260**: 81-106.

MÜCHER, H. J., and MOROZOVA, T. D. 1983. The application of soil micromorphology in Quaternary geology and geomorphology. *In* Soil micromorphology. *Edited by* P. Bullock and C. P. Murphy. A. B. Academic Publishers, Berkhamsted, pp. 151-194.

MULLER, E. H. 1963. Geology of Chautauqua County New York Part II, Pleistocene geology. New York State Museum and Science Service, Bulletin 392, pp. 1-60.

MULLER, E. H. 1965. Quaternary geology of New York. *In* The Quaternary of the United States. *Edited by* H. E. Wright, JR., and D. G. Frey. Princeton University Press, Princeton, pp. 99-112.

MULLER, E. H. 1974. Origins of drumlins. *In* Glacial geomorphology. *Edited by* D. R. Coates. State University of New York, Binghampton, pp. 187-204.

MULLER, E. H., and CADWELL, D. H. 1986. Surficial geologic map of New York - Finger Lakes sheet. New York State Museum, Geological Survey Map and Chart Series no. 40, scale 1:250 000.

MULLER, E. H., and CALKIN, P. E. 1993. Timing of Pleistocene glacial events in New York State. Canadian Journal of Earth Sciences, **30**: 1829 -1845.

MULLINS, H. T., and HINCHEY, E. J. 1989. Erosion and infill of New York Finger Lakes: implications for Laurentide ice sheet deglaciation. Geology, **17**: 622-625.

OWEN, G. 1987. Deformation processes in unconsolidated sands. *In* Deformation of sediments and sedimentary rocks. *Edited by* M. E. Jones and R. M. F. Preston. Geological Society Special Publication 29, pp. 11-24.

PAUL, M. A., and EVANS, H. 1974. Observations on the internal structure and origin of some flutes in glaciofluvial sediments, Blomstrandbreen, north-west Spitsbergen. Journal of Glaciology, **13**: 393-400.

POWERS, M. C. 1953. A new roundness scale for sedimentary particles. Journal of Sedimentary Petrology, **23**: 117-119.

REED, B., GALVIN, C. J., and MILLER, J. P. 1962. Some aspects of drumlins geometry. American Journal of Science, **260**: 200-210.

RICKARD, L. V., and FISHER, D. W. 1970. Geologic map of New York - Finger Lakes sheet. New York State Museum and Science Service Map and Chart Series no. 15, scale 1:250 000.

RIDKY, R. W., and BINDSCHALER, R. A. 1990. Reconstruction and dynamics of the Late Wisconsin "Ontario" ice dome in the Finger Lakes region, New York. Geological Society of America Bulletin, **102**: 1055-1064.

RUDDIMAN, W. F. 1987. Synthesis: the ocean/ice sheet record. *In* North America and adjacent oceans during the last deglaciation, the geology of North America, Vol. K-3. *Edited by* W. R. Ruddiman, and H. E. Wright, JR. Geological Society of America, Boulder, pp. 463-478.

ROONEY, S. T., BLANKENSHIP, D. D., ALLEY, R. B., and BENTLEY, C. R. 1987. Till beneath ice stream b2 : structure and continuity. Journal of Geophysical Research, **92**: 8913-8920.

SAUNDERSON, H. C. 1977. The sliding bed facies in esker sands and gravels: a criterion for full pipe-flow. Sedimentology, **24**: 623-638.

SHARPE, D. R. 1987. The stratified nature of drumlins from Victoria Island and southern Ontario, Canada. *In* Drumlin symposium. *Edited by* J. Menzies, and J. Rose. A. A. Balkema, Rotterdam, pp. 185-214.

SHAW, J. 1979. Genesis of the Sveg tills and rogen moraines of central Sweden: a model of basal melt out. Boreas, **8**: 409-426.

SHAW, J. 1983. Drumlin formation related to inverted erosion marks. Journal of Glaciology, **29**: 461-479.

SHAW, J., and GILBERT, R. 1990. Evidence for large-scale subglacial meltwater flood events in southern Ontario and northern New York State. Geology, **18**: 1169-1172.

SHAW, J., KVILL, D., and RAINS, B. 1989. Drumlins and catastrophic subglacial floods. Sedimentary Geology, **62**: 177-202.

SITLER, R. F., and CHAPMAN, C. A. 1955. Microfabrics of till from Ohio and Pennsylvania. Journal of Sedimentary Petrology, **25**: 262-269.

SLATER, G. 1928. Structure of drumlins on the southern shore of Lake Ontario, New York State. Pan American Geologist, **50**: 232.

SLATER, G. 1929. Structure of drumlins on the southern shore of Lake Ontario. New York State Museum, Bulletin 281, pp. 3-19.

SOUCHEZ, R. A. and LORRAIN, R. D. 1991. Ice Composition and Glacier Dynamics. Springer-Verlag: New York, 207pp.

SUGDEN, D. E. 1977. Reconstruction of the morphology, dynamics and thermal characteristics of the Laurentide Ice Sheet at its maximum. Arctic and Alpine Research, **9**: 21-47.

TARR, R. S. 1905. Drainage features of central New York. Geological Society of America Bulletin, **16**: 229-242.

VERNON, P. 1966. Drumlins and Pleistocene ice flow over the Ards Peninsula, Stranford Lough area, County Down, Ireland. Journal of Glaciology, **6**: 401-409.

WALDER, J. S., and FOWLER, A. 1994. Channelized subglacial drainage over a deformable bed. Journal of Glaciology, **40**: 3-15.

WHALLEY, W. B., GELLATLY, A. F., GORDON, J. E., and HANSOM, J. D. 1990. Ferromanganese rock varnish in north Norway: a subglacial origin. Earth Surfaces Processes and Landforms, **15**: 265-275.

WHITTECAR, G. R., and MICKELSON, D. M. 1979. Composition, internal structures and an hypothesis of formation for drumlins, Waukesha County, Wisconsin, U.S.A.. Journal of Glaciology, **22**: 357-371.

WRIGHT, H. E., JR. 1973. Tunnel valleys, glacial surges, and subglacial hydrology of the Superior lobe, Minnesota. *In* The Wisconsinan stage. *Edited by* R. F. Black, R. P. Goldthwait, and H. B. Willman. Geological Society of America, Memoir 136, pp. 251-276.

APPENDIX I: PARTICLE SIZE CALCULATION IN THE HYDROMETER METHOD

Calculation of Particle Size

(modified from Gee and Bauder, 1986)

Grain sizes were determined from the raw hydrometer data through a series of calculations based on the determination of particle settling rates as defined by Stokes' Law and the assumption that the terminal velocity of the particles was reached almost instantaneously:

$$r = (9\eta s)\cdot[2g(\rho_s - \rho_1)t]^{-½}$$

The actual procedure involved a series of steps beginning with the substraction of the blank solution hydrometer reading from the individual sample readings which were then divided by the initial dry weight of the sample and multiplied by 100 to yield a summation percent. Determination of the mean particle diameter was based on the equation:

$$d = \theta\cdot(t)^{-½}$$

where: d = diameter (µm)

t = time (min.)

θ = sedimentation parameter (µm·min^{½}), defined as:

$$\theta = 1000\ (B\cdot h')$$

where:

$$B=(30\cdot\eta)\cdot[g(\rho_s - \rho_1)]^{-1}$$

and,

$$h' = 16.3 - 0.164R$$

where: h' = effective hydrometer depth (cm)

R = uncorrected hydrometer reading (g·l^{-1})

g = gravitational acceleration (980.35 cm·s^{-2})

ρ_s = soil particle density (assume 2.65 $g \cdot cm^{-3}$)

ρ_1 = solution density ($g \cdot cm^{-3}$)

η = solution viscosity ($g \cdot cm^{-1} \cdot s^{-1}$ - poise)

Furthermore, to calculate the solution density at a given temperature the following equation is used:

$$\rho^{l} = \rho°(1 + 0.630\ C_s)$$

where: $\rho°$ = water density at temperature T ($g \cdot ml$)

C_s = sodium hexametaphosphate concentration ($g \cdot ml$)

Similarily, the solution viscosity at temperature T can be calculated by:

$$\eta = \eta°(1 + 4.25\ C_s)$$

where: $\eta°$ = water viscosity at temperature T (10^{-3} $kg \cdot m^{-1} \cdot s^{-1}$)

Note: the equations for ρ_1 and η are only valid for sodium hexametaphosphate solutions ≤ 50 $g \cdot l^{-1}$.

APPENDIX II: GRAIN SIZE ANALYSIS RESULTS AND SITE DESCRIPTIONS

Table 3.1a Gravel, sand, silt/clay, silt, and clay fractions (%) of diamicton, glacio-fluvial and glacio-lacustrine samples at Chimney Bluffs.

Sample	Gravel	Sand	Silt/Clay	Silt	Clay
93-CB-1	2.0	15.3	82.7	45.3	37.3
93-CB-2	0.0	44.7	55.3	43.5	11.8
93-CB-2b	0.0	41.2	58.8	50.6	8.2
93-CB-3	24.7	47.2	28.1	20.2	7.9
93-CB-5a	27.6	41.4	31.0	26.4	4.6
93-CB-5b	16.7	47.8	35.6	27.8	7.8
93-CB-6	8.2	47.1	44.7	27.1	17.6
93-CB-7a	17.2	48.4	34.4	30.1	4.3
93-CB-7b	13.0	54.3	32.6	27.2	5.4
93-CB-9	12.2	51.1	36.7	31.1	5.6
93-CB-10	19.3	43.2	37.5	34.1	3.4
93-CB-11	12.6	54.7	32.6	25.3	7.4
93-CB-14	16.0	42.6	41.5	29.8	11.7
93-CB-16	23.3	44.2	32.6	26.7	5.8
93-CB-17b	10.6	45.7	43.6	34.0	9.6
93-CB-19b	19.0	40.5	40.5	28.6	11.9
93-CB-19d	10.5	50.5	38.9	31.6	7.4
93-CB-21b	55.8	35.5	8.6	7.1	1.5
93-CB-22	6.9	49.4	43.7	31.0	12.6
93-CB-22b	16.1	43.0	40.9	34.4	6.5
93-CB-27	10.6	47.9	41.5	29.8	11.7
93-CB-28	18.9	44.2	36.8	26.3	10.5
93-CB-33	12.8	47.9	39.4	27.7	11.7

Table 3.1b Gravel, sand, silt/clay, silt, and clay fractions (%) of sand unit samples at Chimney Bluffs.

Sample	Gravel	Sand	Silt/Clay	Silt	Clay
93-CB-11b	7.1	76.5	16.3	14.3	2.0
93-CB-11c	16.9	50.6	32.6	23.6	9.0
93-CB-11d	22.0	48.9	29.0	24.7	4.3
93-CB-12	9.3	58.1	32.6	31.4	1.2
93-CB-15	3.1	77.3	19.6	17.5	2.1
93-CB-17	25.1	42.9	31.9	30.4	1.6
93-CB-19a	4.2	68.8	27.1	25.0	2.1
93-CB-21a	13.1	67.7	19.2	17.2	2.0
93-CB-24a	0.0	41.2	58.8	54.6	4.1
93-CB-24b	37.1	51.5	11.3	7.2	4.1
93-CB-24c	0.0	85.6	14.4	11.3	3.1
93-CB-25	4.2	53.7	42.1	35.8	6.3
93-CB-27b	2.6	87.1	10.3	8.2	2.1
93-CB-32a	5.2	83.3	11.5	8.3	3.1
93-CB-32b	20.0	43.2	36.8	26.3	10.5
93-CB-34	5.2	80.4	14.4	12.4	2.1

Grain Size Scales and Conversion Tables
(after Folk, 1974)

Millimetres	Phi (Φ)	Wentworth Scale
16.00000	-4.0	Pebble
8.00000	-3.0	
4.00000	-2.0	Granule
2.00000	-1.0	Very Coarse Sand
1.00000	+0.0	Coarse Sand
0.50000	+1.0	Medium Sand
0.25000	+2.0	Fine Sand
0.12500	+3.0	Very Fine Sand
0.06250	+4.0	Coarse Silt
0.03100	+5.0	Medium Silt
0.01560	+6.0	
0.00780	+7.0	Fine Silt
0.00390	+8.0	Very Fine Silt
0.00200	+9.0	Clay
0.00098	+10.0	

Site Descriptions

Site 1

This site is characterised by light grey (10YR7/1) rhythmically laminated glaciolacustrine silt and clay (subunit Br; Fig.1) with massive silt laminae ranging up to 0.5 cm thick. Most of the laminae are undisturbed; however, convoluted laminae are present in the lower portion of this section.

Site 2

The base of the site is a 2 m thick unit consisting of light grey (10YR7/1) rhythmically laminated glaciolacustrine silt and clay (Fig. 2) overlying convoluted laminae. Above this unit is a sequence of intercalated laminated silts and clays, sand stringers and sand inclusions up to 0.5 cm thick consisting of very fine light yellowish brown (10YR6/4) sand (subunit Bs, Fig.3).

Site 3

Possible slump of unit A: pinkish grey (7.5YR6/2; 5YR6/2; 5YR7/2), very pale brown (10YR7/3). light brown (&.5YR6/4) and light yellowish brown (19YR6/4) banded massive sandy diamicton (Fig. 4) with grey (10YR6/1) sandy silt layers and coarse sand lenses into adjacent highly convoluted rhythmites of subunit Bs. Sand stringers occur immediately above the sharp irregular contact between subunit Bs and unit A.

Site 4

Crudely stratified coarse gravel lens in diamicton with sharp upper contact and a gradational lower contact comprising a 10-20 cm zone of intercalated sand stringers and gravel units with sandy diamicton.

Site 5

Weakly stratified sand intraclast (0.20 m x 2 m) containing streaks of clay in 2 m

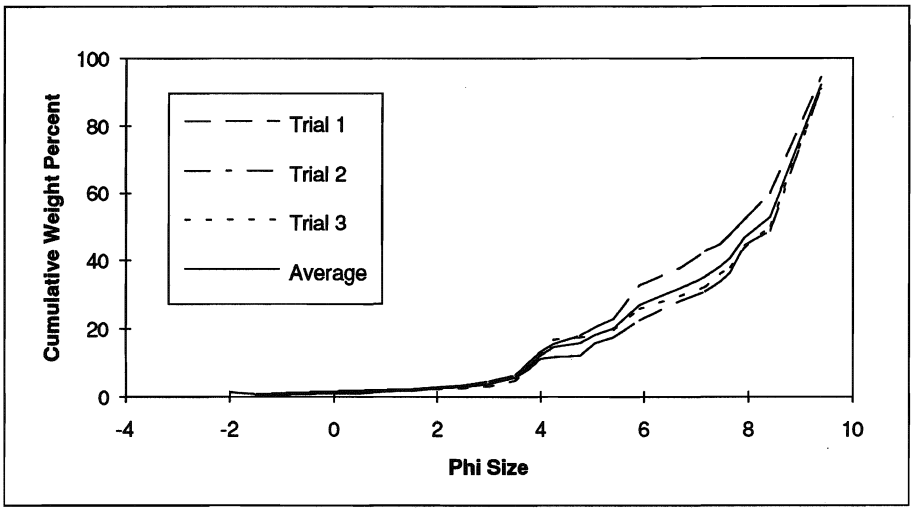

Figure 1 Grain size distribution data for sample 93-CB-1.

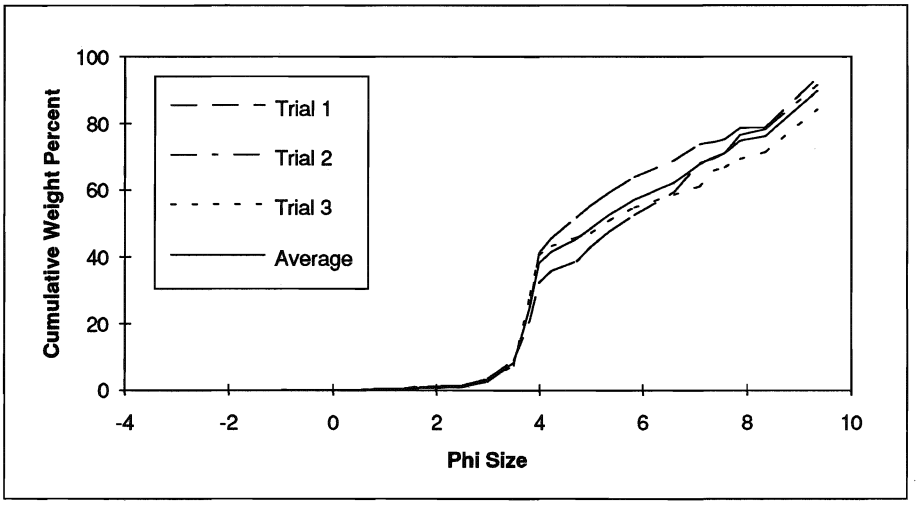

Figure 2 Grain size distribution data for sample 93-CB-2.

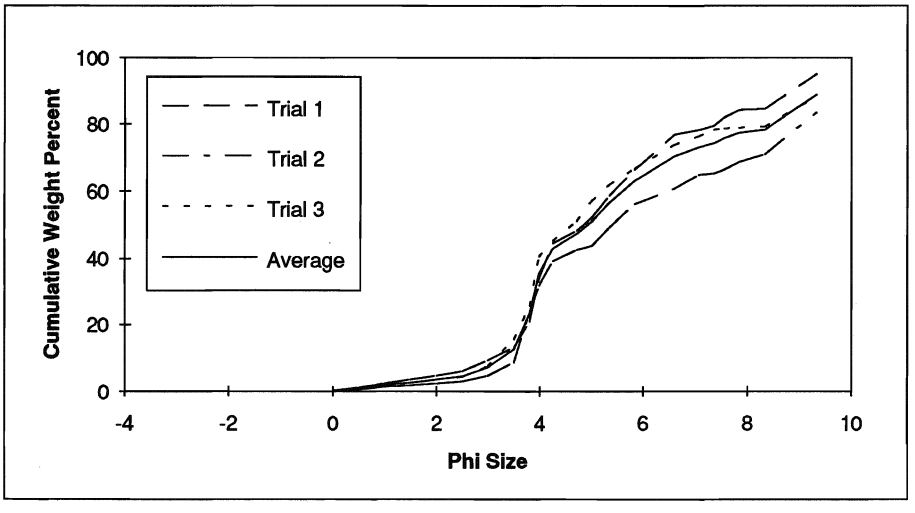

Figure 3 Grain size distribution data for sample 93-CB-2b.

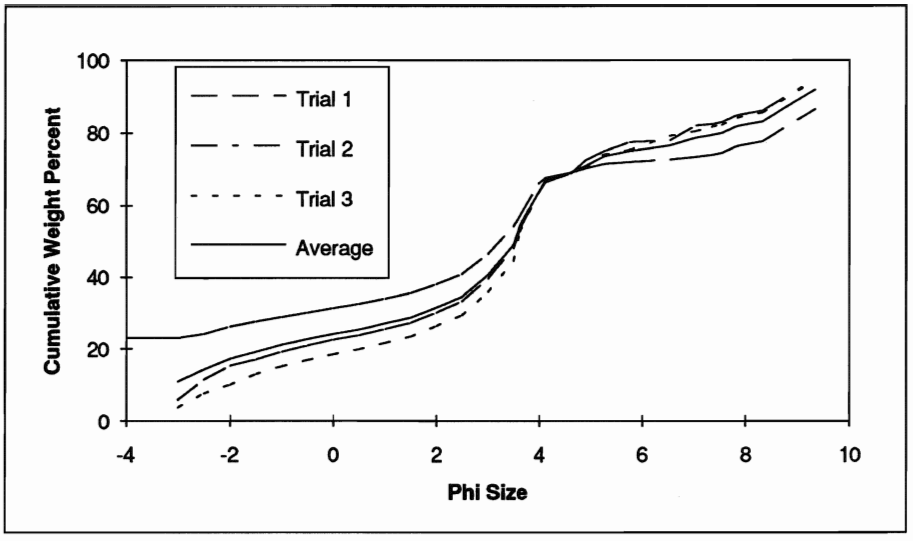

Figure 4 Grain size distribution data for sample 93-CB-3.

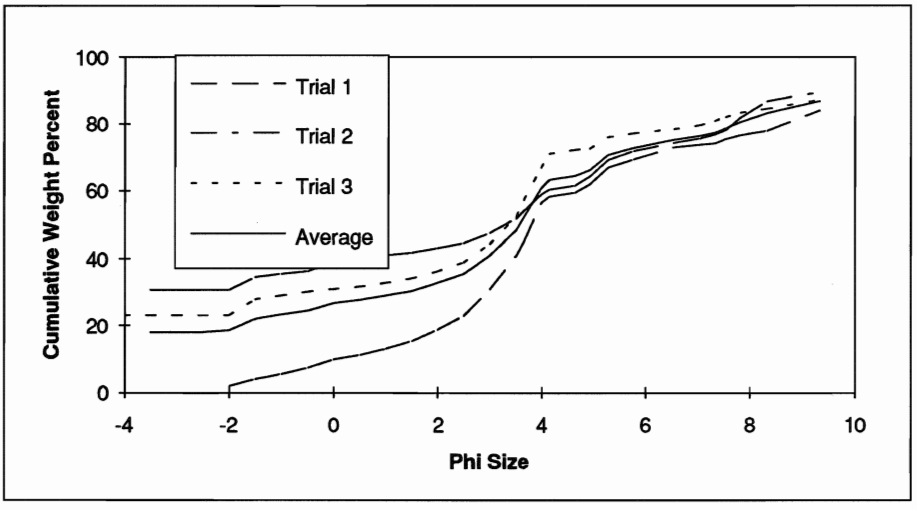

Figure 5 Grain size distribution data for sample 93-CB-5a.

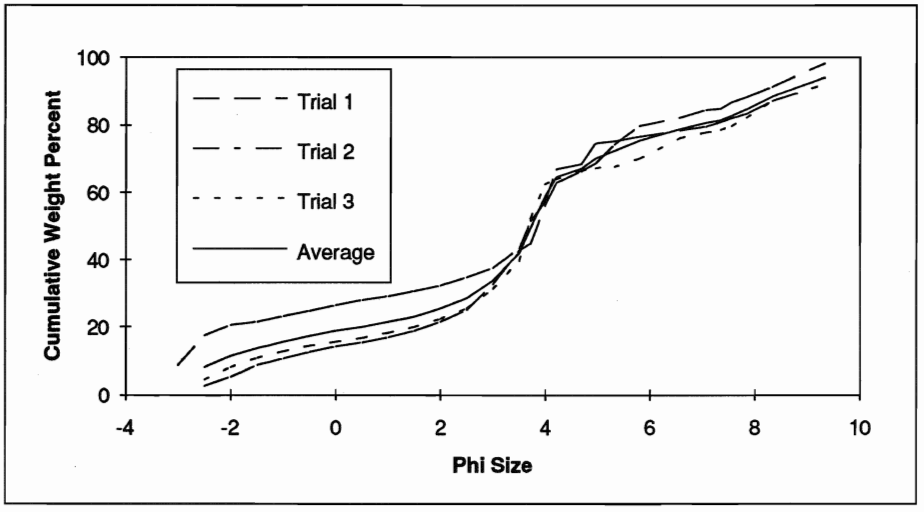

Figure 6a Grain size distribution data for sample 93-CB-5b.

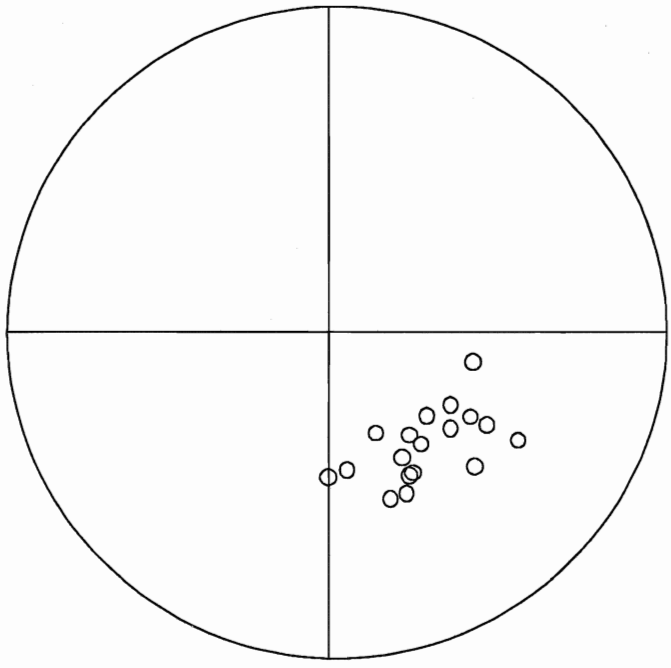

Figure 6b Fissure orientation data for diamicton at *site 5*.

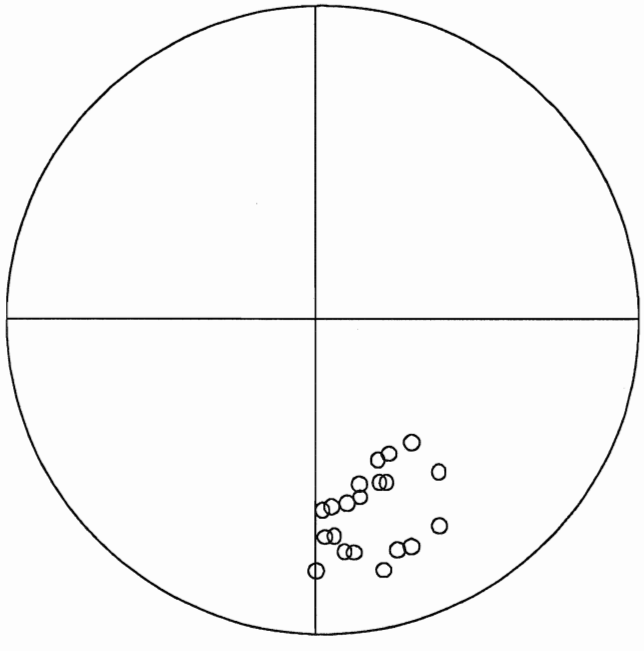

Figure 7a Fissure orientation data for diamicton at *site 6*.

thick beach level slump which grades into a 12 m thick pinkish grey (7.5YR6/2; Fig. 5) and very pale brown (10YR7/3; Fig. 6) banded fissile (Fig. 6b) sandy diamicton. The 4 m thick upper band of very pale brown (10YR4/3) massive sandy diamicton contains many sand stringers and lenses. A sharp erosional contact exists between unit A and a cap of interdigitated stratified light yellowish brown (10YR6/4) sands and gravels (unit B).

Site 6

Two sand lens boudins with coarse sand and clay boudinage structures in fissile (Fig. 7a) pinkish grey (5YR7/2) diamicton containing grey sandy silt layers (Fig. 7a).

Site 7

Light yellowish brown (10YR6/4) sand stringers in very pale brown (10YR7/3; Fig. 8) and pinkish grey (7.5YR6/2; Fig. 9a) banded fissile (Fig. 9b) diamicton.

Site 8 Fissile diamicton with light yellowish brown (10YR6/4) sand intraclast containing coarse sand lenses and sandy silt layers. Fissility in diamicton does not extend into intraclast.

Site 9

Fissile sandy diamicton (Fig. 10) with multiple grey (10YR6/1) sandy silt layers.

Site 10

Sharp erosional contact between fissile (Fig. 11a) diamicton and overlying unit B (Fig. 11b).

Site 11

Fissile pinkish grey (7.5YR6/2) sandy diamicton (Fig. 12) with light brown (7.5YR6/4) sand stringers.

Site 11B

Fissile pinkish grey (7.5YR6/2) sandy diamicton with 1 m thick sand intraclast. Very fine light brown (7.5YR6/4) sand (Fig. 13) comprises the bulk of the intraclast and ranges

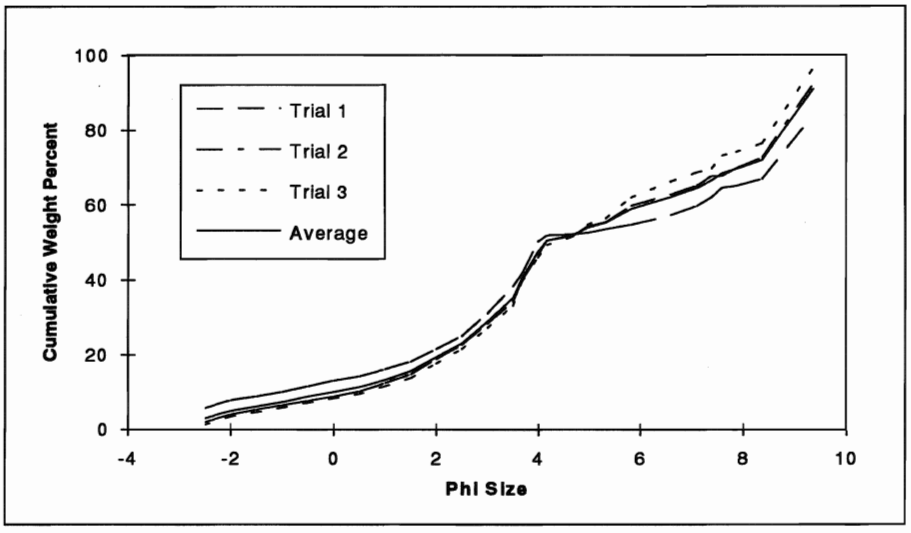

Figure 7b Grain size distribution data for sample 93-CB-6.

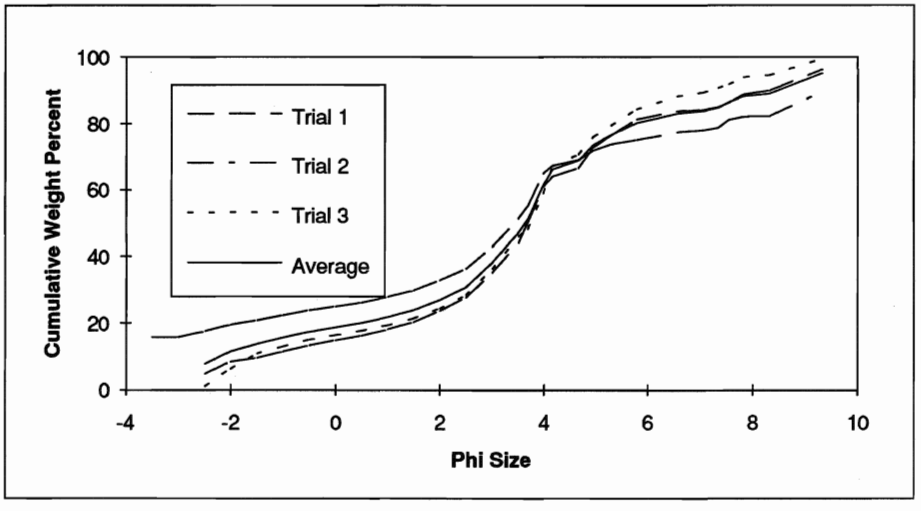

Figure 8 Grain size distribution data for sample 93-CB-7a.

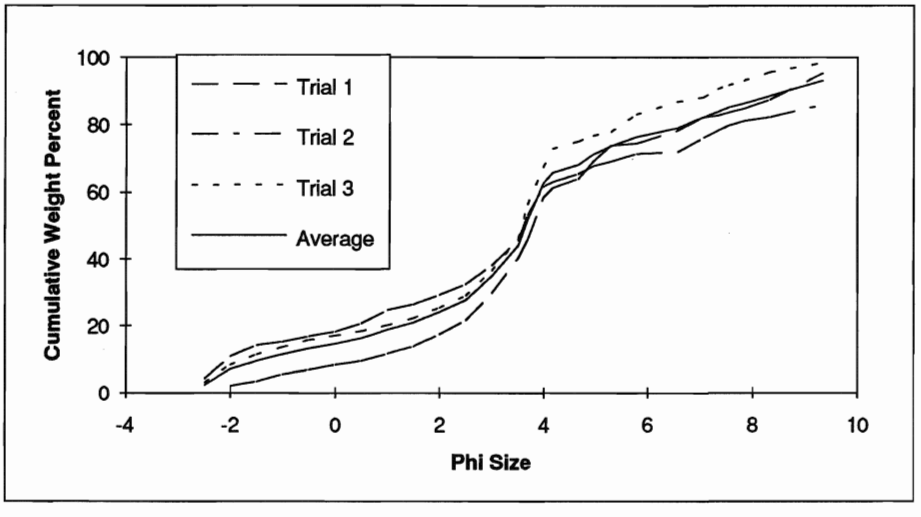

Figure 9a Grain size distribution data for sample 93-CB-7b.

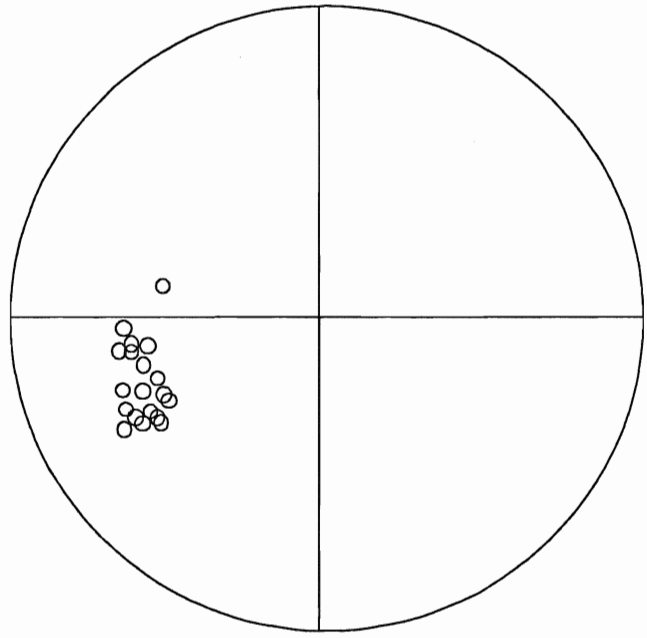

Figure 9b Fissure orientation data for diamicton at *site 7.*

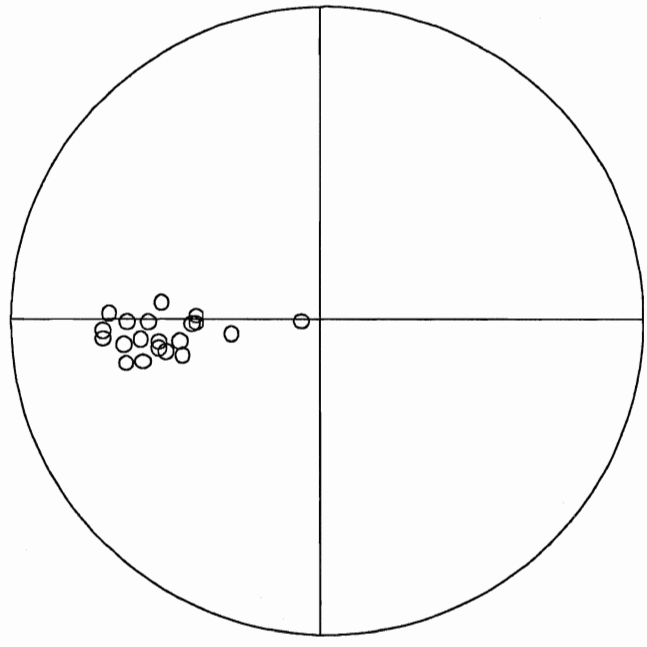

Figure 11a Fissure orientation data for diamicton at *site 10.*

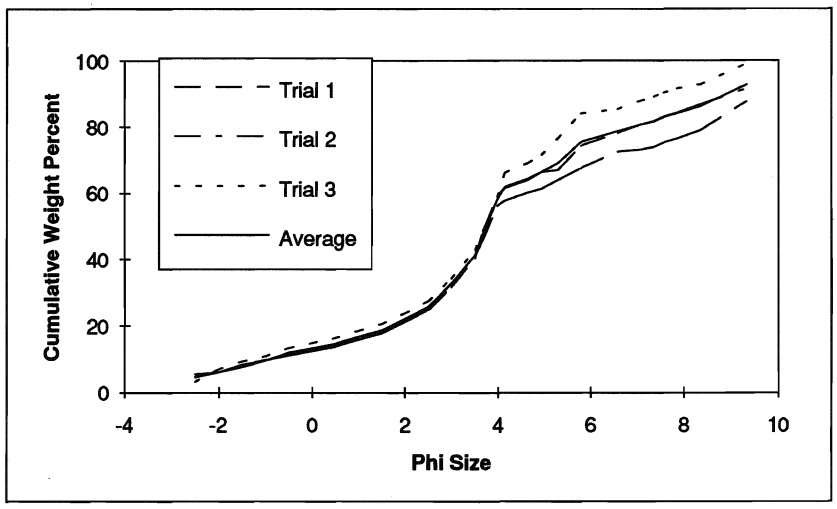

Figure 10 Grain size distribution data for sample 93-CB-9.

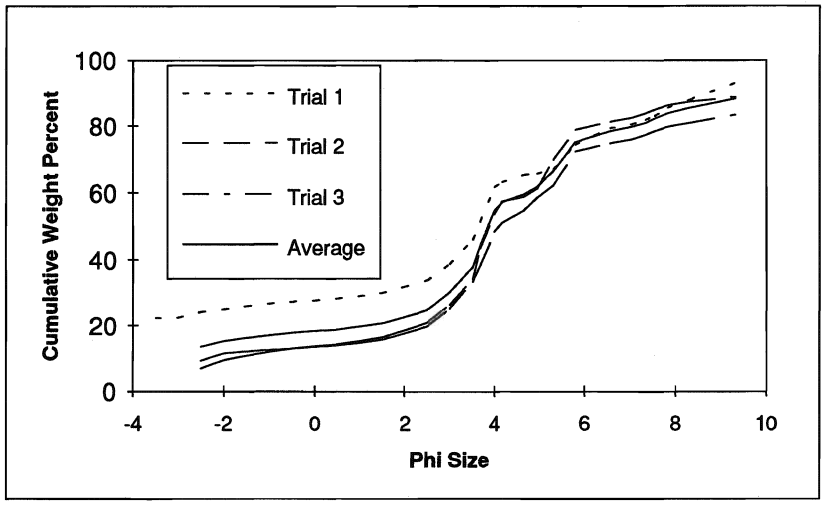

Figure 11b Grain size distribution data for sample 93-CB-10.

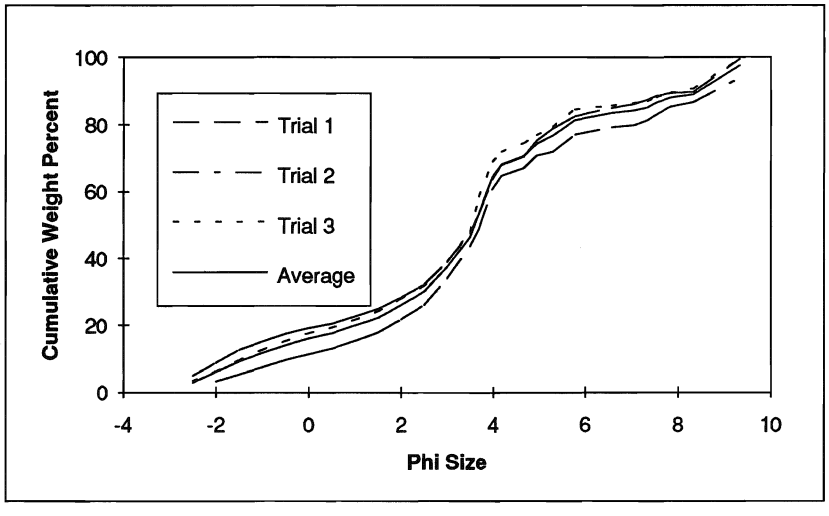

Figure 12 Grain size distribution data for sample 93-CB-11.

from massive to weakly stratified. Coarse silt infilled fractures in addition to diamictic pellets and near-vertical microfaults and shearing. In the diamicton above the intraclast, several large sand units, some of which attenuate into boudinage structures in addition to light grey (10YR7/2) sandy silt layers (Fig. 14) and light brown (7.5YR6/4) sand stringers of varying thicknesses and length are present. The sub-horizontal intraclasts tend to saucer-shaped.

Site 11C

Deformed light brown (7.5YR6/4) very fine sand layer (Fig. 15) with possible laminae in pinkish grey (7.5YR6/2) fissile diamicton.

Site 12

Continuation of pale brown (10YR6/3) very fine sand (Fig. 16a) intraclast from *11B* in fissile (Fig. 16b) pinkish grey (7.5YR6/2) sandy diamicton.

Site 13

Sand intraclast (1 m thick) in fissile pinkish grey (7.5YR6/2) sandy diamicton with intercalated white (10YR8/1) and light brown (7.5YR6/4) very fine sand and light grey (10YR7/1) silt layers. Vague cross-beds, microfaulting in addition to highly irregular angular to sub-rounded silty lenses, clay pellets, coarse sand boudins and streamlined lenses of the surrounding diamicton occur throughout the intraclast. The upper contact is gradational over a zone of 20 - 30 cm and comprises intercalated sand and diamicton, whilst the lower contact is sharp and irregular.

Site 14

Strongly fissile or possibly sheared pinkish grey (5YR6/2) sandy diamicton (Fig. 17) with light brown (7.5YR6/4) "wispy" sand stringers.

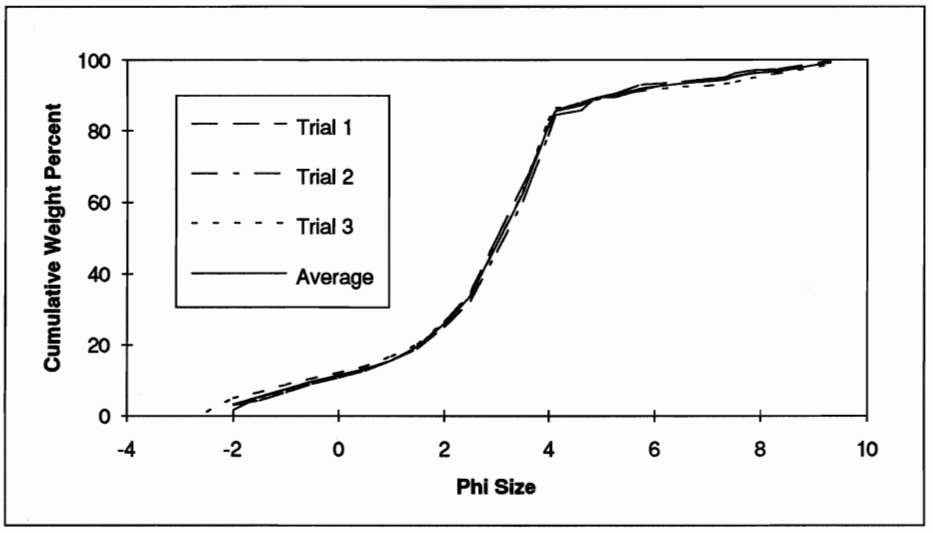

Figure 13 Grain size distribution data for sample 93-CB-11b.

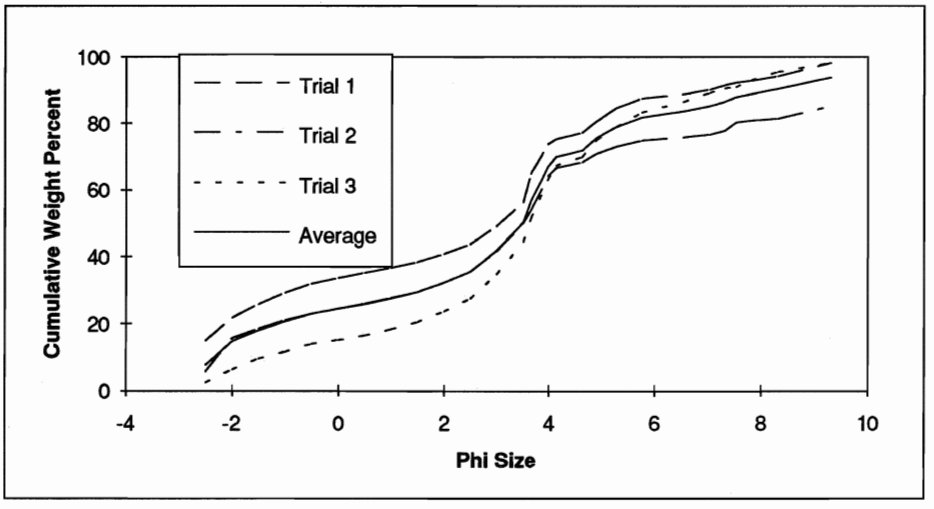

Figure 14 Grain size distribution data for sample 93-CB-11d.

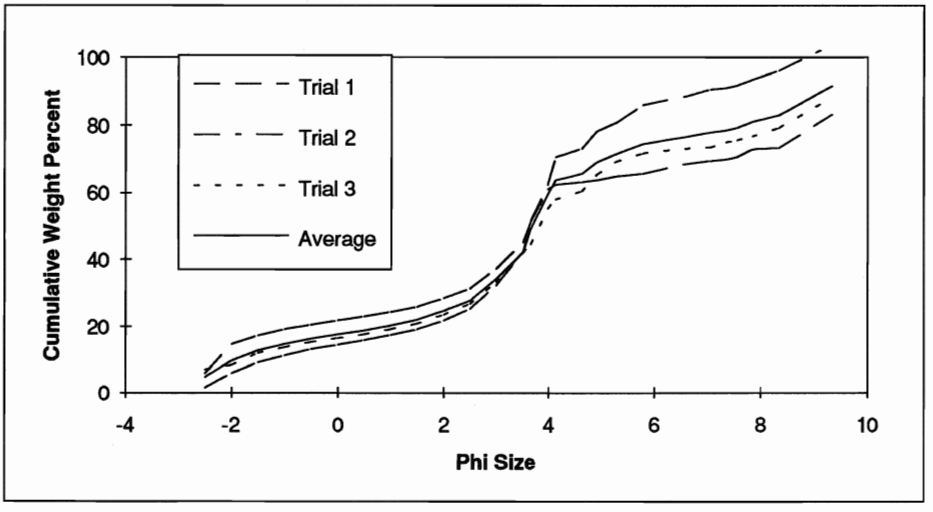

Figure 15 Grain size distribution data for sample 93-CB-11c.

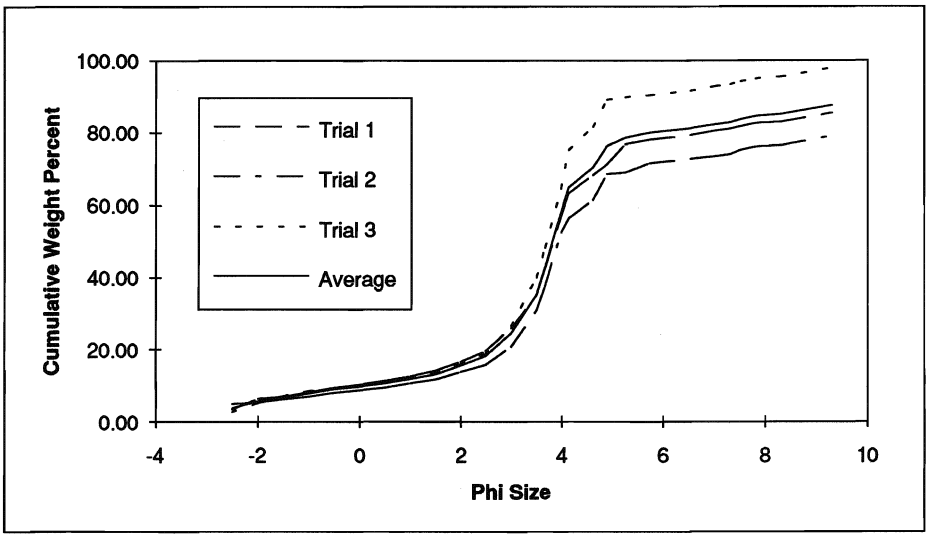

Figure 16a Grain size distribution data for sample 93-CB-12.

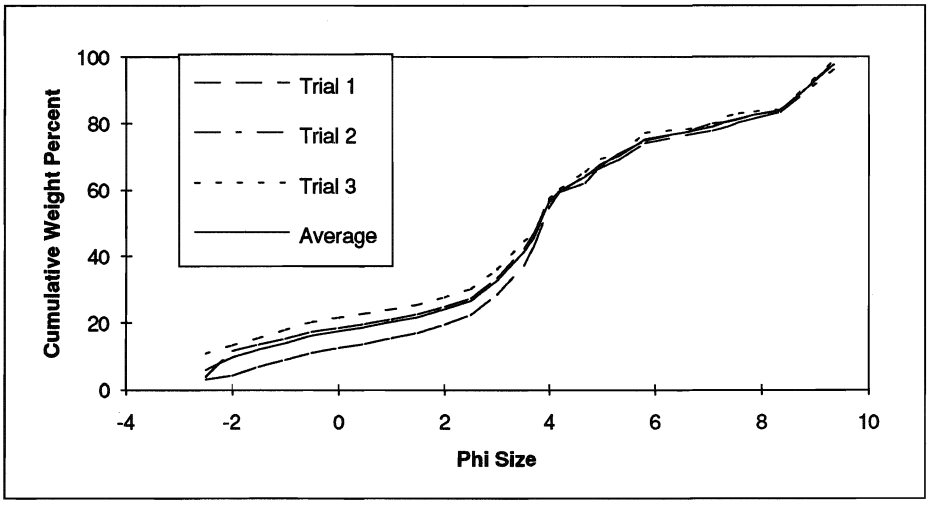

Figure 17 Grain size distribution data for sample 93-CB-14.

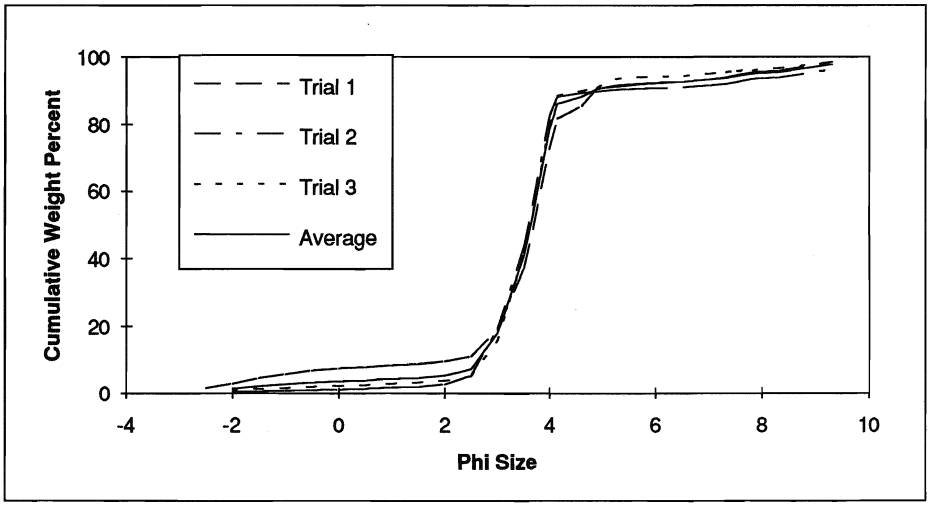

Figure 18 Grain size distribution data for sample 93-CB-15.

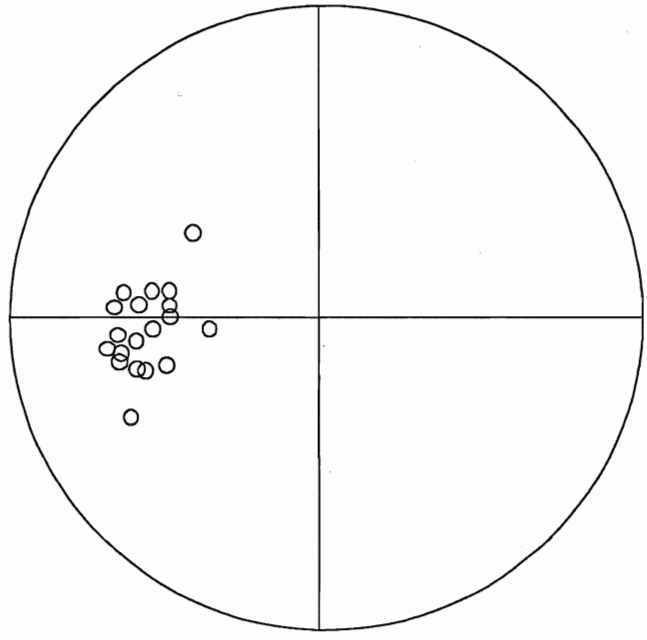

Figure 16b Fissure orientation data for diamicton at *site 12*.

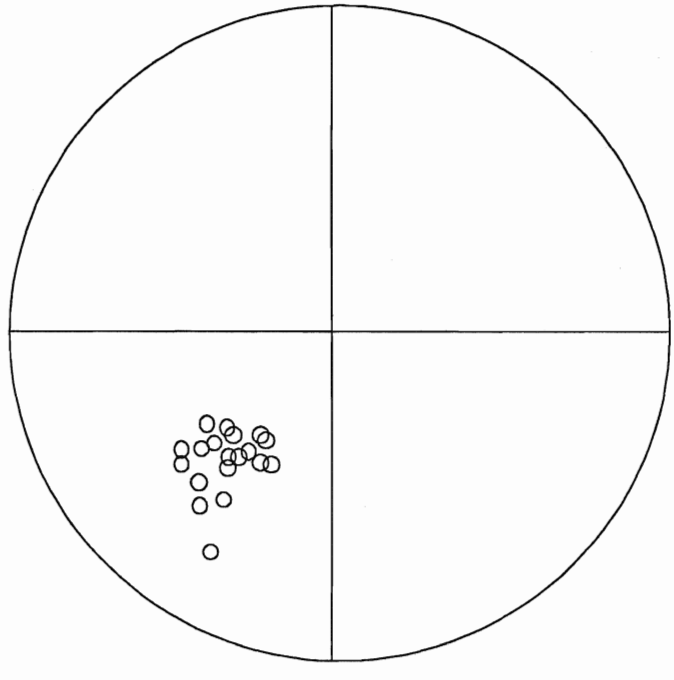

Figure 19a Fissure orientation data for diamicton at *site 16*.

Site 15

Two (10YR7/1) light grey very fine sand (Fig. 18) intraclast boudins with vague cross-beds in fissile pinkish-grey (5YR6/2) diamicton. Intraclasts also contain several streamlined coarse sand lenses, microfaulted silt layers and silt and diamictic pellets.

Site 16

Fissile (Fig. 19a) pinkish grey (7.5YR6/2) sandy diamicton (Fig. 19) overlain by a 1 m thick unit of light yellowish brown (10YR6/4) unit B.

Site 17

This site contains several pale brown (10YR6/3) very fine sand (Fig. 20) intraclasts in addition to numerous grey (10YR6/1) sandy silt layers in fissile (Fig. 21a) pinkish grey (5YR6/2) sandy diamicton (Fig. 21). A sandy silt layer is noted wrapping under a clast. The site also contains a triangular sand intraclast fragment which appears to be rotated. Fractures extend outward from the centre of the block into the surrounding diamicton. These fractures are infilled with diamicton, whilst diamicton fragments are present in the sand unit.

Site 18

Numerous pale brown (10YR6/3) sand stringers in fissile pinkish grey (7.5YR6/2) diamicton.

Site 19

Intercalated light brown (7.5YR6/4) and light grey (10YR7/1) very fine massive sands (Fig. 22) occur in several sand lenses at this site and have irregular "wispy" contacts with the fissile (Fig.23a) pinkish grey (5YR6/2; Fig. 23b) and light brown (7.5YR6/4; Fig.24) banded sandy diamicton. Grey (10YR6/1) clay layers up to 10 cm thick are also in abundance.

Site 20

Unit A pinkish grey (7.5YR6/2) and very pale brown (10YR7/3) banded diamicton

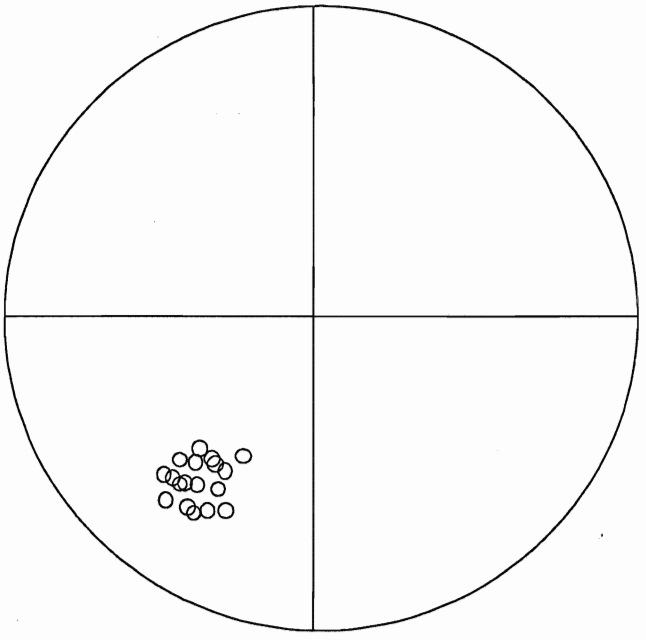

Figure 21a Fissure orientation data for diamicton at *site 17.*

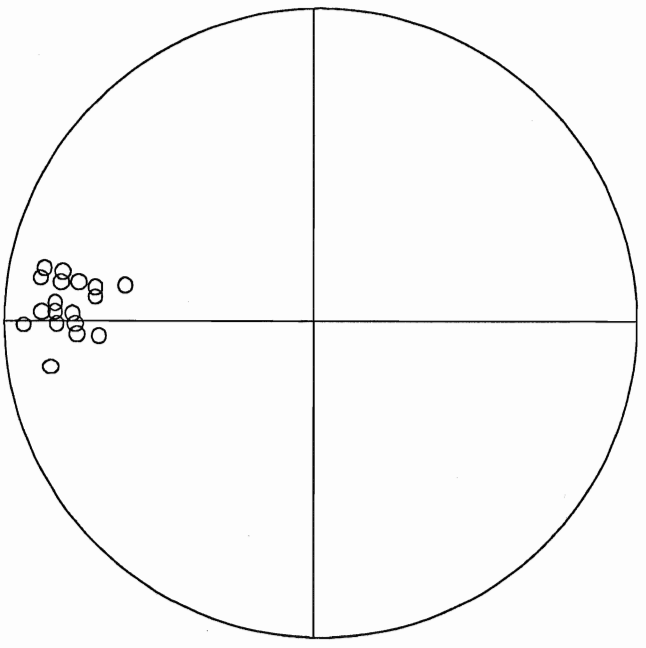

Figure 3.23a Fissure orientation data for diamicton at *site 19.*

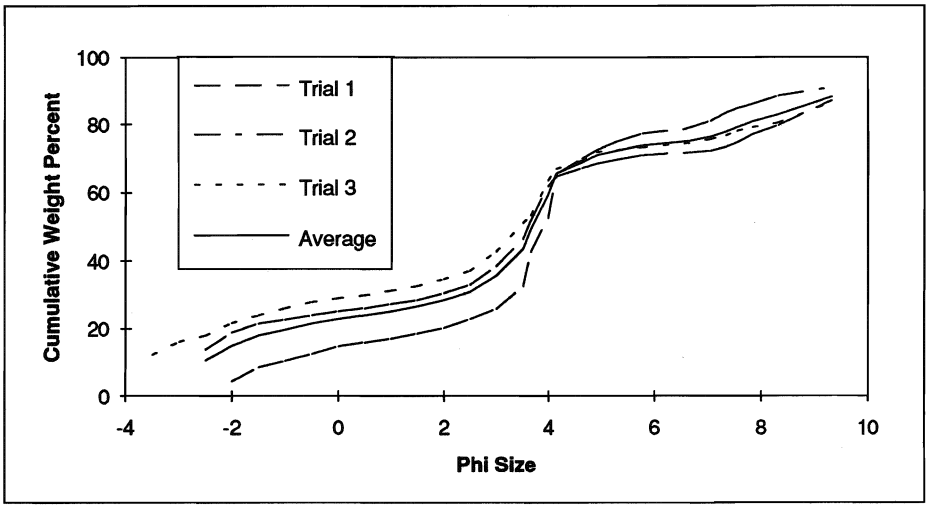

Figure 19b Grain size distribution data for sample 93-CB-16.

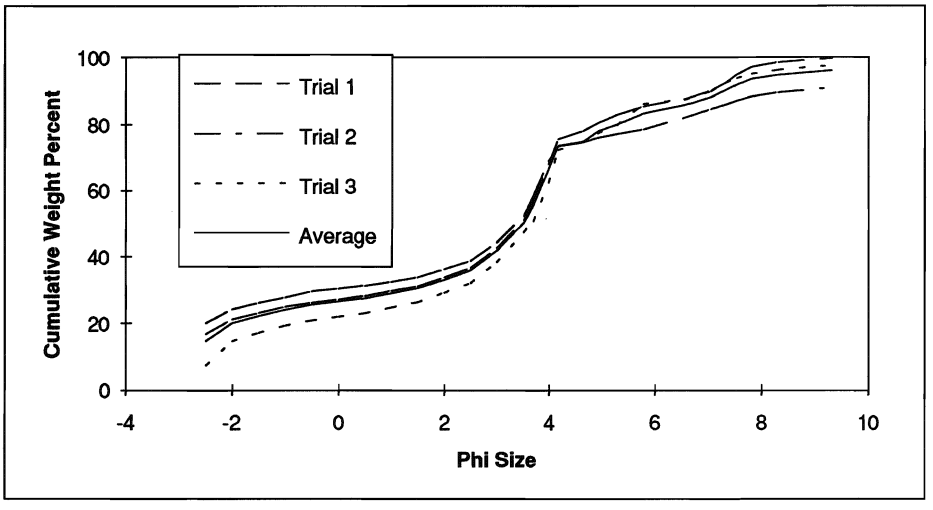

Figure 20 Grain size distribution data for sample 93-CB-17.

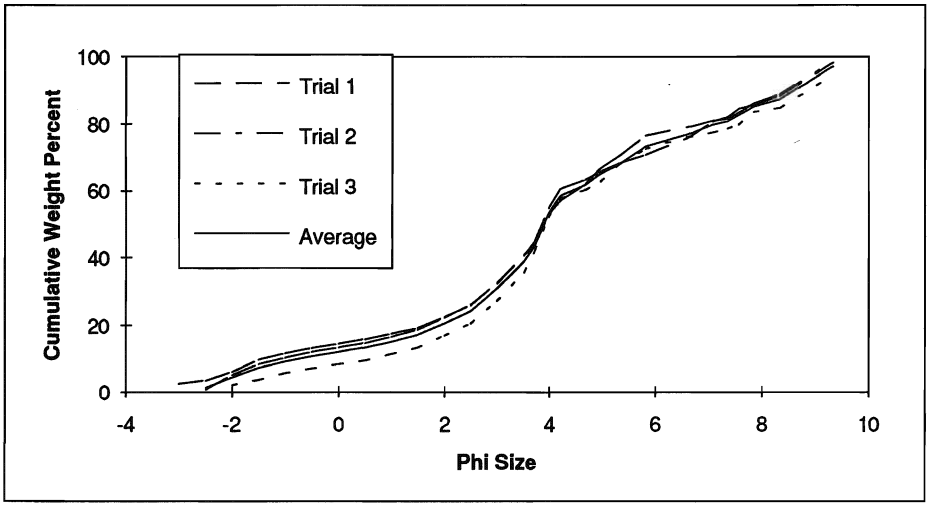

Figure 21b Grain size distribution data for sample 93-CB-17b.

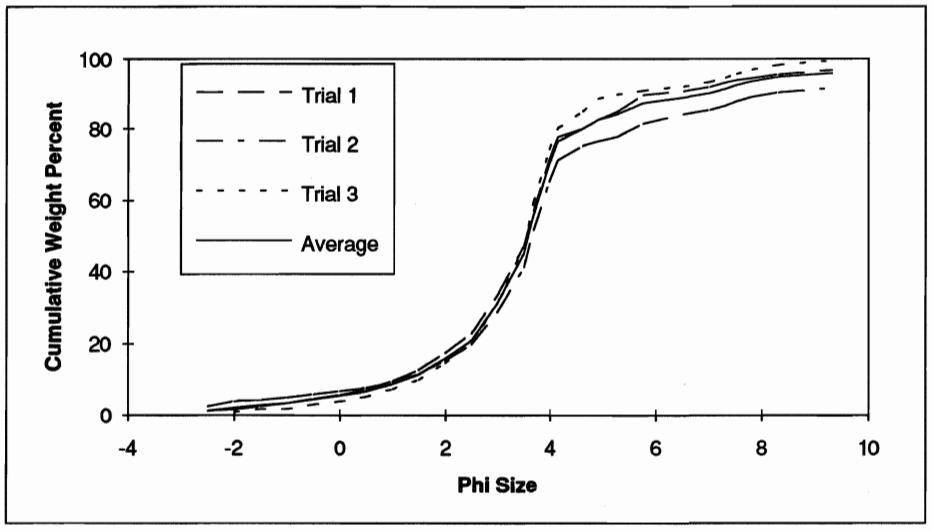

Figure 22 Grain size distribution data for sample 93-CB-19a.

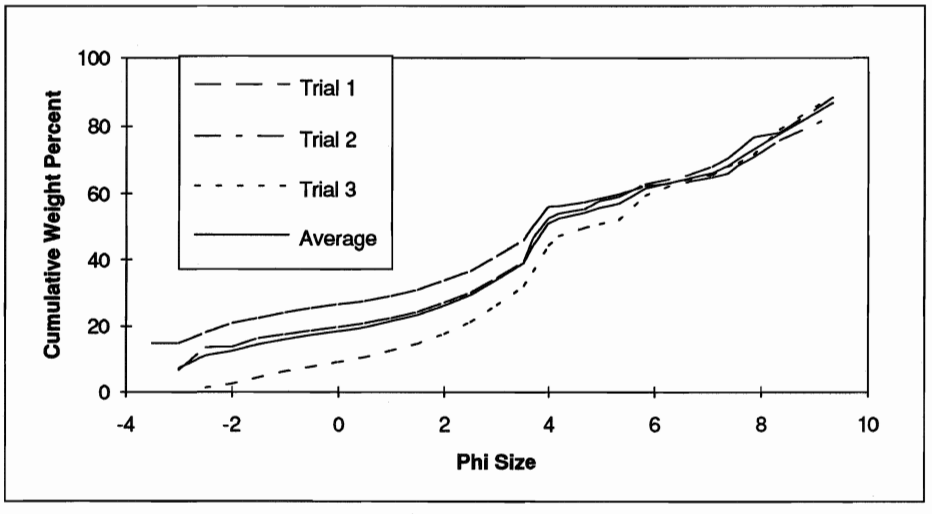

Figure 23b Grain size distribution data for sample 93-CB-19b.

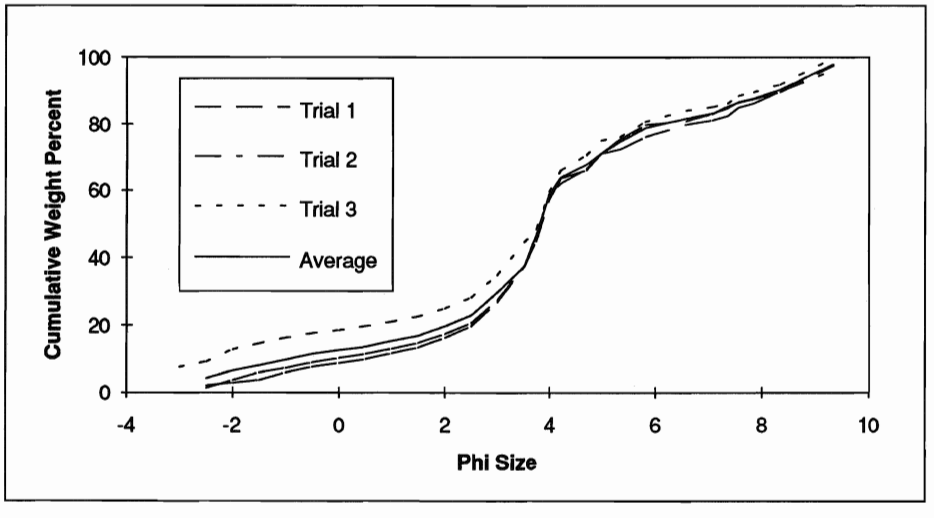

Figure 24 Grain size distribution data for sample 93-CB-19d.

forms a 10 m high bluff at this site which is typical of the bluffs in the area.

Site 21

This site contains a very fine sand layer (Fig. 25) within a pinkish grey (7.5YR6/2) sandy diamicton (Fig. 26).

Site 22

A grey (10YR sandy silt layer (Fig. 27) with overturned folds in fissile pinkish grey (5YR6/2) sandy diamicton (Fig. 28).

Site 23

Sand lens and S-folded sand stringers occur in fissile pinkish grey (7.5YR6/2) diamicton.

Site 24

A 1 m thick sand intraclast with a gravel infilled fault. The upper contact is gradational into diamicton and the intraclast extends 3 m into the bluff face. The intraclast comprises intercalated vaguely cross-bedded pinkish grey (7.5YR6/2) fine to very fine sand, light grey (10YR7/2) sandy silt (Fig.29), light brown (7.5YR6/4) poorly sorted sand lenses (Fig. 30) and diamictic pellets (Fig. 31).

Site 25

Light grey (10YR7/2) very fine sand boudins (Fig. 32) in slump at base of drumlin in which wavy sand and silt laminae are evident in pinkish grey (7.5YR7/2) diamicton..

Site 26

Sand intraclast(0.4 x 2 m) in diamicton comprising intercalated vaguely cross-bedded pale brown (10YR6/3) sand and light brown (7.5YR6/4) coarse sand lenses. Pellets of grey sandy silt (10YR6/1) and pinkish grey (7.5YR6/2) diamicton are found throughout the intraclast and adjacent boudinaged sand lenses.

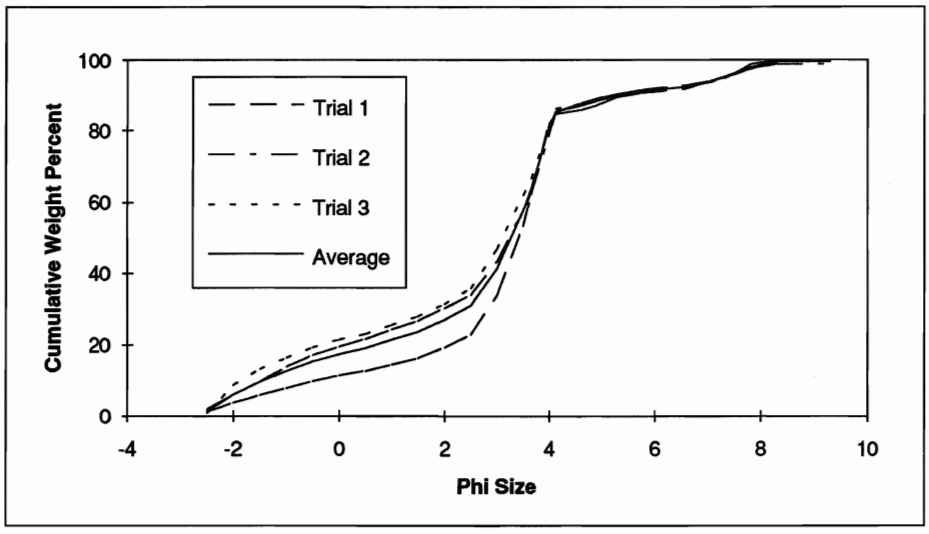

Figure 25 Grain size distribution data for sample 93-CB-21a.

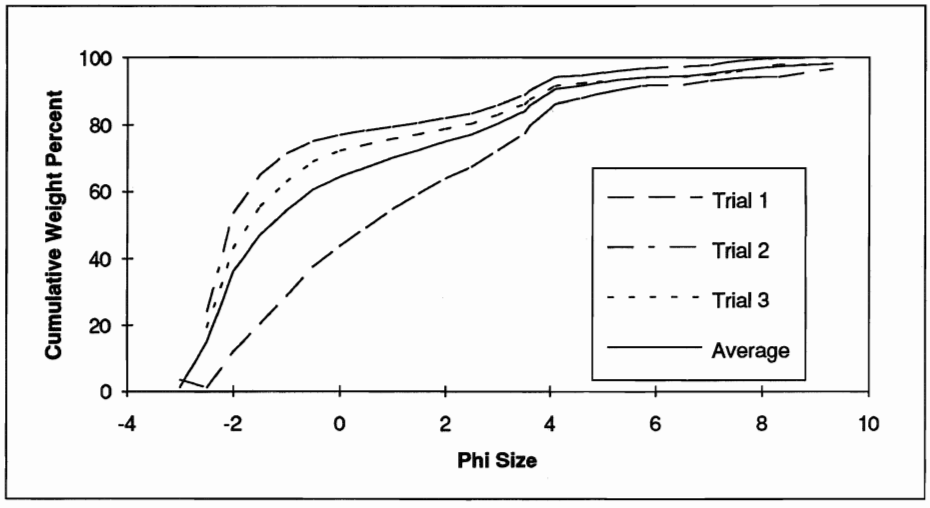

Figure 26 Grain size distribution data for sample 93-CB-21b.

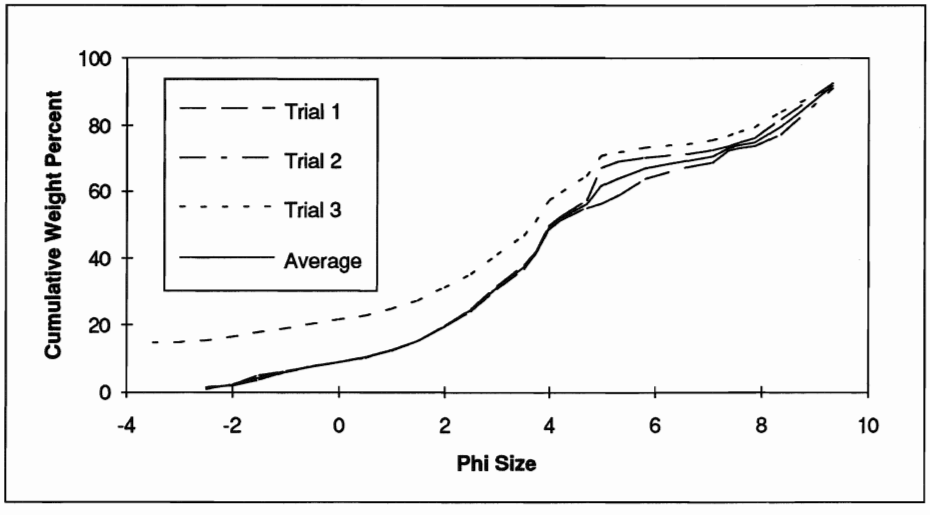

Figure 27 Grain size distribution data for sample 93-CB-22.

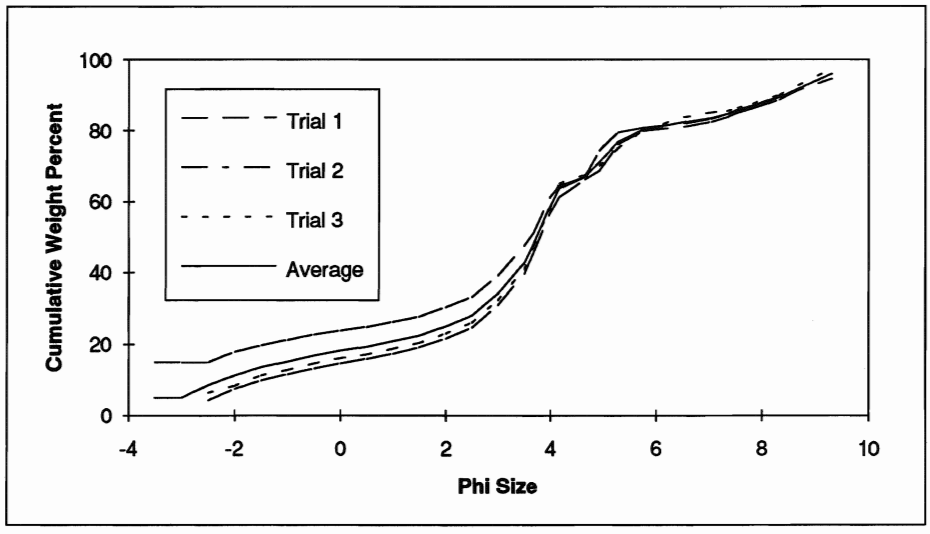

Figure 28 Grain size distribution data for sample 93-CB-22b.

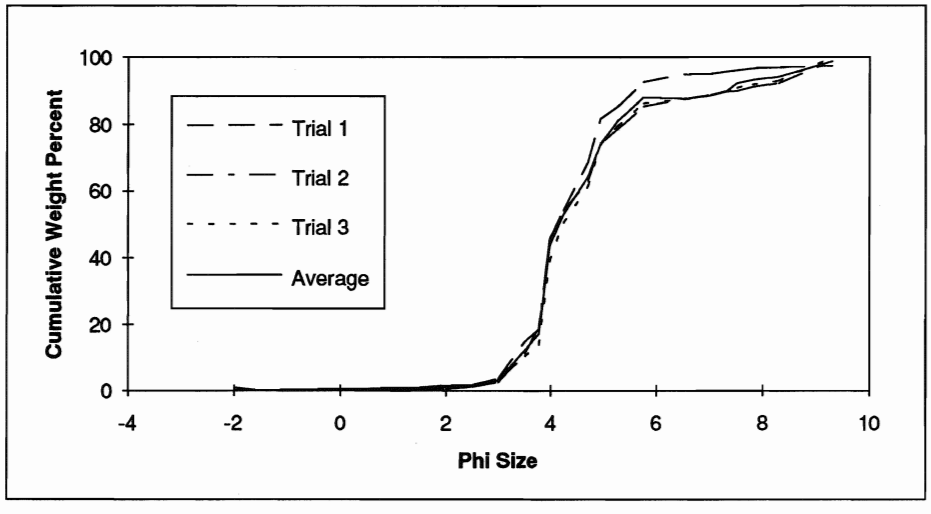

Figure 29 Grain size distribution data for sample 93-CB-24a.

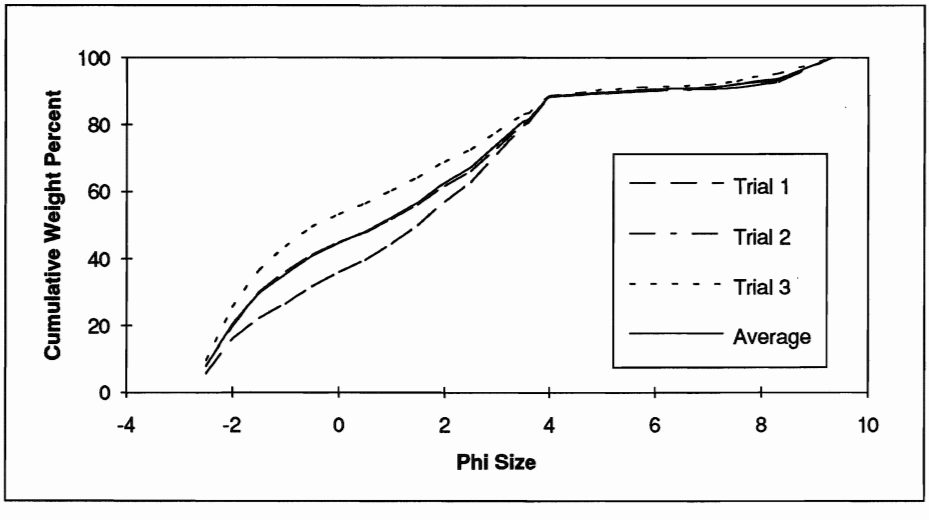

Figure 30 Grain size distribution data for sample 93-CB-24b.

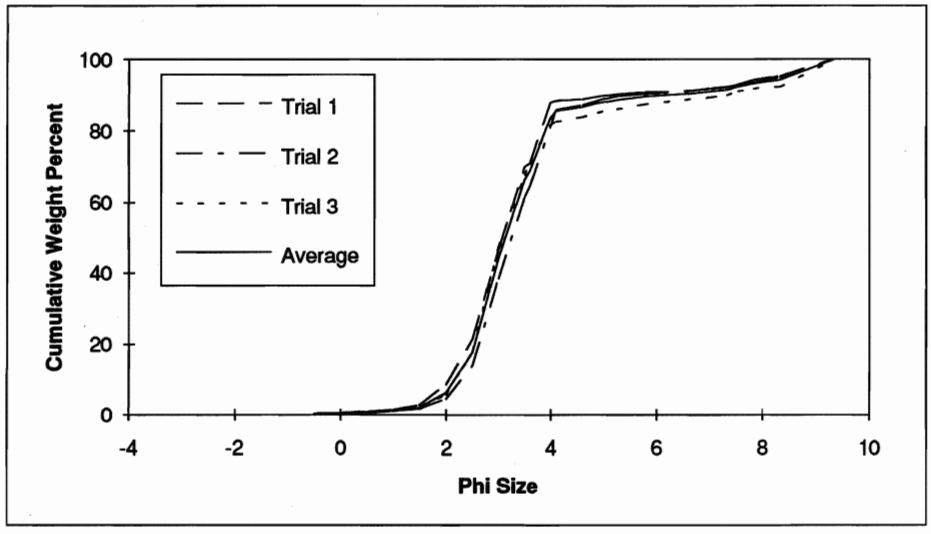

Figure 31 Grain size distribution data for sample 93-CB-24c.

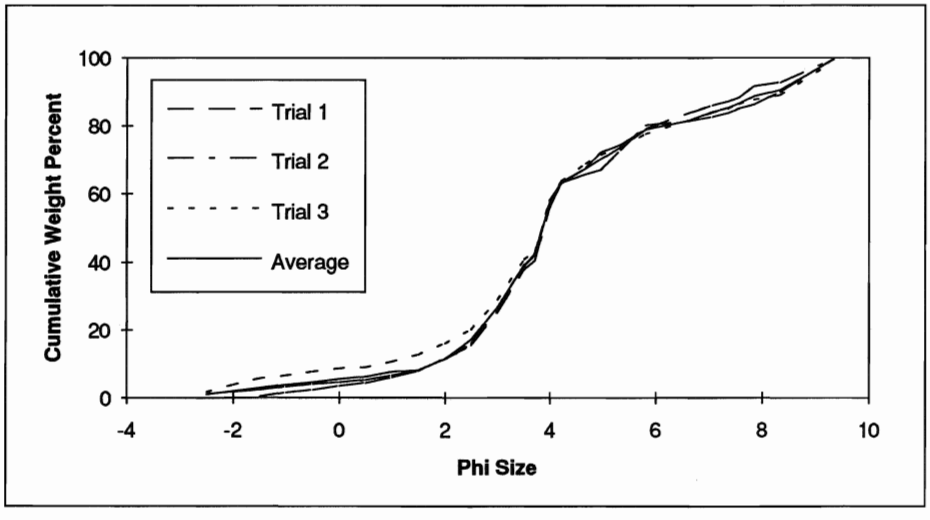

Figure 32 Grain size distribution data for sample 93-CB-25.

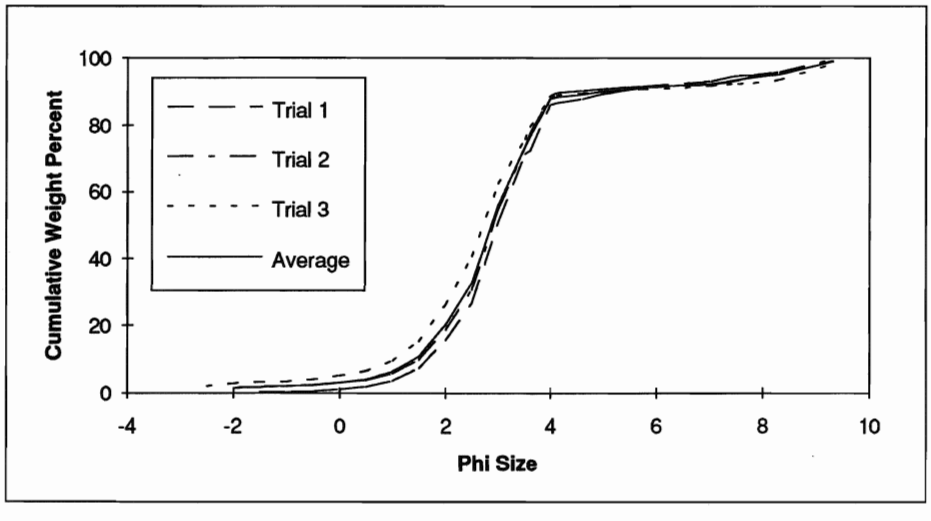

Figure 33 Grain size distribution data for sample 93-CB-27b.

Site 27

Two sand intraclasts are evident at the site. One is a light brown (7.5YR6/4) 0.10 m x 1 m streamlined lens of intercalated massive sands and silts (Fig. 33) whilst the other is a 1 m x 15 m lenticular block. The large one is similar to the intraclast described at site 24 and may represent the eastward extent of the same unit. The upper and lower contacts at this site are sharp and irregular whilst the lateral edge is gradational into the surrounding fissile pinkish grey (7.5YR7/2) sandy diamicton (Fig. 34).

Site 28

Pinkish grey (7.5YR6/2) sandy diamicton (Fig. 35) with weakly defined fissility is capped by a 1 m thick unit B.

Site 29

Typical bluff of vaguely fissile pinkish grey (7.5YR6/2) unit A.

Site 30

Sand intraclast (1 m x 20 m) in non-fissile diamicton comprising intercalated light brown (7.5YR6/4) very fine sands and light grey (10YR7/1) sandy silt with coarse sand lenses. Vague cross-bedding is evident in the sand layers, though somewhat distorted. the upper and lower contacts are gradational interfingered sands and diamicton.

Site 31

Transverse section of pinkish grey (7.5YR6/4) diamicton containing numerous light brown (7.5YR6/4) sand stringers.

Site 32

Erosional contact between 2 m thick unit of light yellowish brown (10YR6/4) stratified sands and gravels (Fig. 36) and underlying fissile pinkish grey (7.5YR6/4) diamicton. Fine to silty sand (Fig. 37) from the overlying unit B has infilled some of the

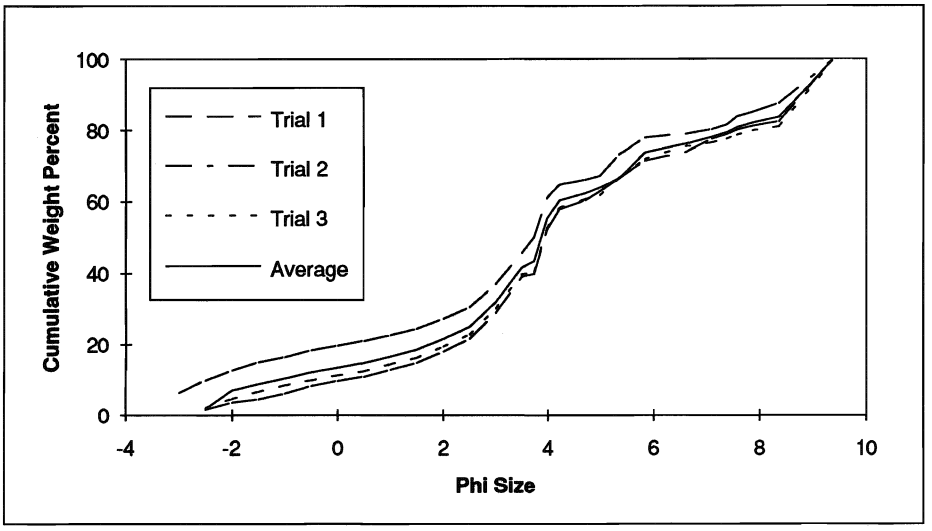

Figure 34 Grain size distribution data for sample 93-CB-27.

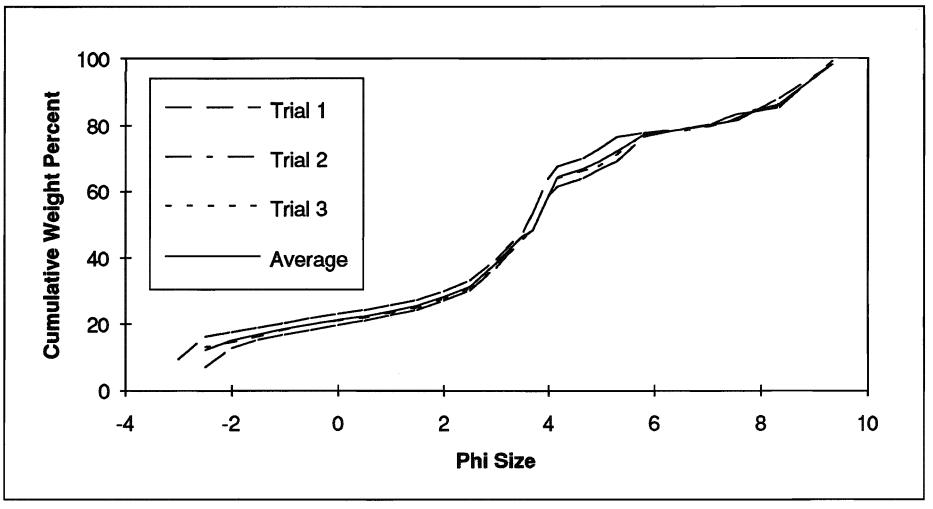

Figure 35 Grain size distribution data for sample 93-CB-28.

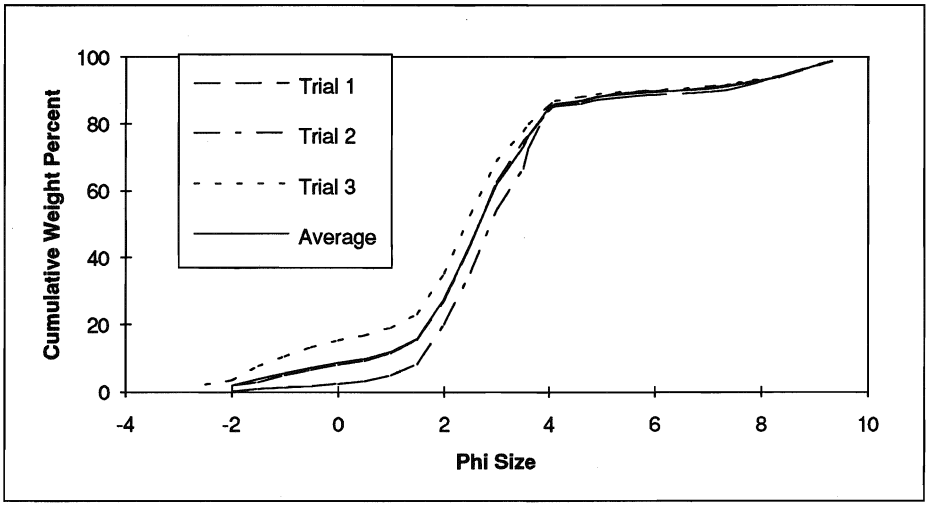

Figure 36 Grain size distribution data for sample 93-CB-32a.

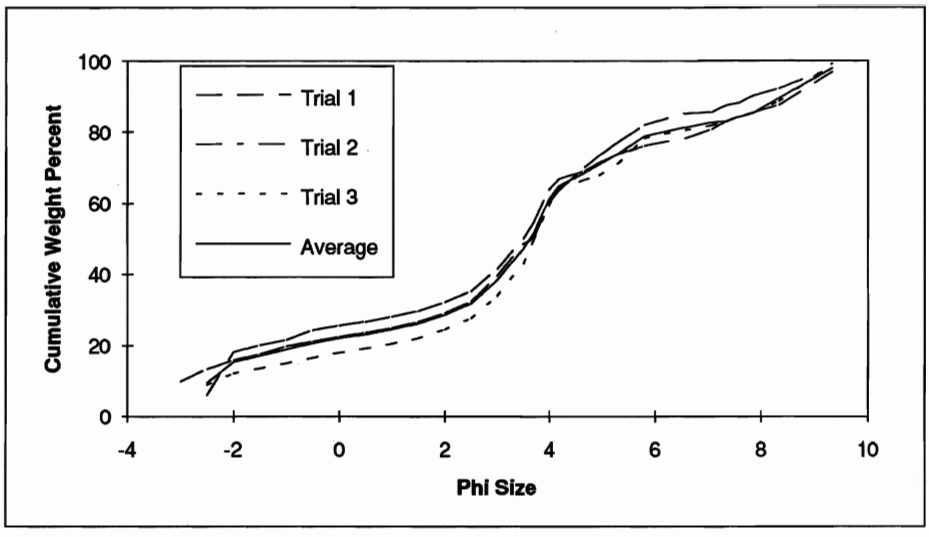

Figure 37 Grain size distribution data for sample 93-CB-32b.

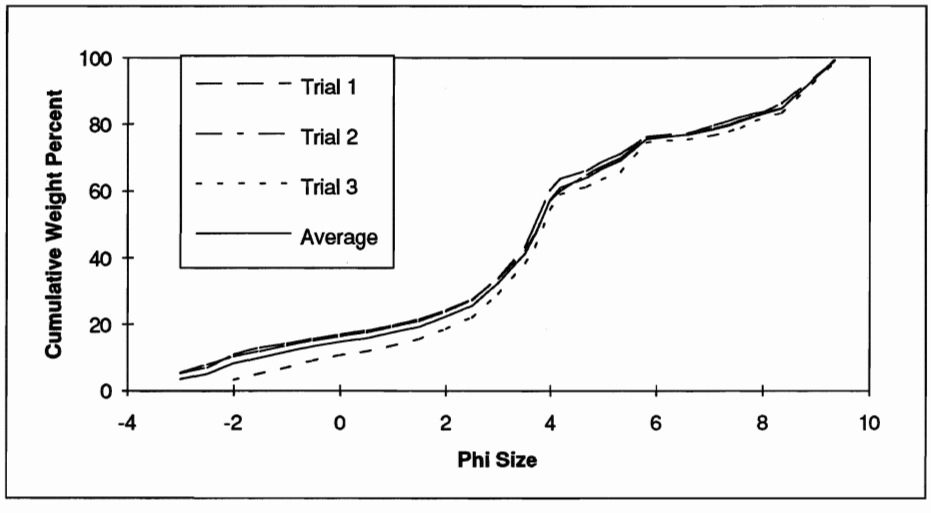

Figure 38 Grain size distribution data for sample 93-CB-33.

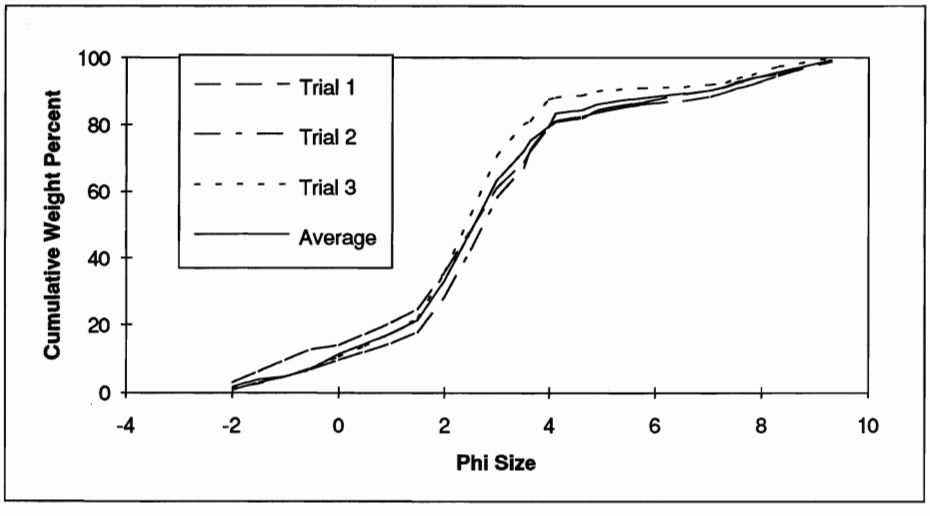

Figure 39 Grain size distribution data for sample 93-CB-34.

fissures in unit A to a depth of 2 m. The poorly sorted sands in Figure 37 suggest that some intermixing with the diamicton has occurred.

Site 33

Light yellowish brown (10YR6/4) unit B has a sharp erosional contact with the underlying very pale brown (10YR7/3) sandy diamicton (Fig. 38). Fragments and stretched out inclusions of diamicton occur throughout the overlying sands and gravels, whilst sand stringers occur in the diamicton.

Site 34

Planar cross-bedded sands are evident in unit B which has a sharp erosional contact with the underlying diamicton, although a small degree of intermixing has occurred.

Site 35

A 25 m high bluff of pinkish grey (7.5YR6/2) diamicton with several grey (10YR6/1) sandy silt layer which increase in number up-sequence in addition to becoming more contorted.

Site 36

Slump of pinkish grey (7.5YR6/2)) diamicton into adjacent convoluted sands. The diamicton also contains many folded medium sand and coarse sand layers which are similar in appearance to the convoluted laminae described at site 1.

Table 5.1 Coefficient of permability (in m/s) for unconsolidated sediments (after Craig, 1987).

APPENDIX IV: EXTRANEOUS LITERATURE

A Drumlin Woodchuck

One thing has a shelving bank,
Another a rotting plank,
To give it cosier skies
And make up for its lack of size.

My own strategic retreat
Is where two rocks almost meet,
And still more secure and snug,
A two-door burrow I dug.

With those in mind at my back
I can sit forth exposed to attack
As one who shrewdly pretends
That he and the world are friends.

All we who prefer to live
Have a little whistle we give,
And flash, at the least alarm
We dive down under the farm

We allow some time for guile
And don't come out for a while
Either to eat or drink.
We take occasion to think.

And it after the hunt goes past
And the double-barrelled blast
(Like war and pestilence
And the loss of common sense),

If I can with confidence say
That still for another day,
Or even another year,
I will be there for you, my dear,

It will be because, though small
As measured against the All,
I have been so instinctively thorough
About my crevice and my burrow.

Robert Frost, 1936